THESIS FOR THE DEGREE OF DOCTOR OF PHILOSOPHY

Development of a Cohesive Zone Model for Adhesive Joints that Includes Environment Degradation

by

Guilherme Miranda Silva de Oliveira Viana

Supervisor:

Lucas Filipe Martins da Silva

Co-Supervisor:

Mariana Doina Banea

January 2018

Departamento de Engenharia Mecânica

Faculdade de Engenharia da Universidade do Porto

Rua Dr. Roberto Frias

4200-465 Porto

Portugal

ABSTRACT

Adhesives used in transportation industries must operate in various environmental conditions. These adhesives must maintain the structural integrity of the joint at high moisture environments and at high and low temperatures. Moisture is absorbed by the adhesive and acts as a plasticizer, increasing adhesive ductility and decreasing its strength. Moisture may also attack the interface between the adhesive and the adherend, being responsible for adhesive failure of the joint. Different temperatures also affect the mechanical properties of the adhesive.

Now-a-days, the design of adhesive joints is a relatively easy task, as there are advanced tools that allow the engineer to reliably predict the mechanical behaviour of the joint in the short term. However, in the long term the adhesive joint will degrade, and its properties will deteriorate. This is arguably the most important disadvantage of adhesive bonding today.

High and low temperatures are one of the environmental factors that affect the performance of adhesive joints as mechanical properties of the adhesive change with temperature. At higher temperatures, the adhesive becomes more ductile and more sensitive to strain rate. Moreover, the performance of the adhesive joint should be assessed under service conditions. In the automotive industry, for instance, it is important to consider also impact loads, as the adhesive joint must be able to resist high impact loads such as those that are cause by vehicle crash.

The main objective of this study is to determine the mechanical behaviour of two structural adhesives used in transportation industries, simultaneously taking into account different levels of moisture and the range of temperatures typically found in these applications: from -40^{o}C to 80^{o}C. The information generated was used to develop a cohesive zone model that can be used to predict the mechanical behaviour of any adhesive joint under moisture and temperature conditions. This will help engineers design more efficient adhesive joints.

The triangular cohesive zone law was used to model the adhesive layer. To define this law, the determination of three parameters is required: the modulus, strength and toughness of the adhesive. These properties were determined in this study as a function of environmental moisture and temperature.

Moisture does not penetrate instantaneously into the adhesive layer. This means that the adhesive that is closer to the edges of the bondline will attain saturation faster than the adhesive in the centre of the joint, which will create a gradient also in the mechanical properties of the adhesive layer.

In this study scaled specimens of a joint used in the railway industry were artificially aged in high moisture environments and tested at high and low temperatures. Using Fick's laws, it is possible to predict the amount of absorbed water at each point of the adhesive layer and consequently attribute a different set of mechanical properties at each point. The shape of the cohesive zone law is different at each point of the adhesive layer. A numerical model that includes a cohesive zone element that is capable of taking into account graded adhesive properties according to absorbed moisture and environmental temperature was developed. The results provided by this model correlate well with values obtained experimentally.

RESUMO

Os adesivos estruturais que são utilizados nas indústrias dos transportes em geral têm de ser capazes de suportar condições ambientais adversas. Estes adesivos têm de manter a integridade estrutural da junta em condições de humidade elevada e sob altas e baixas temperaturas. A humidade actua no adesivo como um plasticizante, aumentando a sua ductilidade e diminuindo a sua resistência. A humidade também pode atacar a interface entre adesivo e substracto, podendo ser responsável por ruptura adesiva da junta. Altas e baixas temperaturas também afectam as propriedades mecânicas da junta.

Actualmente, o projecto de juntas adesivas é relativamente simples. Existem ferramentas avançadas que permitem fazer previsões fiáveis do comportamento mecânico a curto prazo. No entanto, a longo prazo as propriedades mecânicas da junta degradar-se-ão. Esta é possivelmente a pior desvantagem das juntas adesivas em relação a outros métodos de ligação.

Altas e baixas temperaturas afectam as propriedades dos adesivos e, consequentemente, o comportamento mecânico de juntas adesivas. A temperaturas mais elevadas, o adesivo torna-se mais dúctil e mais sensível à taxa de deformação, pelo que o desempenho da junta deve ser determinado à temperatura de serviço. Na indústria automóvel, por exemplo, é importante considerar também taxas de deformação elevadas porque a junta tem de ser capaz de suportar cargas de impacto, como aquelas que resultam de colisões entre veículos.

O principal objectivo deste estudo é a determinação das propriedades mecânicas de dois adesivos estruturais utilizados em indústrias de transportes, considerando diferentes níveis de humidade e de temperatura simultaneamente. A informação gerada foi utilizada para desenvolver um elemento coesivo que pode ser utilizado na determinação do comportamento mecânico de juntas adesivas sujeitas a diferentes condições de humidade e temperatura. Este elemento pode ajudar engenheiros na previsão do comportamento de juntas adesivas a longo prazo e no projecto de juntas mais eficientes.

A lei de dano triangular foi utilizada para modelar a camada de adesivo. Para definir esta lei, é necessária a determinação de três parâmetros: o módulo, a resistência e a tenacidade. Estes três parâmetros foram determinados em função da humidade e temperatura ambientais.

A humidade não penetra instantaneamente na camada de adesivo. Isto significa que as zonas de adesivo que estão mais próximas das extremidades da zona de sobreposição absorverão

humidade mais rapidamente. Isto criará um gradiente na humidade do adesivo e, consequentemente, nas suas propriedades mecânicas.

Neste estudo, provetes de dimensões reduzidas, que imitam um tipo de junta utilizada na indústria ferroviária, foram expostos a uma diversidade de condições de humidade e temperatura encontrados neste tipo de indústria. Utilizando as leis de Fick, é possível determinar a quantidade de água absorvida pelo adesivo em cada ponto da camada de adesivo e, consequentemente, atribuir diferentes propriedades mecânicas ao adesivo em cada ponto. A forma da lei coesiva é diferente em cada elemento da camada de adesivo. Um modelo numérico que inclui um elemento coesivo capaz de tomar em consideração propriedades graduadas do adesivo, de acordo com o seu nível de humidade e temperatura, foi desenvolvido. Existe boa correlação entre os resultados do modelo e os valores obtidos experimentalmente.

ACKNOWLEDGEMENTS

I would like to express my gratitude to my supervisor, prof. Lucas da Silva for and my co-supervisor Mariana Banea for their guidance, technical contribution, dedication and writing review during this work.

I equally wish to thank FEUP's adhesives group members for their friendship, help and support during the development of this thesis Ana Loureiro, Ana Queirós, Eduardo Marques, Filipe Chaves, José Machado, Marcelo Costa, Ricardo Carbas and Rodrigo Avendaño.

Acknowledgements to master students Rodrigo Avendaño (who later joined the group), Daniel Rosendo and Pedro Fernandes for their contributions to this work.

Special thanks to the Brazilian colleagues and friends Daniel Kawasaki, Júlia Bonaldo, Pedro Zugliani and Rosemere Lima and for their very important contribution at the last stages of this study.

Thanks to prof. Raul Campilho for his precious advice and willingness to help whenever it was needed.

My sincere gratitude to D. Emilia Soares for her help and to members of the workshop Mr. José Fernando Rocha Almeida, Mr. Albino Alves Calisto Dias, Pedro Miguel Almeida Falcão Alves and André Alves as well as to members of the testing laboratory Mr. Miguel Figueiredo and Mr. Rui Silva.

I am very thankful and would like to express my sincere gratitude to my family and friends for their encouragement, support and affection, without which it would not have been possible to conclude this work.

An important contribution was given by Nagase Chemtex®, which partially funded and supplied samples of adhesive for this study.

In last place, I would like to thank the Portuguese Foundation of Technology for partially financing this work through research grant EXCL/EMS-PRO/0084/2012.

Table of Contents

LIST OF PUBLICATIONS

1. G. Viana, M. Costa, M.D. Banea, L.F.M da Silva, A review on the temperature and moisture degradation of adhesive joints, Proceedings of the Institution of Mechanical Engineers, Part L: Journal of Materials: Design and Applications, 2017, vol. 231, issue 5, pp. 488-501.
2. G. Viana, M. Costa, M.D. Banea, L.F.M da Silva, Behaviour of environmentally degraded epoxy adhesives as a function of temperature, The Journal of Adhesion, 2017, vol. 93, issue 1-2, pp. 95-112.
3. G. Viana, M. Costa, M.D. Banea, L.F.M da Silva, Water Diffusion in Double Cantilever Beam Adhesive Joints, Latin American Journal of Solids and Structures, 2017, vol. 14, issue 2, pp. 188-201.
4. G. Viana, M. Costa, M.D. Banea, L.F.M da Silva, Moisture and temperature degradation of double cantilever beam adhesive joints, Journal of Adhesion Science and Technology, 2017, vol. 31, issue 16, pp. 1824-1838.
5. G. Viana, J. Machado, R. Carbas, M. Costa, L.F.M. da Silva, M. Vaz, M.D. Banea, Strain rate dependence of adhesive joints for the automotive industry at low and high temperatures, Journal of Adhesion Science and Technology, submitted.
6. P. Fernandes, G. Viana, R.J.C. Carbas, M. Costa, L.F.M. da Silva and M.D. Banea, The Influence of Water on the Fracture Envelope of an Adhesive Joint, Theoretical and Applied Fracture Mechanics, 2017, vol. 89, pp. 1-15.
7. G. Viana, R.J.C. Carbas, M. Costa, M.D. Banea, L.F.M. da Silva, A new cohesive element to model environmental degradation of adhesive joints in the rail industry, International Journal of Adhesion and Adhesives, submitted.

SUMMARY OF THESIS

1. Introduction

a. Background

Adhesives used in the automotive industry and in the transports industry in general must operate under a variety of environmental conditions. They need to maintain the structural integrity of the joint at low and high temperature (roughly between -40^{o}C and 80^{o}C) and, at the same time, withstand high and low levels of moisture. Adhesives, which are polymeric materials, show great sensitivity to this kind of conditions [1, 2]. However, some adhesives can withstand these conditions, particularly epoxy adhesives. “Crash resistant” epoxy adhesives are an example of adhesives that are increasingly being used mainly in the automotive industry as they are at the same time relatively strong and ductile, they provide very tough joints, which is key to have high absorption of energy in case of collision.

The application of adhesive bonding in transportation industries has been steadily growing. Transportation industries in general are interested in reducing the weight of their vehicles, in order to improve the performance and reduce fuel consumption and pollutant emissions. Although its application in these industries has been steadily growing, the use of adhesive bonding is still limited, as more traditional joining methods, such as riveting or bolting, continue to be preferred due to their higher reliability. The main factor holding adhesive bonding back is arguably the uncertainty regarding the adhesive’s mechanical properties in the long term. Moisture and extreme temperatures are the main factors contributing to the degradation of adhesive properties.

In order to properly design an adhesive joint that is subjected to environmental degradation, a good prediction of the mechanical behaviour of the joint must be made. To achieve this purpose, the temperature and moisture dependent mechanical properties of the adhesive must be determined [3-7]. Moisture penetrates slowly into the adhesive layer: the edges of the adhesive layer absorbed more water than center [4, 8]. Figure 1 shows the moisture distribution in an adhesive layer as calculated using the finite element method (FEM). Consequently, there will be a gradient in the moisture concentration of the adhesive, meaning that there will also be a gradient in the mechanical properties of the adhesive [8, 9].

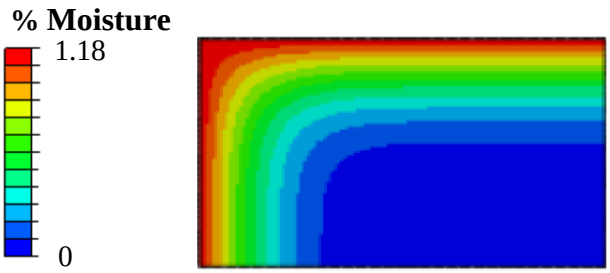

Figure 1: Moisture distribution in the adhesive layer of an adhesive joint (only a quarter of the adhesive joint shown).

Cohesive zone models are often used together with the Finite element method to predict crack initiation and propagation within the adhesive layer [4, 10, 11]. This allows to the engineer to accurately predict the mechanical behaviour and the strength of complex adhesive joints. The cohesive zone model relies on the cohesive zone law to predict crack initiation and propagation. The simplest and most common cohesive zone law is the triangular zone law, pictured in Figure 2.

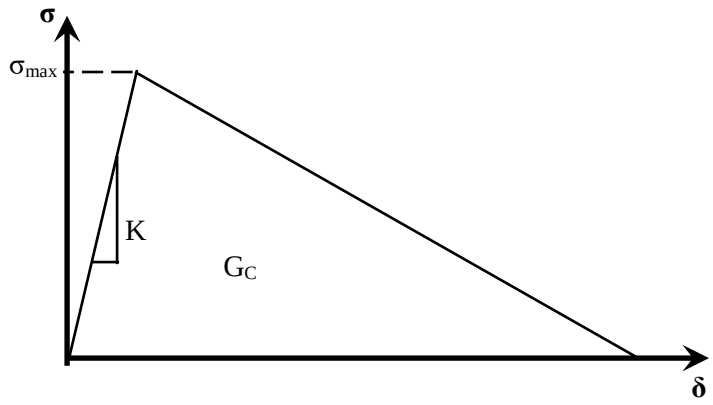

Figure 2: Triangular cohesive zone model.
K: Stiffness
σ_{max}: Strength of the adhesive
G_C: Toughness of the adhesive

The cohesive zone law defines a relationship between the displacement and stress. First the stress rises linearly until the yield stress of the adhesive is reached. Then, softening initiates. In the triangular cohesive zone law, softening is linear but in other laws it can be more complex, such as exponential or trapezoidal. This allows the model to capture the more ductile or fragile behaviour of the adhesive. The triangular law, on the other hand, is the simplest law and the easiest to implement.

The modulus, yield stress and toughness of the adhesive give the initial stiffness, maximum stress and area of the cohesive zone law. These three properties are enough to define the triangular cohesive zone law. However, other laws need more require the determination of more properties, which add to the complexity of the model.

Absorbed moisture is responsible for plasticization of the adhesive, which means that the adhesive will become weaker and more ductile. This will change the shape of the cohesive zone law. As water concentration is not uniform across the width of the adhesive joint, the shape of the triangle at each element must be different. A cohesive zone element that can change its properties as a function of local moisture and temperature will allow for more reliable strength predictions [10].

In order to validate the proposed cohesive zone element, an aluminium rail used in the railway industry to attach the seats of a train was considered. The possibility of bonding this rail to the train floor instead of using the currently used mechanical fasteners was studied. Scaled specimens of this joint were manufactured and environmentally exposed. A finite element model using the developed cohesive zone element was put forward. Results given by the numerical model generally matched well with experimental results.

b. Objectives

The main objective of this research was to develop a cohesive zone model that includes two environmental degradation mechanisms of adhesive joints simultaneously: moisture and temperature. This cohesive zone model can be used to predict the strength of adhesive joints that are subjected to simultaneously high/low temperatures and humid environments and was used in this study to predict the mechanical behaviour of a scaled adhesive joint used in the railway industry. Two epoxy adhesives were studied.

The specific objectives are listed below:

- to determine the moisture absorption properties of the two adhesives studied;
- to determine the moisture and temperature dependent mechanical properties of both adhesives studied;
- to experimentally determine the mechanical behaviour of a joint used in the railway industry;

- to develop a cohesive zone model that can help predict the mechanical behaviour of adhesive joints as a function of environmental moisture and temperature.

c. Research methodology

The following approach was used to complete the objectives of this PhD:

- A literature review on the moisture and temperature degradation of adhesive joints was done in **Paper 1**. Techniques used to model adhesive joints under moist environments were also addressed in this paper.
- The failure strength of the bulk adhesive as a function of environmental moisture and temperature was determined. The water absorption characteristics of each studied adhesive was assessed. This information is published in **Paper 2**.
- Fracture tests were performed in **Paper 3** and in **Paper 4**. In **Paper 3**, double cantilever beam specimens were immerged in distilled water salt water and the partially saturated specimens were tested regularly over a period of time. In **Paper 4**, the mode I toughness of both studied adhesives were determined as a function of environmental moisture and temperature.
- In **Paper 5**, the effect of strain rate and temperature on the strength of adhesive joints for the automotive industry is assessed. A finite element model was used to predict the mechanical behaviour of adhesive joints under quasi-static and impact conditions.
- **Paper 6** presents a study about the effect of moisture on the fracture envelop of an adhesive using the "open-faced technique". Experimental results obtained by using a special apparatus that subjects the adhesive to diverse mixed mode ratio were successfully modelled using the finite element method.
- Scaled specimens of a rail used in the railway industry to attach the seats of a train were produced and tested at low and high temperatures. Prior to testing, the specimens were exposed to distilled water and to salt water, so that the adhesive layer was partially saturated at the time the specimen was tested. A cohesive zone element that includes moisture and temperature degradation was developed and used to predict the failure load of the scaled adhesive joint. The results are shown in **Paper 7**.

d. Outline of the thesis

This PhD thesis is constituted by seven papers and a summary. The abstract of each paper is summarized below:

Paper 1 G. Viana, M. Costa, M.D. Banea, L.F.M. da Silva

Abstract of Paper 1: Despite offering very attractive advantages over traditional joining methods, one of the setbacks of adhesive bonding is its long term strength in aggressive environments, such as environments with high moisture and extreme temperatures. With the rise of new lightweight materials and their recent use in everyday vehicles, transportation industries have been very interested in determining the long term behaviour of adhesive joints. The aim is to build durable, lighter vehicles, which consume less energy and emit less pollution.

The two main factors that affect the strength of vehicle adhesive joints are exposure to moist environments and high and low temperatures. There are some works concerning the effect of these two factors separately and some predictive models have been developed, which help the engineer to design reliable, safe and efficient adhesive joints. However, the combined effect of temperature and moisture is not yet totally understood.

Paper 2 G. Viana, M. Costa, M.D. Banea, L.F.M. da Silva

Abstract of Paper 2: Structural adhesives are increasingly being used in the aerospace and automotive industries. They allow for light weight vehicles, fuel savings and reduced emissions. However, the environmental degradation of adhesive joints is a major setback in its wide implementation. Moisture degradation of adhesive joints includes plasticization, attacking of the interface, swelling of the adhesive and consequent creation of residual stresses. This may lead to reversible and irreversible damage. The main factors affecting the strength of adhesive joints under high and low temperatures are the degradation of the adhesive mechanical properties and the creation of residual stresses induced by different coefficients of thermal expansion (between the adhesive and the adherends). The effect of the combined effect of moisture and temperature is not yet fully understood. The aim of this study is to shed light on this subject.

In this work water absorption tests were conducted at different moisture conditions in order to assess the diffusion coefficient, maximum water uptake and glass transition temperature. Aged and unaged small dogbone tensile specimens were tested under different temperature

conditions. The glass transition temperature of the adhesives as a function of the water uptake was assessed. The aim is to determine the evolution of the properties of two epoxy adhesives as a function of two variables (environmental temperature and moisture).

As a consequence of water sorption, the glass transition temperature of the adhesives studied dropped significantly. This has an effect on the mechanical properties of the adhesives, especially at high temperature. At lower temperatures, although some plasticization occurs, its effect is not as significant.

Paper 3 G. Viana, M. Costa, M.D. Banea, L.F.M. da Silva

Abstract of Paper 3: Structural adhesives are increasingly being used in the aerospace and automotive industries. They allow for light weight vehicles, fuel savings and reduced emissions. However, the environmental degradation of adhesive joints is a major setback in its wide implementation. Moisture degradation of adhesive joints includes plasticization, attacking of the interface, swelling of the adhesive and consequent creation of residual stresses. This may lead to reversible and irreversible damage.

In this work double cantilever beam (DCB) specimens using two different adhesives for the automotive industry were subjected to two different ageing environments. They were tested periodically until the toughness of the adhesives stabilized, which means that they were fully degraded. An association was made between the toughness of the adhesive and the amount of water that it had absorbed. This way it was possible to indirectly measure the water uptake in an adhesive joint taking into account the water uptake properties of the adhesives studied, which had been determined in another study.

It was found that diffusion of water into the studied adhesive joints was faster than diffusion through the bulk adhesive alone. A model that takes into account diffusion through the interface between the adhesive and the adherends was proposed.

Paper 4 G. Viana, M. Costa, M.D. Banea, L.F.M. da Silva

Abstract of Paper 4: In this work, the Double Cantilever Beam (DCB) test is analysed in order to evaluate the combined effect of temperature and moisture on the mode I fracture toughness of adhesives used in the automotive industry. Very few studies focus on the combined effect of temperature and moisture on the mechanical behaviour of adhesive joints. To the authors' knowledge, the simultaneous effect of these conditions on the fracture toughness of adhesive joints has never been determined.

Specimens using two different adhesives for the automotive industry were subjected to two different ageing environments (immersion in distilled water and under 75% of relative humidity). Once they were fully degraded, they were tested at three different temperatures (-40ºC, 23ºC and 80ºC), which covers the range of temperature an adhesive for the automotive industry is required to withstand. The aim is to improve the long term mechanical behaviour prediction of adhesive joints. The DCB substrates were made of a high strength aluminium alloy to avoid plastic deformation during test. The substrates received a phosphoric acid anodisation to improve their long term adhesion to the adhesive.

Results show that even though a phosphoric acid anodization was applied to the adherends, when the aged specimens were tested at room temperature and at 80ºC, they suffered interfacial rupture. At -40ºC, however, cohesive rupture was observed and the fracture toughness of the aged specimens was higher.

Paper 5 G. Viana, J. Machado, R. Carbas, M. Costa, L.F.M. da Silva, M. Vaz, M.D. Banea

Abstract of Paper 5: In this study the impact and quasi-static mechanical behaviour of single lap joints (SLJ) using a new crash resistant epoxy adhesive has been characterized as a function of temperature. Single lap adhesive joints were tested using a drop weight impact machine (impact tests) and using an universal test machine. Induction heating and nitrogen gas cooling was used in order to achieve an homogeneous distribution of temperature along the overlap of +80ºC and -20ºC, respectively. Adherends made of mild steel, similar to the steel used in automobile construction, were chosen in order to study the yielding effect on the strength of the SLJ. Results showed that at room temperature (RT) and low temperature (LT), failure was dictated by the adherends due to the high strength of the adhesive. At high temperature (HT), a decrease was found in the maximum load and energy absorbed by the joint due to the reduced strength of the adhesive at this temperature. The results were successfully modelled using the commercially available finite element software Abaqus®. Good correlation was found between experimental and numerical results, which allows the reduction of experimental testing.

Paper 6 P. Fernandes, G. Viana, R.J.C. Carbas, M. Costa, L.F.M. da Silva, M.D. Banea

Abstract of Paper 6: This research aims at determining the fracture envelope of an adhesive as a function of the water content. The fracture toughness of an adhesive joint was determined under pure mode I, II and mixed mode I+II loadings, in three different environments: dry, aged in salt water and aged in distilled water. The fracture toughness under mode I and II were determined using Double Cantilever Beam (DCB) and End-Notched Flexure (ENF) tests, respectively. The characterization of the fracture toughness under mixed-mode was done using an apparatus capable of applying a wide range of loadings that go from pure mode I to almost pure mode II. To accelerate the diffusion process and obtain a uniform water concentration in the adhesive joint, a modified DCB specimen (ODCB specimen) was adopted. Finite Element (FE) analysis was used to determine the gradient of water concentration in both specimens and to validate the use of the modified DCB specimens, comparing the fracture toughness obtained using DCB and ODCB specimens. It was found that the toughness of the adhesive changed as a function of the ageing environment. For the salt water environment, the mechanical properties increased, while for the distilled water environment, degradation of the mechanical properties was observed.

Paper 7 G. Viana, R. Carbas, M. Costa, L. F. M. da Silva, M. D. Banea

Abstract of Paper 7: This work addresses the strength of adhesive joints used in the rail industry. The capability of structural adhesives to bond an aluminium rail used to assemble the seats inside the train is investigated. Scaled specimens of these joints were mechanically tested under a wide range of temperatures (from -40ºC to 80ºC) before and after ageing in distilled water in order to simulate real life conditions.

A three dimension numerical simulation was carried out to understand the magnitude of stresses present in the adherends and in the adhesive layer. A new developed cohesive element was used along with the finite element method to predict the behaviour of an adhesive joint after environmental degradation.

Results show that even though a phosphoric acid anodization was applied to the adherends, sopme specimens suffered interfacial rupture. A new cohesive zone element has been developed and was used to predict cohesive failure of the adhesive. The model gave accurate

results and was able to successfully predict cohesive failure of every joint that failed cohesively in the adhesive layer.

2. Adhesives tested

In this thesis, two different kinds of toughened epoxy adhesive were considered:

- SikaPower 4720, a bi-component that cures at room temperature for 24h and is supplied by Sika® Portugal (Vila Nova de Gaia)
- Nagase ChemteX XNR6852-1, a single component that cures for 3h at 150ºC and is supplied by Nagase (Osaka, Japan)

Exceptionally, the adhesive used for the single-lap joints under quasi-static and impact loads in Paper 5 was a more recent version of the adhesive supplied by Nagase ChemteX (XNR6852-1), which has improved strength under impact conditions.

Tests show that XNR6852-1 performs better than SikaPower 4720: it is stronger, more ductile, absorbs less water, has a higher Tg, is tougher and is not severely affected by moisture. SikaPower 4720 has the advantage of being a bi-component, which does not require conditioning in cold atmosphere and can cure at room temperature.

3. Test methods

In this study, to characterize the mechanical behaviour of the adhesive as a function of temperature and absorbed moisture, a triangular cohesive zone model was used. This triangle changes its shape depending on the mentioned environmental factors. To define the triangle at each temperature and moisture condition, an extensive battery of experimental tests had to be carried out [12-14].

To determine the effect of moisture on the mechanical properties of the adhesive, it is necessary to test water saturated adhesive specimens. However, to expose adhesive joints until saturation takes generally several years. Due to the difficulty in obtaining fully saturated specimens in a timely manner, two approaches were adopted:

1. Smaller specimens were employed. These specimens, due to their small width, allowed to reduce the time required to saturate the adhesive layer [9, 13, 14];
2. Open faced specimens were used [15]. Instead of exposing the adhesive layer inside the joint, a very thin adhesive plate of bulk adhesive was manufactured and exposed outside the joint. Because the exposed area of the bulk adhesive plate is much higher than the adhesive layer in a joint, saturation is reached in a matter of days. After saturation, this bulk adhesive plate is bonded to the substrates using a stronger adhesive. The stronger adhesives ensures that failure can only occur in the exposed adhesive layer.

Bulk tensile tests were performed to determine the Young's modulus and Yield stress of each studied adhesive. The mode I fracture toughness was determined using small double cantilever beam (DCB) specimens. Open-faced specimens were used to determine the effect of absorbed moisture on the fracture envelop of the adhesive. Reduced size specimens were preferred to determine mode I fracture toughness due to a set of advantages:

1. Smaller specimens can be produced easily in larger quantities;
2. They are small enough to be tested at high and low temperatures in the available test machines
3. These specimens do not need to be environmentally exposed for as long as standard specimens, as their exposed surface area is greater.

Water absorption tests were performed to determine the speed of water intake of each adhesive. The moisture dependent Tg of both adhesives was measured using a new method based on DMA [16] in order to assess the decay of the glass transition temperature with absorbed moisture. In the following subsections, the experimental methods used in this thesis is explained with more detail.

3.1 Bulk specimens

Bulk specimens were manufactured from bulk adhesive plates. As the studied adhesives are relatively stiff, machining of bulk adhesive plates was feasible and the quality of the finish product was very high. Specimens manufactured with this method include bulk water sorption specimens, Tg specimens and bulk tensile specimens. In order to manufacture the required bulk adhesive plate, a mould was used (represented in *Figure 3*).

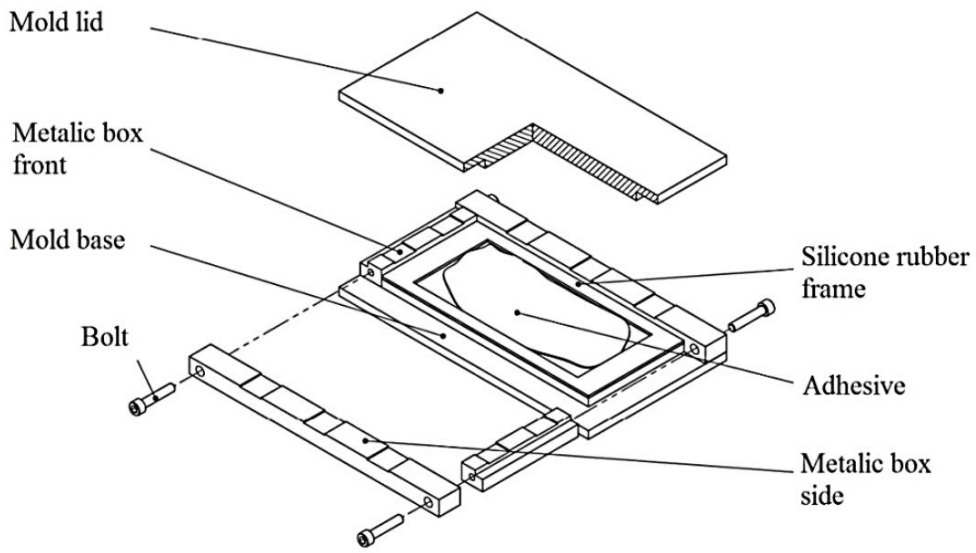

Figure 3: Exploded view of the mould used to produce bulk adhesive plates.

A silicone rubber frame was used to ensure the required thickness of the adhesive plate. After the adhesive has been applied, the mould is closed and placed in a hot plates press for the cure schedule. In the case of adhesives that cure at room temperature, the plate is left under pressure for 24h and left to cure outside the press for at least 14 days before being tested or subjected to environmental exposure.

The manufactured bulk adhesive plate must be machined with the shape of the suitable bulk adhesive specimen, in this case either Tg specimens, water absorption specimens or bulk tensile specimens, as represented in *Figure 4*.

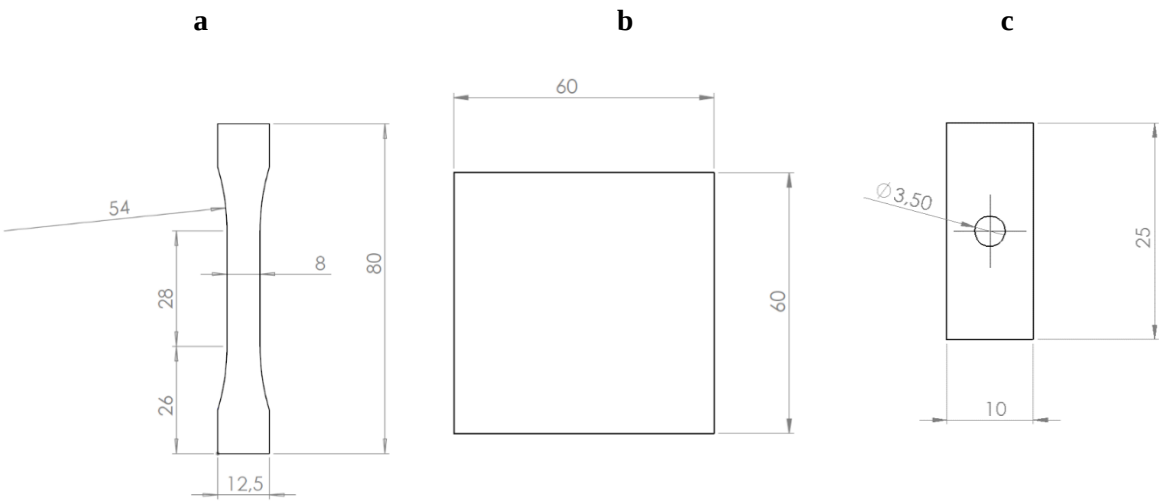

Figure 4: Types of bulk adhesive specimens used in this thesis:

a. Small bulk tensile specimens;
b. Water absorption specimens;
c. Tg specimens.

3.1.1 Water absorption

Before exposing the specimens to their aging environment, they must be kept in a dry desiccator in order to eliminate any water that may have been absorbed from the air. Then, the initial weight of each water sorption specimen is measured with a high resolution scale and exposed to the suitable environment. It is important that every face of the specimen is being exposed. The weight of each specimen must be periodically measured until saturation is attained. The results are plotted against $\sqrt{t/l^2}$. An example of such a graph is given in *Figure 5*.

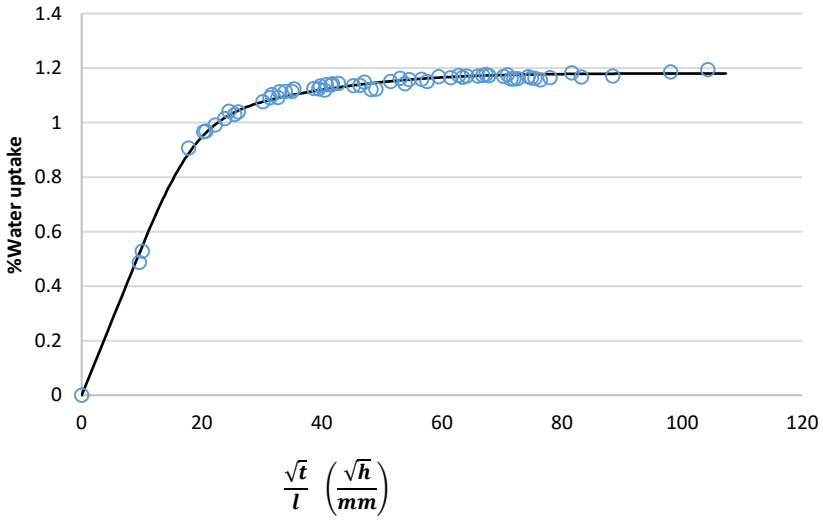

Figure 5: Example of the absorption curve of an epoxy adhesive.

In this case (one dimension absorption), the water concentration of at each point of the adhesive is given by:

$$\frac{c}{c_\infty} = 1 - \frac{4}{\pi}\sum_{n=0}^{\infty}\frac{(-1)^n}{(2n+1)}exp\left[\frac{-D(2n+1)^2\pi^2 t}{4l^2}\right] \times \cos\left[\frac{(2n+1)\pi x}{2l}\right] \quad \text{Eq.1}$$

Where c_∞ is the concentration of water in the surface layers, which is supposed to be attained instantaneously, l is half of the layer's width, t is the time. The center of the adhesive is located in $x = 0$.

Equation (2) is the integration of equation (1). Instead of giving the water concentration in each point, which is hard to obtain experimentally, it gives the fractional mass uptake of the entire specimen [26].

$$\frac{mwt_t}{mwt_\infty} = 1 - \frac{8}{\pi^2}\sum_{n=0}^{\infty}\frac{1}{(2n+1)^2}exp\left[\frac{-D(2n+1)^2\pi^2 t}{4l^2}\right] \quad \text{Eq.2}$$

mwt_∞ is the moisture level at equilibrium and mwt_t is the moisture level at instant t.

3.1.2 Tensile tests of bulk adhesive

Tensile tests of both studied adhesives were determined using tensile bulk specimens produced from bulk adhesive plates, as described in section 3.1. Tests were carried out at room temperature, -40ºC and 80ºC. This range of temperatures was achieved by using a climatic chamber coupled to a universal testing machine.

At each temperature condition, three kind of specimens were considered: dry specimens, specimens exposed to a saturated solution of NaCl and specimens exposed to distilled water. This allowed to study the effect of moisture and temperature degradation in the mechanical properties of the bulk adhesive simultaneously (see Paper 2).

3.2 Joint specimens

To manufacture high quality adhesive joints, it is necessary to prepare the surfaces to bond. The surfaces should be rough to increase the surface area and to improve mechanical interlocking between adherend and adhesive. The maximum amount of contaminants should

be removed and sometimes, depending on the application and on the materials to bond, a surface treatment should be applied.

The surface of each adherend was grit blasted and degreased with acetone prior to the application of the adhesive. A mould was used to line the adherends in place. This mould was introduced in a hot plates press to perform the suitable cure schedule according to the adhesive used.

In the case of environmentally exposed adhesive joints using aluminium adherends, to avoid corrosion of substrates and consequent loss of joint strength, the surface of the substrate received a phosphoric acid anodisation, as described in standard ASTM D3933 [17], prior to application of adhesive. This is proven to improve the wettability of the surface and its resistance to moist environments [18], This consists in immerging the surfaces to anodise in a 12% concentration phosphoric acid solution while an electric current flows between the adherends (positive pole) and solution (negative pole). The difference in electric potential between substrates and solution should be between 14 and 16 Volts.

Specific information about each kind of specimen can be found in the following sub sections.

3.2.1 Fracture tests

To design adhesive joints, the availability of reliable damage models depends on the knowledge of the fracture toughness of the adhesive. The fracture toughness varies according to the mode of loading (between modes I, II and III, as explained in *Figure 6*).

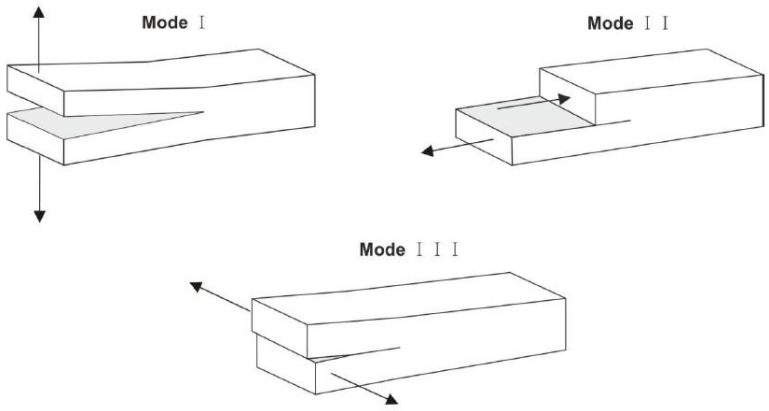

Figure 6: Modes of crack propagation.

Mixed mode loadings are also possible as, in adhesive joints, the crack is constrained by the adherends.

Water penetrates very slowly into the adhesive layer. This means that the saturation of the adhesive layer in a standard DCB specimen is attained several years after. Numerical predictions show that the small specimens used in this thesis saturate in a matter of months, which allows to obtain important information about the toughness of the adhesive in a timely manner. This technique was used in Paper 3 and Paper 4.

An alternative approach can also be taken. Instead of reducing the dimensions of the specimen, "open-faced specimens" can be used [18-20]. First a very thin plate of adhesive must be exposed. The absorption of water is very fast, as it is very thin and has a very surface area. After, the saturated plate should be bonded to the adherends using a stronger adhesive (secondary adhesive). As the exposed layer of adhesive is weaker than the secondary adhesive, the crack propagates through the adhesive that had been exposed. If the crack propagates through the secondary adhesive, the test cannot be considered valid. This technique was adopted in Paper 6.

3.2.2 Single-lap joints

Due to its simplicity and capability to provide relatively strong joints, the single lap joint is the kind of joint that is most commonly used in the industry. It is also often used to assess the performance of adhesives in real life applications.

Despite being loaded mostly in shear, peel stresses that arise especially at the ends of the overlap due to load misalignment [21] can compromise the strength of the joint. Shear stress is also not uniform: it is higher at the ends of the overlap and lower in the middle. Because the stress in this joint is not uniform, it cannot be used to determine properties of the adhesive but is a good indicator of the suitability of an adhesive for a given application [22].

Tests were made to assess the quasi-static and impact strength of single-lap joints at low, high and room temperature using XNR 6852. Details are given in Paper 5.

4. Numerical modelling

The Finite element method (FEM) has shown acceptable results in the analysis of adhesive joints, traditionally by using stress/strain criteria. These criteria are based on the analysis of stresses and strains of the structures. With the help of the FEM, it is possible to know the stress and displacement field around a certain point. However, real structures have points where the stress concentration factor tends to infinite. In these singular points, the solution provided by the FEM is highly mesh-dependent and not accurate. This kind of problem can be minimized with the use of the point stress criterion [23], in which the stresses are computed at a pre-defined distance from the singular point, and with the use of average stress criterion [23], in which an average stress is computed along a determined path.

Unlike the stress/strain based criteria, fracture mechanics based criteria have the ability to determine, taking into account the existence of singular points in the structure, when a crack may start to propagate. However, these methods are difficult to implement in adhesive joints because, although every material has its defects, their size or location is very difficult to determine.

Cohesive zone models (CZM) have the advantage of combining the stress/strain based criteria with fracture mechanics, accurately predicting the behaviour of the materials. CZM can predict the formation and propagation of cracks [23]. As soon as, in a given node, the strength of the material is reached, softening initiates. Depending on the properties of the material, several cohesive laws can be used to simulate the softening of the material. These include triangular, linear-parabolic, polynomial, exponential and trapezoidal laws. Although cohesive laws can be adjusted to better fit the behaviour of the material, the triangular CZM, due to its simplicity, is very widely used and provides good results for most real situations [24][37]. In this thesis, every simulation was carried out with the use of a triangular cohesive zone model, as described in Paper 7. The triangular cohesive law has an initial elastic behaviour. After the maximum stress is achieved, linear softening initiates. When the stress reaches the value of zero, no load can be transmitted, which is the same as saying that a crack has been created.

The elastic domain is defined by a constitutive matrix [K] containing stiffness parameters.

$$t = \begin{Bmatrix} t_n \\ t_s \end{Bmatrix} = \begin{bmatrix} K_{nn} & K_{ns} \\ K_{ns} & K_{ss} \end{bmatrix} \cdot \begin{Bmatrix} \varepsilon_n \\ \varepsilon_s \end{Bmatrix} = K_s \qquad \text{Eq.3}$$

K_{ab} are the values attributed to the stiffness matrix $[K]$. n corresponds to mopde I and s corresponds to mode II.

For thin adhesive layers, the following approximations can be used:

$$K_{nn} = E \quad \text{Eq.4}$$

$$K_{ss} = G \quad \text{Eq.5}$$

$$K_{ns} = 0 \quad \text{Eq.6}$$

For the damage initiation, the quadratic criterion was used:

$$\left\{\frac{\langle t_n \rangle}{t_n^0}\right\}^2 + \left\{\frac{t_s}{t_s^0}\right\}^2 = 1 \quad \text{Eq.7}$$

"⟨ ⟩" are the Macaulay brackets, which indicate that compressive loads do no contribute to damage initiation.

Linear or quadratic energetic criteria can be used:

Linear criterion: $$\frac{G_n}{G_n^c} + \frac{G_s}{G_s^c} = 1 \quad \text{Eq.8}$$

Quadratic criterion: $$\left(\frac{G_n}{G_n^c}\right)^2 + \left(\frac{G_s}{G_s^c}\right)^2 = 1 \quad \text{Eq.9}$$

5. Conclusion

This work focused on the development of a cohesive zone model for adhesive joints that considers environmental degradation. With this in mind, the moisture and temperature dependent mechanical properties of two adhesives were determined. In order to predict the velocity of moisture diffusion into the adhesive joint, the diffusion properties of the adhesive were measured. With this information, it was possible to attribute a distinct set of properties to each cohesive element. This results in the accurate prediction of the mechanical behaviour of adhesive joints subject to moist environments.

Bulk adhesive specimens were used to determine the Young's modulus and strength of both adhesives studied as a function of environmental moisture and temperature. Due to the difficulty in obtaining fully saturated specimens in a timely manner, alternative ways to saturate

the adhesive were used. This enabled to measure the mode I toughness of both adhesives as a function of the environmental conditions addressed in this study.

The strength of single lap adhesive joints as a function of temperature under quasi-static and impact conditions was also addressed in this study. Taking into account the determined strain rate dependent properties of adhesive and adherend, a finite element model was created to predict the strength of adhesive joints under impact loads and high and low temperatures.

The experimental information reunited allowed to create a cohesive zone element that can be used to predict the mechanical behaviour of adhesive joints under different conditions of moisture and temperature.

6. Future work

6.1 Include the effect of fatigue loads in the developed cohesive element

It would be very interesting to include the effect of fatigue loads in the developed cohesive element. The effect of environmental moisture on the fatigue behaviour of the two adhesives analysed in this thesis was studied by Costa et al. [25]. This would not be as hard as if work had be started from the very beginning, as most experimental work has already been performed.

6.2 Effect of different surface treatments and primers

In this study, failure of some adhesive joints was dictated by the interface between adhesive and adherend. This kind of failure results in a significantly lower strength of the joint that is very hard to predict. To most industries this is not acceptable. The logical way to prevent adhesive failure from happening is to improve wettability and corrosion resistance of the substrates. This can be done by choosing a more appropriate surface preparation and applying a compatible primer to the adherend surface.

6.3 Rate effects

To many transport industries and to the automotive industry in general, adhesive joints are required to withstand high impact loads. This means that the adhesive is loaded under very

high strain rates. It would be very interesting to study the behaviour of the adhesive under these conditions and include this behaviour into the developed cohesive zone model.

REFERENCES

[1] Zhou, J. M., Lucas, J. P., Polymer **40**, 5505-5512 (1999).
[2] Zhang, Y., Adams, R. D., da Silva, L. F. M., J Adhesion **90**, 327-345 (2014).
[3] Jurf, R. A., Vinson, J. R., J Mater Sci **20**, 2979-2989 (1985).
[4] Han, X., Crocombe, A. D., Anwar, S. N. R., Hu, P., Int J Adhes Adhes **55**, 1-11 (2014).
[5] Li, W. D., Ma, M., Han, X., Tang, L. P., Zhao, J. N., Gao, E. P., J Adhesion **92**, 916-937 (2016).
[6] Banea, M. D., da Silva, L. F. M., Campilho, R. D. S. G., J Adhes Sci Technol **28**, 1367-1381 (2014).
[7] Hu, P., Han, X., da Silva, L. F. M., Li, W. D., Int J Adhes Adhes **41**, 6-15 (2013).
[8] Crocombe, A. D., Int J Adhes Adhes **17**, 229-238 (1997).
[9] Sugiman, S., Crocombe, A. D., Aschroft, I. A., Int J Adhes Adhes **40**, 224-237 (2013).
[10] Sugiman, S., Crocombe, A. D., Aschroft, I. A., Engineering Fracture Mechanics **98**, 296-314 (2013).
[11] Banea, M. D., da Silva, L. F. M., Campilho, R. D. S. G., J Adhes Sci Technol **26**, 939-953 (2012).
[12] Viana, G., Costa, M., Banea, M. D., da Silva, L. F. M., The Journal of Adhesion **93**, 95-112 (2016).
[13] Viana, G., Costa, M., Banea, M. D., Silva, L. F. M. d., J Adhes Sci Technol **31**, 1824-1838 (2017).
[14] Viana, G., Costa, M., Banea, M. D., da Silva, L. F. M., Latin American Journal of Solids and Structures **14**, 188-201 (2017).
[15] Fernandes, P., Viana, G., Carbas, R., Costa, M., da Silva, L., Banea, M., Theoretical and Applied Fracture Mechanics **89**, (2017).
[16] Zhang, Y., Adams, R. D., Da Silva, L. F. M., J Adhesion **89**, 785-806 (2013).
[17] ASTM. Standard Guide for Preparation of Aluminum Surfaces for Structural Adhesives Bonding (Phosphoric Acid Anodizing). 2017. p. 5.
[18] Goglio, L., Rezaei, M., J Adhesion **89**, 769-784 (2013).
[19] Goglio, L., Rezaei, M., Rossetto, M., J Adhes Sci Technol **28**, 1382-1393 (2014).
[20] Wylde, J. W., Spelt, J. K., Int J Adhes Adhes **18**, 237-246 (1998).
[21] da Silva, L., das Neves, P., Adams, R. D., Spelt, J. K., Int J Adhes Adhes **29**, 310-330 (2009).
[22] da Silva, L. F. M., Dillard, D., Blackman, B., Adams, R. D., Testing adhesive joints - Best practices, (Wiley, Weinheim, 2012). Chapter,
[23] Advances in Numerical Modelling of Adhesive Joints, Springer Briefs in Computational Mechanics. 2012.
[24] Liljedahl, C. D. M., Crocombe, A. D., Wahab, M. A., Ashcroft, I. A., International Journal of Fracture **141**, 147-161 (2006).
[25] Costa, M., Viana, G., da Silva, L. F. M., Campilho, R. D. S. G., Materialwissenschaft und Werkstofftechnik (2016).

APPENDED PAPERS

PAPER 1

Review article

Institution of MECHANICAL ENGINEERS

Journal of MATERIALS: DESIGN AND APPLICATIONS

Proc IMechE Part L:
J Materials: Design and Applications
0(0) 1–14

DOI: 10.1177/1464420716671503
pil.sagepub.com

SAGE

A review on the temperature and moisture degradation of adhesive joints

G Viana[1], M Costa[1], MD Banea[2] and LFM da Silva[3]

Abstract

Despite offering very attractive advantages over traditional joining methods, one of the setbacks of adhesive bonding is its long-term strength in aggressive environments, such as environments with high moisture and extreme temperatures. With the rise of new lightweight materials and their recent use in everyday vehicles, transportation industries have been very interested in determining the long-term behavior of adhesive joints. The aim is to build durable, lighter vehicles, which consume less energy and emit less pollution. The two main factors that affect the strength of vehicle adhesive joints are exposure to moist environments and high and low temperatures. There are some works concerning the effect of these two factors separately and some predictive models have been developed, which help the engineer to design reliable, safe, and efficient adhesive joints. However, the combined effect of temperature and moisture is not yet totally understood. This paper presents a review on the temperature and moisture degradation of adhesive joints.

Keywords

Moisture degradation, temperature degradation, environmental degradation, numerical modeling of adhesive joints, structural adhesive joints

Date received: 7 June 2016; accepted: 6 September 2016

Introduction

Structural adhesives are increasingly being used in several industries. Adhesive joints allow for uniform stress distributions, higher fatigue resistance, and for joining dissimilar materials. The only viable way of joining fiber-reinforced plastics is with a structural adhesive.[1,2] This translates into stronger and lighter and fatigue-resistant structures. Adhesive joints are increasingly being used in civil engineering, particularly in timber structures.[3,4] Transport industries, in particular, are very interested in this kind of technology as it allows higher energy efficiencies and reduced emissions.

The automotive industry, in particular, has been investing in the development of adhesive bonding in recent years. Automotive manufacturers are interested in reducing the weight of their vehicles in order to improve their efficiency and reduce emissions. However, vehicles must be able to withstand important loads during their lifetime, probably the most demanding for the adhesive joint being impact loads, that are caused when the vehicle crashes. These stresses must be withstood under a great variety of temperatures (usually between $-40\,^{\circ}C$ and $80\,^{\circ}C$) and relative humidity, so that the safety of the passengers can be assured.

Moisture is absorbed by the adhesive in two different ways: as free water, which occupies the free spaces of the adhesive and is responsible for plasticization. Water is also absorbed as bound water, which forms single or multiple hydrogen bonds with the adhesive's polymer chain, resulting in swelling of the adhesive, plasticization and consequent decrease of strength and glass transition temperature (T_g). Usually, if the water uptake is done at low temperatures, as soon as the adhesive is dried, its mechanical properties are usually recovered. It is usually, therefore, a reversible process.

High temperatures are also responsible for degrading the adhesive properties. Sometimes for short exposure times, the adhesive joint's properties are improved due to post cure effects. However, after a certain amount of time, its properties start to decrease.[5]

[1]Instituto de Ciência e Inovação em Engenharia Mecânica e Engenharia Industrial (INEGI), Oporto, Portugal
[2]Federal Centre of Technological Education in Rio de Janeiro (CEFET), Rio de Janeiro, Brazil
[3]Departamento de Engenharia Mecânica, Faculdade de Engenharia da Universidade do Porto (FEUP), Oporto, Portugal

Corresponding author:
LFM da Silva, Departamento de Engenharia Mecânica, Faculdade de Engenharia da Universidade do Porto (FEUP), 4200-465 Oporto, Portugal.
Email: lucas@fe.up.pt

The environmental degradation of adhesive joints is still a major setback in their wide implementation. Studies have been made regarding the moisture and temperature degradation of adhesives, which include reduction of their mechanical properties, induced plasticization, and decrease of T_g. The deleterious effects are usually greater in adhesive joints due to the creation of residual stresses between the adhesive and the adherends and due to the degradation of the interface between the adhesive and the adherends, which may cause interfacial failure. In order to improve the strength of the adhesive–adherend interface, a suitable surface treatment should be used.

This paper is a review on recent developments on the effect of environmental conditions on the mechanical response of adhesive joints and on the methods used to predict their behavior. The paper is organized in the following sections: the first section handles on the temperature degradation of adhesive joints (adhesive properties, residual stresses, and its influence in the adhesive joints), followed by a review on the moisture degradation of adhesive joints. The last sections are about the combined effect of temperature and moisture of adhesive joints and about modeling techniques for aged adhesive joints.

Temperature degradation

Adhesive properties

Generally, adhesive mechanical properties show temperature dependence. At high temperatures, the yield stress and Young's modulus are usually reduced while at low temperatures, the adhesive is generally very stiff and strong.[6] The ductility has the opposite evolution: high at high temperatures and low at low temperatures. A review on low and high temperature degradation of adhesive joints was performed by Marques et al.[7]

Due to their polymeric nature, the capability of adhesives to support extreme temperatures is limited. Even high temperature adhesives show usually some degree of degradation above 200 °C. Nonetheless, there are adhesives capable of supporting relatively high temperatures, about 300 °C, such as some ceramic adhesives, or low temperatures, down to −100 °C, such as room temperature vulcanizing (RTV) silicon adhesives. However, it is not foreseeable that in the near future a single adhesive will be able to withstand this range of temperatures. In order to design an adhesive joint for being used under high or low temperatures, a suitable adhesive must be chosen. The capability of an adhesive to support low or high temperatures is closely related to its T_g. Below T_g, the adhesive is in a glassy state, it tends to be stiff, strong, and with limited ductility. On the other hand, above T_g, the adhesive is generally weak and flexible. Therefore, in order to avoid loss of adhesive strength, the adhesive should be generally used below T_g. Adhesives for high temperature use have usually high T_g while adhesives for low temperature applications have usually a low T_g.

T_g depends not only on the kind of adhesive that is used, but also on the cure cycle of the adhesive and on its thermal history,[8–10] which will consequently influence the behavior of the adhesive at high temperatures.

Banea et al.[11] determined the toughness of an epoxy adhesive for the automotive industry as a function of temperature. A significant temperature dependence was found: above T_g there is a very significant drop in mode I fracture toughness (G_{IC}) while below it is fairly constant.

Adhesives are polymeric materials and, as a result, they allow mobility of their chains, especially at high temperatures, where viscoelasticity and creep play an important role in their mechanical behavior. Creep is a time-dependent deformation that occurs below the yield stress of the adhesive.

In order to model the creep behavior of adhesives, one has to account not only for their elastic deformation, but also for their viscous deformation. It is usually done using one or more elements with a spring and a dashpot either in parallel (Maxwell's element) or in series (Kelvin–Voigh element),[12] as illustrated in Figure 1. The spring accounts for the elasticity part of the behavior and the dashpot for the viscous part.

Creep tests are generally expensive and time-consuming. Mizah et al.[13] developed a machine that

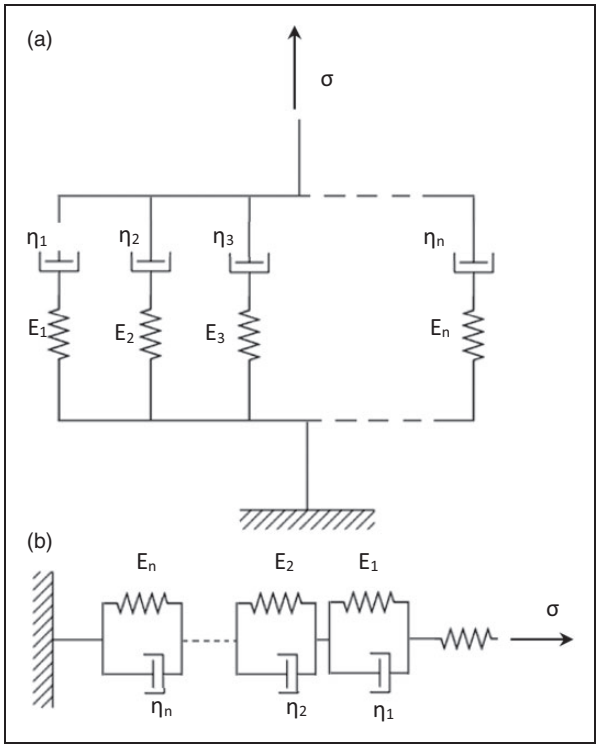

Figure 1. Maxwell's (a) and Kelvin–Voigh's (b) elements.

is able to test several specimens at the same time, thus reducing the time and cost.

Thermal stresses

Stresses induced by thermal expansion are usually not negligible in adhesive joints subjected to high and low temperatures. Adhesives and substrates have usually different coefficients of thermal expansion. As the temperature rises, the constrained materials tend to accumulate stresses that can be responsible for the reduction of the joint's strength.

If the adhesive cures at high temperature, as it cools down after cure, residual thermal stresses as well as shrinkage stresses arise and, as the molecular mobility is low at this temperature, they do not relax easily, which means that residual stresses in adhesive joints do no occur only at extreme temperatures. However, there is a temperature at which no thermal stresses exist, called the stress-free temperature (T_{SF}), which was first introduced by Hart-Smith.[14] Yu et al.[15]developed a dilatometer to measure the shrinkage of the adhesive during cure.

The magnitude of the thermal stresses depend on many factors, such as the mechanical properties of the adhesive, the geometry of the joint, the stiffness of the adherends, and the work temperature. It can be evaluated by the thermal load (ΔT)

$$\Delta T = T_0 - T_{SF} \quad (1)$$

where T_0 is the operating temperature and T_{SF} is the temperature at which cure is initiated (slightly below the actual cure temperature). Because T_{SF} is very close to the actual cure temperature, if one assumes that T_{SF} and the cure temperature are the same, no significant error is committed. This relationship is only valid as long as the adhesive operates below T_g. Above T_g, the adhesive is much more flexible and insensitive to residual stresses. When the adhesive is cooled down again, in order to compute ΔT, one should take into account T_g and not T_{SF}.[16]

In order to measure the coefficient of thermal expansion of adhesives, either the common dilatometry using strain gages or the bi-material curved beam method[17,18] can be used. This last method consists in subjecting a beam made of two different materials, usually a metal, whose coefficient of thermal expansion (CTE) is known and the adhesive whose CTE is to be measured. The beam is subjected to high or low temperatures and its deformation, which depends on the adhesive's CTE, is measured.

Although thermal stresses always arise in bonded joints subjected to wide ranges of temperature, the situation in which they are the most significant is when substrates with very dissimilar CTE are bonded. Usually, fiber-reinforced polymers have a very low CTE in the longitudinal direction (CTE = -0.5E-6 °C^{-1}). When bonding these materials with metals, particularly with aluminium (CTE = 24E-6 °C^{-1}) using stiff adhesives, such as epoxies, usually very significant thermal stresses arise.

Humfeld and Dillard[19] studied the behavior of adhesive joints after subjecting them to temperature cycles. When loading an adhesive joint at high temperature, as a result of the viscoelasticity of the adhesive, thermal stresses tend to relax quickly. However, when the joint is cooled down to ambient temperature, the residual stresses come back. At this lower temperature, there is no significant mobility of the polymer's chains and the stresses are locked in. With each cycle, the stresses tend to increase, leading to cracking of the adhesive and ultimately to the failure of the adhesive joint.

Adhesive joints at low and high temperatures and optimization

Real adhesive joints will be subject not only to quasi-static loads, but also to impact loads, especially in the automotive industry, where impact loads must be taken into account in order to ensure the crashworthiness of a vehicle. With this in mind, Avendaño et al.[20,21] assessed the impact and quasi-static behavior of single-lap joints for the automotive industry as a function of temperature (from -30 °C to 80 °C). They used both an acrylic adhesive and a crash-resistant epoxy adhesive and carbon fiber reinforced polymer and biopolymer adherends. This material has been used in order to design innovative inner car structures for being more environmentally friendly than other materials. The higher the temperature, the higher the ductility of the materials and, therefore, the higher its strain rate dependence, which causes the failure loads at impact to much higher than failure loads under quasi-static conditions.

As described in the previous section, T_g of the adhesive is one of the factors to take into account when designing an adhesive joint, especially if the joint is going to be subjected to high or low temperatures, as demonstrated by Banea et al.,[6] who studied the mechanical behavior of single-lap joints under low and high temperatures (-40 °C to 80 °C) using a polyurethane and an epoxy adhesive. The strength of the epoxy adhesive joints was maximum at room temperature and decreased by 10% and 32% at -40 °C and 80 °C, respectively. At 80 °C, the reason is the loss of adhesive strength while at -40 °C it is due to the loss of ductility. The specimens tested at room temperature have the best compromise between strength and ductility of the adhesive. The strength of the joints using the polyurethane adhesive increased as the temperature decreased. This was because the T_g of this adhesive was very low (-60 °C).

On the other hand, thermal stresses may also play a very important role in the strength of adhesive joints, especially if the cure temperature of the adhesive is very high, as reported by Banea et al.,[22] who have

determined the strength of aluminium single-lap joints under a wide range of temperatures, from room temperature up to 200 °C. The adhesive chosen was a high temperature, high strength epoxy adhesive, whose T_g is 155 °C. At room temperature, the joint strength was lower than expected due to the residual stresses created by a high cure temperature. The strength of the joint grew with temperature until T_g. Above T_g, the joint's strength dropped very quickly due to the loss of adhesive strength.

Hu et al.[23] and Li et al.[5] studied the temperature degradation of unbalanced single-lap and T-joints respectively for the automotive industry using mild steel and an aluminum alloy. They subjected the adhesive joints to thermal cycles between −30 °C[23] or −40 °C[5] and 80 °C. With the increase in temperature, the strength of both kinds of joint decreased quickly at the beginning of the exposure and slower at the end.

It is known that adhesive joints often exhibit peak loads along the overlap length, which may compromise their load-carrying capability. In order to solve this problem, and obtain a more uniform load distribution and superior joint strength, Hart-Smith[14] proposed the use of mixed adhesive joints. In this joint, instead of applying only a very stiff and resistant adhesive along the entire overlap length, two adhesives are used: a stiff adhesive at the middle of the overlap and a flexible adhesive at the ends, where stress concentration exists.

Instead of applying this technique only at room temperature, da Silva and Adams[24,25] widened their application for low and high temperature use. The flexible adhesive at the ends of a double-lap joint is now a low temperature adhesive and the stiff adhesive that is supposed to be applied in the middle is substituted by a high temperature adhesive. Using carbon fiber reinforced polymer and titanium-bonded double-lap joints, they have experimentally proven that the mixed adhesive joint is a real improvement over joints with only a high temperature adhesive or only a low temperature adhesive. Later, Marques et al.[7,26] applied the same concept in a joint representative of an aerospace heatshield using a room temperature vulcanizing silicon (RTV) and a strong and stiff epoxy adhesive to bond a cordierite heat shield to an aluminum substrate.

The natural evolution of the mixed adhesive joint is a joint with a functionally graded adhesive, a joint whose adhesive properties vary continuously along the overlap length. This was proposed by Carbas et al.,[3,27] who invented an apparatus to produce single-lap joints using differential cure temperature. The temperature of cure was set to provide the maximum stiffness at the middle of the overlap and minimum at the ends, so that the stress distribution along the overlap length was as uniform as possible. Kawasaki et al.[28] obtained mixed adhesive joints by mixing two acrylic adhesives with different ratios along the overlap length.

Moisture degradation

Water absorption

Bulk adhesive. Adhesives, like all polymers, due to their high level of molecular mobility are permeable to all gases and liquids. This includes water that is present in the environment, to which adhesive joints are exposed, for example in the automotive industry. Water only diffuses through the amorphous phase of the polymer, as the crystalline phase is too tightly packed to allow the penetration of other molecules.

In order to model the diffusion in an adhesive, several models have been proposed. The most simple and common are the Fickian laws of diffusion.[29] Although being more suitable for modeling the water diffusion in adhesives above their glass transition temperature, the Fickian laws of diffusion are also able to describe the water uptake behavior of most of the adhesives in their glassy state.

Fick's first law states that the flux in the x-direction (F) is proportional to the gradient of chemical potential. In order to simplify, as we are only studying one material (the adhesive), it is possible to substitute the gradient of chemical potential by the concentration gradient ($\mathrm{d}c/\mathrm{d}x$). The proportionality constant is the diffusion coefficient (D).

$$F = -D\,{}^{\mathrm{d}c}/_{\mathrm{d}x} \tag{2}$$

Fick's second law states that the build-up or decay of diffusant is the sum of the fluxes across the six faces of a cube (if Cartesian coordinates are used).

$${}^{\mathrm{d}c}/_{\mathrm{d}t} = D\left({}^{\delta^2 c}/_{\delta x^2} + {}^{\delta^2 c}/_{\delta y^2} + {}^{\delta^2 c}/_{\delta z^2}\right) \tag{3}$$

where t is the time.

If a long adhesive layer, which is wide and narrow, or a plate of bulk adhesive in which the thickness ($2L$) is very small when compared to the remaining directions are considered, one can assume that the flow of diffusant is one-directional. In that case, the concentration of diffusant as a function of the distance to the center of the adhesive is given by the following equation

$${}^{C}/_{C_1} = 1 - \left({}^{4}/_{\pi}\right)\sum_{n=0}^{\infty}\left[{}^{(-1)^n}/_{(2n+1)}\right] \exp\left[{}^{-D(2n+1)^2\pi t}/_{4L^2}\right]\cos\left[{}^{(2n+1)\pi x}/_{2L}\right] \tag{4}$$

C_1 is the concentration of the diffusant at the border of the adhesive, which is in theory attained instantaneously.

The solution to equation (4) gives the mass absorbed (M_t) at instant t

$${}^{M_t}/_{M_e} = 1 - \sum_{n=0}^{\infty}\frac{8\,\exp\left({}^{-D(2n+1)^2\pi t}/_{l^2}\right)}{(2n+1)^2\pi^2} \tag{5}$$

This means that the parameters needed to characterize Fickian sorption are the diffusion coefficient and the equilibrium moisture uptake.

The phenomenon of diffusion shares mathematics with the phenomenon of heat conduction and it is possible to model the moisture uptake of the adhesive simply as a heat conduction problem. The equivalent parameters to permeability coefficient, diffusion coefficient, and solubility coefficient are thermal conductivity, thermal diffusivity, and heat capacity, respectively.

The water uptake behavior of structural adhesives depends greatly on the environmental conditions. Generally, the equilibrium mass uptake increases with the environmental moisture.[30–34] Some authors[30,35] have measured the equilibrium moisture uptake of epoxy adhesives and have found that it remains constant with environmental temperature while other authors[33,36–38] have obtained significant differences on the equilibrium moisture uptake when subjecting the adhesive to warmer environments.

The water uptake behavior of structural adhesives is also affected by the stress state. Real adhesive joints in their real application must be able to sustain significant loads while subjected to moist environments. Liljedahl et al.[39] determined the water uptake of stressed bulk adhesive specimens and found a significant increase on the diffusion coefficient and on the amount of absorbed water, which has also an impact on the mechanical properties of the adhesive.

Fickian sorption is the most common type of sorption in adhesives.[40] It happens when diffusion is much slower than relaxation and the water uptake is directly proportional to the square root of exposure time ($n = 0.5$). When the opposite happens, one is in the presence of case II diffusion. In this case, a fully saturated and swollen front advances against the unpenetrated polymer and the water uptake is proportional to the exposure time ($n = 1$).

$$\frac{mwt_t}{mwt_\infty} = kt^n \tag{6}$$

Although the single Fickian sorption is the most common type of water sorption in adhesives, other types of behavior also exist, in which n is between 0.5 and 1. These behaviors are named "anomalous". These anomalous behaviors are often described using a dual Fickian model. This consists in assuming that the diffusion is Fickian but occurs through two different mechanisms simultaneously and, therefore, in order to describe the sorption behavior, two different diffusion coefficients and water uptakes are necessary. Other types of Fickian-like behavior include the sequential dual Fickian[31] and delayed dual Fickian.[41]

Adhesive may have single Fickian behavior under certain conditions, and anomalous behavior under other set of conditions.[38] Usually non-Fickian behavior is promoted by higher temperatures and higher relative humidity.[32]

Dual Fickian behavior may also be enhanced by smaller adhesive thickness.[32,42] The first stage apparently corresponds to water occupying the free spaces of the adhesive, which happens very quickly in thin specimens. Afterwards, only bound water (water that strongly couples with some hydrophilic functional groups in the polymer) is absorbed, which happens in a slower manner, leading to the second stage.[32]

In some adhesives, at high temperatures, close to the adhesive's T_g, mass loss may occur due to chemical modification and physical damage of the adhesive.[38]

There is also evidence that while a bulk adhesive may have a Fickian diffusion behavior, the same adhesive in a joint may present a case II diffusion behavior.[43] When in a joint, the adhesive is constrained by the substrates and when water is absorbed, residual stresses are created, which leads to stress-enhanced diffusion that may promote case II diffusion.

Frequently, if the saturated adhesive is subjected to a very dry environment, it loses all the water that was absorbed. However, due to crazes and cracks that are created or enlarged during ageing, the speed of diffusion sometimes increases.[42]

The Langmuir model introduces the notion of "free water" and "bound water".[44] Free water is the water that, when absorbed, stays in the small crazes and voids of the adhesive. This kind of absorbed water is responsible for the change in mechanical properties of the adhesive, swelling and change in T_g.[45]

In this model, it is assumed that free water molecules can become bound molecules and vice-versa. The probability per unit time of a free water molecule to become a bound water molecule is γ and the probability per unit time of a bound molecule to become a free molecule is β. This way, when saturation is attained, the adhesive is in a state of dynamic equilibrium, in which

$$\gamma n_\infty = \beta N_\infty \tag{7}$$

n_∞ and N_∞ are the number of free and bound water molecules per unit volume at equilibrium, respectively. In the one-dimensional case, the molecular number densities at position z satisfy the following equations

$$D\frac{\partial^2 n}{\partial z^2} = \frac{\partial n}{\partial t} + \frac{\partial N}{\partial t} \tag{8}$$

$$\frac{\partial N}{\partial t} = \gamma n - \beta N \tag{9}$$

For an infinite plate immersed in water, whose thickness (e) is equal to 2δ and $z = 0$ is the central plane, the upper and lower surfaces are defined by $z = \delta$ and $z = -\delta$, respectively.

The initial boundary conditions are given by

$$n(z,\mathbf{0}) = N(z,\mathbf{0}) = \mathbf{0}, \text{ for } |z| < \delta$$

$$n(\delta,t) = n_\infty \text{ and } n(-\delta,t) = n_\infty \text{ for all } t$$

$$\begin{aligned} n(z,t) = n_\infty \Bigg[1 - \frac{1}{4}\sum_{n=0}^{\infty} \frac{(-1)^n}{(2n+1)(r^+_{2n+1} - r^-_{2n+1})} \\ \times \left(r^+_{2n+1} e^{-r^-_{2n+1}} - r^-_{2n+1} e^{-r^+_{2n+1}} \right) \\ \times \cos\left(\frac{\pi(2n+1)z}{2\delta} \right) \Bigg] \\ + n_\infty \frac{4}{\pi\beta} \sum_{n=0}^{\infty} \frac{(-1)^n}{(2n+1)(r^+_{2n+1} - r^-_{2n+1})} \\ \times \left(r^+_{2n+1}\, r^-_{2n+1} \right) \left[e^{-r^-_{2n+1}} - e^{-r^+_{2n+1}} \right] \\ \times \cos\left(\frac{\pi(2n+1)z}{2\delta} \right) \end{aligned} \tag{10}$$

where

$$\begin{aligned} r^\pm_{2n+1} = \frac{1}{2}\left(k(2n+1)^2 + \gamma + \beta \right) \\ \pm \sqrt{\left(k(2n+1)^2 + \gamma + \beta \right)^2 - 4k\beta(2n+1)^2} \end{aligned} \tag{11}$$

And

$$k = \frac{\pi^2 D}{4\delta^2} \tag{12}$$

The Langmuir model has proven to be able to successfully model adhesives that do not follow Fick's laws.[44,46,47]

Adhesive–adherend interface. Water can also penetrate in the adhesive layer through the interface between adhesive and adherend. In fact, some studies suggest that water can be absorbed by the interface much faster than by the bulk adhesive.[48,49] Water penetrates in the interface through the process of adsorption. This is the process by which molecules of a substance, in this case H_2O, collect on the surface of another substance (the substrates). The molecules are attracted to the surface but do not enter into the solid's interior, as in absorption.

Gravimetric methods are usually used in order to measure the water uptake of an adhesive.[50] This consists simply in subjecting a plate of bulk adhesive to an aging environment, such as distilled water, air with a particular relative humidity, or other environments compatible with what the adhesive will be subjected in its service life, such as toluene,[35] and measuring the weight change over time with a precision scale. In order to simulate an environment with a particular relative humidity, a saturated salt solution can be used. Different kinds of salt can be used depending on the relative humidity that is required.[51] This method is, however, very difficult to use in an adhesive joint, which usually uses a very low amount of adhesive, whose weight change cannot be measured with common precision scales. In order to overcome this difficulty and determine the average water uptake or the moisture profile in an adhesive joint, other techniques have been used. Among these techniques is the Fourier transform infrared spectroscopy, transmission spectroscopy,[49] and nuclear reaction analysis.[43]

Zanni-Deffarges and Shanahan[48] have tested torsional joints and bulk tensile and compressive specimens after aging them for different amounts of time. The modulus of both the bulk specimens and the torsional joints were monitored as a function of the aging time. Taking the evolution of the Young's modulus as a function of the aging time into account, approximations to the diffusion coefficients of the joints and the bulk specimens were computed and it was found that the diffusion coefficient of the joints was much higher than the bulk specimens'. Viana et al.[52] have taken a similar approach. They aged adhesively bonded double cantilever beam specimens and tested them periodically. Based on the obtained G_{IC} as a function of the aging time, the moisture uptake of the joint was inferred. With this data, a model was made that was used to compute the diffusion coefficient of the interface between the adhesive and the adherends.

Kinloch et al.[53] concluded that relatively viscous adhesives may have difficulty penetrating in the pores and gaps of substrates, which may lead to premature rupture of adhesive joints, which are subjected to moist environments, either due to the hydration of the uppermost regions of the oxide layer or due to weakening of the adhesive–adherend interface. If a low viscosity primer is applied prior to bonding on a phosphoric acid anodized surface, the results are much improved because the primer will fill in the gaps which would be otherwise filled with water and would cause hydration of the upper layers of oxide.

Bulk properties of the adhesive

Swelling. Swelling is the volumetric change of an adhesive due to its absorbed moisture alone.

Water may be absorbed by the adhesive in two main ways:

1. As free water, occupying the free spaces of the adhesive, which does not cause any change in the volume of the adhesive;
2. As bound water, making hydrogen bonds with the adhesive's molecular chain. As water is a polar molecule, it can form molecular bonds with the hydroxyl groups, normally present in adhesives,[46,54] increasing the intersegmental hydrogen bond and, as a consequence, the volume of the adhesive.

As free water only occupies the free spaces of the adhesive and is very quickly absorbed, only the bound water is responsible for swelling. This means that the volumetric change in the adhesive is not proportional to the change in its mass. The adhesive will become denser as water is absorbed.[54] This way, one can speak about "efficiency of swelling".

Figure 2 shows the ratio of change in specimen volume as a function of the net volume of absorbed water normalized by the volume of dry adhesive (V_0). The bold line in the middle, which has the slope of 1, represents the swelling of the adhesive that would be expected if the entire volume of absorbed water contributed to the change of volume of the adhesive.

Initially, in region I, water starts to occupy the free volumes of the adhesive (which does not cause any swelling) as well as making hydrogen bonds with the resin (which causes swelling).[46,54] After this stage, in region II, the process of interchain hydrogen bond dominates, as virtually all the micro cavities of the adhesive are full with free water. The absorption of water is made almost entirely by making hydrogen bonds with the adhesive.[46,54] Adamson[54] postulated that there is still a third stage, when water enters the densely crosslinked structures, which contain some free volume but do not swell as much, resulting in a lower swelling efficiency.

Swelling of the adhesive is responsible for the creation of residual stresses in the adhesive layer, which may enhance water diffusion in an adhesive joint.[30,43]

Some authors state that strains induced by swelling are larger than strains induced by the coefficient of thermal expansion mismatch.[39] However, if these strains are taken into account when predicting the mechanical behavior of the joint, its strength is underestimated. This is because the absorbed water tends to enhance the creep behavior of the adhesive, which is responsible for reducing significantly residual stresses in the adhesive joint.[39]

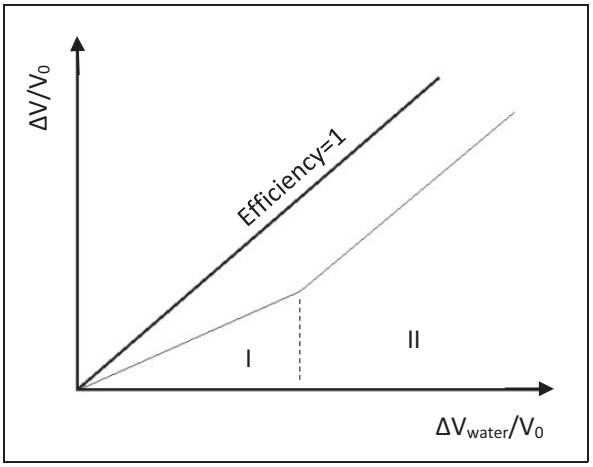

Figure 2. Schematic representation of the swelling curve of an adhesive.

Glass transition temperature. Absorbed moisture influences the mobility of the adhesive polymer. This has an impact both on the glass transition temperature and on the mechanical properties of the adhesive. However, the impact may be more or less significant depending on the kind of adhesive. The T_g of a glassy, very crosslinked polymer is higher than that of a more ductile amorphous polymer.

In order to measure the variation of T_g of an adhesive before and after aging, usually the dynamic mechanical analysis technique is used. However, this technique requires the adhesive to be kept at relatively high temperature for a considerable amount of time. This may change the results because the adhesive may suffer post cure and change its T_g while the test is being made. Also, water that the adhesive may have absorbed will evaporate, at least partially, and the right T_g value will not be read. Adams et al.[55] have developed a technique based on the DMA with which it is possible to determine T_g of an adhesive very quickly, avoiding significant post cure of the adhesive and reducing the amount of water that may evaporate. This technique has been used successfully by Viana et al.[56] and by Zhang et al.[35] to measure T_g of moisture degraded adhesives.

This method consists in keeping a vibrating beam with a bolted adhesive plate in its center at resonance. This adhesive plate introduces damping in the specimen. The beam is supported by two thin stretched twines along the direction perpendicular to Figure 3, at each side of the vibrating beam. The temperature of the specimen is then raised and the amplitude of the vibration is recorded. It is known that, at T_g, the adhesive presents its maximum damping.[55] From the theory of forced vibration, the damping is proportional to the inverse of the amplitude. In order words, T_g is the temperature at which the amplitude of the specimen is at its minimum. A schematic representation of the test setup is shown in Figure 3.

In this method, it is very important always to keep the beam at resonance frequency, which changes throughout the test. With this in mind, the frequency of the power supply that feeds the driving coil is controlled by a feedback system that takes into account the frequency read by the pickup coil.

As water penetrates into the epoxy adhesive, some molecules form single hydrogen bonds mainly hydroxyl or amine.[54,57] This bound water acts as a plasticizer and is responsible for the decrease in T_g (type I bound water).[45] However, in some cases water absorption can slightly increase T_g.[45] This is due to the creation of secondary cross linking between the main polymer chain and water molecules. This kind of bound water (type II bound water) poses a higher activation energy than type I bound water, which makes it more difficult to remove. The amount of type II bound water depends strongly on the temperature and time of exposure.

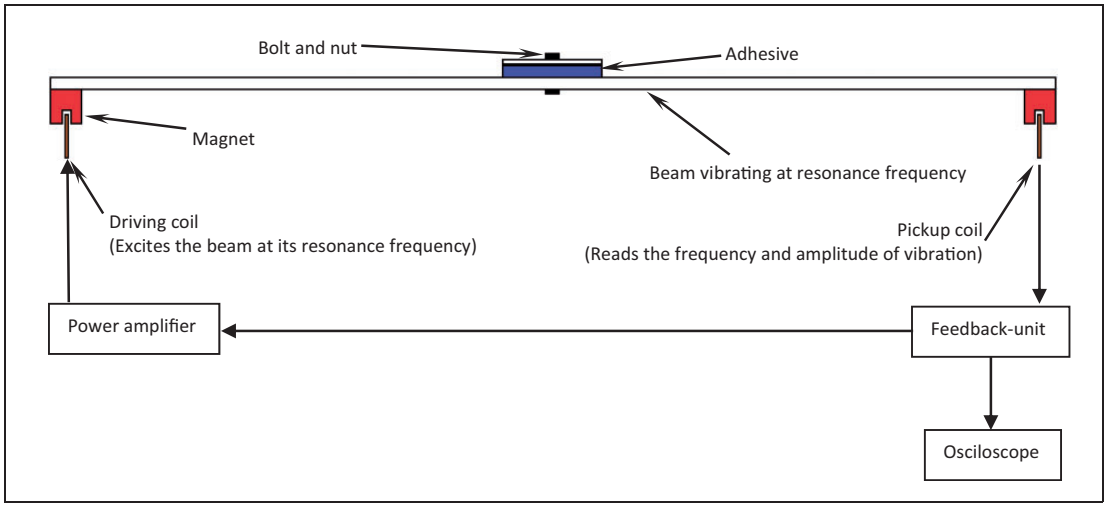

Figure 3. Schematic representation of the principle of operation of the DMA type test developed by Adams et al.[55]

Viana et al.[56] studied the evolution of T_g of two epoxy adhesives for the automotive industry. They found high T_g under dry conditions; however, when the adhesives were degraded in a distilled water environment at 32.5 °C the evolution of their T_g showed very distinct evolutions: in one case it dropped by a small amount of 15 °C from 117 °C to 104 °C while T_g decrease of another adhesive was from 97 °C to 11 °C, which has very significant implications in its strength even at room temperature.

The degradation of T_g of epoxy adhesives with water and toluene absorption was addressed by Zhang et al.[35] Because toluene is an organic molecule containing benzene rings, just like the epoxy, its uptake was about 30 times greater than the water uptake. This translates into a lower T_g for the specimens that were aged in a toluene environment. After aging and drying, the adhesives recovered their T_g almost entirely.

Mechanical properties. Absorbed water is responsible for changing the mechanical properties of adhesives.[58] Water causes a reduction on the yield stress and stiffness of adhesives[56,59,60] and also influences its fatigue behavior.[61,62]

The tensile modulus and tensile strength degrade roughly in a linear way as a function of the absorbed moisture.[39,59,63] Sugiman et al.[59] obtained higher tensile stress degradation ($\approx$39%) than the tensile modulus degradation ($\approx$27%). Lin and Chen[42] found them to degrade roughly by the same relative amount (about 29%). Barbosa et al.[64] and Lin and Chen,[42] who have also studied the moisture sorption–desorption–resorption characteristics of an epoxy adhesive, found that although the strength and tensile modulus of a moisture degraded epoxy adhesive recovered after drying, they did not reach the original value, meaning that moisture degradation of adhesives may not be fully reversible.

Viana et al.[56] proved that if T_g of an adhesive falls below room temperature after moisture absorption, the mechanical properties of the adhesive suffer serious degradation, including a drastic reduction of tensile strength, modulus, and strain to failure.

Liljedahl et al.[39] found that the stress relaxation of dry adhesives was negligible (with initial stresses of 6 and 10 MPa), while the relaxation of wet adhesives was very rapid, which is a consequence of adhesive plasticization.[65]

Moisture degradation of adhesive joints

Moisture degradation techniques. Moisture degradation of adhesive joints includes not only the degradation of the adhesive layer, but also the degradation of the adherends and the adherend–adhesive interface. In order to assess the degradation and its effect on the mechanical behavior of the adhesive joint, one would simply leave the joint in the aging environment for a certain amount of time and test them when it reaches total saturation or when it has absorbed a sufficient amount of water. However, if only diffusion through the bulk adhesive is considered, most adhesive joints take very long to saturate. In order to accelerate the degradation of adhesive joints, it is tempting to increase the temperature. However, this technique is admonished by Meiser et al.[66] Two other techniques can be used:

1. Open-faced specimens: This technique consists of producing the specimens in two steps. The first adhesive layer is applied on the face of one of the adherends. Then the adhesive is subjected to its aging environment and when the adhesive layer is saturated, a second layer of adhesive is applied and the second substrate is bonded. The second layer of adhesive can be of the same adhesive that is being tested or other, stronger, adhesive.

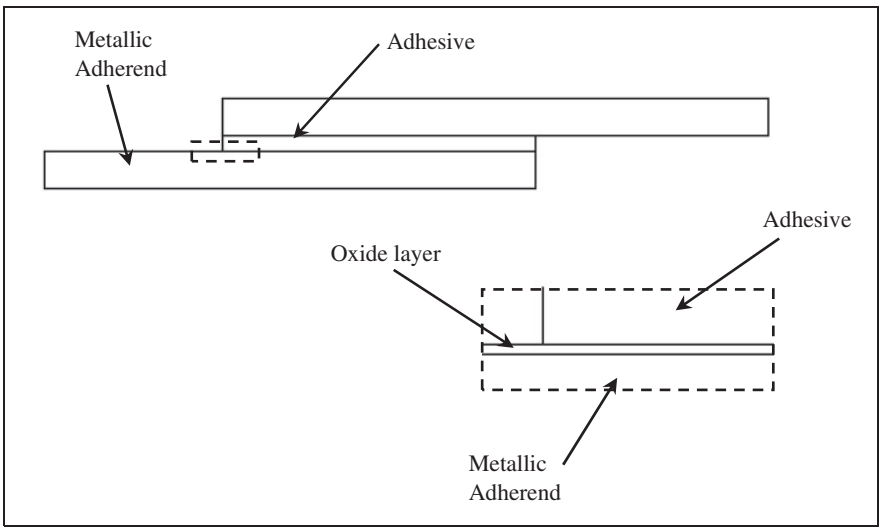

Figure 4. Schematic representation of the adhesive–adherend interface of the metal-bonded substrates.

The most important thing is that failure occurs in the primary adhesive. With this technique, water is allowed to diffuse through the thickness direction of the adhesive (usually shorter than 1 mm) instead of diffusing through its width, which would take much longer. Another advantage is that the moisture uptake is uniform in the entire adhesive layer.

Goglio et al.[67] found that the strength of unaged open-faced single-lap joints was reduced by about 10% when compared to the strength of closed specimens.

2. Specimens with reduced thickness: Some authors have used specimens with smaller width in order to allow for a faster saturation. Viana et al.[56] used reduced DCB specimens while Sugiman et al.[59] and Han et al.[68] used reduced single-lap joint specimens. Costa et al.[69] studied the effect of size reduction of these specimens. Campilho et al.[70] studied the effect of reducing the height of DCB substrates.

Moisture degradation of adhesive joints is not only controlled by the degradation of the adhesive layer. If the substrates are made of moisture-sensitive materials, such as reinforced polymers, the absorbed moisture will deteriorate their mechanical behavior.[30] In case metallic adherends are used, moisture may degrade the adhesive–adherend interface. In order to eliminate or diminish this damage, a suitable surface pretreatment should be used.[71]

The effect of surface treatments. The role of the interface in the failure mechanism of metallic adhesive joints is also very important. Most engineering metals are covered with a thin layer of oxide that is also prone to degradation and that must be also taken into account.[53,71,72]

In order to strengthen the oxide layer and the adhesive–adherend interface, it is common to treat the surface of the substrates, by either anodizing them or applying a primer, etching, roughening, degreasing, etc. A review of surface pretreatments for aluminum alloys was made by Critchlow and Brewis[71] (Figure 4)

Kinloch et al.[53] studied the effect of surface pretreatments (phosphoric acid anodization (PAA), phosphoric acid anodization followed by application of a low viscosity primer (PAAP), and grit blasting followed by degreasing (GBD)) on the fatigue resistance of aluminum-bonded joints. They concluded that the primer-coated phosphoric acid anodized substrates yielded the best results despite having obtained adhesive failure between the adhesive and the primer. According to the authors, GBD joints allowed a high degree of stress concentration due to poor wetting of the surface and due to the presence of microvoids at the interface. The PAA joints performed slightly better; however, the adhesive was apparently not able to penetrate the porous surface of the anodized substrate, leading to a slight hydration of the uppermost regions of the oxide layer. The best results were obtained with the PAAP joints, as the low viscosity primer was able to penetrate the porous structure, preventing its hydration.

Goglio and Rezaei[72] studied the strength degradation of open-faced single-lap joints as a function of aging time using different surface treatments. Among the pretreatments that were tested, phosphoric acid anodization yielded the best results and was enough to allow a mostly cohesive failure of the adhesive layer.

Mubashar et al.[41] used a surface treatment named ACDC anodizing, which developed an oxide layer with a needle-like structure. This structure was also responsible for the mechanical interlocking, which promotes adhesion between the adhesive and the adherends.

Other studies regarding the moisture degradation of adhesive joints show that primer-coated anodized substrates allow for cohesive failure of the adhesive.[41,59,73]

Generally, phosphoric acid anodized and primer-coated adherends perform better under moist environments. However, other surface treatments such as phosphoric acid anodization alone or ACDC anodization might be enough to avoid interfacial fracture of the joint.

Mechanical behavior of moisture degraded adhesive joints. Adhesive joints made with composite adherends are especially prone to moisture degradation. Composite adherends are typically made of fibers (e.g. carbon fibers or glass fibers) bonded with a polymer matrix. The moisture absorbed by the fibers is generally negligible and only the matrix absorbs a significant amount of water. This means that only the matrix loses its mechanical properties[37,74] and swells, which in turn creates residual stresses between the fibers and the matrix. Additionally, absorbed water is responsible for loss of adhesion between the matrix and the fibers.[75] These three effects are responsible for the loss of adherend properties.

It is not only water that is absorbed after adhesive cure that influences the mechanical behavior of the adhesive joint. Water present on the adherend surface when the adhesive is applied has also a very significant impact on joint properties.[76]

Sugiman et al.[59] studied the mechanical behavior of aged and unaged aluminum monolithic single-lap adhesive joints and laminated doublers loaded in bending. Specimens were tested right after the adhesive reached saturation (1 year of aging) and 1 year after reaching saturation (2 years of aging) in a 50 °C distilled water environment. All specimens failed cohesively at the adhesive and the adherends did not suffer plastic deformation. The single-lap joints lost roughly the same strength after 1 year and 2 years of aging, 22.1% and 24.4% respectively, which means that the properties of the adhesive were moisture dependent only and did not change with time. The laminated doublers loaded in bending, on the other hand, lost 14.1% and 20.3% after 1 year and 2 years, respectively. This is because these joints were not saturated even after 2 years of aging.

Mubashar et al.[41] studied the sorption–desorption effect on ACDC anodized and primer-coated aluminum single-lap joints. Two different kinds of aluminum alloy were used: a thermally treated alloy and a nontreated alloy, so that in one case the substrates would deform plastically and in the other would not. Joints were aged in 50 °C water and were tested regularly up to 182 days. Specimens failed mostly in a cohesive way, either in the primer layer or in the adhesive layer. The fractional area of primer fracture was monitored and increased from 0% to 34% in the soft aluminum joints and from 19% to 41% in the hard aluminum joints. The strength of the high strength aluminum joints decreased from 12 kN to 9.5 kN, while in the soft aluminum joints the decrease was from 8.8 kN to 7.8 kN. After aging, the specimens were dried and the strength of the joints made with hard aluminum was recovered. However, the strength of the joints made with soft aluminum was not fully recovered.

The strength evolution of adhesively bonded and single-lap joints under a salt spray environment was assessed by Li et al.[77] The strength reduced as a function of the aging time until it gradually stabilized. After this stabilization, no further degradation of the joint occurred.

Real adhesive joints will be subjected to creep loads and moisture throughout their life. It is known that the moisture uptake of adhesives is stress dependent and greater the absorption of water by an adhesive, the more affected its mechanical properties will be. The work of Han et al.[68] focused on this subject. A fully coupled moisture displacement that was able to predict the strength of single-lap joints was developed based on the moisture and creep displacement obtained with degraded bulk adhesive specimens.

Combined temperature and moisture degradation

Both the adhesive absorbed moisture and the difference in the coefficients of thermal expansion between the adhesive and the adherends may introduce residual stresses in the adhesive joint. However, the swelling of the adhesive can also be responsible for decreasing the thermal stresses originated after curing the adhesive at high temperatures, as was experimentally proven by Loh et al.[32]

Despite the separate effect of temperature and moisture on the mechanical behavior of adhesive joints being relatively well known, its combined effect is not yet very well studied and very few authors have addressed this subject. One of the earliest studies regarding this subject was performed by Jurf and Vinson[78] and addressed the evolution of T_g and the static response of single-lap adhesive joints shortly after being cured and after being aged under a 63% RH and 95% RH environments. The experimental mechanical tests were performed between room temperature and a temperature above the T_g of each adhesive. It was concluded that aging the specimens has the same effect as raising the environmental temperature or equivalently lowering T_g.

Viana et al.[56] studied the evolution of T_g with absorbed moisture and the mechanical behavior of moisture degraded bulk tensile adhesive specimens with low and high temperatures. It was concluded that as water is absorbed by the adhesive, its tensile behavior is degraded. This phenomenon is especially significant at higher temperatures due to the plasticizing effect of moisture in the adhesive, which is

responsible for lowering its T_g, which caused the degraded adhesive specimens to be closer to T_g than the dry adhesive specimens. At lower temperatures, the effect of moisture in the mechanical properties of the adhesive was not as significant because the adhesives were already well below T_g.

Numerical modeling of degraded adhesive joints

When modeling the mechanical behavior of an aged adhesive joint, one must pay attention to the degraded properties of the adhesive if the failure is cohesive in the adhesive[59,60,73,79,80] or, pay attention to the degraded properties of the interface[30,34,39,80] if interfacial failure occurs. Adhesives generally become more ductile and weaker when exposed to moist environments and the interface is prone to lose its toughness. In an adhesive joint, this frequently means that there is a gradient in the mechanical properties of the adhesive layer and on the interface as the exposed faces of the adhesive joint always absorb water faster than the joint's center, which will cause the edges of the joint to lose its properties faster than in the center if the joint is exposed for a limited time and has not reached saturation yet. As a consequence, the numerical simulation must be able to simulate a joint with graded properties. In order to assess the gradient of mechanical properties in the adhesive layer or in the interface, it is necessary to know the amount of water at each point, which means that the water uptake into the adhesive joint must be computed, either using an analytical[82] or numerical method.[60,68,79,80]

Crocombe[82] was the first to make such a simulation. The strength of single-lap adhesive joints with and without adhesive fillets was predicted using the adhesive failure strain as a criterion. It was found that, after 30 days of immersion in tap water, the joints were more prone to fail at their center, where the adhesive ductility was lower due to the lower water uptake. Later, Hua et al.[60] made a similar simulation. They used the von Mises yielding criterion as the failure criterion. This critical strain was calculated using dry and partially moist mixed-mode flexure tests (MMF). It was found that the critical strain given by bulk specimens was higher than the actual critical strain in the adhesive joint. Maybe the wet-adhesive–adherend interface was more susceptible to moisture degradation.

Carrere et al.[83] developed a method for predicting the mechanical behavior of carbon-epoxy laminates using a finite fracture mechanics approach. In this model, the damage threshold is influenced by the aging but the kinetics of the crack propagation remains almost constant.

Usually, because water penetrates into the adhesive bondline through two directions, a 3D analysis must be undertaken in order to consider the gradient in the mechanical properties in both dimensions of the adhesive layer.[60] However, there are two cases in which a simpler 2D analysis may be enough to accurately predict the mechanical behavior of the adhesive joint:

1. A rectangular adhesive layer, in which the length is considerably smaller than the width. In this case, the gradient in the width direction will be negligible. Only the gradient in the length direction will be important;
2. When permeable adherends, such as FRP, are used. These adherends allow water to be absorbed through its thickness, allowing for a more uniform water absorption by the adhesive layer.[60]

Most adhesive joints degrade under service conditions. They absorb water while supporting a mechanical load. It is known that mechanical loading enhances degradation and water absorption of adhesives.[39,68] Some authors have modeled the mechanical behavior of adhesive joints using sequentially coupled analyses. This kind of analysis is normally made in two steps:

1. Calculating the moisture profile using a diffusion analysis;
2. Calculating the parameters used in the model, which are a function of the moisture amount in the adhesive, predicted in the previous step. Graded properties are attributed to the adhesive, as the moisture concentration is usually not constant along the entire overlap.

Usually the moisture uptake of the adhesive is determined using unstressed bulk specimens. However, some studies state[39,68] that the diffusion of water into adhesives is affected by the stress state of the adhesive. The sequentially coupled analysis does not take into account the stress enhanced diffusion. To overcome this setback, fully coupled models[73] have been developed. Using these models, the stress state of the adhesive is influenced by the water uptake, which will in turn be influenced by the stress state of the adhesive. In practice, this means that real adhesive joints, which are usually stressed during its work life, will absorb more water and their properties will be more degraded.

In order to model the degradation of stressed adhesive joints subjected to moisture environments and to obtain their residual strength, Han et al.[73] used two steps:

1. Step 1: Modeling the long-term aging process in the adhesive joint under combined thermal-hygro-mechanical service loading conditions with a fully-coupled methodology, an analogy between moisture diffusion and conduction of heat was made and thermal-displacement-coupled elements were used in the adhesive layer.[68] The von Mises

stress was used to characterize the stress dependence of the moisture uptake. In this step, a constant creep load was applied to the adhesive joint. The moisture uptake and equivalent creep strain were defined as field variable and used in step 2.
2. Step 2: Simulation of the quasi-static tensile loading process in adhesive joints using cohesive zone models that had been previously aged (in step 1). The properties of the adhesive were set to be a function of the field variables defined in step 1.

When an adhesive is aged under a moist environment, swelling occurs due to the absorbed bond water. However, it has been shown by several authors[39,80,84] that in an adhesive joint, no significant residual stresses arise due to relaxation of the adhesive and the strength of the joint remains almost unchanged.[39]

Conclusion

A literature review on the temperature and moisture degradation of adhesive joints has been made. Temperature and moisture influence the bulk behavior of the adhesive. Moisture-induced plasticization of the adhesive lowers its yield stress and stiffness and increases its strain to failure.

Low temperatures are responsible for the creation of residual stresses in the adhesive joint and this has an impact on the adhesive joint strength. Residual stresses also arise in adhesive joints subjected to high temperatures environments but due to polymer chain relaxation, they do not become very significant unless the joint is subjected to high and low temperature cycles. Moisture creates swelling of the adhesive, which generally does not cause significant residual stresses in the adhesive joint due to its plasticizing effect. It can, however, help in the reduction of thermal stresses.

Moisture is responsible for lowering the adhesive's T_g and this has an influence on the behavior of the adhesive, especially at high temperatures. At lower temperatures, as the adhesive is already well below T_g, its influence is not as significant. Despite the separate influence of moisture and temperature on the adhesive joint's mechanical behavior being relatively well known, its combined effect is not yet well known as very few authors have addressed this subject.

A review on methodologies used to predict the mechanical behavior of aged adhesive joints was also made. Generally, a sequentially coupled analysis is made: first the moisture uptake in the adhesive joint is calculated and then the mechanical behavior of the joint is computed based on the moisture-dependent properties of the adhesive. However, the moisture uptake of the adhesive is also dependent on its stress state and real adhesive joints are always subjected to some kind of stress. This translates into a more complex fully coupled analysis, in which the stress state of the adhesive is influenced by the moisture uptake and vice versa.

Declaration of conflicting interests

The author(s) declared no potential conflicts of interest with respect to the research, authorship, and/or publication of this article.

Funding

The author(s) disclosed receipt of the following financial support for the research, authorship, and/or publication of this article: This study was supported by Fundação para a Ciência e Tecnologia through grant EXCL/EMS-PRO/0084/2012.

References

1. Banea MD, da Silva LFM, Campilho RDSG, et al. Smart adhesive joints: An overview of recent developments. *J Adhes* 2014; 90: 16–40.
2. Banea MD and da Silva LFM. Adhesively bonded joints in composite materials: An overview. *Proc IMechE, Part L: J Materials: Design and Applications* 2009; 223: 1–18.
3. Carbas RJC, Viana GMSO, da Silva LFM, et al. Functionally graded adhesive patch repairs of wood beams in civil applications. *J Compos Construct* 2015; 19.
4. Fecht S, Vallee T, Tannert T, et al. Adhesively bonded hardwood joints under room temperature and elevated temperatures. *J Adhes* 2014; 90: 401–419.
5. Li W, Pang B, Han X, et al. Predicting the strength of adhesively bonded T-joints under cyclic temperature using a cohesive zone model. *J Adhes* 2015; 92: 892–907.
6. Banea MD and da Silva LFM. The effect of temperature on the mechanical properties of adhesives for the automotive industry. *Proc IMechE, Part L: J Materials: Design and Applications* 2010; 224: 51–62.
7. Marques EAS, da Silva LFM and Flaviani M. Testing and simulation of mixed adhesive joints for aerospace applications. *Compos Part B: Eng* 2015; 74: 123–130.
8. Carbas RJC, Marques EAS, da Silva LFM, et al. Effect of cure temperature on the glass transition temperature and mechanical properties of epoxy adhesives. *J Adhes* 2014; 90: 104–119.
9. Carbas RJC, da Silva LFM, Marques EAS, et al. Effect of post-cure on the glass transition temperature and mechanical properties of epoxy adhesives. *J Adhes Sci Technol* 2013; 27: 2542–2557.
10. Zhang Y, Adams RD and da Silva LFM. Effects of curing cycle and thermal history on the glass transition temperature of adhesives. *J Adhes* 2014; 90: 327–345.
11. Banea MD, da Silva LFM and Campilho RDSG. Mode I fracture toughness of adhesively bonded joints as a function of temperature: Experimental and numerical study. *Int J Adhes Adhes* 2011; 31: 273–279.
12. Majda P and Skrodzewicz J. A modified creep model of epoxy adhesive at ambient temperature. *Int J Adhes Adhes* 2009; 29: 396–404.
13. Mizah BR, Sekiguchi Y and Sato C. Novel method to measure the creep strength of adhesively bonded butt joints subjected to constant loading using a hydro-pneumatic testing machine. *J Adhes* 2016; 92: 65–79.

14. Hart-Smith LJ. Adhesive bonded single lap joints. NASA Contractual Report 1973, NASA CR-112235.
15. Yu H, Adams RD and da Silva LFM. Development of a dilatometer and measurement of the shrinkage behaviour of adhesives during cure. *Int J Adhes Adhes* 2013; 47: 26–34.
16. da Silva LFM and Adams RD. Effect of temperature on the mechanical and bonding properties of a carbon-reinforced bismaleimide. *Proc IMechE, Part L: J Materials: Design and Applications* 2008; 222: 45–52.
17. Yu JH, Guo S and Dillard DA. Bimaterial curvature measurements for the CTE of adhesives: Optimization, modeling, and stability. *J Adhes Sci Technol* 2003; 17: 149–164.
18. da Silva LFM and Adams RD. Stress-free temperature in a mixed-adhesive joint. *J Adhes Sci Technol* 2006; 20: 1705–1726.
19. Humfeld GR and Dillard DA. Residual stress development in adhesive joints subjected to thermal cycling. *J Adhes* 1998; 65: 277–306.
20. Avendaño R, Carbas RJC, Marques EAS, et al. Effect of temperature and strain rate on single lap joints with dissimilar lightweight adherends bonded with an acrylic adhesive. *Compos Struct* 2016; 152: 34–44.
21. Avendaño R, Carbas RJC, Chaves F, et al. Impact loading of single lap joints of dissimilar lightweight adherends bonded with a crash-resistant epoxy adhesive. *J Eng Mater Technol* 2016.
22. Banea MD, da Silva LFM and Campilho RDSG. Effect of temperature on the shear strength of aluminium single lap bonded joints for high temperature applications. *J Adhes Sci Technol* 2014; 28: 1367–1381.
23. Hu P, Han X, Li WD, et al. Research on the static strength performance of adhesive single lap joints subjected to extreme temperature environment for automotive industry. *Int J Adhes Adhes* 2013; 41: 119–126.
24. da Silva LFM and Adams RD. Adhesive joints at high and low temperatures using similar and dissimilar adherends and dual adhesives. *Int J Adhes Adhes* 2007; 27: 216–226.
25. da Silva LFM and Adams RD. Joint strength predictions for adhesive joints to be used over a wide temperature range. *Int J Adhes Adhes* 2007; 27: 362–379.
26. Marques EAS, Magalhaes DNM and da Silva LFM. Experimental study of silicone-epoxy dual adhesive joints for high temperature aerospace applications. *Materialwiss Werkstoff* 2011; 42: 471–477.
27. Carbas RJC, da Silva LFM and Critchlow GW. Adhesively bonded functionally graded joints by induction heating. *Int J Adhes Adhes* 2014; 48: 110–118.
28. Kawasaki S, Nakajima G, Haraga K, et al. Functionally graded adhesive joints bonded by honeymoon adhesion using two types of second generation acrylic adhesives of two components. *J Adhes* 2016; 92: 517–534.
29. Aris R. *The mathematics of diffusion*. Oxford: Clarendon Press, 1975.
30. Liljedahl CDM, Crocombe AD, Wahab MA, et al. Modelling the environmental degradation of the interface in adhesively bonded joints using a cohesive zone approach. *J Adhes* 2006; 82: 1061–1089.
31. Ameli A, Datla NV, Papini M, et al. Hygrothermal properties of highly toughened epoxy adhesives. *J Adhes* 2010; 86: 698–725.
32. Loh WK, Crocombe AD, Wahab MMA, et al. Modelling anomalous moisture uptake, swelling and thermal characteristics of a rubber toughened epoxy adhesive. *Int J Adhes Adhes* 2005; 25: 1–12.
33. Vanlandingham MR, Eduljee RF and Gillespie JW. Moisture diffusion in epoxy systems. *J Appl Polym Sci* 1999; 71: 787–798.
34. Crocombe AD, Hua YX, Loh WK, et al. Predicting the residual strength for environmentally degraded adhesive lap joints. *Int J Adhes Adhes* 2006; 26: 325–336.
35. Zhang Y, Adams RD and da Silva LFM. Absorption and glass transition temperature of adhesives exposed to water and toluene. *Int J Adhes Adhes* 2014; 50: 85–92.
36. Chiang MYM and Fernandez-Garcia M. Relation of swelling and Tg depression to the apparent free volume of a particle-filled, epoxy-based adhesive. *J Appl Polym Sci* 2003; 87: 1436–1444.
37. Suh DW, Ku MK, Nam JD, et al. Equilibrium water uptake of epoxy/carbon fiber composites in hygrothermal environmental conditions. *J Compos Mater* 2001; 35: 264–278.
38. Zhou JM and Lucas JP. The effects of a water environment on anomalous absorption behavior in graphite-epoxy composites. *Compos Sci Technol* 1995; 53: 57–64.
39. Liljedahl CDM, Crocombe AD, Wahab MA, et al. The effect of residual strains on the progressive damage modelling of environmentally degraded adhesive joints. *J Adhes Sci Technol* 2005; 19: 525–547.
40. Pethrick RA. Design and ageing of adhesives for structural adhesive bonding - A review. *Proc IMechE, Part L: J Materials: Design and Applications* 2015; 229: 349–379.
41. Mubashar A, Ashcroft IA, Critchlow GW, et al. Moisture absorption-desorption effects in adhesive joints. *Int J Adhes Adhes* 2009; 29: 751–760.
42. Lin YC and Chen X. Moisture sorption-desorption-resorption characteristics and its effect on the mechanical behavior of the epoxy system. *Polymer* 2005; 46: 11994–12003.
43. Liljedahl CDM, Crocombe AD, Gauntlett FE, et al. Characterising moisture ingress in adhesively bonded joints using nuclear reaction analysis. *Int J Adhes Adhes* 2009; 29: 356–360.
44. Popineau S, Rondeau-Mouro C, Sulpice-Gaillet C, et al. Free/bound water absorption in an epoxy adhesive. *Polymer* 2005; 46: 10733–10740.
45. Zhou JM and Lucas JP. Hygrothermal effects of epoxy resin. Part II: Variations of glass transition temperature. *Polymer* 1999; 40: 5513–5522.
46. Li YM, Miranda J and Sue HJ. Hygrothermal diffusion behavior in bismaleimide resin. *Polymer* 2001; 42: 7791–7799.
47. Karter HG and Kibler KG. Fundamental and operational glass transition temperatures of composite resins and adhesives. *J Compos Mater* 1978; 12: 118–131.
48. Zannideffarges MP and Shanahan MER. Diffusion of water into an epoxy adhesive - comparison between bulk behavior and adhesive joints. *Int J Adhes Adhes* 1995; 15: 137–142.
49. Wapner K and Grundmeier G. Spatially resolved measurements of the diffusion of water in a model adhesive/silicon lap joint using FTIR-transmission-microscopy. *Int J Adhes Adhes* 2004; 24: 193–200.

50. da Silva LFM, Dillard D, Blackman B, et al. *Testing adhesive joints - Best practices*. Weinheim: Wiley, 2012.
51. Winston PW and Bates DH. Saturated solutions for the control of humidity in biological-research. *Ecology* 1960; 41: 232–237.
52. Viana G, Costa M, Banea MD, et al. Water diffusion in double cantilever beam adhesive joints. *Latin Am J Solids Struct* 2016.
53. Kinloch AJ, Little MSG and Watts JF. The role of the interphase in the environmental failure of adhesive joints. *Acta Mater* 2000; 48: 4543–4553.
54. Adamson MJ. Thermal-expansion and swelling of cured epoxy-resin used in graphite-epoxy composite-materials. *J Mater Sci* 1980; 15: 1736–1745.
55. Zhang Y, Adams RD and da Silva LFM. A rapid method of measuring the glass transition temperature using a novel dynamic mechanical analysis method. *J Adhes* 2013; 89: 785–806.
56. Viana G, Costa M, Banea MD, et al. Behaviour of environmentally degraded epoxy adhesives as a function of temperature. *J Adhes* 2016; DOI: 10.1080/00218464.2016.1179118.
57. Moy P and Karasz FE. Epoxy-water interactions. *Polym Eng Sci* 1980; 20: 315–319.
58. Costa M, Viana G, da Silva LFM, et al. Determination of the fracture envelope of an adhesive joint as a function moisture. *Materialwiss Werkstoff* 2016.
59. Sugiman S, Crocombe AD and Aschroft IA. Experimental and numerical investigation of the static response of environmentally aged adhesively bonded joints. *Int J Adhes Adhes* 2013; 40: 224–237.
60. Hua Y, Crocombe AD, Wahab MA, et al. Modelling environmental degradation in EA9321-bonded joints using a progressive damage failure model. *J Adhes* 2006; 82: 135–160.
61. Costa M, Viana G, da Silva LFM, et al. Environmental effect on the fatigue degradation of adhesive joints: A review. *J Adhes* 2016; DOI: 10.1080/00218464.2016.1179117.
62. Costa M, Viana G, da Silva LFM, et al. Effect of humidity on the fatigue behaviour of adhesively bonded aluminium joints. *Latin Am J Solids Struct* 2016.
63. Loh WK, Crocombe AD, Wahab MMA, et al. Environmental degradation of the interfacial fracture energy in an adhesively bonded joint. *Eng Fract Mech* 2002; 69: 2113–2128.
64. Barbosa AQ, da Silva LFM and Ochsner A. Hygrothermal aging of an adhesive reinforced with microparticles of cork. *J Adhes Sci Technol* 2015; 29: 1714–1732.
65. da Silva LFM and Sato C. *Design of adhesive joints under humid conditions*. Berlin Heidelberg: Springer-Verlag, 2013.
66. Meiser A, Willstrand K and Possart W. Influence of composition, humidity, and temperature on chemical aging in epoxies: A local study of the interphase with air. *J Adhes* 2010; 86: 222–243.
67. Goglio L, Rezaei M and Rossetto M. Moisture degradation of open-faced single lap joints. *J Adhes Sci Technol* 2014; 28: 1382–1393.
68. Han X, Crocombe AD, Anwar SNR, et al. The effect of a hot-wet environment on adhesively bonded joints under a sustained load. *J Adhes* 2014; 90: 420–436.
69. Costa M, Viana G, Canto C, et al. Effect of the size reduction on the bulk tensile and double cantilever beam specimens used in cohesive zone models. *Proc IMechE, Part L: J Materials: Design and Applications* 2015; DOI: 1464420715610248.
70. Campilho RDSG, Moura DC, Banea MD, et al. Adherend thickness effect on the tensile fracture toughness of a structural adhesive using an optical data acquisition method. *Int J Adhes Adhes* 2014; 53: 15–22.
71. Critchlow GW and Brewis DM. Review of surface pretreatments for aluminium alloys. *Int J Adhes Adhes* 1996; 16: 255–275.
72. Goglio L and Rezaei M. Effect of different substrate pre-treatments on the resistance of aluminum joints to moist environments. *J Adhes* 2013; 89: 769–784.
73. Han X, Crocombe AD, Anwar SNR, et al. The strength prediction of adhesive single lap joints exposed to long term loading in a hostile environment. *Int J Adhes Adhes* 2014; 55: 1–11.
74. Ray BC. Temperature effect during humid ageing on interfaces of glass and carbon fibers reinforced epoxy composites. *J Colloid Interface Sci* 2006; 298: 111–117.
75. Bao LR and Yee AF. Moisture diffusion and hygrothermal aging in bismaleimide matrix carbon fiber composites - Part I: Uni-weave composites. *Compos Sci Technol* 2002; 62: 2099–2110.
76. Markatos DN, Tserpes KI, Rau E, et al. Degradation of mode-I fracture toughness of CFRP bonded joints due to release agent and moisture pre-bond contamination. *J Adhes* 2014; 90: 156–173.
77. Li WD, Ma M, Han X, et al. Strength prediction of adhesively bonded single lap joints under salt spray environment using a cohesive zone model. *J Adhes* 2016; 92: 916–937.
78. Jurf RA and Vinson JR. Effect of moisture on the static and viscoelastic shear properties of epoxy adhesives. *J Mater Sci* 1985; 20: 2979–2989.
79. Hua Y, Crocombe AD, Wahab MA, et al. Continuum damage modelling of environmental degradation in joints bonded with EA9321 epoxy adhesive. *Int J Adhes Adhes* 2008; 28: 302–313.
80. Sugiman S, Crocombe AD and Aschroft IA. Modelling the static response of unaged adhesively bonded structures. *Eng Fract Mech* 2013; 98: 296–314.
81. Loh WK, Crocombe AD, Wahab MMA, et al. Modelling interfacial degradation using interfacial rupture elements. *J Adhes* 2003; 79: 1135–1160.
82. Crocombe AD. Durability modelling concepts and tools for the cohesive environmental degradation of bonded structures. *Int J Adhes Adhes* 1997; 17: 229–238.
83. Carrere N, Tual N, Bonnemains T, et al. Modelling of the damage development in carbon/epoxy laminates subjected to combined seawater ageing and mechanical loading. *Proc IMechE, Part L: J Materials: Design and Applications* 2016. DOI: 10.1177/1464420716648353.
84. Reedy ED and Guess TR. Butt joint strength: effect of residual stress and stress relaxation. *J Adhes Sci Technol* 1996; 10: 33–45.

PAPER 2

The Journal of Adhesion

ISSN: 0021-8464 (Print) 1545-5823 (Online) Journal homepage: http://www.tandfonline.com/loi/gadh20

Behaviour of environmentally degraded epoxy adhesives as a function of temperature

G. Viana, M. Costa, M. D. Banea & L. F. M. da Silva

To cite this article: G. Viana, M. Costa, M. D. Banea & L. F. M. da Silva (2017) Behaviour of environmentally degraded epoxy adhesives as a function of temperature, The Journal of Adhesion, 93:1-2, 95-112, DOI: 10.1080/00218464.2016.1179118

To link to this article: https://doi.org/10.1080/00218464.2016.1179118

Accepted author version posted online: 21 Apr 2016.
Published online: 03 Aug 2016.

THE JOURNAL OF ADHESION
2017, VOL. 93, NOS. 1–2, 95–112
http://dx.doi.org/10.1080/00218464.2016.1179118

Taylor & Francis
Taylor & Francis Group

Behaviour of environmentally degraded epoxy adhesives as a function of temperature

G. Viana[a], M. Costa[a], M. D. Banea[b], and L. F. M. da Silva[c]

[a]Polo FEUP, Instituto de Ciência e Inovação em Engenharia Mecânica e Engenharia Industrial (INEGI), Oporto, Portugal; [b]Federal Centre of Technological Education in Rio de Janeiro (CEFET), Rio de Janeiro, Brazil; [c]Departamento de Engenharia Mecânica, Faculdade de Engenharia da Universidade do Porto (FEUP), Oporto, Portugal

ABSTRACT

Structural adhesives are increasingly being used in the aerospace and automotive industries. They allow for light weight vehicles, fuel savings, and reduced emissions. However, the environmental degradation of adhesive joints is a major setback in its wide implementation. Moisture degradation of adhesive joints includes plasticization, attacking of the interface, swelling of the adhesive and consequent creation of residual stresses. This may lead to reversible and irreversible damage. The main factors affecting the strength of adhesive joints under high and low temperatures are the degradation of the adhesive mechanical properties and the creation of residual stresses induced by different coefficients of thermal expansion (between the adhesive and the adherends). The effect of the combined effect of moisture and temperature is not yet fully understood. The aim of this study is to shed light on this subject.

In this work bulk water absorption tests were conducted at different moisture conditions in order to assess the diffusion coefficient, maximum water uptake, and glass transition temperature. Aged and unaged small dogbone tensile specimens were tested under different temperature conditions. The glass transition temperature of the adhesives as a function of the water uptake was assessed. The aim is to determine the evolution of the properties of two epoxy adhesives as a function of two variables (environmental temperature and moisture).

ARTICLE HISTORY
Received 17 February 2016
Accepted 9 April 2016

KEYWORDS
Moisture degradation; temperature tests; tensile tests

1. Introduction

Structural adhesives are increasingly being used in the transport industries. They allow for light weight vehicles, energy savings, and reduced emissions. The main advantages include more uniform load distribution, higher fatigue resistance than other traditional joining methods, and the ability to join dissimilar materials [1]. Also, due to their high vulnerability to stress concentration, the only viable way to join composite materials, such as fibre

CONTACT L. F. M. da Silva lucas@fe.up.pt Departamento de Engenharia Mecânica, Faculdade de Engenharia da Universidade do Porto (FEUP), Rua Dr. Roberto Frias, 4200-465 Oporto, Portugal.
Color versions of one or more of the figures in the article can be found online at www.tandfonline.com/gadh.

reinforced plastic, is with a structural adhesive [2]. However, the environmental degradation of adhesive joints is a major setback in their wide implementation.

Moisture degradation of adhesives includes reduction of their mechanical properties, inducing plasticization. The deleterious effects are greater in adhesive joints as the degradation of the adhesive–adherend interface may cause interfacial failure.

The water diffusion in adhesives is frequently controlled by the Fick's laws but non-Fickian diffusion is not uncommon. Other models have been developed, such as the dual Fickian diffusion [3], delayed dual Fickian [4], and the Langmuir model [5]. The rate at which the water is absorbed and the maximum water uptake depends on environmental factors such as the relative humidity and temperature and on the thickness [3,6] and the stress state of the adhesive [7].

As the water diffuses into the adhesive, some of this moisture becomes bound water. Bound water generally increases with exposure time and temperature [8,9]. Unlike the free water that occupies the free space of the adhesive, this bound water is responsible for the volumetric changes that are observed in adhesives under high humidity environments, which may cause residual stresses in adhesive joints [10]. Zhou and Lucas [8,9] have found two types of bound water: Type I involves water molecules forming a single hydrogen bond while Type II results from water forming multiple hydrogen bonds. Type I bound water acts as a plasticizer, increasing the chains segment mobility. It is responsible for decreasing the glass transition temperature (Tg) [8]. If the temperature is high and the exposure time is long, Type II bound water may also occur. This type of bound water is responsible for creating secondary cross-linking [9], which lessens the extent of Tg depression [8]. While Type I bound water can be removed at low temperature, in order to remove Type II bound water, the adhesive must be subjected to relatively high temperatures [8].

The main factors affecting the strength of adhesive joints under high and low temperatures are the degradation of the mechanical properties and the creation of residual stresses induced by different coefficients of thermal expansion between the adhesive and adherends, especially when the substrates are made with different materials. It was found that the residual stresses caused by the shrinkage of the adhesive during cure have not a major effect on the strength of the joint [11]. Generally, the strength of adhesive joints decreases with increasing and decreasing temperatures [12–18]. The fracture toughness of adhesives also shows a strong temperature dependence [19,20]. Banea et al. [16] found that below Tg, the fracture toughness of an epoxy adhesive changed little, while above Tg, it decreased dramatically.

Although the separate effect of moisture and temperature on the mechanical properties of epoxy adhesives is now-a-days relatively well understood, very few studies focus on the mechanical properties of aged adhesives at high and low temperatures. This work aims at shedding light on this subject. This will allow for a more accurate long-term prediction of the mechanical behaviour of adhesive joints.

In this study, two different ageing environments were considered: distilled water, which is the most aggressive environment, and a saturated solution of NaCl, which is equivalent to exposing the specimens in a 75% relative humidity environment [21].

Bulk dogbone tensile specimens were aged under these environments and tested at three different temperatures: −40°C, 23°C, and 80°C, which cover the range of temperatures an adhesive for the automotive industry must be able to withstand. This way it was possible to obtain the properties of the dry adhesive, the saturated adhesive (aged in distilled water), and an intermediate state (adhesive aged in salt water) under the three different temperatures considered. The tests were performed in three different moments: right after the specimens were dried in a dry desiccator for at least two weeks, after 74 days of ageing, when they were fully saturated with water, and after one year of ageing, so that the influence of the ageing time could be assessed.

In order to determine the moisture diffusion behaviour of the adhesives, bulk water sorption tests were made. The diffusion coefficients and maximum water absorption were measured for each ageing environment considered.

A rapid method based on the dynamic mechanical analysis (DMA) was used to measure Tg of aged and unaged adhesives. In this method, the specimen is kept at resonance and the value of Tg is determined by the temperature at which the maximum damping occurs [22].

2. Materials

2.1 *Adhesives*

The epoxy adhesive XNR 6852-1 was supplied by NAGASE CHEMTEX® (Osaka, Japan). This adhesive is a one-part system that cures at 150°C for 3 hr.

The epoxy adhesive SikaPower 4720 was supplied by SIKA® (Portugal, Vila Nova de Gaia). This adhesive is a two-part system that cures at room temperature for 24 hr.

These adhesives were developed for the automotive industry and were recommended by Sika® and Nagase® for this durability study.

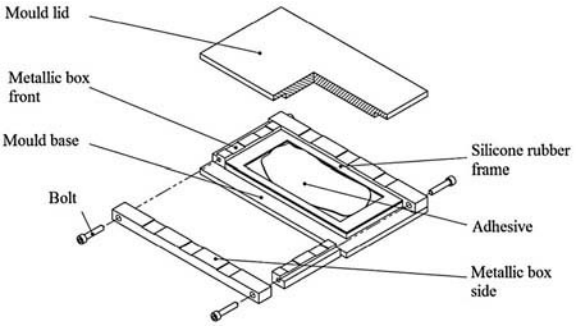

Figure 1. Mould used in the manufacture of adhesive bulk plates.

2.2 *Specimen Fabrication*

The bulk specimens were produced by curing the adhesive between steel plates of a mould. (Fig. 1). A silicone rubber frame was used to avoid the adhesive from flowing out and to ensure the thickness of the adhesive plate (1 mm in the water sorption specimens and 2 mm in the bulk tensile specimens and Tg specimens). Both adhesives were cured under 2 MPa hydrostatic pressure in a hotplates press. The temperature of cure was set at 150°C for XNR6851-1 adhesive and at room temperature (23°C) for the SikaPower 4720 adhesive, according to the manufacturer's specification. Bulk tensile specimens (Fig. 2), water absorption specimens (Fig. 2), and Tg specimens (Fig. 3) were machined from these plates.

The thickness of the water sorption specimens is small compared with the remaining dimensions, so that water sorption along its width and length can be neglected and simple one-dimensional sorption across the thickness direction can be considered without incurring significant error.

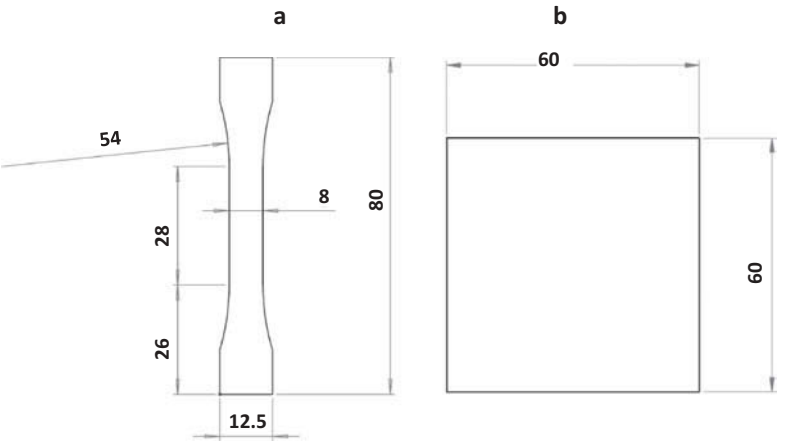

Figure 2. Dogbone tensile specimen geometry (a) and bulk water sorption specimen (b). Dimensions in millimetres.

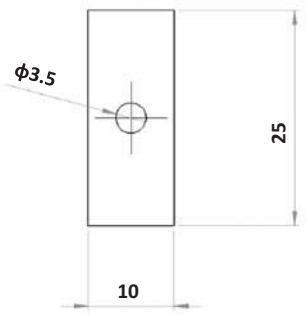

Figure 3. Glass transition temperature specimen. Dimensions in millimetres.

Small bulk tensile specimens were used, allowing a time efficient production and easy storage during immersion. Although the selected geometry did not follow a standard, it was optimized in previous work to provide accurate elastic properties and reduce the amount of adhesive used. More information about this specimen geometry can be found in another study [23].

The Tg specimens are a 2-mm thick plate with a hole in its centre that are bolted to an aluminium beam. More information about these specimens can be found in Section 3.1 and in previous studies [22,24].

3. Experimental Procedure

3.1 *DMA Type Test*

In order to perform the Tg tests, a method based on the DMA was used [22]. This method consists in keeping a vibrating beam with a bolted adhesive plate in its centre at resonance. This adhesive plate introduces damping in the specimen. The beam is supported by two thin stretched twines along the direction perpendicular to Fig. 4, at each side of the vibrating beam. The temperature of the specimen is then raised and the amplitude of the vibration is recorded. It is known that, at Tg, the adhesive presents its maximum damping [22]. From the theory of forced vibration, the damping is proportional to the inverse of the amplitude. In order words, Tg is the temperature at which the amplitude of the specimen is at its minimum. A schematic representation of the test setup is shown in Fig. 4.

In this method it is very important always to keep the beam at resonance frequency, which changes throughout the test. With this in mind, the frequency of the power supply that feeds the driving coil is controlled by a feedback system that takes into account the frequency read by the pickup coil.

Because the measurement of Tg using this method takes so little time (less than 10 minutes), significant post cure of the adhesive is avoided

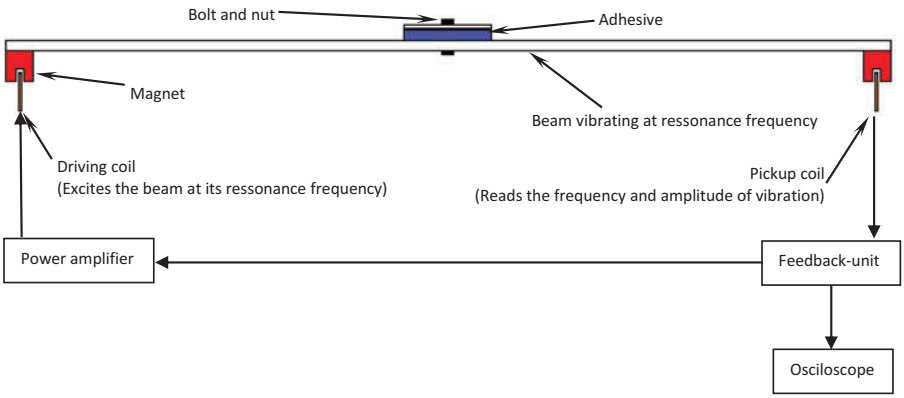

Figure 4. Schematic representation of the principle of operation of the DMA type test used in this study.

[25]. Also, if the test took a long time to perform, such as the standard DMA test, some moisture would evaporate from the aged specimens, giving wrong results.

In this study the Tg of both adhesives as a function of the absorbed water was assessed. The specimens were kept immersed in distilled water and a saturated solution of NaCl for at least 75 days, when equilibrium water uptake had been attained, before being tested.

3.2 *Bulk Water Sorption Tests*

Before exposing the specimens to their aging environment, they were kept in a dry desiccator for two weeks in order to eliminate any water that may be absorbed from the air. Then, the initial weight of each water sorption specimen was measured with a 0.001 g resolution scale and they were placed in two different environments: a saturated NaCl water solution (referred in this paper as "salt water", which is equivalent to a 75% RH environment) and distilled water at 32.5°C. The specimens remained hanging inside closed containers, so that every face could be exposed to the ageing environment.

The weight of each specimen was periodically measured until saturation was attained.

The results were modelled using simple Fickian diffusion and dual Fickian diffusion.

For the one-dimensional case, the water concentration at each point of the adhesive, according to the Fick's laws, was [26]

$$\frac{c}{c_\infty} = 1 - \frac{4}{\pi}\sum_{n=0}^{\infty}\frac{(-1)^n}{(2n+1)}exp\left[\frac{-D(2n+1)^2\pi^2 t}{4l^2}\right] \times \cos\left[\frac{(2n+1)\pi x}{2l}\right], \quad (1)$$

where c_∞ is the concentration of water in the surface layers, which is supposed to be attained instantaneously, l is half of the layer's width, and t is the time. The center of the adhesive is located at $x = 0$.

Equation (2) is the integration of Equation (1). Instead of giving the water concentration in each point, which is hard to obtain experimentally, it gives the fractional mass uptake of the entire specimen [26]:

$$\frac{mwt_t}{mwt_\infty} = 1 - \frac{8}{\pi^2}\sum_{n=0}^{\infty}\frac{1}{(2n+1)^2}exp\left[\frac{-D(2n+1)^2\pi^2 t}{4l^2}\right]. \quad (2)$$

mwt_∞ is the moisture level at equilibrium and mwt_t is the moisture level at instant t.

Throughout this paper the moisture content (mwt_t) is expressed in terms of percentage as a function of $\sqrt{t}/l^2$.

3.3 *Bulk Tensile Tests*

Bulk dogbone specimens of both studied adhesives were aged under the same environmental conditions used with the water sorption specimens (75% RH and distilled water). The specimens were tested in three moments: after being produced and dried in a dry desiccator, after being aged for 75 days, and after being aged for 12 months, so that the evolution of the adhesive properties with time could be assessed. Dry specimens, which were kept in a dry container were also tested.

The tensile tests were performed in an INSTRON® model 3367 universal test machine (Norwood, Massachusetts, USA) with a capacity of 30 kN, at the constant displacement rate of 1 mm/min. Loads and displacements were recorded up to failure. Since contact extensometers are not advisable when testing polymers under high temperatures because they damage the specimens, an optic method was used. This optic method consists in taking photos of the specimen every 5 s using a high-resolution digital camera. After the test, the photos are read by a Matlab® subroutine in which the strain of the specimen is computed. The strain is computed between two parallel lines that must be drawn on the specimen.

A climatic chamber coupled with the universal testing machine allowed the testing at three different temperatures, covering the range of temperatures required for adhesives used in the automotive industry: low temperature (−40°C), room temperature (23°C), and high temperature (80°C).

4. Experimental Results and Discussion

4.1 *DMA Type Tests*

Figure 5 shows the Tg of both adhesives as a function of the ageing environment.

The Tg is maximum when the adhesives are dry and tends to lower with an increasingly aggressive environment. This happens due to the bond water absorbed by the adhesive, which acts as a plasticizer [8].

The Tg of SikaPower 4720 adhesive is more dependent on the ageing environment than that of XNR 6852-1 adhesive, as it changes only 15°C between the specimens aged in distilled water and the dry specimens. The Tg of SikaPower 4720 adhesive is relatively high in the dry state, drops to 76.1°C when aged in salt water and is below room temperature if aged in distilled water.

4.2 *Bulk Water Sorption*

Figures 6–8 show the fractional mass uptake of the adhesives studied, as well as the respective Fickian fit. Both the dual Fickian and simple Fickian models were used to characterize the moisture diffusion in the adhesives.

The rate of mass uptake was maximum at the beginning of the exposure and kept diminishing until equilibrium was attained. As it would be expectable, the final moisture level of the specimens that were kept in salt water was lower than that of the specimens immersed in distilled water.

XNR 6852-1 adhesive shows a dual Fickian behaviour when immersed in both distilled water and in salt water.

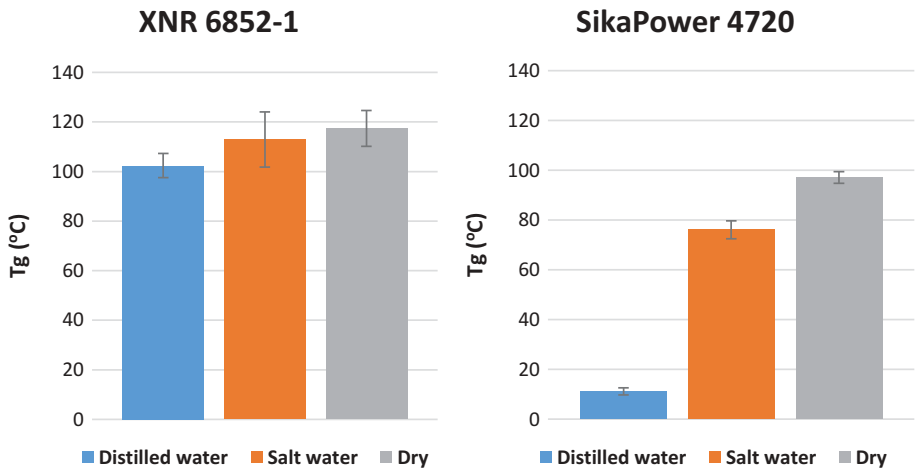

Figure 5. Glass transition temperature of XNR 6852-1 and SikaPower 4720 adhesive as a function of the ageing environment.

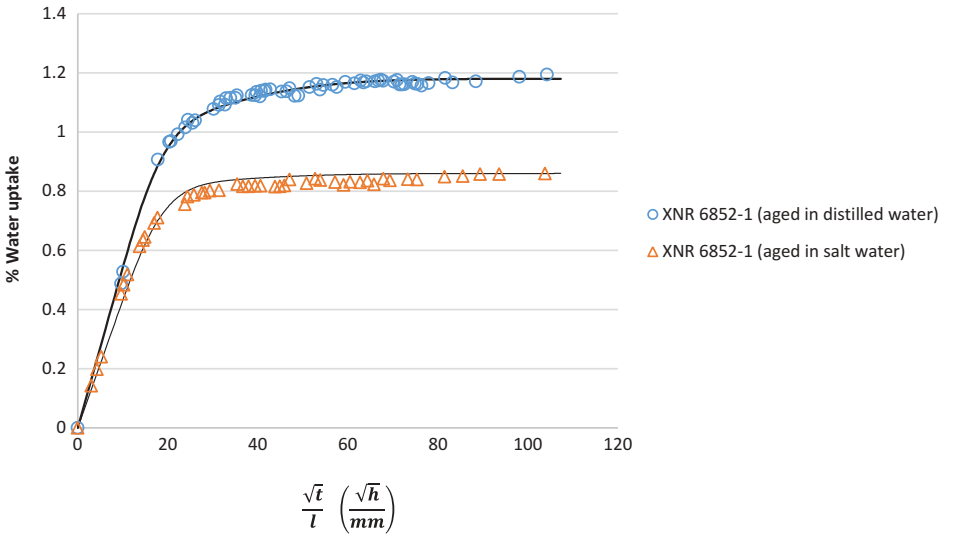

Figure 6. Water uptake behaviour of the XNR 6852-1 adhesive when aged in salt water and distilled water and respective dual Fickian fit.

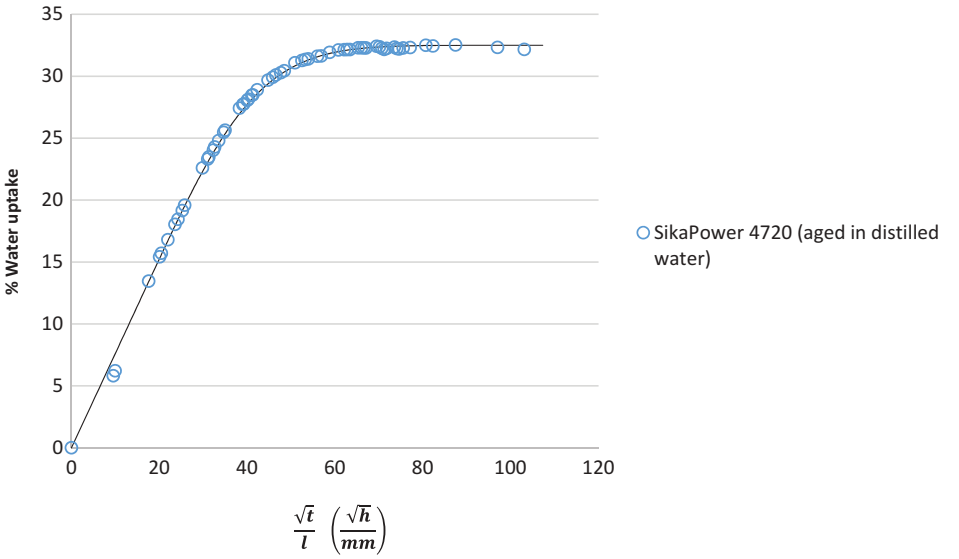

Figure 7. Water uptake behaviour of the SikaPower 4720 adhesive when aged in distilled water and Fickian fit.

When aged in distilled water, SikaPower 4720 adhesive shows a simple Fickian behaviour. Under these conditions, this adhesive shows a very high water uptake, unusual for an epoxy adhesive. This probably happens because under these ageing conditions the Tg of the adhesive is lower than the temperature of the bath. When immersed in salt water the adhesive is above its Tg,

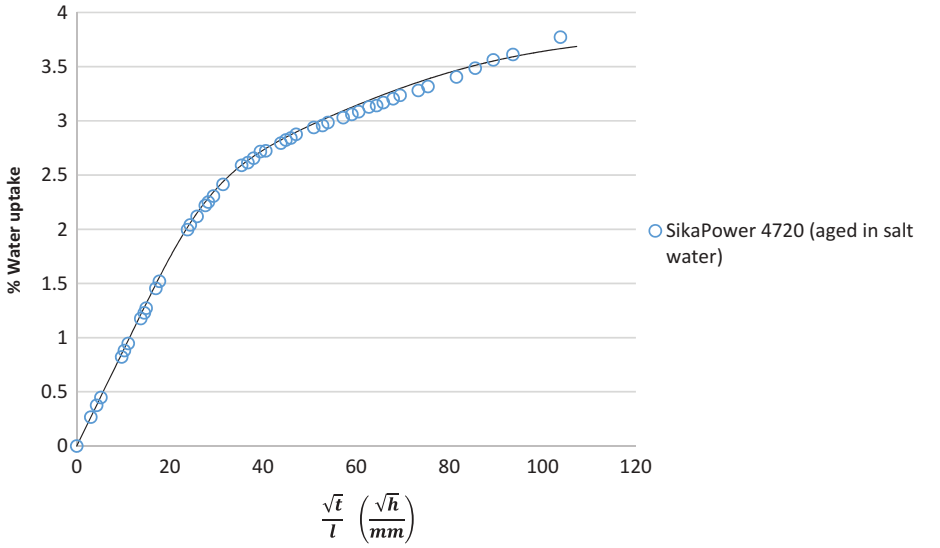

Figure 8. Water uptake behaviour of the SikaPower 4720 adhesive when aged in salt water and Fickian fit.

Table 1. Water Sorption Parameters of Both Adhesives.

		D_1 (m^2/s)	mwt_1	D_2 (m^2/s)	mwt_2
XNR 6852-1	Distilled water	6.0E-13	0.0095	8E-14	0.0023
	Salt water	6.0E-13	0.0080	8E-14	0.0006
SikaPower 4720	Distilled water	1.2E-13	0.325	–	–
	Salt water	2.6E-13	0.020	2.5E-14	0.018

shows a more common water uptake, and a clear dual Fickian behaviour. Despite having been aged for more than three months, this adhesive apparently did not reach saturation. The diffusion parameters were calculated considering that the maximum water uptake is the last that was measured.

The water uptake parameters of both adhesives are summarized in Table 1.

4.3 *Bulk Tensile Tests*

The bulk tensile tests were made at three different times:

(1) After the adhesives had been dried in a dry desiccator for at least two weeks;
(2) After the adhesives had been aged and had reached the equilibrium water uptake (75 days);
(3) After the adhesives had been aged for one year.

In the following subsections representative stress–strain curves of both adhesives are shown as a function of the ageing environment and test

temperature. The curves that represent the mechanical behaviour of the aged specimens and that are shown in following subsections are those obtained after one year of ageing, which are not significantly different from those obtained after 75 days of ageing.

4.3.1. *23°C Tensile Tests*

Figure 9 presents the stress–strain curves of the two adhesives tested at 23°C with different fractional moisture contents. The ductility increased with the adhesive's water content. The yield strength and the Young's modulus decreased in both adhesives. This effect is more evident in SikaPower 4720 adhesive than in XNR 6852-1 adhesive. The ductility of SikaPower 4720 adhesive that was aged in distilled water, however, decreased, which may be a consequence of testing above Tg or an indication that chemical degradation may have occurred. As can be seen in Fig. 10, XNR 6852-1 adhesive showed a ductile fracture while SikaPower 4720 showed a brittle fracture.

4.3.2. *40°C Tensile Tests*

The yield strength and tensile modulus of both adhesives increased when tested at −40°C. The fractional water uptake had little impact on the properties of SikaPower 4720 adhesive when tested at −40°C and does not seem to have a significant impact on XNR 6852-1 adhesive (Fig. 11).

From Fig. 12, one can see that both adhesives showed a brittle fracture.

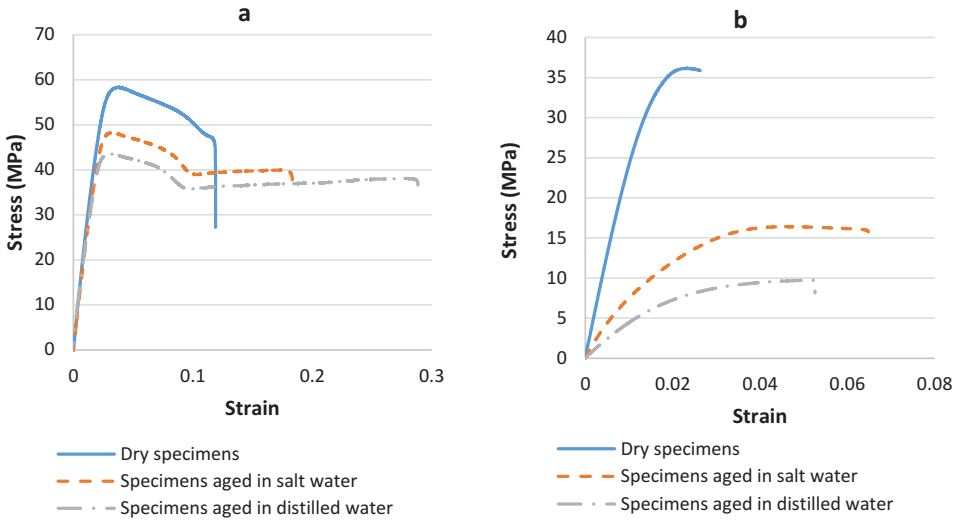

Figure 9. Stress–strain curves of the XNR 6852-1 adhesive (a) and the SikaPower 4720 adhesive (b) as a function of the ageing environment tested at room temperature.

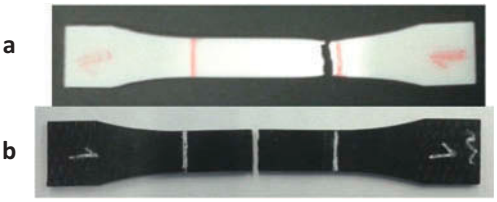

Figure 10. Specimens of the XNR 6852-1 adhesive (a) and of the SikaPower 4720 adhesive (b) after being tested at room temperature.

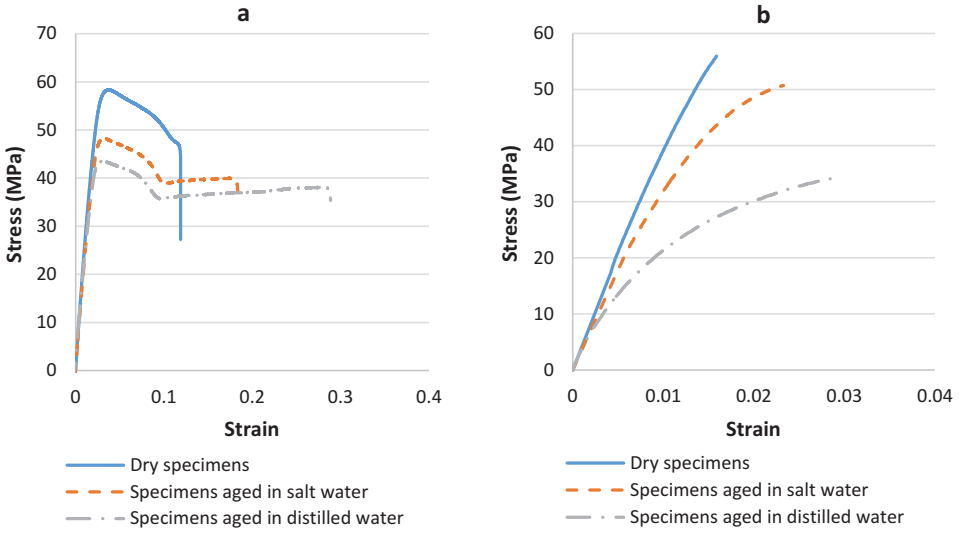

Figure 11. Stress–strain curves of the XNR 6852-1 adhesive (a) and the SikaPower 4720 adhesive (b) as a function of the ageing environment tested at −40°C.

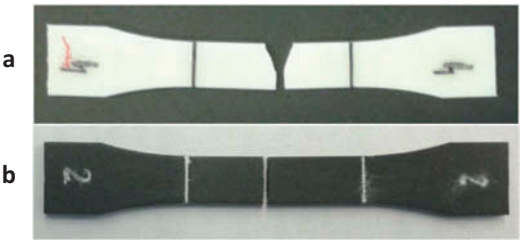

Figure 12. Specimens of the XNR 6852-1 adhesive (a) and of the SikaPower 4720 adhesive (b) after being tested at −40°C.

4.3.3. *80°C Tensile Tests*

Despite having broken close to the grips and not in the necking region, XNR 6852-1 adhesive had more than 100% elongation. Before rupturing, XNR 6852-1 specimens were already in the plastic region, consequently the yield strength of the adhesive could be assessed. It was not possible to determine

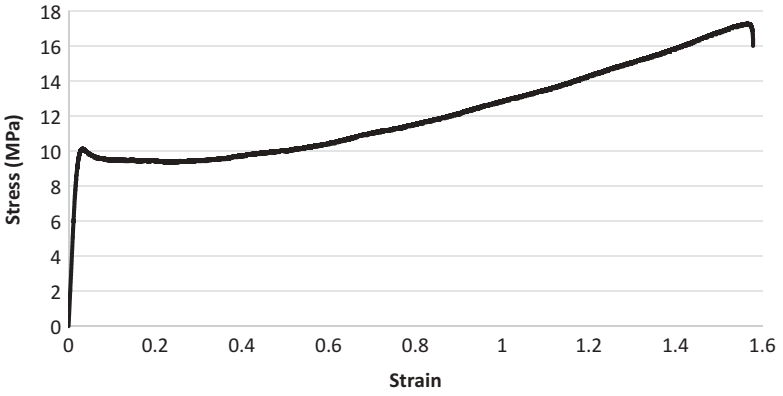

Figure 13. Entire stress–strain curve of a dry XNR 6852-1 specimen tested at 80°C up to failure.

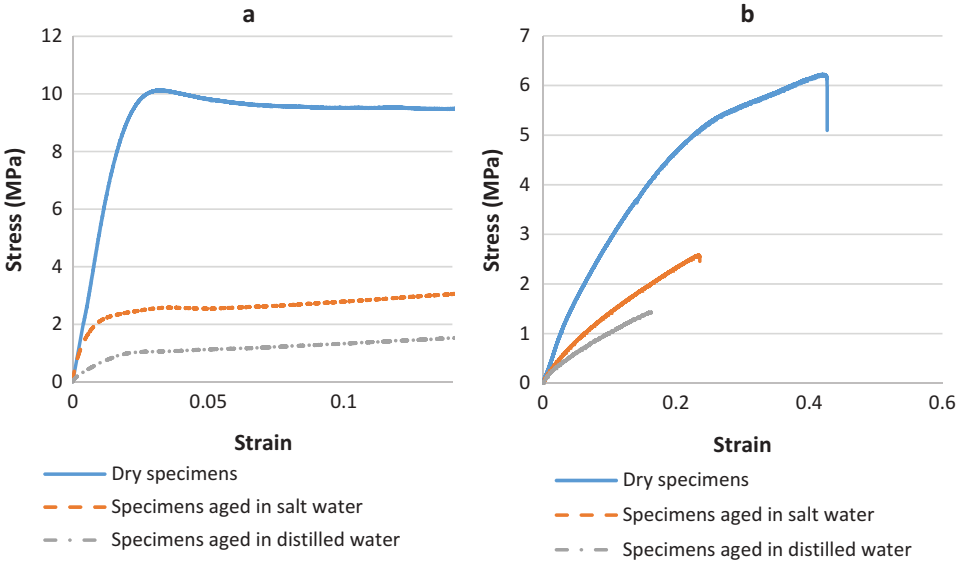

Figure 14. Stress–strain curves of the XNR 6852-1 adhesive (a) and the SikaPower 4720 adhesive (b) as a function of the ageing environment tested at −80°C.

how high the ductility is but, as the specimens broke with more than 100% of strain, one can be sure that it must be higher than 100%. Figure 13 shows a typical stress–strain curve of the dry adhesive tested at 80°C. In Fig. 14, the entire curves were omitted so that the reader can focus on the elastic part of the graph.

The ductility of SikaPower 4720 adhesive also increased when tested at high temperature. At this temperature, the yield stress and the tensile modulus of the adhesives were strongly moisture dependent.

As can be seen in Fig. 15, the XNR 6852-1 adhesive exhibited a very ductile fracture, while SikaPower 4720 showed a brittle fracture.

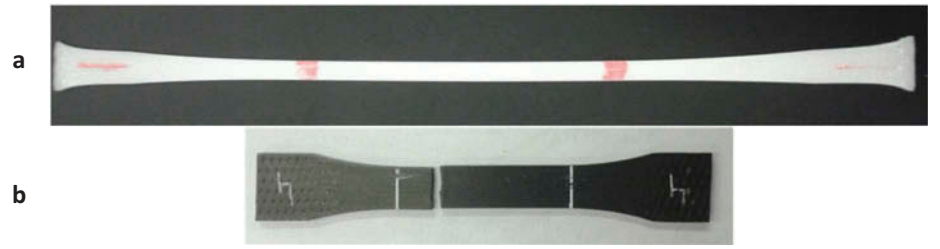

Figure 15. Specimens of XNR 6852-1 adhesive (a) and of SikaPower 4720 adhesive (b) after being tested at 80°C.

4.3.4. *Discussion*

As moisture diffuses into the adhesives, it increases the mobility of its chains. This phenomenon is responsible for lowering Tg of both adhesives and is clearer in SikaPower4720. As a result of increased chain mobility, the stiffness and yield stress of both adhesives also tend to decrease. However, this effect was not clearly visible when the specimens were tested at −40°C because low temperatures tend to decrease the mobility of polymer chains. At this temperature the decrease of polymer chain mobility is much higher than the increase of chain mobility caused by moisture absorption.

XNR6852-1 shows a very significant moisture dependence when tested at 80°C due to its proximity to Tg. At this temperature, the dry specimens are considerably away from Tg while the aged specimens are much closer. As a consequence, the aged specimens show a considerably lower stiffness and yield stress than the dry specimens.

Aged specimens of SikaPower4720 are actually above Tg when tested at 80°C, therefore the dry specimens of this adhesive show a considerably higher strength and stiffness than those that were aged.

The decrease of the yield strength of the adhesives due to the moisture uptake is more pronounced at 80°C than at −40°C. At this temperature, the effect of moisture on the yield stress of the adhesive is minimum and at 80°C maximum.

The yield stress and the Young's modulus of both adhesives were independent of exposure time and tended to level off toward saturation, as was also concluded in other studies [27]. The moisture and temperature-dependent yield stress and moduli of both adhesives are shown in Figs. 16 and 17 and in Figs. 18 and 19, respectively. The higher the temperature, the more the yield stress and modulus of the adhesives was dependent on water uptake.

Results show that the yield strength and stiffness of both adhesives were more affected by the test temperature than by the moisture uptake. This is illustrated in Figs. 16, 17, 18, and 19.

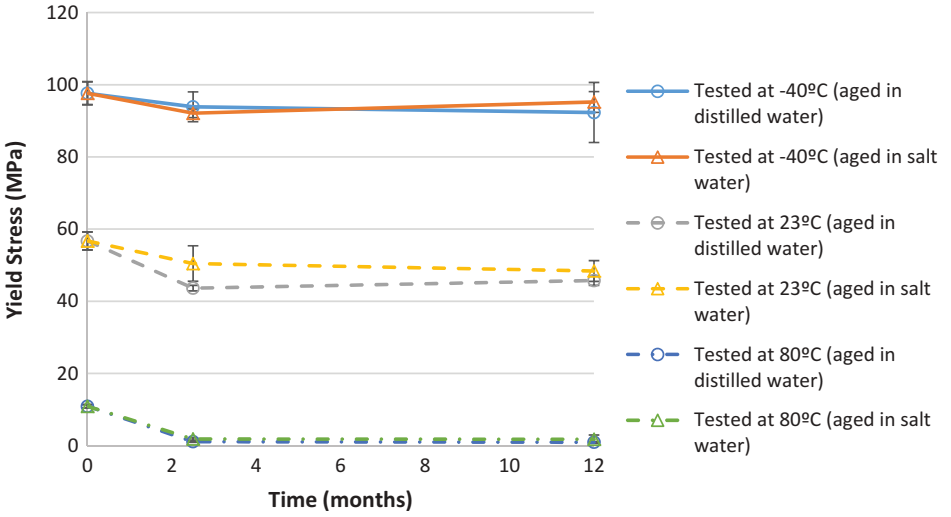

Figure 16. Evolution of the yield stress of XNR 6852-1 adhesive.

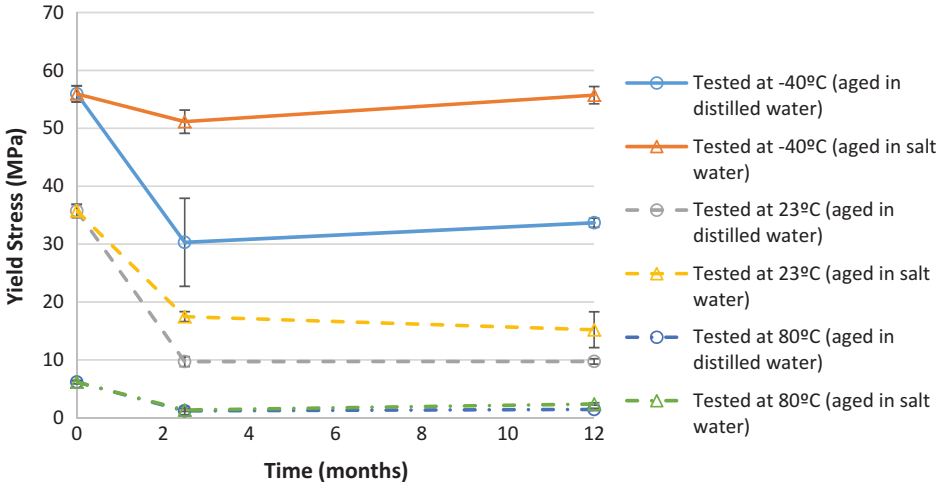

Figure 17. Evolution of the yield stress of XNR 6852-1 adhesive.

5. Conclusion

This work focused on the effect of water uptake and testing temperature on the mechanical behaviour of two epoxy adhesives for the automotive industry. The following conclusions could be drawn:

(1) The Tg of both adhesives decreases with moisture uptake. Similar results have been obtained in numerous studies [8,28].
(2) The Tg of XNR 6852 adhesive is less dependent on the ageing environment than that of SikaPower 4720.

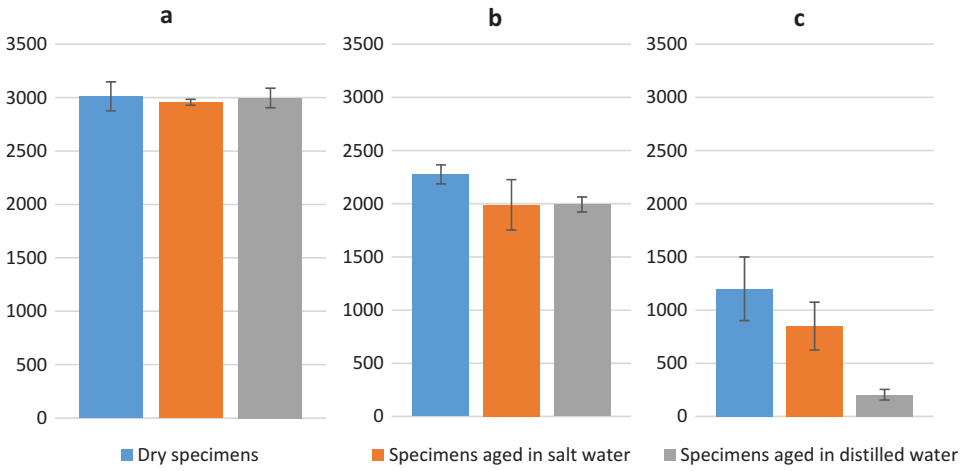

Figure 18. Young's modulus of XNR 6852-1 as a function of moisture uptake and test temperature (values in MPa): (a) tested at −40°C, (b) tested at 23°C, and (c) tested at 80°C.

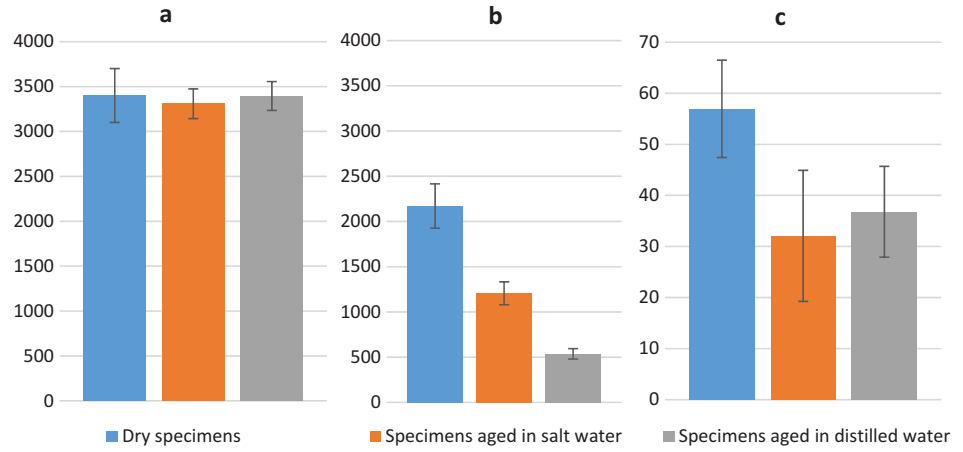

Figure 19. Young's modulus of SikaPower as a function of moisture uptake and test temperature (values in MPa): (a) -tested at −40°C, (b) tested at 23°C, and (c) tested at 80°C.

(3) The moisture uptake of SikaPower 4720 when aged in distilled water is very high for an epoxy adhesive. This is probably a result of two phenomena:
   (a) The Tg of the adhesive is very sensitive to moisture uptake.
   (b) Once Tg approaches the temperature of the ageing environment, the adhesive is more prone to establish hydrogen bonds with the water molecules, further increasing the water uptake and the drop in Tg.

(4) The Tg of SikaPower 4720 adhesive is lower than room temperature when it is aged in distilled water. This has severe consequences on the tensile properties of the adhesive, especially when tested at 80°C.

(5) The tensile properties of both adhesives studied were not dependent on the ageing time.
(6) The tensile properties of the adhesives are affected by temperature and moisture. Moisture causes plasticization in the adhesives, reducing their strength, stiffness, and increasing their ductility. Such results have been obtained by many researchers at room temperature [27,29,30]. However, the adhesive can be more or less dependent on this moisture depending on the test temperature:
    (a) At high temperature XNR 6852-1 aged specimens are very close to their Tg, which makes their stiffness and strength considerably lower than the unaged specimens. In this situation the effect of the moisture uptake is maximum.
    (b) At high temperature SikaPower 4720 aged specimens also show such behaviour. At this temperature the dry specimens are below Tg, while the aged specimens are above it. This causes a reduction in the strength and stiffness of the aged specimens.
    (c) At low temperature, the strength and stiffness of both adhesives increase and the ductility decreases. The effect of the moisture uptake is not very significant.

Acknowledgements

The authors would like to thank Sika for supplying the SikaPower 4720 adhesive and Nagase Chemtex for supplying the XNR 6852-1 adhesive.

Funding

This study was financed by the Fundação para a Ciência e Tecnologia through grant EXCL/EMS-PRO/0084/2012.

References

[1] Banea, M. D., da Silva, L. F. M., Campilho, R. D. S. G., and Sato, C., *J Adhes*. **90**, 16–40 (2014).
[2] Banea, M. D., and da Silva, L. F. M., *Proc. Inst. Mech. Eng. Part L: J. Mater. Des. Appl.* **223**, 1–18 (2009).
[3] Loh, W. K., Crocombe, A. D., Wahab, M. M. A., and Ashcroft, I. A., *Int. J. Adhes. Adhes*. **25**, 1–12 (2005).
[4] Mubashar, A., Ashcroft, I. A., Critchlow, G. W., and Crocombe, A. D., *Int. J. Adhes. Adhes*. **29**, 751–760 (2009).
[5] Ameli, A., Datla, N. V., Papini, M., and Spelt, J. K., *J. Adhes*. **86**, 698–725 (2010).
[6] Lin, Y. C., and Chen, X., *Polymer* **46**, 11994–12003 (2005).
[7] Han X., Crocombe, A. D., Anwar, S. N. R., Hu, P., and Li, W. D., *J. Adhes*. **90**, 420–436 (2014).

[8] Zhou, J. M., and Lucas, J. P., *Polymer* **40**, 5513–5522 (1999).
[9] Zhou, J. M., and Lucas, J. P., *Polymer* **40**, 5505–5512 (1999).
[10] Adamson, M. J., *J. Mater. Sci.* **15**, 1736–1745 (1980).
[11] Adams, R. D., Coppendale, J., Mallick, V., and Al-Hamdan, H., *Int. J. Adhes. Adhes.* **12**, 185–190 (1992).
[12] Deb, A., Malvade, I., Biswas, P., and Schroeder, J., *Int. J. Adhes. Adhes.* **28**, 1–15 (2008).
[13] Banea, M. D., and Silva, L. F. M., *J. Adhes.* **85**, 261–285 (2009).
[14] Srivastava, V. K., *Int. J. Adhes. Adhes.* **23**, 59–67 (2003).
[15] Grant, L. D. R., Adams, R. D., and da Silva, L. F. M., *Int. J. Adhes. Adhes.* **29**, 535–542 (2009).
[16] Banea, M. D., de Sousa, F. S. M., da Silva, L. F. M., Campilho, R. D. S. G., and Pereira, A. M. D., *J. Adhes. Sci. Technol.* **25**, 2461–2474 (2011).
[17] Marques, E. A. S., da Silva, L. F. M., Banea, M. D., and Carbas, R. J. C., *J. Adhes.* **91**, 556–585 (2015).
[18] Banea, M. D., and da Silva, L. F. M., *Proc IMechE, Part L: J. Mater.-Des. Appl.* **224**, 51–62 (2010).
[19] Banea, M. D., da Silva, L. F. M., and Campilho, R. D. S. G., *Int. J. Adhes. Adhes.* **31**, 273–279 (2011).
[20] Pethrick, R. A., *Proc IMechE, Part L: J. Mater.: Des. Appl.* **229**, 349–379 (2014).
[21] Winston, P. W., and Bates, D. H., *Ecology* **41**, 232–237 (1960).
[22] Zhang, Y., Adams, R. D., and da Silva L. F. M., *J. Adhes.* **89**, 785–806 (2013).
[23] Costa, M., Viana, G., Canto, C., da Silva, L., Banea, M., Chaves, F., et al., *Proc IMechE, Part L: J. Mater.: Des. Appl.* Epub ahead of print 7 October 2015. doi:10.1177/1464420715610248.
[24] Carbas, R. J. C., Marques, E. A. S., da Silva, L. F. M., and Lopes, A. M., *J. Adhes.* **90**, 104–119 (2014).
[25] Zhang, Y., Adams, R. D., and da Silva, L. F. M., *J. Adhes.* **90**, 327–345 (2014).
[26] Silva, L. F. M. D., and Sato, C., *Design of Adhesive Joints under Humid Conditions*, (Springer-Verlag, Berlin, Heidelberg, 2013). Chs. 2–7.
[27] Sugiman, S., Crocombe, A. D., and Aschroft, I. A., *Int. J. Adhes. Adhes.* **40**, 224–237 (2013).
[28] Zhang, Y., Adams, R. D., and da Silva, L. F. M., *Int. J. Adhes. Adhes.* **50**, 85–92 (2014).
[29] Barbosa, A. Q., da Silva, L. F. M., and Öchsner, A., *J. Adhes. Sci. Technol.* **29**, 1714–1732 (2015).
[30] Lin, Y. C., and Chen, X., *Polymer* **46**, 11994–12003 (2005).

PAPER 3

Latin American Journal of Solids and Structures
www.lajss.org

Water Diffusion in Double Cantilever Beam Adhesive Joints

Abstract

Structural adhesives are increasingly being used in the aerospace and automotive industries. They allow for light weight vehicles, fuel savings and reduced emissions. However, the environmental degradation of adhesive joints is a major setback in its wide implementation. Moisture degradation of adhesive joints includes plasticization, attacking of the interface, swelling of the adhesive and consequent creation of residual stresses. This may lead to reversible and irreversible damage.

In this work double cantilever beam (DCB) specimens using two different adhesives for the automotive industry were subjected to two different ageing environments. They were tested periodically until the toughness of the adhesives stabilized, which means that they were fully degraded. An association was made between the toughness of the adhesive and the amount of water that it had absorbed. This way it was possible to indirectly measure the water uptake in an adhesive joint taking into account the water uptake properties of the adhesives studied, which had been determined in another study.

It was found that diffusion of water into the studied adhesive joints was faster than diffusion through the bulk adhesive alone. A model that takes into account diffusion through the interface between the adhesive and the adherends was proposed.

Keywords

Hygrothermal ageing,adhesive joints; moisture degradation, double cantilever beam, diffusion

G. Viana [a]
M.Costa [a]
M.D. Banea[b]
L.F.M. da Silva[c]

[a] Instituto de Ciência e Inovação em Engenharia Mecânica e Engenharia Industrial (INEGI), 4200-465 Oporto, Portugal
[b] Federal Centre of Technological Education in Rio de Janeiro (CEFET), Av. Maracanã, 229, Rio de Janeiro, Brazil
[c] Departamento de Engenharia Mecânica, Faculdade de Engenharia da Universidade do Porto (FEUP), 4200-465 Oporto, Portugal

http://dx.doi.org/10.1590/1679-78253040

Received 02.05.2016
Accepted 16.11.2016
Available online 29.11.2016

1 INTRODUCTION

Structural adhesives are increasingly being used in the transport industries. They allow for light weight vehicles, energy savings and reduced emissions. The main advantages include more uniform load distribution, higher fatigue resistance than other traditional joining methods and the ability to

join dissimilar materials (Banea et al. 2014). Also, due to their high vulnerability to stress concentration, the only viable way to join composite materials, such as fiber reinforced plastic, is with a structural adhesive (Banea and da Silva 2009). However, the environmental degradation of adhesive joints is a major setback in their wide implementation (Costa et al. 2016d).

Moisture degradation of adhesives include reduction of their mechanical properties, inducing plasticization (Costa et al. 2016a, Costa et al. 2016b, Costa et al. 2016c, Sugiman, Crocombe and Aschroft 2013, Wylde and Spelt 1998). The deleterious effects are greater in adhesive joints as the degradation of the adhesive-adherend interface may cause interfacial failure.

The water diffusion in adhesives is frequently controlled by the Fick's laws. Fickian sorption happens when the diffusion is much slower than relaxation. In this situation, the uptake will be proportional to the square root of exposure time. When the opposite occurs, one is in the presence of case II diffusion, in which the water uptake is directly proportional to the exposure time. In this case, a fully saturated and swollen front advances against the unpenetrated polymer (2013).

Although fickian diffusion is the most common uptake behavior in adhesives, non-fickian diffusion is not uncommon. Other models have been developed, such as the dual fickian diffusion (Loh et al. 2005), delayed dual fickian (Mubashar et al. 2009) and the Langmuir model (Ameli et al. 2010). In many cases the water uptake may be fickian under certain environmental situations and non-fickian under others. Generally non fickian behaviour is more prone to happen at higher temperatures (Zhou and Lucas 1995), higher relative humidity (Ameli et al. 2010, Loh et al. 2005) and smaller thicknesses of the bulk adhesive specimen (Loh et al. 2005). There is also evidence that while a bulk adhesive may have a fickian diffusion behaviour, the same adhesive in a joint may have a case II diffusion behaviour (Liljedahl et al. 2009).

The rate at which the water is absorbed and the maximum water uptake depend on environmental factors, such as the relative humidity and temperature and on the thickness (Loh et al. 2005, Y.C. Lin 2005) and the stress state of the adhesive (X. Han 2014).

As the water diffuses into the adhesive, some of this moisture becomes bound water. Bound water generally increases with exposure time and temperature (Zhou and Lucas 1999a, Zhou and Lucas 1999b). Unlike the free water that occupies the free space of the adhesive, this bound water is responsible for the volumetric changes that are observed in adhesives under high humidity environments, which may cause residual stresses in adhesive joints (Adamson 1980). Zhou and Lucas (Zhou and Lucas 1999a, Zhou and Lucas 1999b) have found two types of bound water: Type I involves water molecules forming a single hydrogen bond while type II results from water forming multiple hydrogen bonds. Type I bound water acts as a plasticizer, increasing the chains segment mobility. It is responsible for decreasing the glass transition temperature (Tg) (Barbosa, da Silva and Ochsner 2015, Zhang, Adams and da Silva 2014, Zhou and Lucas 1999b). If the temperature is high and the exposure time is long, type II bound water may also occur. This type of bound water is responsible for creating secondary cross-linking (Zhou and Lucas 1999a), which lessens the extent of Tg depression (Zhou and Lucas 1999b). While type I bound water can be removed at low temperature, in order to remove type II bound water, the adhesive must be subjected to relatively high temperatures (Zhou and Lucas 1999b).

Gravimetric methods are usually used in order to measure the water uptake of an adhesive (2012). This consists simply in subjecting a plate of bulk adhesive to an ageing environment, such

as distilled water, a salt solution, air with a particular relative humidity, or other environments compatible with what the adhesive will be subjected in its service life, such as toluene (Zhang et al. 2014), and measuring the weight change over time with a precision scale. This method is, however, very difficult to use in an adhesive joint, which usually uses a very low amount of adhesive, whose weight change cannot be measured with common precision scales. In order to overcome this difficulty and determine the average water uptake or the moisture profile in an adhesive joint, other techniques have been used. Among these techniques is the FTIR (Fourier transform infrared spectroscopy) -transmission spectroscopy (Wapner and Grundmeier 2004) and nuclear reaction analysis (Liljedahl et al. 2009).

(Zannideffarges and Shanahan 1995) have tested torsional joints and bulk tensile and compressive specimens after ageing them for different amounts of time. The modulus of both the bulk specimens and the torsional joints were monitored as a function of the ageing time. Taking the evolution of the Young's modulus into account, approximations to the diffusion coefficients of the joints and the bulk specimens were computed and it was found that the diffusion coefficient of the joints was much higher than the bulk specimens'.

(Kinloch, Little and Watts 2000) have concluded that relatively viscous adhesives may have difficulty penetrating in the pores and gaps of substrates, which may lead to premature rupture of adhesive joints, which are subjected to moist environments, either due to the hydration of the uppermost regions of the oxide layer or due to weakening of the adhesive-adherend interface. If a low viscosity primer is applied prior to bonding on a phosphoric acid anodized surface, the results are much improved because the primer will fill in the gaps which would be otherwise filled with water.

In this study, the toughness of two epoxy adhesives that were subjected to two different ageing environments: distilled water and a saturated water solution of NaCl (referred throughout this paper as "salt water" and is equivalent to subjecting the specimens to a 75% RH environment (Winston and Bates 1960)). The specimens were tested periodically until no change in the fracture toughness was perceptible. At this point it was considered that the specimens were fully saturated. It was found that the time it took for the specimens to saturate was shorter than if only the properties of the bulk adhesive were considered. Based on this information, the approximate diffusion coefficients of the interfaces were computed. This allows a more accurate prediction of the water diffusion in complex adhesive joints, which leads to more accurate predictions of the strength of aged adhesive joints.

2 MATERIALS

2.1 Adhesives

The adhesives, which were developed for the automotive industry and were recommended by Sika® and Nagase® for this durability study are the following:

- The epoxy adhesive XNR 6852-1, supplied by NAGASE CHEMTEX® (Osaka, Japan). This adhesive is a one-part system that cures at 150°C for 3 h. It has a high strength and high displacement to failure;

- The epoxy adhesive SikaPower 4720, supplied by SIKA® (Portugal, Vila Nova de Gaia). This adhesive is a two-part system that has the advantage of curing at room temperature for 24 hours.

The stress-displacement curves of bulk tensile specimens of these adhesives obtained in a previous study (Viana et al. 2016) are shown in Figure 1.

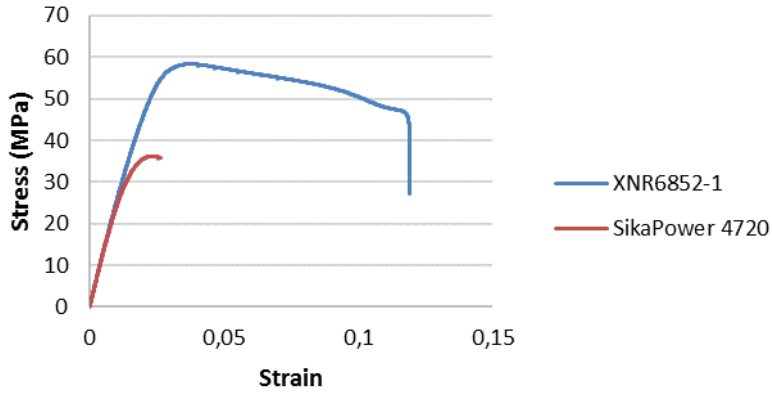

Figure 1: Stress-displacement curves of both adhesives used.

2.1 Substrates

In order to measure the toughness of adhesive joints, DCB specimens were used. To avoid plastic deformation while testing, the substrates were made of the high strength aluminium alloy 6082-T6. In a standard DCB specimen, whose length is much greater than the width, water sorption occurs almost entirely along the width direction (Hua et al. 2006). However, they take very long time to reach saturation. Instead of using this standard specimen geometry, a smaller geometry (shown in Figure 2) was used.

Some studies about the effect of DCB specimen geometry on the fracture energy (G_{IC}) of the adhesive layer have been undertaken (Campilho et al. 2014, Costa et al. 2015). Results show that the geometry of the substrates may have influence on the measured toughness of the adhesive. This suggests that G_{IC} may not be a material parameter, but a geometry-dependent quantity instead. In this study, in order to allow for a fast ingress of water into the adhesive layer, small DCB specimens were used. The results obtained should be compared only between specimens of the same geometry.

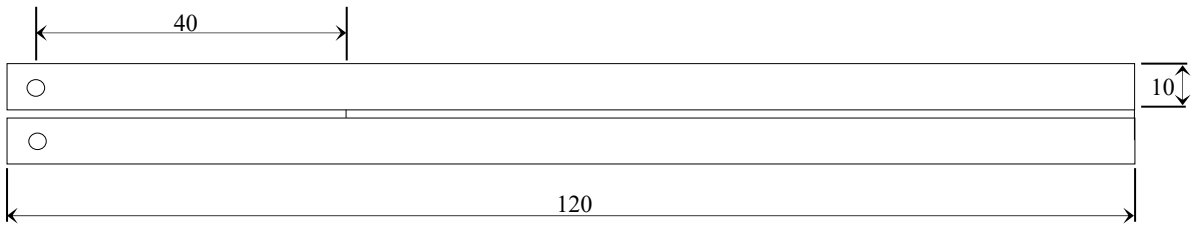

Figure 2: Geometry of the DCB specimens (dimensions in mm).

3 EXPERIMENTAL PROCEDURE

3.1 Specimen Fabrication

Prior to bonding, the surfaces of the DCB substrates were abraded with a 80 grit CSi sandpaper, cleaned in an ultrasonic acetone bath and received a phosphoric acid anodisation. Less than a day after being anodized, the specimens were bonded and left to cure for 3h at 150°C or for 24h at room temperature, according to the indication of the manufacturer of each adhesive used. After the cure cycle the excess adhesive was removed and the specimens were left to dry for at least 3 weeks in a dry desicator. After this time, the specimens of each adhesive were divided into three groups:

- Dry specimens, which were ready to be tested;
- Specimens to be aged in a saturated solution of NaCl at 32.5°C (refered throughout this paper as "salt water"), which is equivalent to ageing them in a 75% RH environment (Winston and Bates 1960);
- Specimens to be aged in distilled water at 32.5°C.

In this study, specimens with reduced dimensions were used. This allowed time efficient production and ageing.

3.2 Test Procedure

After all specimens had been produced and dried in a dry desicator, they were separated into the three different groups mentioned in the previous section. The dry specimens were immediately tested while the specimens to be aged were placed in their respective ageing environment and tested periodically at a displacement rate of 0.5 mm/min until their toughness stabilized, meaning that they were fully degraded by the absorbed water.

The effect of moisture uptake in the adhesives studied tends to be more pronounced at 80°C than at room or lower temperatures (Viana et al. 2016). For this reason, it was decided that the tests should be made at 80°C, as it would be possible to better associate the toughness of the adhesive to the moisture that the joint has absorbed. A climatic chamber coupled with an universal test machine (INSTRON® model 3367) allowed to test the specimens at 80°C. Right before testing, the specimens were left inside the climatic chamber at 80°C for 10 minutes to make sure that the temperature was exactly 80°C in the entire specimen.

4 EXPERIMENTAL RESULTS

After testing, the fracture surfaces were observed visually. As can be seen in Figure 3, the failure modes were interfacial for every case.

The toughness of the aged specimens was measured regularly. The results were plotted as a function of the ageing time, as can be seen in Figure 4. The longer the specimens were kept immersed in water (either distilled water or salt water), the greater the drop in their toughness was, until it starts to level off.

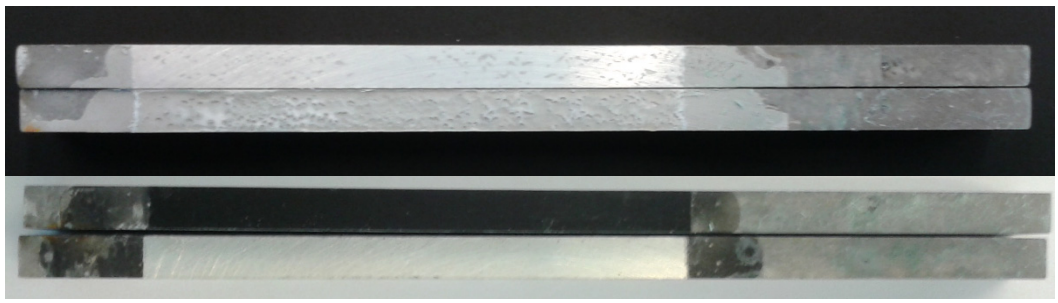

a. XNR 6852-1
b. SikaPower 4720

Figure 3: Fracture surfaces of both adhesives used.

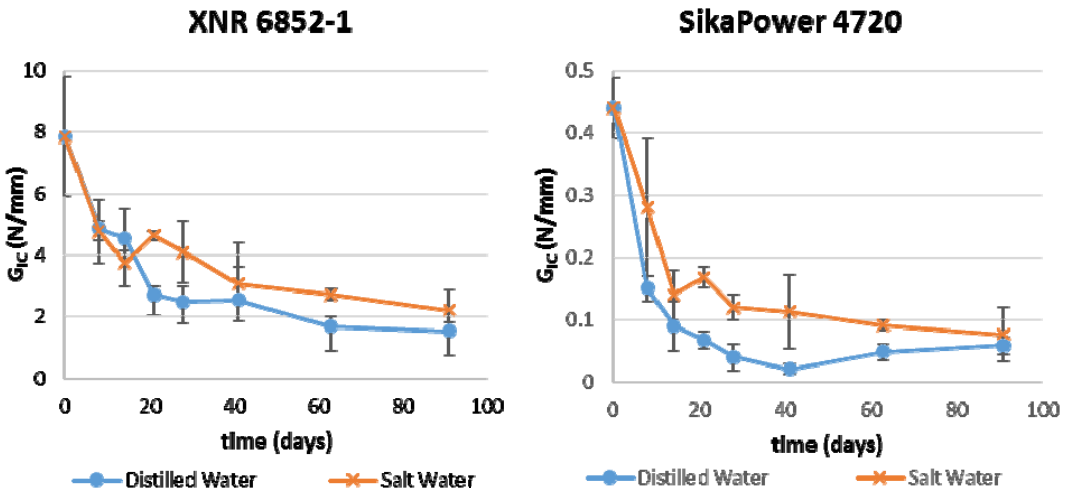

Figure 4: Fracture energy of both adhesives studied as a function of ageing time and ageing environment.

The rate of toughness loss was maximum at the beginning of the exposure and kept diminishing until equilibrium was attained. As it would be expectable, the final toughness of the specimens that were kept in salt water was higher than that of the specimens immersed in distilled water.

Once the toughness reached a plateau, it was considered that the specimens were fully saturated. This way, it is possible to make a correlation between the measured toughness and the water content of the specimen, taking also into account the equilibrium water uptake of the bulk adhesive measured in a previous study (Viana et al. 2016). Although some specimens did not reach a clear plateau, it is perceptible that the toughness of the specimens would not decrease significantly further, meaning that they were almost fully saturated.

It was considered that these specimens were dry when they were first tested and fully saturated at the time of the last toughness measurement. Considering that the G_{IC} that was measured changes linearly with the moisture concentration of the adhesive, using linear interpolation, the moisture concentration as a function of the ageing time was calculated. Figure 5 shows the calculated water uptake of both adhesives as a function of the square root of time.

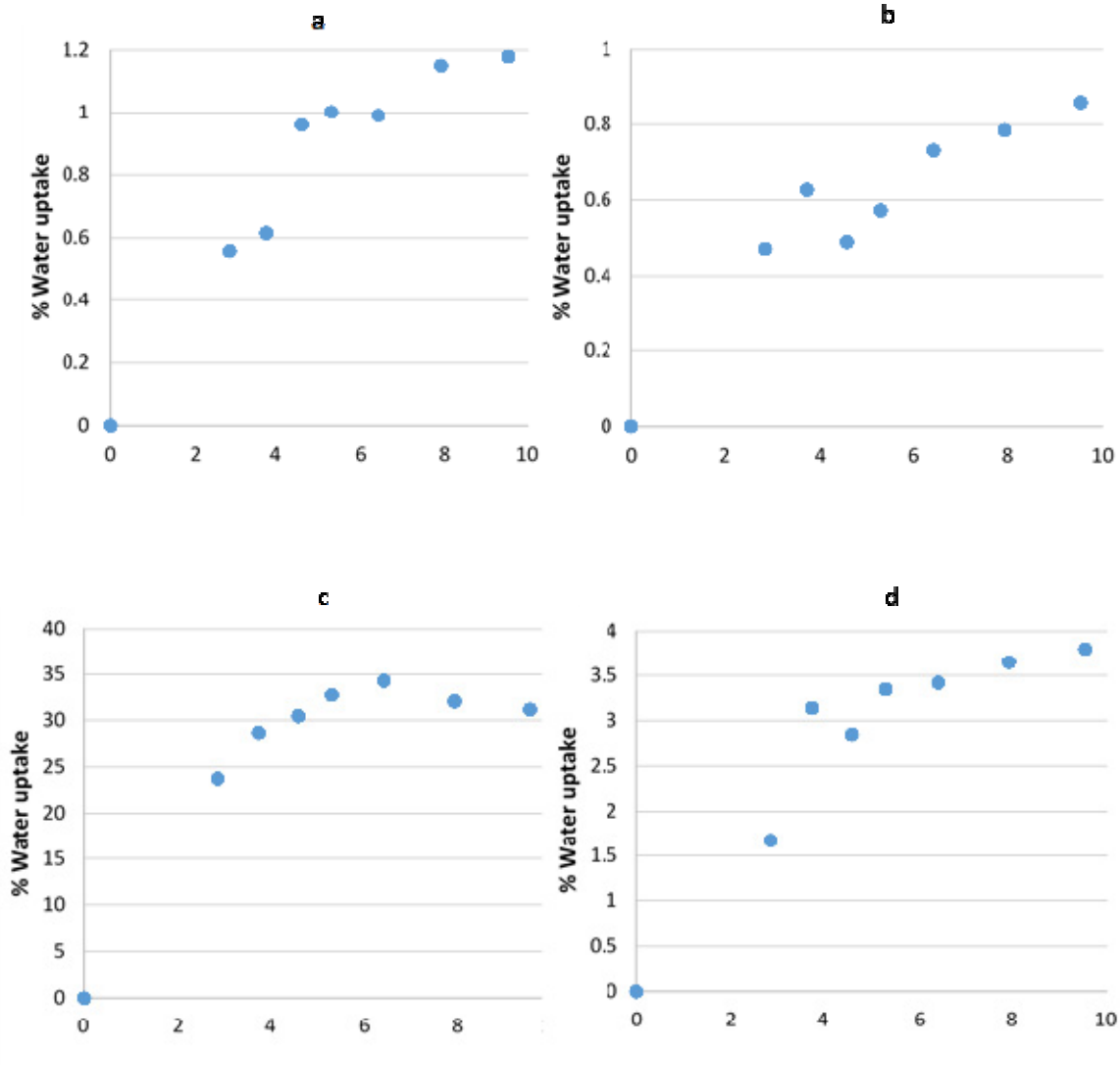

a. XNR 6852-1 aged in distilled water
b. XNR 6852-1 aged in salt water
c. SikaPower 4720 aged in distilled water
d. SikaPower 4720 aged in salt water

Figure 5: Water uptake of both adhesives used as a function of ageing time and ageing environment.

5 NUMERICAL MODELLING

The water uptake in the adhesive joint was modeled using the Finite element method (FEM). As the bondline is very long, diffusion only in the width direction is enough to predict the water absorption of the adhesive joint (Hua et al. 2006). The adhesive joints reached their maximum moisture uptake sooner than expected if only sorption in the bulk adhesive was considered, taking into account the adhesive diffusion properties determined in a previous study (Viana et al. 2016). This is

thought to be due to interfacial diffusion of water. In order to model this phenomenon, two types of model were adopted:

1. A **one dimensional model**, in which the overall water uptake of the joint was modeled. The diffusion along the width of the joint was modeled using unidimensional beam elements. The diffusion coefficient attributed to these elements were fitted so that the numerical prediction would match the moisture uptake that was calculated, taking into account the experimentally measured toughness. This way it was possible to compute the overall diffusion coefficient ($D_{average}$) of the joint through an inverse method;
2. A **two dimensional model**, in which the water uptake of the bulk adhesive and the water uptake in the adhesive-adherend interface were modeled separately. In this model, the increase in the diffusion speed is attributed to capillary diffusion happening at the interface between the adhesive and the adherends. In order to model this phenomenon, two layers were considered (see Figure 6):
   a. A layer of adhesive, whose diffusion properties were determined in a previous study (Viana et al. 2016) (see Table 1). Depending on the ageing environment, these adhesives may present Fickian or dual Fickian behavior. For this reason, two diffusion coefficients and two equilibrium moisture uptakes are presented;
   b. A very thin layer that represents the interface. The diffusion coefficient of this layer was fitted so that the water uptake of the adhesive would match the water uptake that was calculated from the experimentally measured toughness.

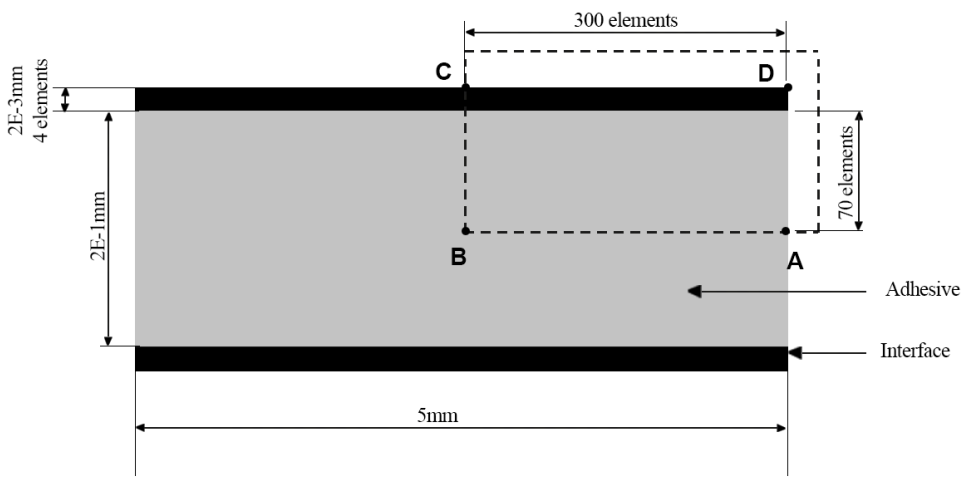

Figure 6: Geometry of the model used to predict interfacial moisture uptake.
Due to the symetry, only the dotted rectangle was modeled.

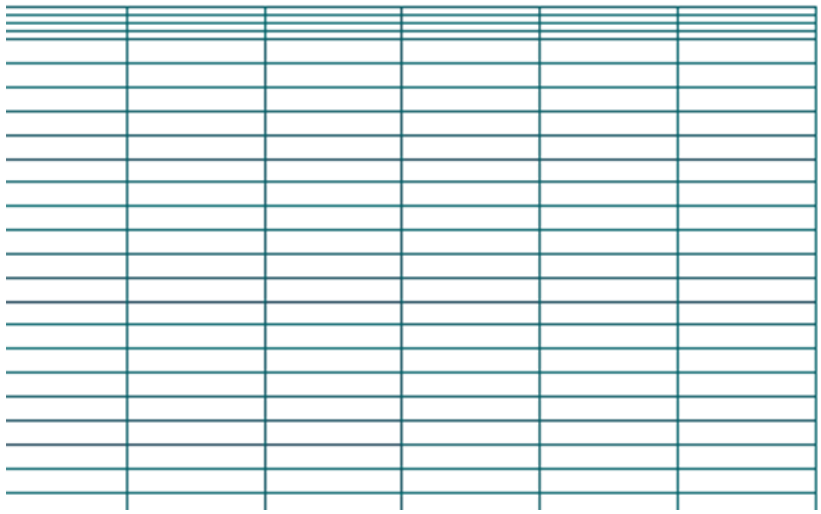

Figure 7: Detail of the mesh used used in the two dimensional model (area contoured in Figure 6).

		D_1 (m^2/s)	mwt_1	D_2 (m^2/s)	mwt_2
XNR 6852-1	Distilled Water	6.0E-13	0.0095	8E-14	0.0023
	Salt Water	6.0E-13	0.0080	8E-14	0.0006
SikaPower 4720	Distilled Water	1.2E-13	0.325	-	-
	Salt Water	2.6E-13	0.020	2.5E-14	0.018

mwt1- Equilibrium moisture content 1
mwt2- Equilibrium moisture content 2

Table 1: Moisture diffusion parameters of both adhesives studied.

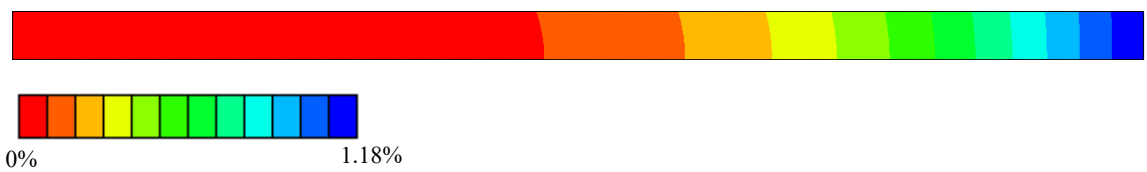

Figure 8: Numerical prediction of the moisture profile of XNR 6852-1 after 24 hours of ageing. The upper bar represents one quarter of the adhesive layer and the lower bar indicates, through a code of colours, its prediction of moisture uptake.

	Ageing environment	$D_{average}(m^2/s)$ (Obtained with the 1D model)	$D_{interface}(m^2/s)$ (Obtained with the 2D model)
XNR 6852-1	Distilled water	1.8E-12	5.5E-11
	Salt water	1.5E-12	5.0E-11
SikaPower 4720	Distilled water	4.5E-12	2.2E-10
	Salt water	1.6E-12	6.2E-11

Table 2: Moisture diffusion parameters of the joints bonded with both adhesives studied.

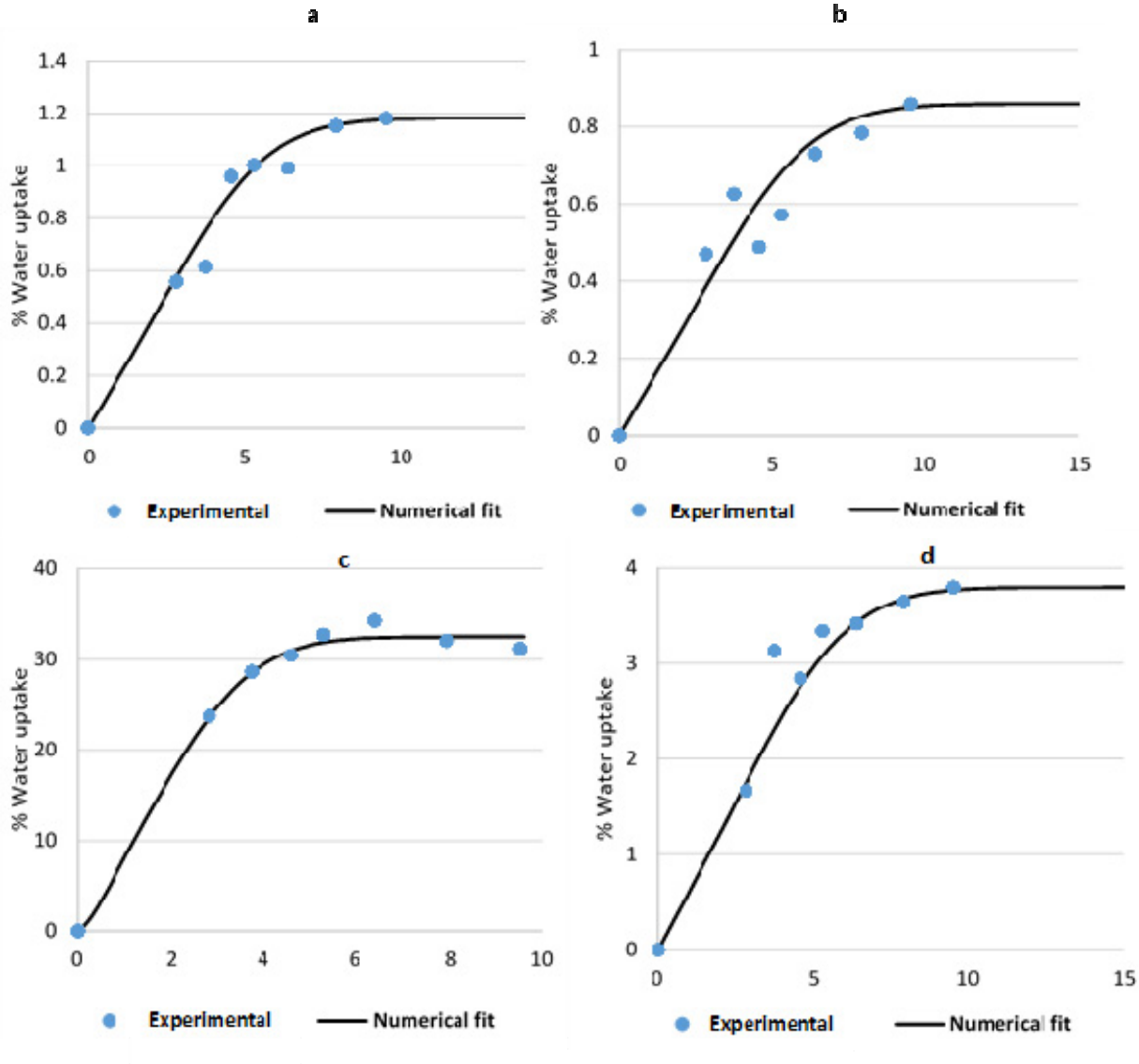

a. XNR 6852-1 aged in distilled water
b. XNR 6852-1 aged in salt water
c. SikaPower 4720 aged in distilled water
d. SikaPower 4720 aged in salt water

Figure 9: Experimental and numerical prediction of the adhesive joints studied.

This way it was possible to compute the diffusion coefficient of the interface ($D_{interface}$) through an inverse method.

As the coefficient of diffusion was set to be higher at the interface, diffusion of water occurs preferentially in this region, which is then responsible for bringing moisture deeper into the adhesive layer. This moisture is quickly absorbed by the adhesive. Figure 8 shows the computed moisture uptake of XNR 6852-1 adhesive after 24 hours of immersion.

The phenomenon of diffusion shares mathematics with the phenomenon of heat conduction and it is possible to model the moisture uptake of the adhesive simply as a heat transfer problem. The equivalent parameters to permeability coefficient, diffusion coefficient and solubility coefficient are thermal conductivity, thermal diffusivity and heat capacity respectively. In both the one dimensional model and the two dimensional model the heat transfer elements available at the Abaqus® library DC1D2 and DC2D4 for the 1D and 2D analyses, respectively, were used.

Due to the symmetry of the problem, in order to reduce the computation effort and to increase the speed of the analysis only one quarter of the section of the specimens was modelled (see Figure 6). A detail of the mesh is shown in Figure 7. Across line segments [AB], [BC] and [CD], represented in Figure 6, no mass transfer was allowed. In the line segment [AD] equilibrium moisture uptake is attained instantly because it is in contact with the ageing environment.

Using this methodology, both the average diffusion coefficient and the diffusion coefficient of the interface were determined. They are shown in Table 2. The comparison between the experimental diffusion and the numerical predictions are shown in Figure 9. Although there is some dispersion in the results, which is expected given the method used, the numerical prediction fits the experimental results well.

6 DISCUSSION

Experimental results show that the water diffusion in bonded joints was faster than in the bulk adhesive. Other authors have obtained similar results, using different methods (Liljedahl et al. 2009, Wapner and Grundmeier 2004, Zannideffarges and Shanahan 1995). The comparison between the diffusion coefficients obtained in these studies are summarized in Table 3. From the analysis of this table, it is possible to conclude that when in an adhesive joint, the adhesive usually absorbs water faster than when in bulk.

Reference	Method		D (m^2/s)	Ageing temperature
(Zannideffarges and Shanahan 1995)	Mechanical loading (change in adhesive's modulus)		5.3E-12	70°C
	Gravimetric measurement		1.4E-12	
(Wapner and Grundmeier 2004)	FTIR-transmission microscopy		1.13E-13	21°C
(Frantzis 1998)	Gravimetric measurement		1.0E-13	
Present study	Mechanical loading (change in adhesive's toughness)	SikaPower 4720	[1.5-4.6]E-12*	32.5°C
		XNR 6852-1	[1.5-1.8]E-12*	
	Gravimetric measurement	SikaPower 4720	[1.2-2.6]E-13*	
		XNR 6852-1	6E-13	

*These values vary if the adhesive is aged in salt water or distilled water.

Table 3: Comparison between the average diffusion coefficients determined in this work and those found in other studies.

This behaviour might be explained by the fact that in an adhesive joint, as the adhesive is constrained by metallic adherends, the shrinkage due to curing could lead to a less dense structure near the interface and facilitate local water uptake. The orientation of the polymer closer to the substrates could be different and enhance diffusion in that region. Water can diffuse at the interface by capillary diffusion through voids that exist between the adhesive and the adherends(Zannideffarges and Shanahan 1995). On the other hand, the presence of these voids allow the rapid ingress of water and enable pockets of water to be developed along the interface, which may promote diffusion in this region (Kinloch et al. 2000). Another possibility has to do with the creation of stresses due to the swelling of the adhesive. This residual stress may enhance the diffusion and promote case II diffusion, as suggested by Liljedahl et al. (Liljedahl et al. 2009).

The speed of interfacial moisture diffusion depends on the roughness of the substrate and on the capacity of the adhesive to fill in the gaps of the adherends. In order to avoid this problem, maybe if a low viscosity primer capable of filling in the small gaps that exist in the adhesive surface is applied, adsorption of water by the substrates would be reduced (Kinloch et al. 2000) and the water uptake would be slower.

7 CONCLUSION

This work focused on the measurement of the toughness of aged DCB adhesive joints. Tests were made after different ageing times and a strong reduction in the toughness of the adhesive was found. From the variation of toughness of the specimens, the moisture uptake of the adhesive was calculated. The speed of moisture ingress into the adhesive was higher than expected if only the moisture uptake through the bulk adhesive was considered. It is thought that this is due to capillary diffusion enhanced by voids that exist at the interface between the adhesive and the adherends. A finite element model was proposed in order to predict the average diffusion coefficient and the diffusion coefficient of the interface. The numerical prediction fits the experimental results well. This information can help predict the moisture uptake of more complex joints.

In order to predict the mechanical behaviour of adhesive joints, it is very important to be able to predict the moisture uptake in each point of the adhesive layer. This study sheds some light on this subject and allows a better prediction of the water uptake in adhesive joints. However, more work is needed in order to assess the influence of the roughness of the substrates and the capability of the adhesive to fill the voids of the substrates on the interfacial diffusion coefficient.

Aknowledgements

The authors would like to thank Sika for supplying SikaPower 4720 adhesive and Nagase Chemtex for supplying XNR 6852-1 adhesive. This study was financed by the Fundação para a Ciência e Tecnologia through grant EXCL/EMS-PRO/0084/2012.

References

Adamson, M.J. (1980), Thermal-Expansion and Swelling of Cured Epoxy-Resin Used in Graphite-Epoxy Composite-Materials, *Journal of Materials Science,* 15**,** 1736-1745.

Ameli, A., Datla, N.V., Papini, M., Spelt, J.K. (2010), Hygrothermal Properties of Highly Toughened Epoxy Adhesives, *Journal of Adhesion,* 86**,** 698-725.

Banea, M.D., Silva, L.F.M. da (2009), Adhesively bonded joints in composite materials: an overview, *Proceedings of the Institution of Mechanical Engineers, Part L: Journal of Materials: Design and Applications,* 223**,** 1-18.

Banea, M.D., Silva, L.F.M. da, Campilho, R.D.S.G., Sato, C. (2014), Smart Adhesive Joints: An Overview of Recent Developments, *Journal of Adhesion,* 90**,** 16-40.

Barbosa, A.Q., Silva, L.F.M. da, Ochsner, A. (2015), Hygrothermal aging of an adhesive reinforced with microparticles of cork, *Journal of Adhesion Science and Technology,* 29**,** 1714-1732.

Campilho, R.D.S.G., Moura, D.C., Banea, M.D., Silva, L.F.M. da (2014), Adherend thickness effect on the tensile fracture toughness of a structural adhesive using an optical data acquisition method, *International Journal of Adhesion and Adhesives,* 53**,** 15-22.

Costa, M., Viana, G., Canto, C., Silva, L. da, Banea, M., Chaves, F., Campilho, R., Fernandes, A. (2015), Effect of the size reduction on the bulk tensile and double cantilever beam specimens used in cohesive zone models, *Proc IMechE, Part L: Journal of Materials: Design and Applications***,** 1-15.

Costa, M., Viana, G., Silva, L.F.M. da, Campilho, R.D.S.G. (2016a), Determination of the fracture envelope of an adhesive joint as a function moisture, *Materialwissenschaft und Werkstofftechnik*.

Costa, M., Viana, G., Silva, L.F.M. da, Campilho, R.D.S.G. (2016b), Effect of humidity on the fatigue behaviour of adhesively bonded aluminium joints, *Latin American Journal of Solids and Structures*, 13, 174-187.

Costa, M., Viana, G., Silva, L.F.M. da, Campilho, R.D.S.G. (2016c), Effect of humidity on the mechanical properties of adhesively bonded aluminium joints, *Journal of Materials Design and Applications***,** 1-10.

Costa, M., Viana, G., Silva, L.F.M. da, Campilho, R.D.S.G. (2017), Environmental effect on the fatigue degradation of adhesive joints: a review, *The Journal of Adhesion*, 93, 127-146.

Frantzis, P. (1998), Environmental Attack on Adhesive Joints: Part I:Test Equipment, *International Journal Series A Solid Mechanics and Material Engineering,* 41**,** 231-242.

Hua, Y., Crocombe, A.D., Wahab, M.A., Ashcroft, I.A. (2006), Modelling environmental degradation in EA9321-bonded joints using a progressive damage failure model, *Journal of Adhesion,* 82**,** 135-160.

Han, X., Crocombe, A.D., Anwar, S.N.R., Hu, P., Li, W.D. (2014), The Effect of a Hot–Wet Environment on Adhesively Bonded Joints Under a Sustained Load, *The Journal of Adhesion,* 90**,** 420-436.

Kinloch, A.J., Little, M.S.G., Watts, J.F. (2000), The role of the interphase in the environmental failure of adhesive joints, *Acta Materialia,* 48**,** 4543-4553.

Liljedahl, C.D.M., Crocombe, A.D., Gauntlett, F.E., Rihawy, M.S., Clough, A.S. (2009), Characterising moisture ingress in adhesively bonded joints using nuclear reaction analysis, *International Journal of Adhesion and Adhesives,* 29**,** 356-360.

Lin, Y.C., Chen, X. (2005), Moisture sorption–desorption–resorption characteristics and its effect on the mechanical behavior of the epoxy system, *Polymer***,** 11994–12003.

Loh, W.K., Crocombe, A.D., Wahab, M.M.A. Ashcroft, I.A. (2005), Modelling anomalous moisture uptake, swelling and thermal characteristics of a rubber toughened epoxy adhesive, *International Journal of Adhesion and Adhesives,* 25**,** 1-12.

Mubashar, A., Ashcroft, I.A., Critchlow, G.W., Crocombe, A.D. (2009), Moisture absorption-desorption effects in adhesive joints, *International Journal of Adhesion and Adhesives,* 29**,** 751-760.

Silva, L.F.M. da, Dillard, D., Blackman, B. & Adams, R.D. (2012), Testing adhesive joints - Best practices.

Silva, L.F.M. da, Sato, C. (2013), Design of Adhesive Joints under Humid Conditions.

Sugiman, S., Crocombe, A.D., Aschroft, I.A. (2013), Experimental and numerical investigation of the static response of environmentally aged adhesively bonded joints, *International Journal of Adhesion and Adhesives,* 40**,** 224-237.

Viana, G., Costa, M., Banea, M.D., Silva, L. da (2017), Behaviour of environmentally degraded epoxy adhesives as a function of temperature (2017), *The Journal of Adhesion*, 93, 95-112.

Wapner, K., Grundmeier, G. (2004), Spatially resolved measurements of the diffusion of water in a model adhesive/silicon lap joint using FTIR-transmission-microscopy, *International Journal of Adhesion and Adhesives,* 24**,** 193-200.

Winston, P.W., Bates, D.H. (1960), Saturated Solutions for the Control of Humidity in Biological-Research, *Ecology,* 41**,** 232-237.

Wylde, J.W., Spelt, J.K. (1998), Measurement of adhesive joint fracture properties as a function of environmental degradation, *International Journal of Adhesion and Adhesives,* 18**,** 237-246.

Zannideffarges, M.P., Shanahan, M.E.R. (1995), Diffusion of Water into an Epoxy Adhesive - Comparison between Bulk Behavior and Adhesive Joints, *International Journal of Adhesion and Adhesives,* 15**,** 137-142.

Zhang, Y., Adams, R.D., Silva, L.F.M. da (2014), Absorption and glass transition temperature of adhesives exposed to water and toluene, *International Journal of Adhesion and Adhesives,* 50**,** 85-92.

Zhou, J.M., Lucas, J.P. (1995), The Effects of a Water Environment on Anomalous Absorption Behavior in Graphite-Epoxy Composites, *Composites Science and Technology,* 53**,** 57-64.

Zhou, J.M., Lucas, J.P. (1999a), Hygrothermal effects of epoxy resin. Part I: the nature of water in epoxy, *Polymer,* 40**,** 5505-5512.

Zhou, J.M., Lucas, J.P. (1999b), Hygrothermal effects of epoxy resin. Part II: variations of glass transition temperature, *Polymer,* 40**,** 5513-5522.

PAPER 4

Taylor & Francis
Taylor & Francis Group

Journal of Adhesion Science and Technology

ISSN: 0169-4243 (Print) 1568-5616 (Online) Journal homepage: http://www.tandfonline.com/loi/tast20

Moisture and temperature degradation of double cantilever beam adhesive joints

G. Viana, M. Costa, M. D. Banea & L. F. M. da Silva

To cite this article: G. Viana, M. Costa, M. D. Banea & L. F. M. da Silva (2017) Moisture and temperature degradation of double cantilever beam adhesive joints, Journal of Adhesion Science and Technology, 31:16, 1824-1838, DOI: 10.1080/01694243.2017.1284640

To link to this article: https://doi.org/10.1080/01694243.2017.1284640

Published online: 31 Jan 2017.

JOURNAL OF ADHESION SCIENCE AND TECHNOLOGY, 2017
VOL. 31, NO. 16, 1824–1838
https://doi.org/10.1080/01694243.2017.1284640

Taylor & Francis
Taylor & Francis Group

Moisture and temperature degradation of double cantilever beam adhesive joints

G. Viana[b], M. Costa[b], M. D. Banea[c] and L. F. M. da Silva[a]

[a]Departamento de Engenharia Mecânica, Faculdade de Engenharia da Universidade do Porto (FEUP), Oporto, Portugal; [b]Instituto de Ciência e Inovação em Engenharia Mecânica e Engenharia Industrial (INEGI), Oporto, Portugal; [c]Federal Centre of Technological Education in Rio de Janeiro (CEFET), Rio de Janeiro, Brazil

ABSTRACT

In this work, the double cantilever beam (DCB) test is analysed in order to evaluate the combined effect of temperature and moisture on the mode I fracture toughness of adhesives used in the automotive industry. Very few studies focus on the combined effect of temperature and moisture on the mechanical behaviour of adhesive joints. To the authors' knowledge, the simultaneous effect of these conditions on the fracture toughness of adhesive joints has never been determined. Specimens using two different adhesives for the automotive industry were subjected to two different ageing environments (immersion in distilled water and under 75% of relative humidity). Once they were fully degraded, they were tested at three different temperatures (−40, 23 and 80 °C), which covers the range of temperature an adhesive for the automotive industry is required to withstand. The aim is to improve the long term mechanical behaviour prediction of adhesive joints. The DCB substrates were made of a high strength aluminium alloy to avoid plastic deformation during test. The substrates received a phosphoric acid anodisation to improve their long term adhesion to the adhesive. Results show that even though a phosphoric acid anodization was applied to the adherends, when the aged specimens were tested at room temperature and at 80 °C, they suffered interfacial rupture. At −40 °C, however, cohesive rupture was observed and the fracture toughness of the aged specimens was higher.

ARTICLE HISTORY
Received 9 November 2016
Revised 10 January 2017
Accepted 12 January 2017

KEYWORDS
Moisture degradation; temperature degradation; fracture toughness

1. Introduction

Adhesive bonding has been substituting more traditional joining techniques such as riveting or welding, particularly in the transport industry. Some of the advantages include higher fatigue resistance and the ability to join dissimilar materials [1]. Adhesive joints provide more uniform stress distribution than riveted or bolted joints and are a good choice when joining fiber reinforced plastic adherends [2], as these materials are very vulnerable to stress concentrations. One of the main disadvantages of adhesive bonding is the prediction of the mechanical behaviour of aged adhesive joints, as structural adhesives are moisture and temperature sensitive.

CONTACT L. F. M. da Silva lucas@fe.up.pt

Moisture degradation of adhesives includes reduction of modulus and strength and increase in ductility [3–7]. The fracture toughness of the adhesive may increase or decrease, depending on the environmental conditions and ageing time [8,9]. However, in adhesive joints the effects may be more severe, as the moisture degradation of the interface between the adhesive and the adherend may cause adhesive failure.

Several models have been developed to predict the water absorption of adhesives. The simplest and most common is the fickian diffusion model, which is valid when water absorption is much slower than the relaxation of the adhesive. Although being the simplest and most common model, other more complex models have been developed to describe anomalous behaviours, such as dual fickian diffusion [10], delayed dual fickian [11] and the Langmuir model [12]. In many cases the water uptake may be fickian under certain environmental situations and non-fickian under others. Generally, non fickian behaviour is more prone to occur at higher temperatures, higher relative humidity and for smaller thicknesses of bulk adhesive specimens [10]. There is also evidence that while a bulk adhesive may have a fickian diffusion behaviour, the same adhesive in a joint may have a different water uptake behaviour [13].

The rate at which the water is absorbed and the maximum water uptake depend on environmental factors, such as the relative humidity [12,14], temperature [12,15–17], the thickness [10,18] and on the stress state of the adhesive [7,19].

Water diffuses through the adhesive as free water, occupying the free spaces between the polymer chains. Some of this free water will form bridges with the polymer chains and turn into bound water. The amount of bound water increases with higher temperatures and longer exposures [20,21]. Bound water is responsible for the volumetric changes of adhesives that are subjected to moist environments. If, however, the adhesive is constrained (as in an adhesive joint, for example) residual stresses may arise [10,22–24].

Zhou and Lucas [20,21] have found that two kinds of bound water exist:

(1) Type I bound water is responsible for increasing the polymer chains mobility. It acts therefore as a plasticizer: the effects are the decrease of the glass transition temperature of the adhesive (T_g), increase of ductility and decrease of the adhesive's strength;
(2) Type II bound water is water that forms secondary cross-linking between the polymer chains. It has the effect of reducing the extent of the T_g depression.

Type I bound water can be easily removed at relatively low temperatures, while type II bound water requires high temperature to be removed.

When subjecting a structural adhesive joint to extreme temperatures, one must be aware of two different phenomena:

(1) Thermal expansion of adherends and adhesive, which causes residual stresses, especially if the adherends are dissimilar;
(2) Different bulk adhesive properties. Generally, the adhesive gets more ductile and less strong when it is closer to T_g. Banea et al. [25] found that below T_g the toughness of structural adhesives remains largely constant, while above T_g it decreases dramatically [26,27].

Generally the strength of adhesive joints decreases with high and low temperatures [25,28–33].

This study aims at determining the moisture and temperature dependent toughness of two epoxy adhesives for the automotive industry. Although the separate effect of moisture and temperature on the mechanical properties of structural adhesive joints is relatively well studied, its combined effect is not yet well known [34,35]. To the authors' knowledge, there is not any study regarding the combined effect of temperature and moisture on the toughness of structural adhesive joints. This paper aims to shed light on this subject.

In this study, the toughness of two epoxy adhesives that were subjected to two different ageing environments was analysed. After ageing the specimens in distilled water and in a saturated water solution of NaCl (referred throughout this paper as 'salt water'), they were tested at −40, 23 and 80 °C (covering the range of temperatures required for the automotive industry).

2. Materials

2.1. Adhesives

Two adhesives for the automotive industry which were recommended by Sika® and Nagase® for this durability study were selected:

- The epoxy adhesive XNR 6852-1, supplied by NAGASE CHEMTEX® (Osaka, Japan). This adhesive is a one-part system that cures at 150 °C in 3 h.
- The epoxy adhesive SikaPower 4720 was, supplied by SIKA® (Portugal, Vila Nova de Gaia). This adhesive is a two-part system that cures at room temperature in 24 h.

A very important parameter to take into account when testing adhesive joints, especially when the joint is subjected to high temperatures, is the adhesive's T_g. This temperature is usually high when the adhesive is dry but normally decreases when the adhesive is exposed to moist environments [20]. The T_g of both adhesives before and after ageing has been determined in a previous study [3]. Results showed the T_g of XNR 6852-1 not to be very moisture sensitive. SikaPower 4720, on the other hand, is very moisture dependent, and when aged in distilled water its T_g is actually lower than room temperature (see Figure 1), which has severe consequences on its strength and modulus as well as in its water uptake (32.5% at 32.5 °C when aged in distilled water vs. only 3.8% when aged in salt water).

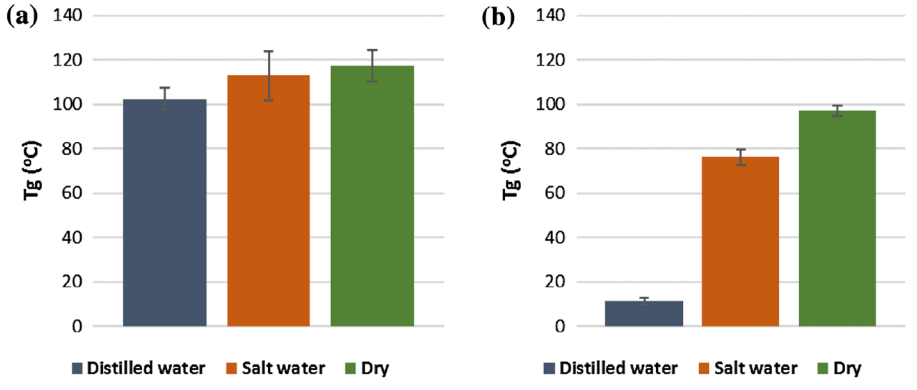

Figure 1. T_g of both adhesives studied [3]: (a) XNR 6852-1, (b) SikaPower 4720.

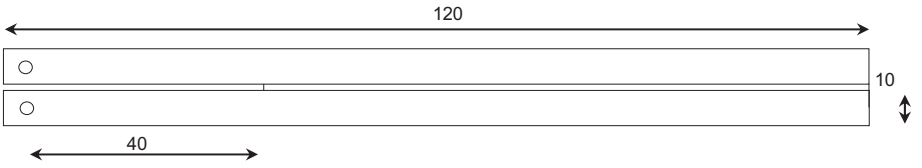

Figure 2. Geometry of the DCB specimens used in this study (dimensions in mm, width = 5 mm).

2.2. Substrates

In order to measure the toughness of adhesive joints, DCB specimens were used. To avoid plastic deformation while testing, the substrates were made of the 6082-T6 high strength aluminium alloy.

In a standard DCB specimen, which has a length much greater than the width, water sorption occurs almost entirely along the width direction [5]. However, due to its dimensions, it takes a very long time to reach saturation. Instead of using this standard specimen geometry, a smaller geometry (shown in Figure 2) was used.

Some studies about the effect of DCB specimen geometry on the fracture energy (G_{IC}) of the adhesive layer have been undertaken [36,37].

3. Experimental procedure

3.1. Specimen fabrication

Prior to bonding, the surfaces of the DCB substrates were abraded with 80 grit SiC sandpaper, cleaned in an ultrasonic acetone bath and received a phosphoric acid anodisation. Less than a day after being anodised, the specimens were bonded and left to cure for 3 h at 150 °C or for 24 h at room temperature, according to the indication of the manufacturer of each used adhesive. After the cure cycle was completed, the excess adhesive was removed and the specimens were left to dry for at least 3 weeks in a dry desiccator. After this time, the specimens of each adhesive were divided into three groups:

- Dry specimens, which were ready to be tested;
- Specimens aged in a saturated solution of NaCl at 32.5 °C (referred throughout this paper as "salt water"), which is equivalent to ageing them in a 75% RH environment [38];
- Specimens aged in distilled water at 32.5 °C.

Prior to testing, each specimen was loaded in pure mode I until a small pre-crack was created. This ensures that the crack tip is not blunt.

As explained above, specimens with reduced dimensions were used. This also allowed time efficient production and ageing.

3.2. Test procedure

After all specimens had been produced and dried in a dry desiccator, they were separated into the three different groups mentioned in the previous section. The dry specimens were immediately tested while the specimens to be aged were placed in their respective ageing environment. At least three valid tests were made for each environmental condition.

Some studies report that water diffusion in an adhesive joint is much faster than water diffusion through the bulk adhesive alone either due to stress enhanced diffusion [13] or due to water penetrating through the interface between adhesive and adherend [39]. Often it is very difficult to predict when an adhesive joint is fully saturated because the thin bond-lines do not absorb enough water to be measured by common precision scales. In order to determine when the specimens reached saturation, some specimens of each adhesive were tested periodically until their toughness stabilized. Using this method, it was concluded that the specimens needed 13 weeks to be fully saturated. The results of this study were already previously published by the authors [40].

After saturation had been attained, the toughness of the remaining specimens that were aged in distilled water and in salt water was measured as a function of the test temperature.

A climatic chamber coupled with a universal test machine (INSTRON® model 3367) allowed to test aged and unaged specimens at −40, 23 and 80 °C. Right before testing at −40 or 80 °C, the specimens were left inside the climatic chamber at the test temperature for 10 min to ensure that the temperature was uniform in the entire specimen. The tests were performed at the constant displacement rate of 0.5 mm/min.

After the mechanical tests, the fracture surfaces of the joints were analysed at the CEMUP laboratory (University of Porto, Portugal) using a high resolution (Schottky) Scanning Electron Microscope (SEM) with X-ray Microanalysis and Electron Backscattered Diffraction analysis: Quanta 400 FEG ESEM / EDAX Genesis X4 M. Samples were coated with a Au/Pd thin film, by sputtering, using the SPI Module Sputter Coater equipment.

4. Results and discussion

DCB specimens of each adhesive were tested at −40, 23 and 80 °C. The tests were performed with dry joints, joints aged in distilled water and joints aged in salt water. For each test a load vs displacement (P–δ) curve was recorded so that the toughness could be measured. In order to determine the fracture toughness, the compliance based beam method [41] was used. This method uses the compliance of the specimen during the test to determine an equivalent crack length that takes also into account the length of the fracture process zone. It is therefore not necessary to measure the actual crack length throughout the test. The mode I fracture toughness (G_{IC}) can be computed using equation 1:

$$G_{IC} = \frac{6P^2}{b^2h^3}\left(\frac{2a_e^2}{E_f} + \frac{h^2}{5G}\right) \tag{1}$$

where P is the load measured by the load cell, b and h are the dimensions of the substrates (in this case 5 and 10 mm, respectively), E_f is a corrected flexural modulus of the specimen, G is the shear modulus of the adherends and a_e is an equivalent crack length that is computed taking into account the compliance of the specimen.

Depending on the temperature and the ageing process, the DCB specimens failed either cohesively in the adhesive layer or in the adhesive-adherend interface, as shown in Figure 3. As will be discussed next, with few exceptions, adhesive failure resulted into low toughness of the specimen.

Results show that at room temperature and at 80 °C water is responsible for shifting the locus of failure from the adhesive to the adhesive-adherend interface, resulting in

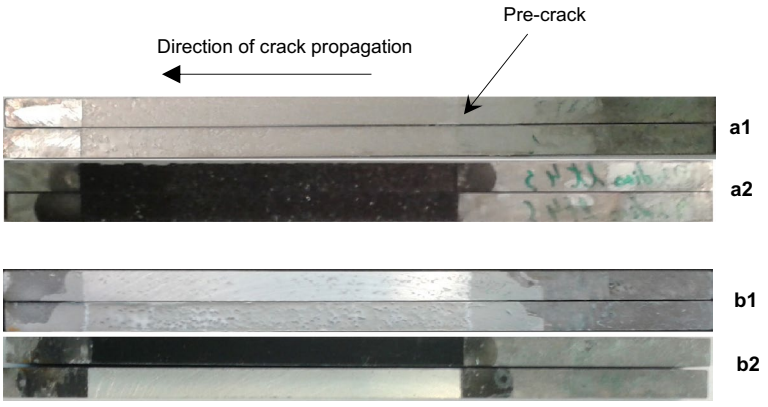

Figure 3. Example of cohesive and interfacial fracture surfaces of both adhesives studied: a1 – Cohesive fracture of XNR6852-1 (dry specimen tested at room temperature). a2 – Cohesive fracture of SikaPower 4720 (distilled water aged specimen tested at −40 °C). b1 – Interfacial fracture of XNR6852-1 (salt water aged specimen tested at room temperature). b2 – Interfacial fracture of SikaPower 4720 (dry specimen tested at 80 °C).

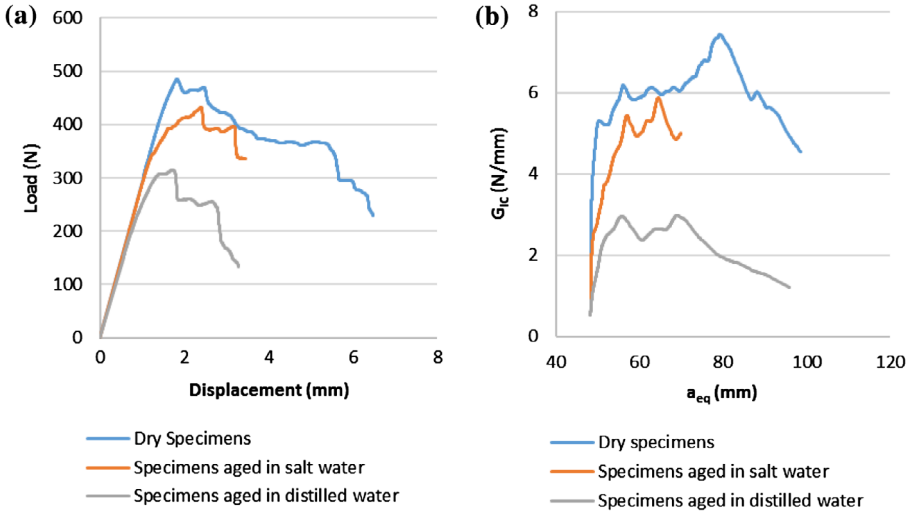

Figure 4. *P*–*δ* curve (a) and R-curve (b) of dry and aged XNR 6852-1 tested at 23 °C.

low toughness. At −40 °C, however, cohesive fracture occurred in every specimen and high values of toughness were determined.

4.1. 23 °C tests

Figures 4 and 5 present examples of *P*–*δ* and *R* curves of the two adhesives tested at 23 °C in the dry state and in two different moist environments. While the dry specimens suffered cohesive failure in the adhesive layer, the aged specimens suffered adhesive failure. The significant decrease in the toughness of the specimens is due to the low interfacial strength after ageing.

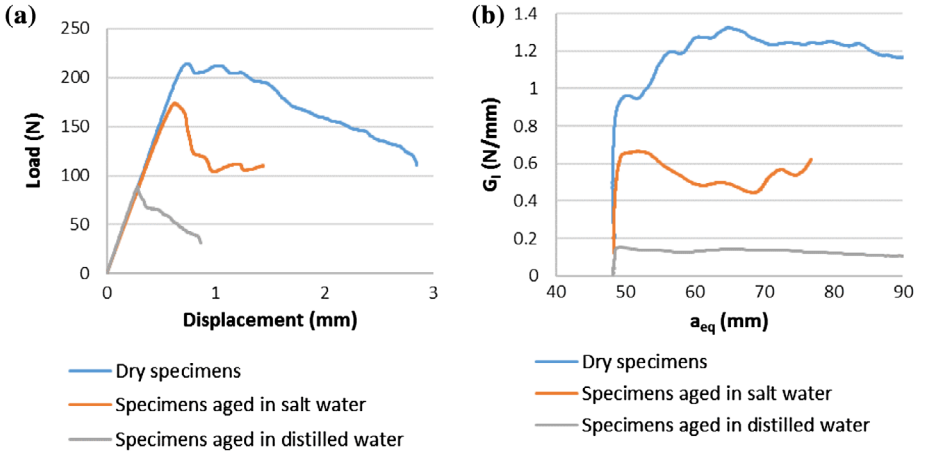

Figure 5. *P–δ* curve (a) and R-curve (b) of dry and aged SikaPower 4720 tested at 23 °C.

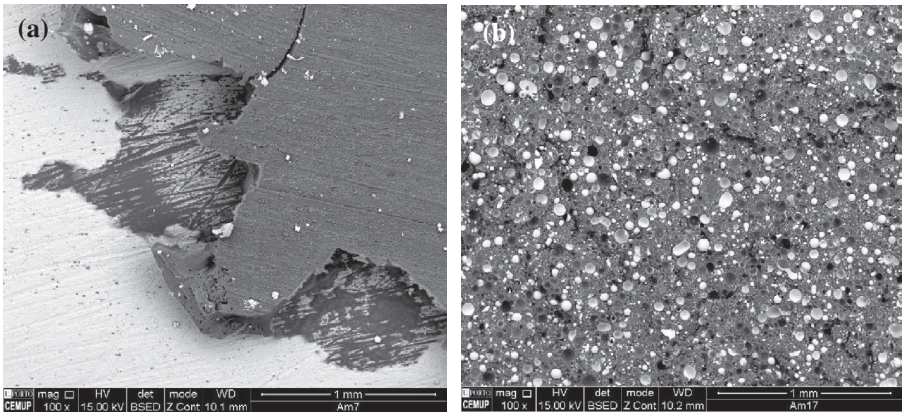

Figure 6. SEM image of a fracture surface of aged XNR 6852-1 (a) and dry SikaPower 4720 (b) tested at room temperature.

For both adhesives, salt water specimens yielded better results than the distilled water specimens.

Despite having failed adhesively, aged XNR 6852-1 joints still hold considerable toughness. Distilled water aged SikaPower 4720 joints, on the other hand, have a very low toughness. This may be due to the low T_g of the adhesive after ageing in this environment.

Figure 6(a) is SEM image of an example of an aged XNR 6852-1 specimen that failed in the adhesive-adherend interface. It is possible to notice that this adhesive is filled with particles of about 10 μm. This is a common method to improve the toughness of the adhesive [42]. There are also some white particles on top of the adhesive layer. These are salt particles that appear on the joint after the salt water has dried.

Figure 6(b) shows a SEM image of the fracture surface of a dry SikaPower 4720 specimen that was tested at 23 °C. The fracture is cohesive through the adhesive layer and shows that this adhesive is also filled with rubber particles with sizes between 57 and 150 μm.

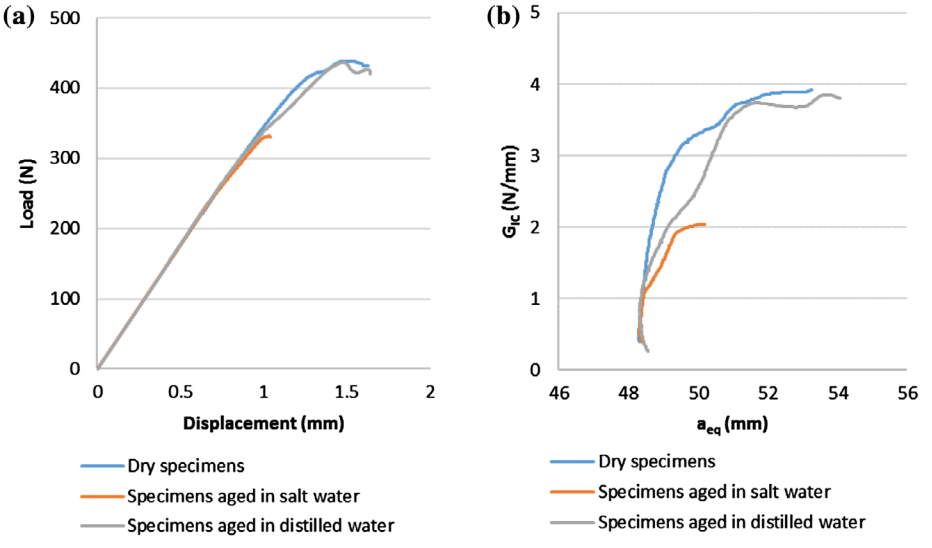

Figure 7. *P–δ* curve (a) and R-curve (b) of dry and aged XNR 6852-1 tested at −40 °C.

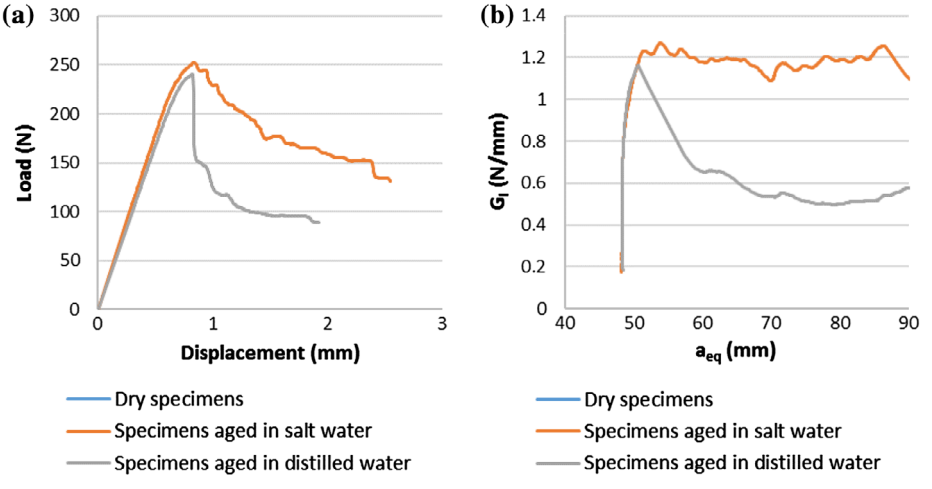

Figure 8. *P–δ* curve (a) and R-curve (b) of dry and aged SikaPower 4720 tested at −40 °C.

4.2. −40 °C tests

Figures 7 and 8 show examples of *P–δ* curves of XNR 6852-1 and SikaPower 4720 joints respectively, which were tested at −40 °C. Every specimen tested at −40 °C showed cohesive fracture in the adhesive.

At the beginning of crack propagation, XNR 6852-1 suffered cohesive stable crack propagation. Later, as the test proceeded, the unstable crack propagation occurred. Results show that dry XNR 6852-1 has a slightly lower toughness at this temperature than at room temperature (see Figure 7(b)). Ageing further lowers the adhesive's toughness at −40 °C. However, the toughness of the aged specimens when tested at −40 °C is higher than when

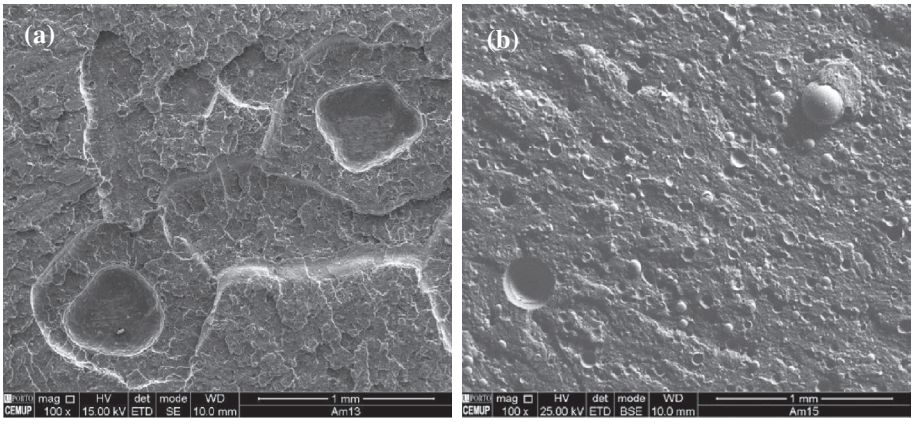

Figure 9. SEM image of a fracture surface of a dry specimens of XNR 6852-1 (a) and SikaPower 4720 (b) tested at −40 °C.

they are tested at 23 °C because, unlike the specimens that were tested at room temperature, these specimens failed cohesively in the adhesive layer.

SikaPower 4720, on the other hand, shows higher moisture dependence when tested at this temperature, as shown in Figure 8. It was not possible to determine the toughness of dry SikaPower 4720 because unstable crack propagation occurred. However, one can assume that it is quite low because they suffered unstable crack propagation within the adhesive layer. It is remarkable that the specimens aged in salt water presented a toughness that is similar to that of the dry room temperature joints. Although the yield stress of this adhesive drops after ageing, its ductility increases as an effect of adhesive plasticization [3], not affecting the fracture toughness significantly. The toughness of SikaPower4720 aged in distilled water was lower than the toughness when the specimens were aged in salt water because ageing this adhesive in distilled water completely degrades its mechanical properties [3].

Figure 9 shows a SEM image of the cohesive fracture obtained from testing both adhesives, both in the dry and in the aged state, at −40 °C. Both adhesives show a fragile fracture surface. A glass sphere with 0.2 mm of diameter is visible on the SikaPower 4720 fracture surface. These spheres are mixed with the adhesive and are used to ensure the proper adhesive thickness. Unlike the joints that were tested at 23 °C, these joints showed a brittle fracture, without significant plastic deformation.

4.3. 80 °C tests

Figures 10 and 11 show examples of P–δ curves and R-curves of XNR 6852-1 and SikaPower 4720 respectively. As adhesive failure was obtained in every test performed at 80 °C, one is not measuring the actual toughness of the adhesive, but the toughness of the interface between adhesive and adherend. Nevertheless, the toughness that was measured is higher than the toughness of the adhesive when the joint is tested at 23 °C, which indicates that, although interfacial failure was observed, failure was not due to interfacial degradation. Aged specimens show a considerably lower fracture energy, meaning that these interfaces were degraded by water. In a previous study [3] it was concluded that although the yield stress of dry XNR 6852-1 significantly lowers with temperature, its ductility increases very

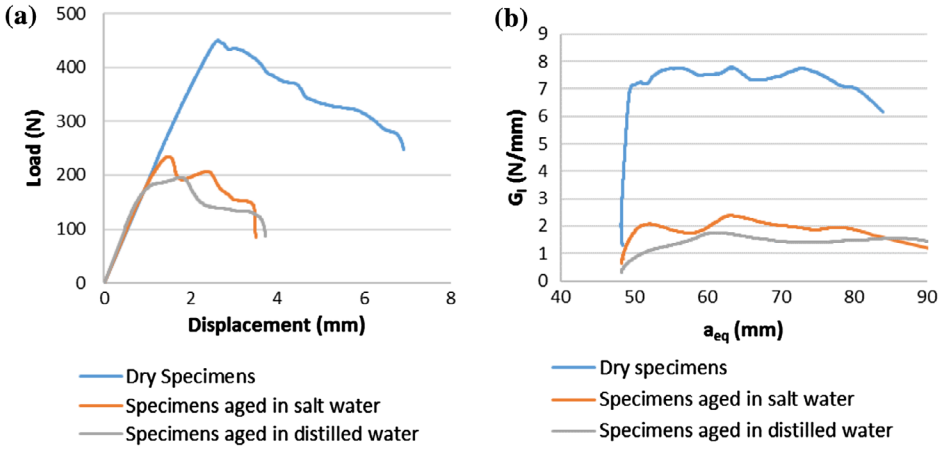

Figure 10. *P–δ* curve (a) and R-curve (b) of dry and aged XNR 6852-1 tested at 80 °C.

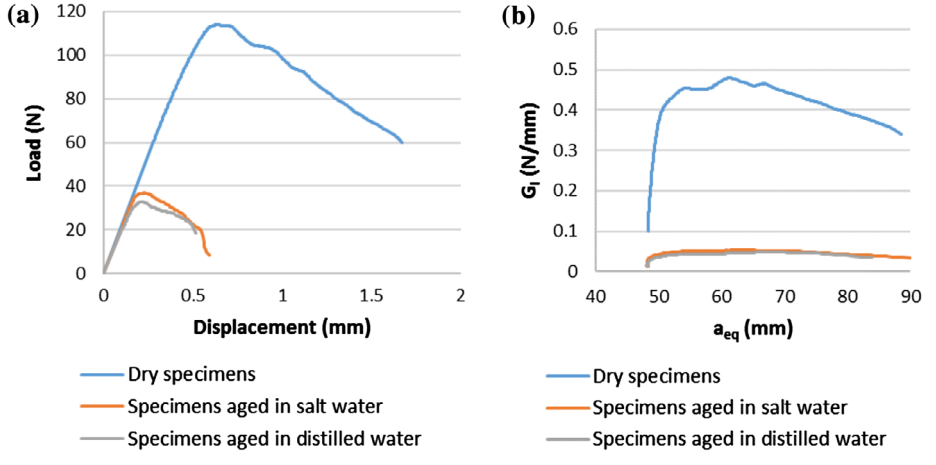

Figure 11. *P–δ* curve (a) and R-curve (b) of dry and aged SikaPower 4720 tested at 80 °C.

significantly, being its final deformation higher than 100% when tested at 80 °C. It was therefore predictable that the toughness of this adhesive would be very high at this temperature, which was experimentally confirmed in this study (see Figure 10). Unlike XNR 6852-1, dry SikaPower 4720 shows lower toughness at 80 °C than at room temperature (see Figure 11). This is a typical consequence of testing the adhesive above T_g [26,43]. The toughness of SikaPower 4720 further decreases after ageing.

The SEM images of the fracture surfaces in Figure 12 show the interfacial failure surfaces of both dry and aged adhesives after testing at 80 °C. Adhesive XNR 6852-1 (Figure 12(a)) shows some plasticity before breaking through the interface. SikaPower 4720, on the other hand, shows a fragile behaviour (Figure 12(b)).

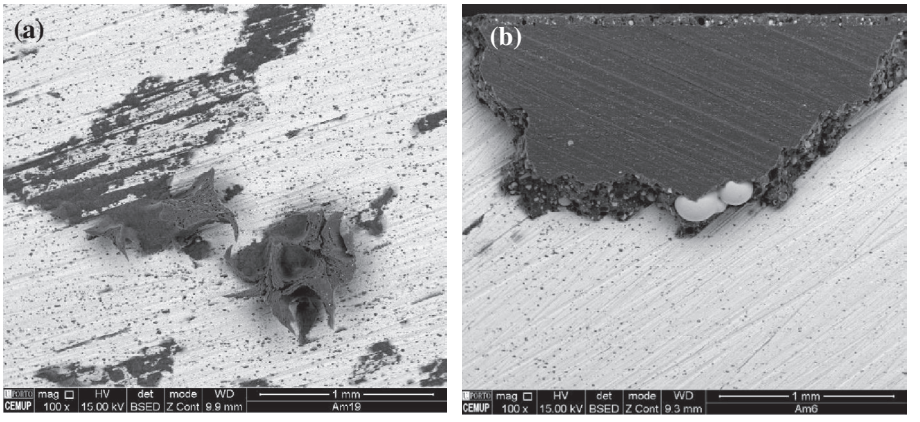

Figure 12. SEM image of a fracture surface of distilled water aged XNR 6852-1 (a) and SikaPower 4720 (b) tested at 80 °C.

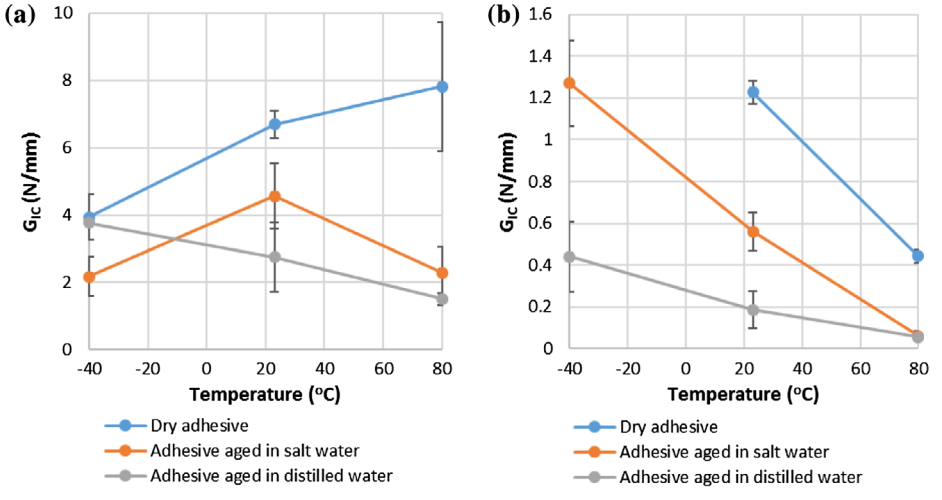

Figure 13. Fracture toughness of XNR 6852-1 (a) and SikaPower 4720 (b) as a function of temperature and ageing environment.

5. Discussion

Inevitably every specimen presents defects. Because the specimens used in this study are smaller than standard specimens, the effect of each defect is much more visible in the *R*-curves and the result is an *R*-curve that may not show a neat plateau. For this reason, only the average toughness was considered as G_{IC}. Figure 13 presents the toughness of both joints made with both adhesives studied as a function of ageing environment and test temperature. Despite the application of a surface treatment that has been shown to improve the performance of bonded aluminium joints in the long term [44,45], it is important to bear in mind that not every failure occurred cohesively in the adhesive layer. Every specimen tested at 80 °C, as well as aged specimens tested at 23 °C suffered adhesive failure. In these situations, one is not measuring the actual toughness of the adhesive, but the toughness

of the adhesive-adherend interface. The fact that in some situations cohesive fracture did not occur allows us, however, to know in what conditions of temperature and moisture interfacial degradation is more likely to happen.

It is known that at low temperature high residual stresses may arise due to mismatch of coefficients of thermal expansion (CTE) between adhesive and adherends [46]. The ductility of the adhesive and modulus of the adhesive is also reduced due to limited chain mobility. As moisture diffuses through the adhesive, it increases the mobility of its chains, increasing its ductility at the expense of some loss of strength.

Usually the toughness of adhesives decreases at low temperature because lower temperatures reduce the mobility of the polymer chains of the adhesive. The result is a stronger but more fragile adhesive [47], with lower toughness [33]. It was found, however, in this study that water can improve the toughness of adhesives at low temperatures. Salt water aged SikaPower 4720 tested at −40 °C resulted in higher fracture toughness than the dry adhesive tested at room temperature. This toughness increase may be due to:

- Adhesive swelling, which can balance the residual stresses cause by CTE mismatch.
- Increased chain mobility created by absorbed moisture.

The same adhesive aged in distilled water shows a very low toughness because ageing in this environment completely degrades this adhesive, as is demonstrated by its equilibrium water uptake and T_g [3].

As can be seen in Figure 13-a, dry and distilled water aged XNR 6852-1 show similar fracture toughness when tested at −40 °C probably due to the same reasons. Salt water aged XNR 6852-1 has a lower toughness. Apparently, the effect of salt water in this case was not enough to significantly improve the toughness of the adhesive at low temperature.

At room temperature the dry specimens failed cohesively in the adhesive layer while the aged specimens failed adhesively at the adhesive-adherend interface. The higher toughness was measured in the dry specimens, while the specimens that suffered adhesive failure showed a significant loss of toughness.

At 80 °C every specimen had adhesive failure. Unfortunately, as fracture occurred at the adhesive-adherend interface, one is not assessing the actual toughness of the adhesive, but the toughness of the interface instead.

Despite having failed at the interface between adhesive and adherend, dry XNR 6852-1 actually had a higher toughness at 80 °C than at room temperature. This means that the interface was not degraded and that the toughness of the adhesive is higher than the toughness of the interface. The interface is therefore the 'weakest link' and controls the failure of the joint. It was found in a previous study [3] that at 80 °C the maximum deformation of this adhesive at 80 °C using bulk tensile specimens was very high (higher than 100%), which corroborates the results obtained in this study.

Unlike XNR 6852-1, the toughness of SikaPower 4720 at 80 °C is lower than at room temperature, as can be seen in Figure 13(b). This is because this adhesive is very close to T_g when tested at 80 °C and already shows some of the characteristics of adhesives tested above T_g, such low strength and modulus [3] and, as was found in this study, low toughness.

6. Conclusion

This work focused on the measurement of the toughness of two epoxy adhesives for the automotive industry as a function of environmental temperature and moisture. The following conclusions can be drawn:

(1) Fracture occurred either within the adhesive layer or in the adhesive-adherend interface. Aged specimens tested at room temperature, as well as specimens tested at 80 °C tend to fail adhesively. Unaged specimens and specimens tested at −40 °C are more prone to fail cohesively;
(2) The toughness of the dry adhesive is lower at −40 °C probably due to the creation of residual stresses and due to lower mobility of the polymer chains. Water at this temperature improved the toughness of the studied adhesives by decreasing the residual stresses and increasing the mobility of the polymer chains.
(3) At room temperature only the dry specimens failed cohesively. Water degraded the adhesive-adherend interface, decreasing the toughness of the joint.
(4) At 80 °C every specimen suffered adhesive failure. The toughness of dry SikaPower 4720 at 80 °C was lower than at room temperature because the test temperature is close to the adhesive's T_g. On the other hand, as the test temperature is not close to T_g, the toughness of dry XNR6852-1 joints was higher at 80 °C. This indicates that probably no interfacial degradation had occurred. The toughness of aged specimens tested at 80 °C was very low either due to the decrease of its T_g or due to the degradation of the adhesive-adherend interface.

Acknowledgements

The authors would like to thank Sika for supplying SikaPower 4720 adhesive and Nagase Chemtex for supplying XNR 6852-1 adhesive.

Disclosure statement

No potential conflict of interest was reported by the authors.

Funding

This work was supported by the Fundação para a Ciência e Tecnologia [grant number EXCL/EMS-PRO/0084/2012].

ORCID

M. D. Banea http://orcid.org/0000-0002-8378-2292
L. F. M. da Silva http://orcid.org/0000-0003-3272-4591

References

[1] Banea MD, da Silva LFM, Campilho RDSG, et al. Smart adhesive joints: an overview of recent developments. J Adhes. 2014;90:16–40.
[2] Banea MD, da Silva LFM. Adhesively bonded joints in composite materials: an overview. Proc Inst Mech Eng Part L J Mater Des Appl. 2009;223:1–18.
[3] Costa M, Viana G, da Silva LFM, et al. Environmental effect on the fatigue degradation of adhesive joints: A review. J Adhes. 2016;93:127–146.
[4] Sugiman S, Crocombe AD, Aschroft IA. Experimental and numerical investigation of the static response of environmentally aged adhesively bonded joints. Int J Adhes Adhes. 2013;40:224–237.
[5] Hua Y, Crocombe AD, Wahab MA, et al. Modelling environmental degradation in EA9321-bonded joints using a progressive damage failure model. J Adhes. 2006;82:135–160.
[6] Barbosa AQ, da Silva LFM, Ochsner A. Hygrothermal aging of an adhesive reinforced with microparticles of cork. J Adhes Sci Technol. 2015;29:1714–1732.
[7] Lin YC, Chen X. Moisture sorption-desorption-resorption characteristics and its effect on the mechanical behavior of the epoxy system. Polymer. 2005;46:11994–12003.
[8] Fernandes P, Viana G, Carbas R, et al. The influence of water on the fracture envelope of an adhesive joint. Theor Appl Fract Mech. 2017. Available from http://dx.doi.org/10.1016/j.tafmec.2017.01.001
[9] Costa M, Viana G, da Silva LFM, et al. Determination of the fracture envelope of an adhesive joint as a function moisture. Materialwiss Werkstofftech. Submitted for publication.
[10] Loh WK, Crocombe AD, Wahab MMA, et al. Modelling anomalous moisture uptake, swelling and thermal characteristics of a rubber toughened epoxy adhesive. Int J Adhes Adhes. 2005;25:1–12.
[11] Mubashar A, Ashcroft IA, Critchlow GW, et al. Moisture absorption-desorption effects in adhesive joints. Int J Adhes Adhes. 2009;29:751–760.
[12] Ameli A, Datla NV, Papini M, et al. Hygrothermal properties of highly toughened epoxy adhesives. J Adhes. 2010;86:698–725.
[13] Liljedahl CDM, Crocombe AD, Gauntlett FE, et al. Characterising moisture ingress in adhesively bonded joints using nuclear reaction analysis. Int J Adhes Adhes. 2009;29:356–360.
[14] Vanlandingham MR, Eduljee RF, Gillespie JW. Moisture diffusion in epoxy systems. J Appl Polym Sci. 1999;71:787–798.
[15] Suh DW, Ku MK, Nam JD, et al. Equilibrium water uptake of epoxy/carbon fiber composites in hygrothermal environmental conditions. J Compos Mater. 2001;35:264–278.
[16] Shanahan MER, Auriac Y. Water absorption and leaching effects in cellulose diacetate. Polymer. 1998;39:1155–1164.
[17] Xiao GZ, Shanahan MER. Water absorption and desorption in an epoxy resin with degradation. J Polym Sci Part B Polym Phys. 1997;35:2659–2670.
[18] Lin YC, Chen X. Moisture sorption–desorption–resorption characteristics and its effect on the mechanical behavior of the epoxy system. Polymer. 2005;11994–12003.
[19] Liljedahl CDM, Crocombe AD, Wahab MA, et al. The effect of residual strains on the progressive damage modelling of environmentally degraded adhesive joints. J Adhes Sci Technol. 2005;19:525–547.
[20] Zhou JM, Lucas JP. Hygrothermal effects of epoxy resin. Part II: variations of glass transition temperature. Polymer. 1999;40:5513–5522.
[21] Zhou JM, Lucas JP. Hygrothermal effects of epoxy resin. Part I: the nature of water in epoxy. Polymer. 1999;40:5505–5512.
[22] Adamson MJ. Thermal-expansion and swelling of cured epoxy-resin used in graphite-epoxy composite-materials. J Mater Sci. 1980;15:1736–1745.
[23] Xiao GZ, Shanahan MER. Swelling of DGEBA/DDA epoxy resin during hygrothermal ageing. Polymer. 1998;39:3253–3260.
[24] Chiang MYM, Fernandez-Garcia M. Relation of swelling and *Tg* depression to the apparent free volume of a particle-filled, epoxy-based adhesive. J Appl Polym Sci. 2003;87:1436–1444.
[25] Banea MD, de Sousa FSM, da Silva LFM, et al. Effects of temperature and loading rate on the mechanical properties of a high temperature epoxy adhesive. J Adhes Sci Technol. 2011;25:2461–2474.

[26] Banea MD, da Silva LFM, Campilho RDSG. Mode I fracture toughness of adhesively bonded joints as a function of temperature: experimental and numerical study. Int J Adhes Adhes. 2011;31:273–279.
[27] Pethrick RA. Design and ageing of adhesives for structural adhesive bonding – a review. Proc IMechE Part L J Mater Des Appl. 2015;229:349–379.
[28] Deb A, Malvade I, Biswas P, et al. An experimental and analytical study of the mechanical behaviour of adhesively bonded joints for variable extension rates and temperatures. Int J Adhes Adhes. 2008;28:1–15.
[29] Banea MD, Silva LFM. Mechanical characterization of flexible adhesives. J Adhes. 2009;85:261–285.
[30] Srivastava VK. Characterization of adhesive bonded lap joints of C/C-SiC composite and Ti-6Al-4V alloy under varying conditions. Int J Adhes Adhes. 2003;23:59–67.
[31] Grant LDR, Adams RD, da Silva LFM. Effect of the temperature on the strength of adhesively bonded single lap and T joints for the automotive industry. Int J Adhes Adhes. 2009;29:535–542.
[32] Marques EAS, da Silva LFM, Banea MD, et al. Adhesive joints for low- and high-temperature use: an overview. J Adhes. 2015;91:556–585.
[33] Banea MD, da Silva LFM. The effect of temperature on the mechanical properties of adhesives for the automotive industry. Proc IMechE Part L J Mater Des Appl. 2010;224:51–62.
[34] Viana G, Costa M, Banea M. A review on the temperature and moisture degradation of adhesive joints. Proc Inst Mech Eng Part L J Mater Des Appl. 2016. doi:http://dx.doi.org/10.1177/1464420716671503.
[35] Costa M, Viana G, da Silva LFM, et al. Environmental effect on the fatigue degradation of adhesive joints: a review. The Journal of Adhesion. 2016;93:127–146. doi:http://dx.doi.org/10.1080/00218464.2016.1179117.
[36] Campilho RDSG, Moura DC, Banea MD, et al. Adherend thickness effect on the tensile fracture toughness of a structural adhesive using an optical data acquisition method. Int J Adhes Adhes. 2014;53:15–22.
[37] Costa M, Viana G, Canto C, et al. Effect of the size reduction on the bulk tensile and double cantilever beam specimens used in cohesive zone models. Proc Inst Mech Eng Part L J Mater Des Appl. 2016;230:968–982.
[38] Winston PW, Bates DH. Saturated solutions for the control of humidity in biological research. Ecology. 1960;41:232–237.
[39] Zannideffarges MP, Shanahan MER. Diffusion of water into an epoxy adhesive – comparison between bulk behavior and adhesive joints. Int J Adhes Adhes. 1995;15:137–142.
[40] Viana G, Costa M, Banea MD, et al. Water diffusion in double cantilever beam adhesive joints. Lat Am J Solids Struct. 2017;14:188–201.
[41] de Moura MFSF, Campilho RDSG, Goncalves JPM. Crack equivalent concept applied to the fracture characterization of bonded joints under pure mode I loading. Compos Sci Technol. 2008;68:2224–2230.
[42] Barbosa AQ, da Silva LFM, Banea MD, et al. Methods to increase the toughness of structural adhesives with micro particles: an overview with focus on cork particles. Materialwiss Werkstofftech. 2016;47:307–325.
[43] Banea MD, da Silva LFM, Campilho RDSG. Effect of temperature on tensile strength and mode I fracture toughness of a high temperature epoxy adhesive. J Adhes Sci Technol. 2012;26:939–953.
[44] Goglio L, Rezaei M. Effect of different substrate pre-treatments on the resistance of aluminium joints to moist environments. J Adhes. 2013;89:769–784.
[45] Kinloch AJ, Little MSG, Watts JF. The role of the interphase in the environmental failure of adhesive joints. Acta Mater. 2000;48:4543–4553.
[46] Humfeld GR, Dillard DA. Residual stress development in adhesive joints subjected to thermal cycling. J Adhes. 1998;65:277–306.
[47] Kang SG, Kim MG, Kim CG. Evaluation of cryogenic performance of adhesives using composite-aluminum double-lap joints. Compos Struct. 2007;78:440–446.

PAPER 5

Strain rate dependence of adhesive joints for the automotive industry at low and high temperatures

G. Viana[1], J. Machado[2], R. Carbas[2], M. Costa[2], L.F.M. da Silva[1], M. Vaz[1], M.D. Banea[3]

[1]Departamento de Engenharia Mecânica, Faculdade de Engenharia da Universidade do Porto (FEUP),
4200-465 Oporto, Portugal, Phone -22 508 14 91, Fax-22 508 22 01

[2]Instituto de Ciência e Inovação em Engenharia Mecânica e Engenharia Industrial (INEGI), 4200-465 Oporto, Portugal

[3]Federal Centre of Technological Education in Rio de Janeiro (CEFET), Av. Maracanã, 229, Rio de Janeiro, Brazil

Abstract

In this study the impact and quasi-static mechanical behaviour of single lap joints (SLJ) using a new crash resistant epoxy adhesive has been characterized as a function of temperature. Single lap adhesive joints were tested using a drop weight impact machine (impact tests) and using a universal test machine. Induction heating and nitrogen gas cooling was used in order to achieve a homogeneous distribution of temperature along the overlap of +80ºC and -20ºC, respectively. Adherends made of mild steel, similar to the steel used in automobile construction, were chosen in order to study the yielding effect on the strength of the SLJ. Results showed that at room temperature (RT) and low temperature (LT), failure was dictated by the adherends due to the high strength of the adhesive. At high temperature (HT), a decrease was found in the maximum load and energy absorbed by the joint due to the reduced strength of the adhesive at this temperature. The results were successfully modelled using the commercially available finite element software Abaqus®. Good correlation was found between experimental and numerical results, which allows the reduction of experimental testing.

Keywords: Adhesive Joints; Temperature; Impact; Quasi-static; Automotive Industry

1. Introduction

In recent years there has been an increasing interest in the automotive industry in applying adhesive bonding in structural components of vehicles [1, 2, 3]. Toughened, high performance adhesives can provide exceptional strength while producing lighter structures and, therefore, improve vehicle safety and efficiency [4, 5]. When adhesive joints are used in this area, some factors such as impact loading and temperature variation have a decisive role [6]. Under these conditions the joint must provide enough strength to transmit the load without fracturing, thus ensuring the vehicle's integrity. Although several studies have characterized adhesives under both situations separately, very few have considered them simultaneously [4, 7, 8, 9, 10].

Low temperatures are known to decrease the ductility of adhesives [11]. It is also known that under high strain rate conditions polymers tend to become brittle [12, 13, 14]. Brittle polymers are usually not as strain rate dependent as more ductile polymers [15]. Therefore, when SLJs

using epoxy adhesives are loaded at low temperatures, different strain rates are not expected to give significantly different results at failure [10, 16]. On the other hand, at high temperatures, adhesive ductility increases due to its proximity to the glass transition temperature (*Tg*), which leads to much higher strain rate dependence.

Though above *Tg*, the toughness of structural adhesives is usually very low, below *Tg* it is normally high and independent of temperature, as demonstrated by Banea et al. [17] It is therefore very important to keep the adhesive always below *Tg*, otherwise the adhesive joint may not be capable of resisting to any impact [18].

However, the strength of a SLJ is not just a function of temperature and strain rate. There are many factors in the joint's design that are involved. Many studies have been done on the influence of the selection of different geometries and materials for the components [19, 20]. Failure load has been demonstrated to be strongly dependent on parameters such as the overlap's length or the thickness of the adhesive layer [21]. The combination of different adherends and adhesives with different ductility has also been proved to be critical in the SLJ performance, especially when loaded in tension [4, 22]. The joint's design chosen for this study tried to mirror real applications in the automotive industry.

The energy that is absorbed by the adhesive joint depends mostly on the substrate. High strength adherends do not allow for high energy absorption during impact. In order to absorb high impact energy, mild steel or other ductile materials should be used because they allow for very high deformation before failure, as demonstrated by Harris and Adams [23].

In this study, mild steel bonded SLJs with a prototype of a crash resistant adhesive for the automotive industry were tested under quasi-static and impact conditions at low (-20^{o}C), high (80^{o}C) and room temperature. Mechanical properties of the adhesive at high and low temperature were obtained using bulk adhesive specimens at different strain rates in previous studies [18, 24], which allowed numerical modelling of the performed mechanical tests using a cohesive zone model (CZM).

The adhesives used in this study were a crash resistant toughened epoxy prototype under development, XNR 6852E-3 manufactured by NAGASE CHEMTEX (Osaka, Japan). Results showed that failure was dictated either by failure of the mild steel adherends due to the high strength of the adhesive or due to yielding of the adherends at the edges of the overlap.

This paper presents a numerical model to describe the mechanical behaviour of adhesive joints for the automotive industry. Previous experimental results using a similar adhesive were presented in a conference paper [25].

2. Experimental Procedure

2.1 Materials

2.1.1 Adhesive

The epoxy adhesive XNR 6852E-3, supplied by NAGASE CHEMTEX® (Osaka, Japan) was used in this study. This adhesive is a one-part system that cures at 150ºC for 3 h. A representative stress-strain curve of this adhesive, which was obtained using bulk tensile specimens and tested at room temperature at the constant displacement rate of 1mm/min is shown in Figure 1.

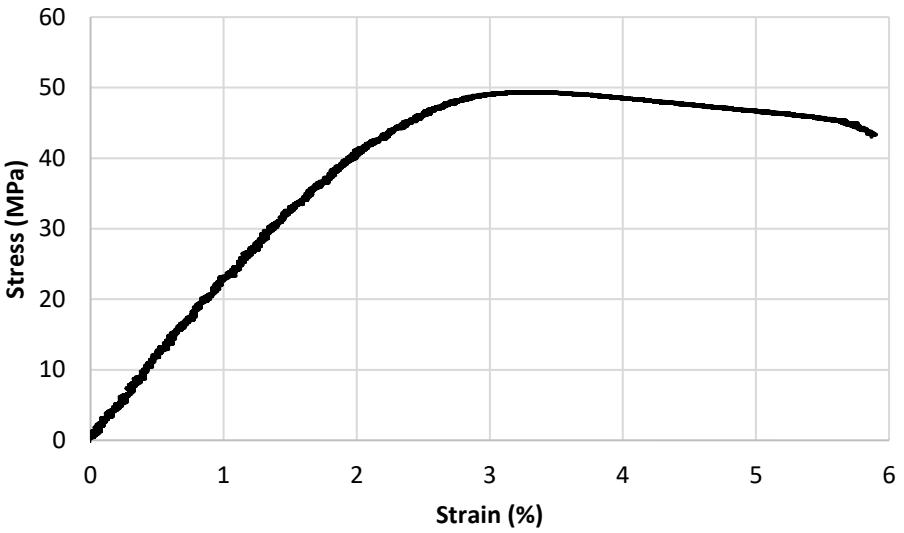

Figure 1: Stress-strain curve of the adhesive used in this study.

A very important parameter to take into account when testing adhesive joints, especially when the joint is subjected to high temperatures, is the adhesive's Tg. Banea et al. [17, 26] have shown that the fracture toughness of adhesives is not very temperature dependent if the adhesive is loaded below its Tg. On the other hand, if the temperature is above Tg, the fracture toughness of the adhesive is very low and this may lead to premature failure of the adhesive joint.

This adhesive has a relatively high Tg (132°C), well above its maximum service temperature (80ºC), which was measured using a rapid method [27].

Bulk dogbone adhesive specimens were used to determine the yield stress and Young's modulus of the adhesive as a function of temperature at 1 mm/min and at 100 mm/min [28]. Mode I

toughness of the adhesive was determined in a previous study and was considered to be largely independent on temperature and strain rate. This assumption has given good results in previous studies [18, 24].

The key properties of this adhesive are shown in Table 1.

Table 1: Key properties of the adhesive used in this study.

Property	Value	Unit
Young's modulus	1728	MPa
Tensile strength	51.5	MPa
Mode I fracture toughness	6.37	N/mm

2.1.2 Adherends

The substrates used to manufacture SLJs were made of 1 mm thick mild steel plates, since this is a very common structural material used in the automotive industry to improve the crashworthiness of vehicles.

In case of impact in vehicles, in order to ensure the safety of the passengers, the energy of impact must be absorbed by the adhesive joint. Unlike hard steel or other more fragile materials, mild steel is capable of absorbing high amounts of energy and is used in vehicles to improve their crashworthiness.

The mild steel used as adherends was characterised using tensile loaded dogbone specimens under 1 mm/min, 10 mm/min and 100 mm/min, following standard ASTM E 8M. The true stress-strain curve that was obtained was used in the finite element model.

The key properties of the substrate material are shown in Table 2.

Table 2: Key properties of the steel alloy used in this study.

Property	Value	Unit
Young's modulus	210	GPa
Yield stress	160	MPa

2.2 Specimen Fabrication

The SLJ consists of two steel plates bonded together, as illustrated in Figure 2. By using a mould, the SLJs were bonded with the correct alignment. The thickness of the adhesive layer was 0.2 mm and was controlled accurately by using steel spacers. The mould with the SLJs was left for 3h at 150^{o}C under a pressure of 2MPa so that the adhesive could be properly cured.

Before the application of the adhesive, the overlap surfaces of the adherends were sandblasted and degreased with acetone. The SLJs were extracted from the mould and any excess of adhesive around the overlap was removed. Finally, two steel plates were bonded to the ends of the substrates using a room temperature curing epoxy adhesive. A hole was drilled at each end to allow the assembly with the machine holding device.

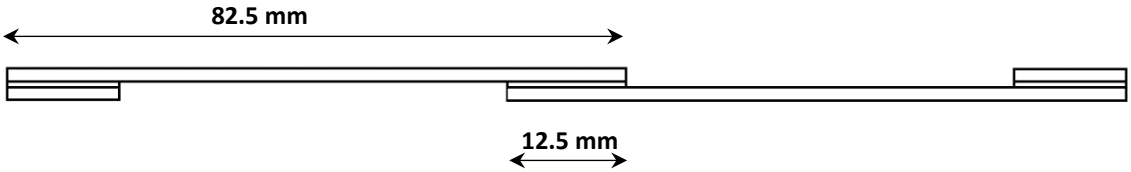

Figure 2: Dimensions of the single lap joints used in this study. Width=25mm.

2.3 Test procedure

2.3.1 Quasi-static tests

The quasi-static tests were performed in a universal test machine INSTRON® model 3367 (Norwood, Massachusetts, USA) with a capacity of 30 kN.

A climatic chamber coupled with the universal test machine was used to perform bulk and SLJ tensile tests at low temperature (-20^{o}C), room temperature (≈23^{o}C) and high temperature (80^{o}C). A thermocouple was used to make sure that the specimens were at the right temperature before starting the test.

2.3.2 Impact tests

The drop-weight impact tests were conducted in a Rosand® Instrumented Falling weight impact tester, type 5 H.V. (Stourbridge, West Midlands, U.K.). This machine drops a mass (m) from a predefined height (H) until it impacts on the device that holds the specimen (Figure 3).

The tests performed in this study were made by dropping a mass of 30kg from 1.02 m, which gives a potential energy of 300J. The impact speed (v) is established by the height from where the mass was dropped, according to Equation 1.

$$v = \sqrt{2gH} \quad (1)$$

Where *g* is the acceleration of gravity.

The energy applied in the impact (*E*) is given by Equation 2.

$$E = mgH \quad (2)$$

Before the mass is dropped, the specimen must be correctly assembled in the holding device, which transmits the impact load received to the lower adherend. The upper adherend is fixed while the lower receives the impact. A vertical guide avoids lateral deviations after the impact so that the displacement that is measured is aligned with the load. The load is recorded over time by a load cell attached to the falling mass. The data is then treated by the software of the machine to give the final load vs displacement curve.

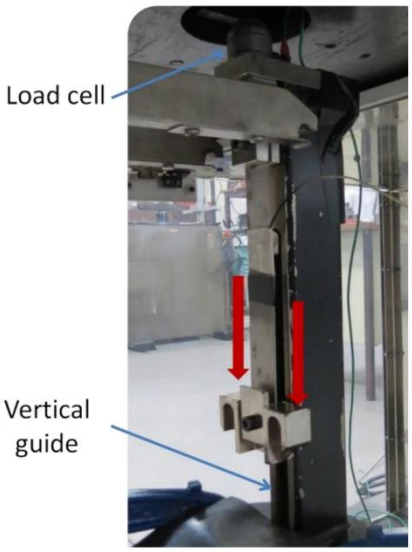

Figure 3: Impact test setup.

In order to perform impact tests at low temperatures, liquid nitrogen was sprayed to the overlap area of the specimens until the temperature stabilized at -20ºC. The high temperature impact tests were made using a home built induction coil to warm the specimens up to 80ºC. The high

heat conductivity of the steel adherends allows the temperature to be uniform along the entire overlap area. The temperature was monitored using a thermocouple and a thermographic camera.

The impactor was dropped 20 seconds after the test temperature was achieved to make sure that the entire overlap was at the same temperature.

3. Numerical Details

Impact and quasi-static numerical models were developed to predict the mechanical behaviour of the adhesive joints analysed in this study. Both are simple models, which diverge only on the boundary conditions and on the input of properties.

Large deformation in the width direction of steel substrates was observed in the experimentally tested joints. For this reason, a 3D model, which is able to capture this behaviour was developed, as well as a simpler 2D model, which cannot predict this kind of deformation. The results provided by both models are compared in the present paper.

Abaqus®/standard was used to model the quasi-static single lap joints while Abaqus®/explicit was used to model the impact specimens and decrease computational effort. The mesh was the same in impact and quasi-static simulation to facilitate comparison between the two models. Though the explicit solution usually requires a finer mesh, the mesh that was used was enough to ensure that the model was numerically stable. Table 1 shows the elements available in the Abaqus® library that were used to model adherends and adhesive.

Table 3: Elements used to model adherend and adhesive behaviour.

	Adhesive	**Adherend**
2D	COH2D4	CPS4R
3D	COH3D8	C3D8

COH2D4 and COH3D8 are 2D and 3D cohesive elements respectively with 4 nodes (2D element) and 8 nodes (3D element). CPS4R is a reduced integration 4 node 2D element and C3D8 is a full integration solid element, which was used to avoid hourglass deformations.

3.1 Boundary Conditions

3.1.1 Quasi-static model

The tip of one of the arms of the specimen was given a clamped boundary condition, which means that every degree of freedom is constrained. This simulates the specimen holding device. A displacement along the length direction of the specimen was attributed to the opposite arm. The load in the constrained arm and the displacement of the opposite arm were recorded.

3.1.2 Impact model

In the impact model, just like in the quasi-static model, one of the arms of the SLJ was set to not allow any displacement or rotation. The entire mass of the impactor was attributed to the end of the opposite arm of specimen. The initial velocity of this volume was set to be 4474 mm/s, parallel to the length of the steel substrates, which was the velocity of the impactor at the moment of impact. This velocity decreased until the specimen broke, as the specimen absorbed the kinetic energy of the impactor.

A scheme of the boundary conditions is shown in Figures 4 and 5. A more detailed view of the mesh used in the 2D model is shown in Figure 6.

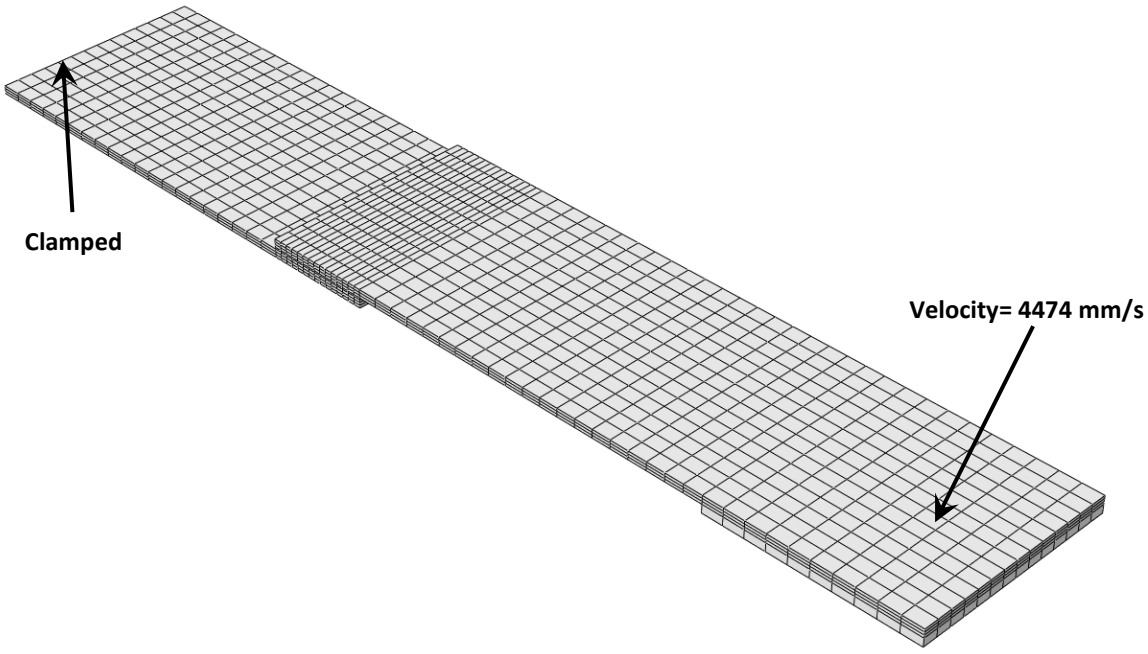

Figure 4: Mesh and boundary conditions used in the 3D model.

Figure 5: Mesh and boundary conditions used in the 2D model.

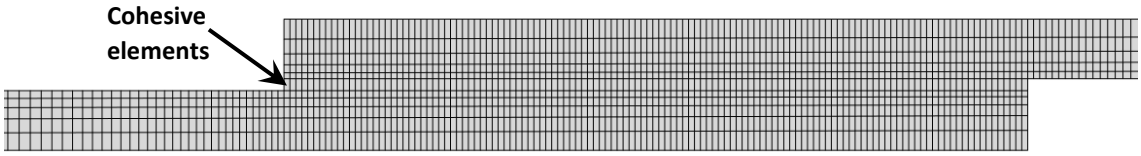

Figure 6: Detail of the mesh used in the 2D model. Cohesive elements were placed between the upper and bottom substrates, as indicated.

3.2 Modelling the Adherends

The true stress-strain curves obtained under three different strain rates according to the description in section 2.1.2 were simplified using three approximation points, as can be seen in Figure 7.

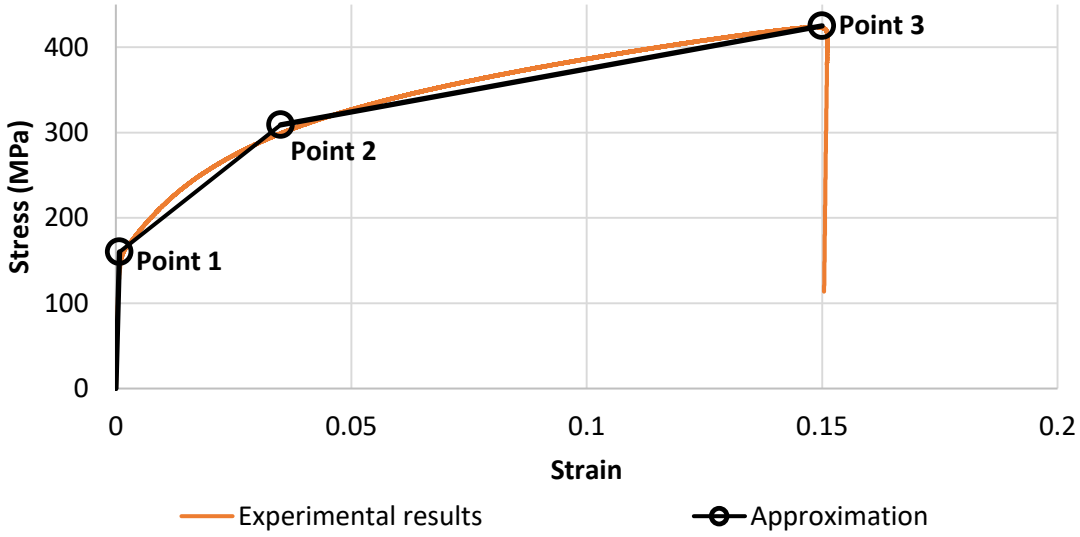

Figure 7: Technique used to model the mild steel adherends. Curve obtained for a cross head speed of 1 mm/min.

The shape of the stress-strain curve of the mild steel adherends changes with the test rate and, consequently, the position of the three approximation points. Table 2 shows the coordinates of each approximation point.

Table 4: Coordinates of each approximation point as a function of test rate.

	Strain	Stress (MPa)		
		1 mm/min	10 mm/min	100 mm/min
Point 1	Strain at the elastic limit	160	175	200
Point 2	0.04	309	315	335
Point 3	Strain at failure	425	447	454

To obtain the properties of the adherends at the test speed at which impact occurred, the stress at each approximation point was extrapolated using a logarithmic regression. Taking into account the stress at each approximation point under the test rates of 1 mm/s, 10 mm/s and 100 mm/s of test rate. An example of this regression for approximation point 1 is presented in Figure 8.

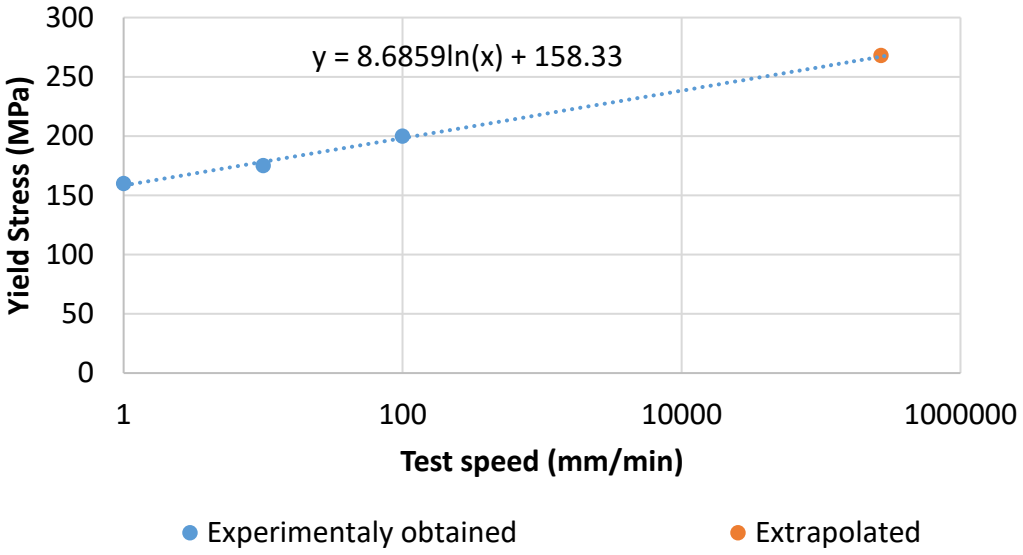

Figure 8: Technique used to determine the approximation points of the steel adherends at high test rates.

The set of properties considered in the numerical model was chosen according to the velocity at which the test was conducted: extrapolated properties were considered for modelling impact tests while the properties obtained at 1mm/min were used when modelling quasi-static tests.

3.3 Modelling the Adhesive

The adhesive was modelled using triangular cohesive zone models. To model using this method, it is necessary to introduce the modulus, yield stress and toughness of the adhesive. The modulus and yield stress of the adhesive were obtained in a previous study [28] as a function of temperature at the test rates of 1 mm/min and 100 mm/min. Mode I energy release rate of the used adhesive was obtained at room temperature at 1mm/min. This toughness was considered to be largely independent on temperature and strain rate. This assumption has given good results in previous studies [18, 24]. The yield stress and Young's modulus were extrapolated using a logarithmic regression. Figure 9 shows the extrapolation of the yield stress of the adhesive at 23ºC.

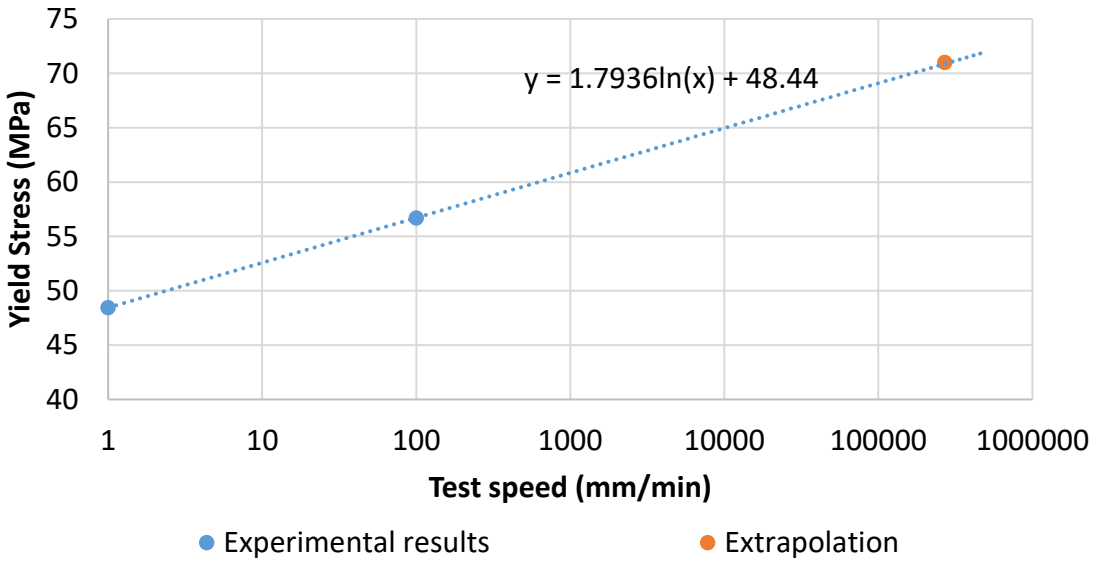

Figure 9: Technique used to determine the behaviour of the adhesive at high test rates.

4. Experimental results

In the following subsections, representative load-displacement (*P*-*δ*) curves obtained in quasi-static and impact tests are shown as a function of test temperature. At least three valid specimens were tested at each test condition. Every adherend suffered plastic deformation in the regions corresponding to the edges of the overlap, including those that were tested at 80ºC and failed at lower loads (see Figure 12). The existence of plastic deformation is an indication that it is the adherend and not the adhesive that is absorbing most of the impact energy. When the joint fails through the adhesive layer, it is due to stress concentration at the ends of the overlap, which is increased by adherend yielding [29].

4.1 23ºC Tests

Figure 10 shows representative *P-δ* curves obtained by testing SLJs under quasi-static and impact conditions.

The adhesive joints that were tested under quasi-static conditions at room temperature failed cohesively in the adhesive layer. By analysing the adherends after failure, it is apparent that significant plastic deformation has occurred, which means that failure was controlled by yielding of the mild steel adherends at the ends of the overlap (see Figure 10-b).

Specimens tested under impact conditions suffered a ductile fracture in one of the adherends, as can be seen in Figure 10-c. This was responsible for very high energy absorption. Under high strain rates, both materials, adhesive and adherend, become stronger. Adhesives, as polymers in general, are significantly more strain rate dependent than most metals such as mild steel. Under high strain rates, the adhesive becomes much stronger, which explains the high deformation and failure of the steel substrates.

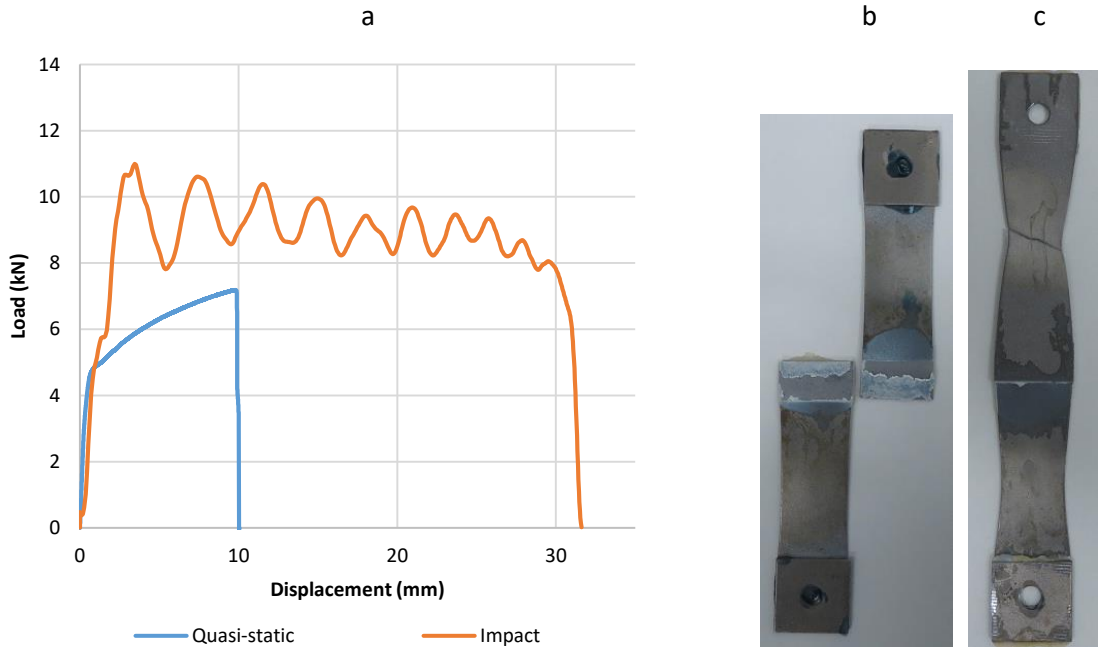

Figure 10: Representative P-δ curves of the impact and quasi-static specimens tested at 23ºC (a)
Failure mode of the quasi-static tests (b)
Failure mode of the impact specimens (c)

4.2 -20ºC Tests

Quasi-static tested joints failed within the adhesive layer at a displacement and load slightly higher than joints tested at room temperature due to the higher strength of the adhesive at this temperature, as can be concluded by analysing Figure 11.

Under impact, the joint suffered a ductile fracture in the mild steel adherends, which resulted in high energy absorption. However, at lower temperatures, the substrates showed a less ductile behaviour than the specimens tested at room temperature and were not able to absorb as much energy as impact room temperature tested specimens.

By comparing Figure 11 and Figure 10, it can be noted that the failure displacement of the quasi-static specimens is higher at low temperature than at room temperature. Though this may seem counter intuitive, it makes sense because the displacement that is being measured is the displacement at failure of the entire joint and not the displacement at failure of the adhesive alone. The temperature dependence of the steel adherends can, under these conditions, be neglected. The contribution of the displacement of the adhesive alone is very low when compared to the contribution of the steel adherends. As the adhesive is stronger at -20°C than at 23°C, it is natural that the joint can withstand higher displacements at -20°C before it fails in the adhesive layer.

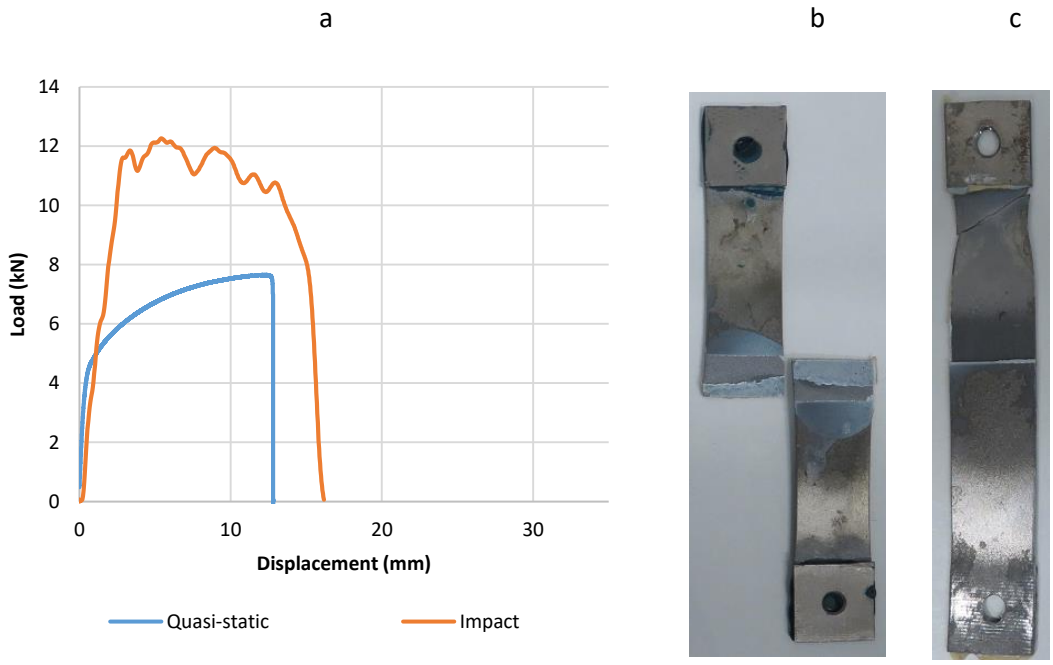

Figure 11: Representative P-δ curves of the impact and quasi-static specimens tested at -20°C (a)
Failure mode of the quasi static-tests (b)
Failure mode of the impact specimens (c)

4.3 80°C Tests

At 80°C both the impact and quasi-static tested specimens failed cohesively in the adhesive layer, as can be seen in Figure 12. At this temperature, the adhesive is very strain rate

dependent, which caused the adhesive to withstand higher loads when tested at impact. This led to higher loads being withstood by the joint thus increasing its failure displacement and improving energy absorption. As in every other test, yielding of the steel adherends at the ends of the overlap was observed, which means that it is the adherend that controls failure of the joint. Figure 12 shows representative *P-δ* curves of the joints tested at 80°C, as well as their failure mode.

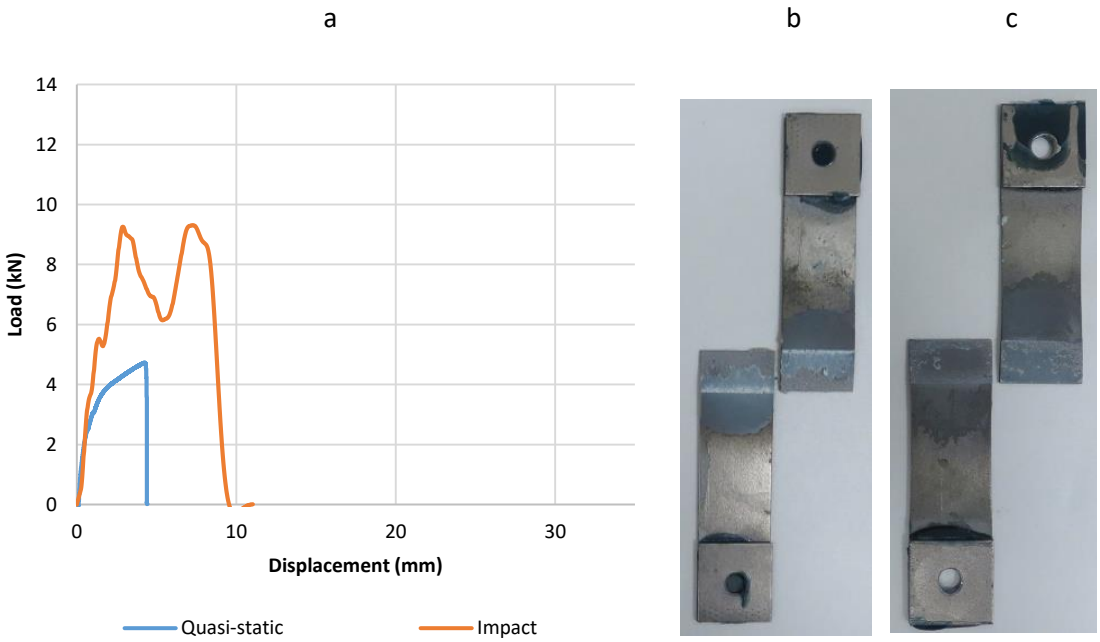

Figure 12: P-δ curves of the impact and quasi-static specimens tested at 80°C (a)
Failure mode of the quasi-static tests (b)
Failure mode of the impact specimens (c)

To summarize, at low and room temperature, impact tested specimens failed cohesively in the mild steel substrates, resulting in high energy absorption. At higher temperatures, the same specimens did not absorb as much energy due to the reduced strength of the adhesive.

Specimens that were tested under quasi-static conditions were not able to absorb as much energy as the impact tested specimens due to the reduced strength of the adhesive under low strain rates.

5. Numerical results

5.1 Quasi-static Simulations

5.1.1 23ºC Tests

Figure 13 shows the comparison between the experimental quasi-static *P-δ* curves and the corresponding numerical predictions using the 2D and 3D models described previously.

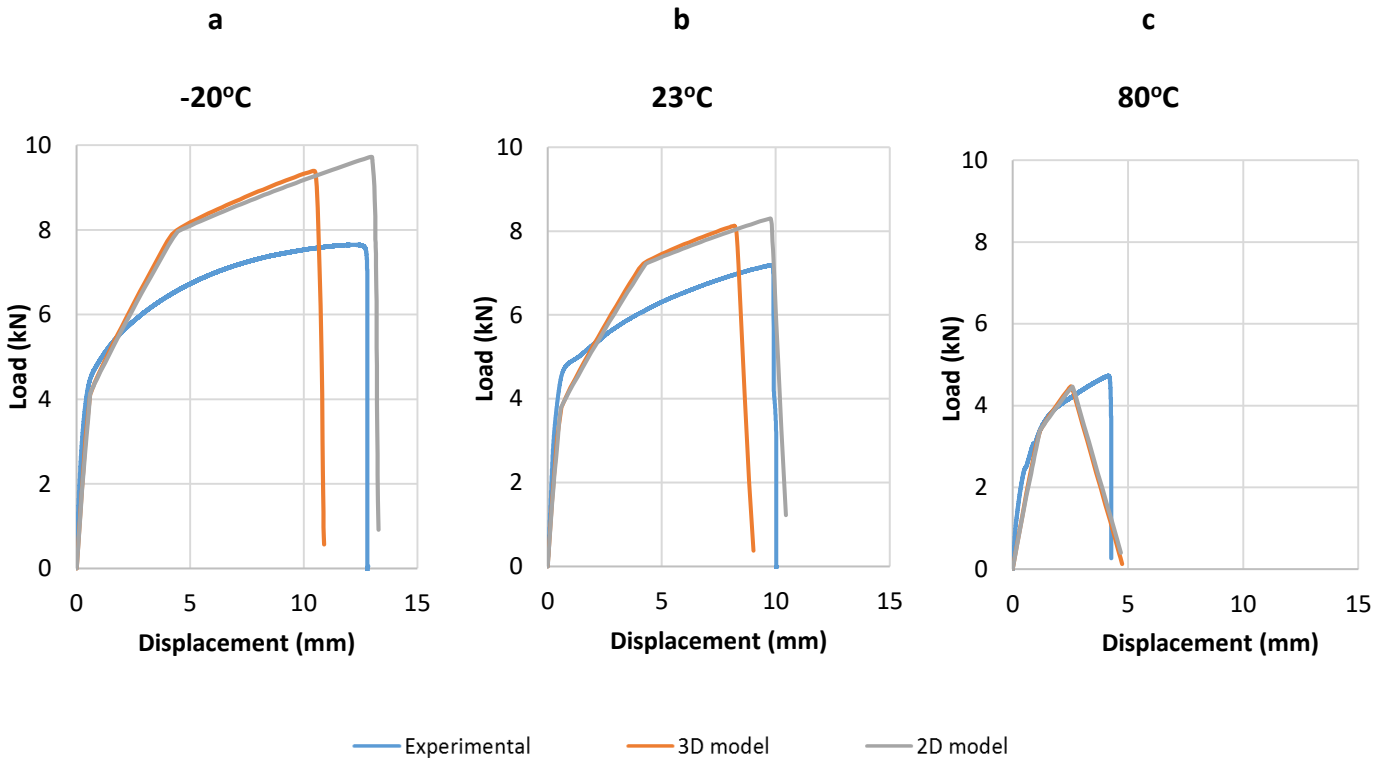

Figure 13: Comparison between numerical and experimental results obtained under quasi-static conditions.

The numerical models were able to predict the behaviour of the tested SLJs. Tough the model over predicted the strength of the joint at -20ºC and 23ºC, it can be said that a reasonable degree of concordance exists between the numerical prediction and the experimental value.

The yield stress of the adhesive was calculated by using bulk adhesive specimens. These bulk specimens may give slightly lower values, especially if there are tested at higher temperatures, when the adhesive is more strain rate dependent. This is probably the reason why the models give a slightly lower maximum displacement of the joint.

Generally, the maximum displacement predicted by 3D models is lower than the maximum displacement given by 2D models because 3D models take into account the stress gradient across the width of the joint (Figure 14). The exception is when the joints are tested at 80ºC

because in this case the adherends do not deform enough to induce significant stress gradients across the width of the specimen.

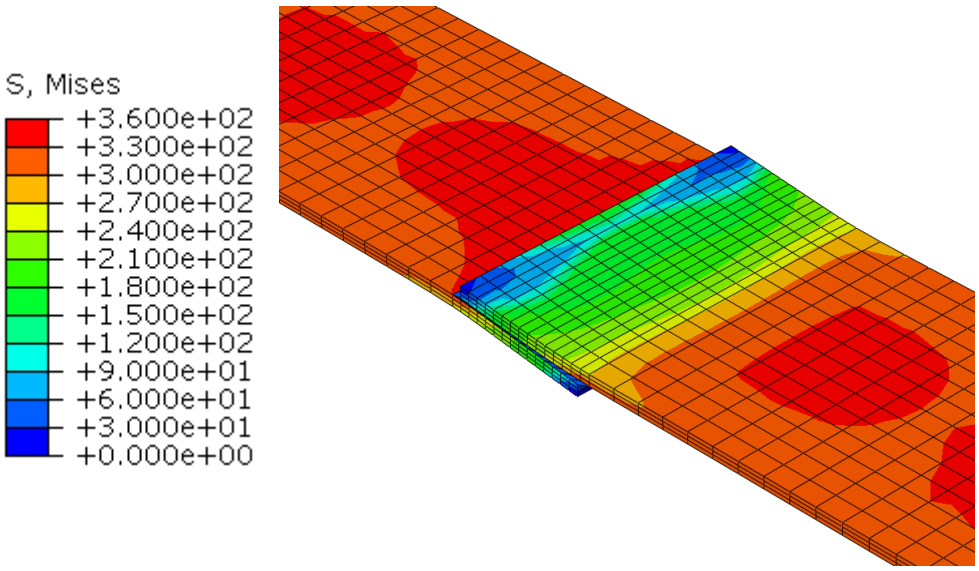

Figure 14: Gradient of stress across the width direction of the single lap joint, von Mises stress criterion (values in MPa).

5.2 Impact Simulations

Figure 15 shows the comparison between the experimental quasi-static *P-δ* curves and the correspondent numerical predictions using the 2D and 3D models described previously.

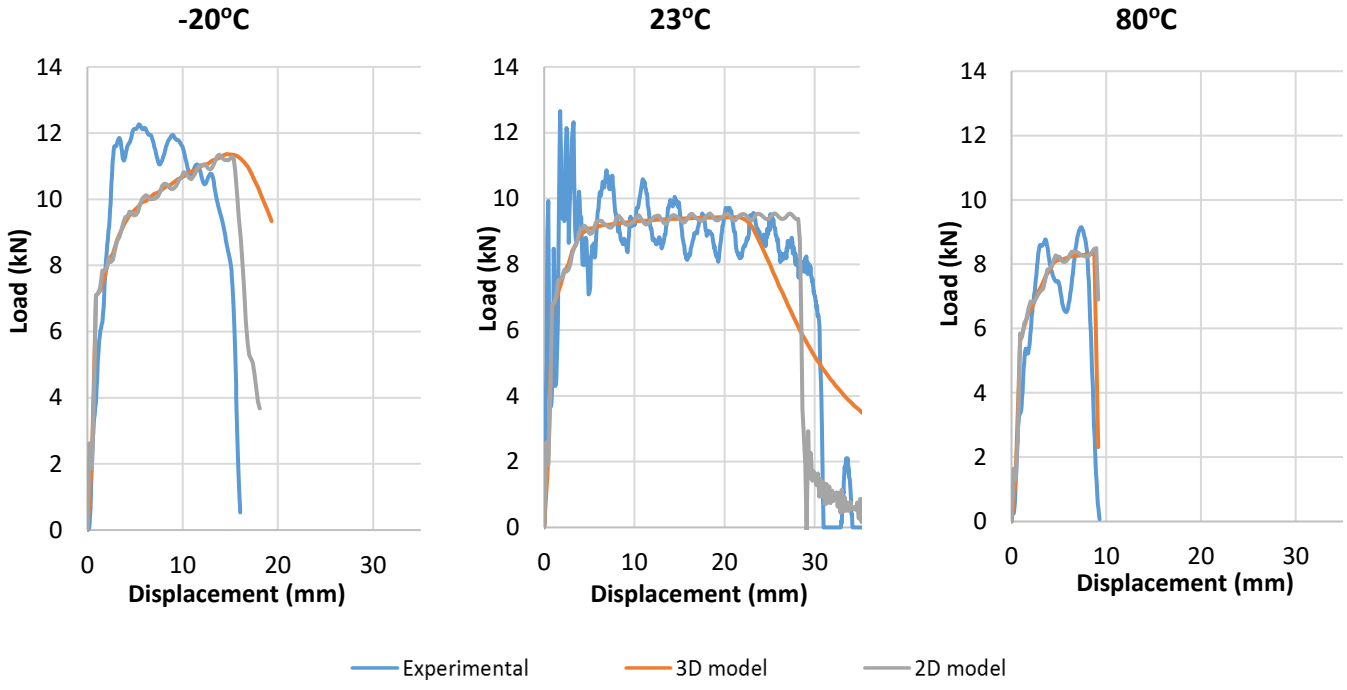

Figure 15: Impact simulations and comparison with experimental results.

The impact models were able to match the experimental results well. After failure, the 2D model predicts a sudden drop of load at every situation, which matches the experimental results. The 3D model predicts a soft drop in load because unlike the 2D model, it can predict deformations in the direction perpendicular to the axis of the specimen.

When failure occurred in the steel adherends (specimens tested under impact and at -20°C and 23°C), the load predicted by the 3D model drops very slowly because the used elements do not take into account complete failure of the adherends. Instead, it predicts very high plastic deformation of the substrates (Figure 16).

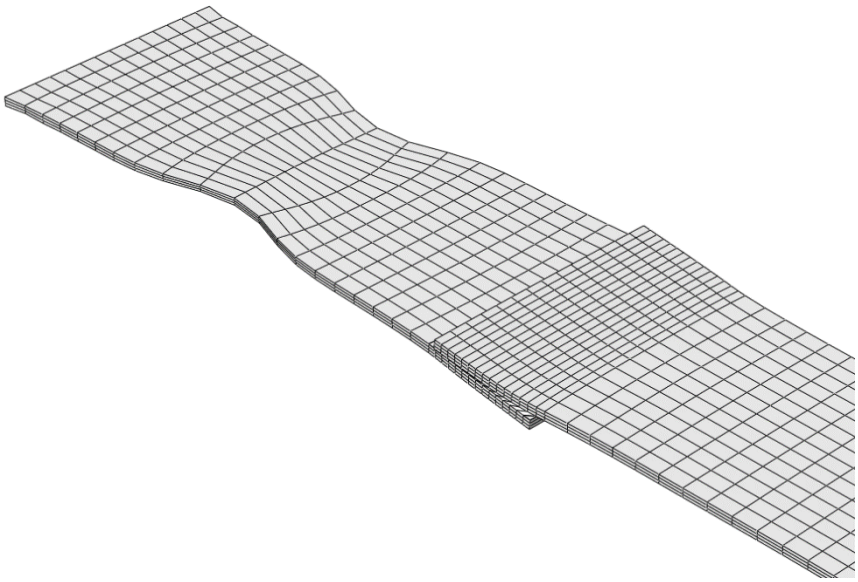

Figure 16: Deformation of mild steel substrates in the 3D impact model.

6 Discussion

At -20°C and at 23°C, quasi-static tested specimens and impact tested specimens showed different modes of failure. At low and room temperatures, while quasi-static tested specimens showed cohesive failure in the adhesive layer, impact tested specimens suffered ductile fracture in the mild steel adherends. Because the toughness of the steel adherends is higher than the adhesive's, the energy that was absorbed by the impact specimens was significantly higher than the energy absorbed by the quasi-static specimens.

At 80°C, the adhesive failed due to the peel stress at the ends of the overlap in both the quasi-static specimens and in the impact specimens. However, due to the higher strength of the adhesive at higher strain rates, the energy absorbed by the impact specimens was higher than the energy absorbed by the quasi-static specimens.

Temperature affected the tested SLJs in different ways:

- Impact tested specimens showed decreasing energy absorption from room temperature tested specimens to low temperature tested specimens because the toughness of the steel used as adherends is lower at lower temperatures.
- Quasi-static tested specimens, on the other hand, which fail in the adhesive layer, showed the opposite trend. These specimens fail due to the peel stress at the ends of the overlap and, as the strength of the adhesive is higher at low temperature, they can actually withstand higher loads at -20°C than at 23°C, which translates into higher energies being absorbed.

The maximum loads that the steel substrates were able to withstand were generally higher in impact conditions than in quasi-static conditions due to the higher strength of mild steel at higher strain rates. Adherend properties changed with temperature as well. Higher temperatures mean softer and more ductile steel. Temperature and strain rate dependence of the steel substrates also have influence on the mechanical performance of the tested SLJs, as stronger adherends induce lower peel stresses at the ends of the overlap, consequently increasing the load and energy absorption of SLJs. Figure 17 makes the comparison between the energy absorbed by the specimens tested in this study under impact and quasi-static conditions as a function of temperature.

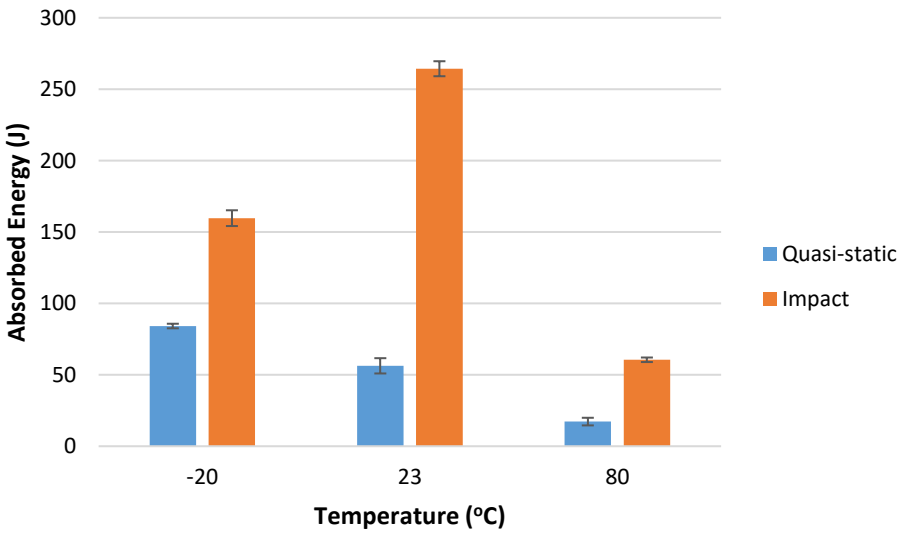

Figure 17: Energy absorbed by quasi-static and impact tested specimens as a function of test temperature.

The energy absorbed by impact specimens at -20°C and 23°C was significantly higher than the energy absorbed by impact specimens at 80°C. This is because the strength of the adhesive at

80°C is sharply reduced due to proximity to *Tg*, which caused these specimens to suffer cohesive failure within the adhesive layer. As failure of impact specimens at -20°C and 23°C occurred in the mild steel adherends, the higher energy absorption of impact specimens at 23°C is related to the higher toughness of the mild steel adherends at this temperature.

Figure 18 shows the comparison between experimental static and impact maximum displacement reached by the specimens and the values given by the numerical models. The numerical models can predict with little error the maximum displacement reached by the specimens in every situation. The 3D model can take into consideration deformation in the direction perpendicular to the loading direction of the specimen and given, therefore higher values than the 2D model.

Under quasi-static conditions failure happens in the adhesive layer. Because the adhesive is stronger at lower temperatures, the joint can withstand higher loads and, therefore the maximum displacement reached by the joint is also higher.

Under impact conditions at -40°C and 23°C the displacement at failure is given by the ductility of the steel adherends. The maximum displacement of specimens tested at 80°C is much lower than at lower temperatures because the steel is not allowed to deform significantly, as failure happens in the adhesive layer due to the reduced strength of the adhesive at higher temperatures.

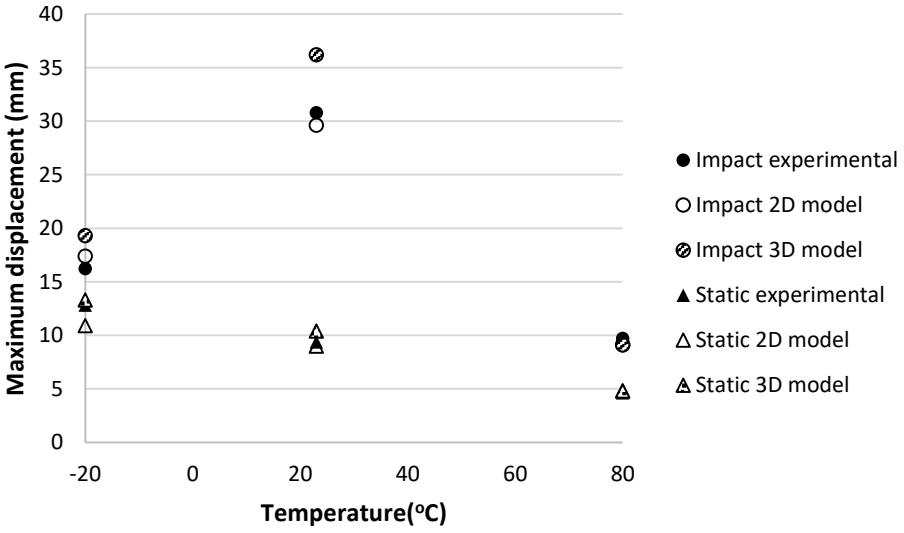

Figure 18: Comparison between static and impact maximum displacement reached by the specimens and comparison to numerical results. Standard deviation lower than 1 mm in every case.

Both the 2D and 3D models used in this study to predict the mechanical behaviour of the tested SLJs matched the experimental results well. Under quasi-static conditions, when extensive plastic deformation of the mild steel substrates was observed, the 2D model gave slightly higher maximum deformations than the 3D model because it did not take into account the stress gradient across the width of the bonded area. The use of FEM has proven to be an excellent tool to predict the mechanical behaviour of adhesive joints under both quasi-static and impact conditions with the variation of temperature.

7 Conclusions

The effect of temperature and strain rate in single lap joints bonded with a crash resistant epoxy was analysed in this paper. Both the mechanical properties of the mild steel adherends and the adhesive showed strain rate dependence, which was successfully modelled using the finite elements software Abaqus®.

Due to strain rate effects, impact tested specimens were able to withstand higher loads and absorb higher amounts of energy before failure than quasi-static tested specimens. At 23°C and at -20°C impact tested specimens failed in the mild steel adherends while quasi-static tested specimens failed in the adhesive layer. The difference in the locus of failure means that the quasi-static tested specimens were able to absorb only a fraction of the impact energy. At 80°C, the energy absorbed by the impact tested specimens was also higher than the energy absorbed by quasi-static tested specimens due to the improved strength of the adhesive.

The energy absorbed by quasi-static tested specimens shows a decreasing trend with temperature, due to the decrease of adhesive yield stress with temperature. However, this trend does not happen in the case of impact specimens, because the absorbed energy depends significantly on the ductility of the adherends, which is lower at lower temperatures.

The mechanical behaviour of the specimens under impact and quasi-static conditions at different temperatures were reasonably predicted by the 2D and 3D finite elements method used in this study.

Acknowledgements

The authors would like to thank Nagase Chemtex for supplying adhesive XNR 6852E-3.

References

1. Da Silva LF, Adams R. Joint strength predictions for adhesive joints to be used over a wide temperature range. International Journal of Adhesion and Adhesives. 2007;27:362-79.
2. Machado J, Marques E, da Silva LF. Adhesives and adhesive joints under impact loadings: An Overview. The Journal of Adhesion. 2017;DOI: 10.1080/00218464.2017.1282349.
3. Viana G, Costa M, Banea M, da Silva L. A review on the temperature and moisture degradation of adhesive joints. Proceedings of the Institution of Mechanical Engineers, Part L: Journal of Materials: Design and Applications. 2017;231:488-501.
4. Banea MD, da Silva LF, Carbas R, Campilho RD. Effect of material on the mechanical behaviour of adhesive joints for the automotive industry. Journal of Adhesion Science and Technology. 2017;31:663-76.
5. May M, Hesebeck O, Marzi S, Böhme W, Lienhard J, Kilchert S, Brede M, Hiermaier S. Rate dependent behavior of crash-optimized adhesives–Experimental characterization, model development, and simulation. Engineering Fracture Mechanics. 2015;133:112-37.
6. Marques E, da Silva L, Banea M, Carbas R. Adhesive joints for low-and high-temperature use: an Overview. The Journal of Adhesion. 2015;91:556-85.
7. Choudhry R, Hassan SF, Li S, Day R. Damage in single lap joints of woven fabric reinforced polymeric composites subjected to transverse impact loading. International Journal of Impact Engineering. 2015;80:76-93.
8. Meschut G., Teutenberg D., Henkel K. Design of low temperature cured adhesive joints in steel-FRPconstructions under crash loads. METC and 2nd ESTAD; 2015.
9. Dean G, Lord G, Duncan B, Comparison of the measured and predicted performance of adhesive joints under impact. National Physical Laboratory, Centre for Materials Measurement and Technology, Great Britain, 1999.
10. Srivastava V. Characterization of adhesive bonded lap joints of C/C–SiC composite and Ti–6Al–4V alloy under varying conditions. International journal of adhesion and adhesives. 2003;23:59-67.
11. Viana G, Costa M, Banea MD, da Silva LFM. Behaviour of environmentally degraded epoxy adhesives as a function of temperature. The Journal of Adhesion. 2016;93:95-112.
12. Bauwens JC. Relation between the compression yield stress and the mechanical loss peak of bisphenol-A-polycarbonate in the β transition range. Journal of Materials Science. 1972;7:577-84.
13. Ree T, Eyring H. Theory of non-Newtonian flow. I. Solid plastic system. Journal of Applied Physics. 1955;26:793-800.
14. Neumayer J, Kuhn P, Koerber H, Hinterholzl R. Experimental Determination of the Tensile and Shear Behaviour of Adhesives under Impact Loading. J Adhesion. 2016;92:503-16.
15. Bezemer A, Guyt C, Vlot A. New impact specimen for adhesives: optimization of high-speed-loaded adhesive joints. International journal of adhesion and adhesives. 1998;18:255-60.
16. Adamvalli M, Parameswaran V. Dynamic strength of adhesive single lap joints at high temperature. International Journal of Adhesion and Adhesives. 2008;28:321-7.

17. Banea MD, da Silva LFM, Campilho RDSG. Effect of Temperature on Tensile Strength and Mode I Fracture Toughness of a High Temperature Epoxy Adhesive. J Adhes Sci Technol. 2012;26:939-53.
18. Avendaño R, Carbas RJC, Marques EAS, da Silva LFM, Fernandes AA. Effect of temperature and strain rate on single lap joints with dissimilar lightweight adherends bonded with an acrylic adhesive. Compos Struct. 2016;152:34-44.
19. Goglio L, Peroni L, Peroni M, Rossetto M. High strain-rate compression and tension behaviour of an epoxy bi-component adhesive. International journal of adhesion and adhesives. 2008;28:329-39.
20. Morin D, Bourel B, Bennani B, Lauro F, Lesueur D. A new cohesive element for structural bonding modelling under dynamic loading. International Journal of Impact Engineering. 2013;53:94-105.
21. Banea MD, Da Silva LFM, Campilho RDSG. The Effect of Adhesive Thickness on the Mechanical Behavior of a Structural Polyurethane Adhesive. J Adhesion. 2015;91:331-46.
22. Thouless M, Adams J, Kafkalidis M, Ward S, Dickie R, Westerbeek G. Determining the toughness of plastically deforming joints. Journal of materials science. 1998;33:189-97.
23. Harris J, Adams R. An assessment of the impact performance of bonded joints for use in high energy absorbing structures. Proceedings of the Institution of Mechanical Engineers, Part C: Journal of Mechanical Engineering Science. 1985;199:121-31.
24. Avendaño R, Carbas RJC, Chaves F, da Silva LFM, Fernandes A. Impact loading of single lap joints of dissimilar lightweight adherends bonded with a crash-resistant epoxy adhesive. Journal of Engineering Materials and Technology. 2016;Accepted for publication.
25. Viana G, Mata R, Costa M, Silva LFMd, Banea MD, Carbas RJC. Impact of adhesive joints for the automotive industry at low and high temperatures. Poster session presented at: AB2015; 2015 Jul 2-3; Porto, Portugal.
26. Banea MD, da Silva LFM, Campilho RDSG. Mode I fracture toughness of adhesively bonded joints as a function of temperature: Experimental and numerical study. Int J Adhes Adhes. 2011;31:273-9.
27. Zhang Y, Adams R, da Silva L. A rapid method of measuring the glass transition temperature using a novel dynamic mechanical analysis method. The Journal of Adhesion. 2013;89:785-806.
28. Araújo H, Machado J, Marques E, da Silva L. Dynamic behaviour of composite adhesive joints for the automotive industry. Composite Structures. 2017;171:549-61.
29. Adams R, Peppiatt N. Stress analysis of adhesive-bonded lap joints. Journal of strain analysis. 1974;9:185-96.

PAPER 6

Theoretical and Applied Fracture Mechanics 89 (2017) 1–15

Contents lists available at ScienceDirect

Theoretical and Applied Fracture Mechanics

journal homepage: www.elsevier.com/locate/tafmec

The influence of water on the fracture envelope of an adhesive joint

P. Fernandes [a], G. Viana [a], R.J.C. Carbas [a,b], M. Costa [a], L.F.M. da Silva [b,*], M.D. Banea [c]

[a] Department of Mechanical Engineering, Faculty of Engineering, University of Porto, Portugal
[b] Institute of Science and Innovation in Mechanical and Industrial Engineering (INEGI), Faculty of Engineering, University of Porto, Portugal
[c] Federal Center of Technological Education in Rio de Janeiro, CEFET/RJ Rio de Janeiro, Brazil

ARTICLE INFO

Article history:
Received 3 October 2016
Revised 7 December 2016
Accepted 8 January 2017
Available online 10 January 2017

Keywords:
Moisture degradation
Structural adhesive
Fracture toughness
Mixed-mode loading
Open specimen
Accelerated ageing

ABSTRACT

This research aims at determining the fracture envelope of an adhesive as a function of the water content. The fracture toughness of an adhesive joint was determined under pure mode I, II and mixed mode I + II loadings, in three different environments: dry, aged in salt water and aged in distilled water. The fracture toughness under mode I and II were determined using Double Cantilever Beam (DCB) and End-Notched Flexure (ENF) tests, respectively. The characterization of the fracture toughness under mixed-mode was done using an apparatus capable of applying a wide range of loadings that go from pure mode I to almost pure mode II. To accelerate the diffusion process and obtain a uniform water concentration in the adhesive joint, a modified DCB specimen (ODCB specimen) was adopted. Finite Element (FE) analysis was used to determine the gradient of water concentration in both specimens and to validate the use of the modified DCB specimens, comparing the fracture toughness obtained using DCB and ODCB specimens. It was found that the toughness of the adhesive changed as a function of the ageing environment. For the salt water environment, the mechanical properties increased, while for the distilled water environment, degradation of the mechanical properties was observed.

1. Introduction

As an alternative to mechanical joints, the use of adhesive joints has been increasing since they provide several advantages over conventional methods. This can be seen in aerospace, automotive and maritime industries as adhesive joints allow for a uniform stress distribution along the width of the bonded area, enhancing the stiffness, load transmission and fatigue resistance of the structure while reducing the weight and thus the cost [1,2].

This type of joint may be exposed to aggressive environments such as high humidity, extreme temperature or radiation. While fracture mechanics characterization tests for adhesive joints may provide relevant properties to guide the design process, the information available to predict the behaviour of the adhesive after being exposed to aggressive environments is scarce. Therefore, the influence of environmental agents on the mechanical properties of the adhesive should be studied [3].

Water may enter the adhesive joint by Comyn [4]: diffusion in bulk adhesive, transport along the interface, capillary action through cracks and crazes or diffusion through the adherend if permeable. Usually this process can be described with Fick's law of diffusion, where the uptake is a function of time, concentration and thickness [5–9]. However, other models have been developed to describe the diffusion process such as: dual fickian diffusion [8], delayed dual fickian [10] and the Langmuir model [11]. External factors also influence the rate at which water is absorbed and the maximum water uptake, such as temperature [8] and the stress state of the adhesive [12]. Water can act as a plasticizer, reducing the interaction forces between molecules and allowing them to rearrange themselves more easily. As a result, this water uptake can lead to changes on the properties of the adhesive due to the plasticization of the adhesive and adherend, which leads to a change of thermal and mechanical properties, involving: lower rigidity at room temperature, decrease of the glass transition temperature (T_g) [5,9,13] and increase of the strain failure at room temperature [9,14]. However, these changes caused by plasticization can be partially or fully reversed with desorption [9,15]. It has also been reported that the presence of water on the adhesive leads to a reduction of its fracture toughness [3,16,17]. Nonetheless, in some cases, an initial increase due to plasticization effects is observed, followed by a decrease due to degradation [9,16].

Fracture mechanics tests such as DCB, ENF and mixed-mode loadings can be used to assess the influence of water on the

* Corresponding author.
E-mail address: lucas@fe.up.pt (L.F.M. da Silva).

http://dx.doi.org/10.1016/j.tafmec.2017.01.001
0167-8442/

adhesive [18]. However, using the standard specimens used in these tests, a long time is required to reach an appreciable level of water concentration. Furthermore, this concentration can also vary in time and space [8,9,16]. As an alternative, some authors used smaller specimens [19] to accelerate the diffusion process, while others modified the specimen by opening it and using a secondary bond [16,18,20]. Based on the second alternative mentioned, a new modified specimen was used in this research, which shortens the diffusion path and avoids the asymmetry of the specimen proposed by Wylde and Spelt [16]. Regardless of the method adopted to accelerate the diffusion process, all the mentioned authors found a reduction in the mechanical properties of the adhesive when it was exposed to aggressive environments for long periods of time. In the particular case of Wylde and Spelt [16], an initial increase of mechanical properties was observed.

In this research, the fracture envelope of a commercial epoxy adhesive used in the automotive industry is characterized as a function of the water content in the adhesive. The fracture characterization of the adhesive joints was performed when the specimens were submitted to pure modes (shear and opening) and mixed mode loadings. Three different environments were tested: dry, a saturated solution of NaCl (salt water) and distilled water. For the dry environment, standard DCB specimens were used, while for the salt water and distilled water environments a modified DCB specimen was adopted.

Furthermore, a FE analysis was performed to determine the gradient of water concentration in the standard DCB specimen, as well as to validate the use of the modified DCB specimens, used to accelerate the ageing process, and predicting the behaviour of the adhesive joint.

2. Experimental details

In order to determine the fracture envelope as a function of water content, DCB specimens standardized by ASTM were used [21]. However, due to the geometry of this specimen, the saturation process would take several years. Thus, in order to accelerate the diffusion process, open-DCB specimens (ODCB) were used, as they are able to replicate the diffusion process that occurs in an adhesive plate.

To be able to compare the influence of water on the fracture envelope using two different specimens, it was necessary to determine the influence of their geometry in the value of the fracture toughness measured experimentally. This analysis was done only for mode I and assumed to be constant for the other modes.

The characterization of the fracture envelopes was done using three loading modes: pure mode I, mixed-mode 55° and mixed-mode 87°. Exceptionally, ENF tests were performed using DCB specimens in a dry environment to determine the G_{IIC} of the adhesive and to be able to input this property in the numerical models.

2.1. Adhesive

The adhesive chosen for this study was SikaPower®-4720 (Supplied by Sika, Vila Nova de Gaia, Portugal) and was used for both DCB and ODCB specimens. It is a two-component high-strength epoxy adhesive specifically designed for metal, particularly aluminium, and composite panel bonding but not intended to be used for body structural parts [22].

The stress-strain curve, as well as the mechanical properties of this adhesive, have been determined previously with tensile tests using bulk specimens [23] (Table 1). On the other hand, the toughness of the adhesive was determined in this research.

Table 1
Mechanical properties of SikaPower®-4720 [23,24].

Property	SikaPower®-4720
Young's modulus, E [MPa]	2170
Tensile strength, σ_{max} [MPa]	25.8
Strain to failure, ε_f [%]	2.7
Shear modulus, G [MPa]	800[a]
Shear strength, τ_{max} [MPa]	14.9[a]
Critical energy release rate in mode I, G_{Ic} [N/mm]	1.15
Critical energy release rate in mode II, G_{IIc} [N/mm]	4.5

[a] Deduced from tensile properties using Von Mises Yield Criterion.

2.2. Ageing environment

The ageing of the adhesive was done by immersing the specimens in a container with either distilled water or salt water (saturated solution of NaCl, which is equivalent to exposure in a 75% RH environment) at 32.5 °C [25,26]. The standard DCB specimens were used to determine the fracture envelope in a dry environment, while the ODCB specimens were used to characterize the fracture envelope in the salt water and distilled water environments.

2.3. DCB specimens

To characterize the fracture envelope, a standard DCB specimen was used, in accordance to ASTM 3433-99 [21]. The adherend's material used for the DCB specimens was aluminium Al7075-T6 supplied by Lanema (Ovar, Portugal). Aluminium was chosen over steel due to the ageing environment, as when exposed to distilled or salt water, the steel adherend would be corroded. This situation can be completely avoided by using phosphoric acid anodized aluminium instead. The choice of this particular aluminium alloy (Table 2) was based on its yield strength, which is high enough to avoid any plastic deformation during the tests.

2.4. ODCB specimens

Open-faced specimens have been used in the past to accelerate the diffusion process [16,18], but this leads to an asymmetric adhesive joint. In this research, a new configuration is proposed. The ODCB specimens are a modification of the standardized DCB specimens. They differ on the fact that, instead of one adhesive layer, the ODCB specimens are constituted by three adhesive layers: one primary bond and two secondary bonds (Fig. 1).

The primary bond is a plate made of the adhesive that is meant to be degraded, in this case SikaPower®-4720. The plate is produced in a mould coated with a release agent and, after 24 h in a hydraulic press, it can be removed from the mould and placed in a dry environment for 5 days, allowing the plate to be completely cured and dried. Afterwards, the adhesive plate is abraded with sandpaper and exposed to the ageing environment. Since the plate is not bonded to any adherend, the area exposed to the environment is much larger than the area of adhesive on a standard DCB specimen, which accelerates the saturation process. After these steps, the aged adhesive plate is abraded with sandpaper again and cleaned with acetone to allow a better adhesion to the secondary bond.

The secondary bond was made with a secondary adhesive, with higher mechanical properties, which is meant to bond the

Table 2
Mechanical properties of aluminium Al7075-T6 supplied by Lanema (Ovar, Portugal).

Maximum strength (Rm)	Yield strength (Rp 0.2)	Hardness (Brinell)
525 MPa	455 MPa	130–150

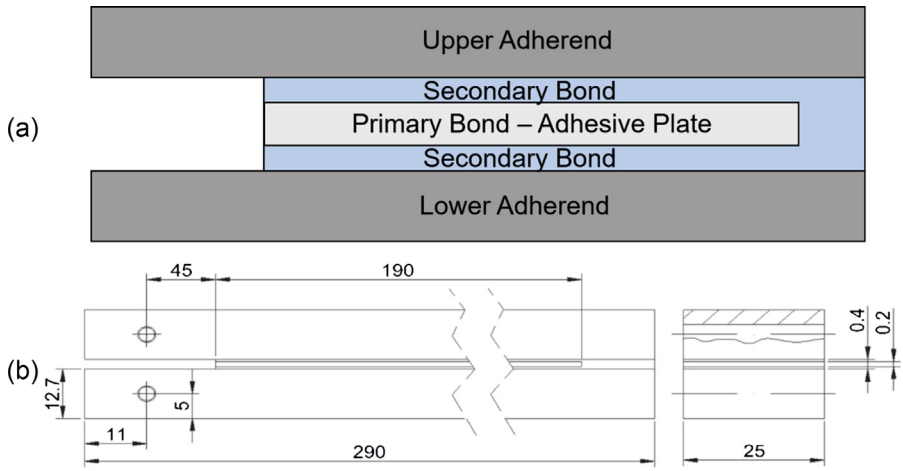

Fig. 1. Scheme (a) and definition draw (b) of an ODCB specimen (dimensions in mm).

degraded adhesive plate to the adherends. For this reason, two layers of the secondary adhesive were used, one on each side of the adhesive plate.

During the experimental tests, it was observed that the secondary bond had no influence in the critical energy release rate and that any difference observed was caused by the change of thickness of the adhesive layer. For this reason, it was possible to choose different secondary bonds for each environment, ensuring that the failure was cohesive in the adhesive plate.

2.4.1. Secondary bond for the salt water environment – Araldite® 420

A two component epoxy, room temperature curing paste adhesive of high strength, toughness and moisture resistance was chosen as secondary adhesive for the salt water environment. This adhesive cured at room temperature for 5 days.

This adhesive was chosen as a secondary bonding for having higher mechanical properties in comparison to the primary adhesive (Table 3). Also, it has been used in the literature as a secondary bond for a similar process [18].

2.4.2. Secondary bond for the distilled water environment – Araldite® 2021

A two component toughened methacrylate adhesive system that cured at room temperature in 1 day was chosen as secondary adhesive for distilled water environment.

This adhesive was chosen for its fast cure cycle, which minimizes the loss of water during the production of the ODCB specimens. It was also chosen for having slightly better mechanical properties than the primary adhesive (Table 4). In this environment, it is acceptable for the secondary bond and primary bond to have similar properties, as only the mechanical properties of the primary bond will be degraded.

Table 3
Mechanical properties of Araldite® 420 A/B [27,28].

Property	Araldite® 420 A/B
Young's modulus, E [MPa]	1800
Tensile strength, σ_{max} [MPa]	28.6
Shear modulus, G [MPa]	692
Shear strength, ζ_{max} [MPa]	16.5
Critical energy release rate in mode I, G_{Ic} [N/mm]	3
Critical energy release rate in mode II, G_{IIc} [N/mm]	12.5

Table 4
Mechanical properties of Araldite® 2021 [29–31].

Property	Araldite® 2021
Young's modulus, E [MPa]	1130
Tensile strength, σ_{max} [MPa]	26.2
Shear modulus, G [MPa]	403.6
Shear strength, τ_{max} [MPa]	18.4
Critical energy release rate in mode I, G_{Ic} [N/mm]	1.6
Critical energy release rate in mode II, G_{IIc} [N/mm]	3.17

2.5. Test method

2.5.1. DCB test

DCB tests were done to determine the G_{Ic} of the adhesive, in accordance to ASTM D3433-99 [21]. To determine this value, three valid test results were used. During the DCB tests, an opening force is applied to the specimens. The load and displacements were recorded by the computers data acquisition system using an Instron® 3367 Universal Testing Machine (Norwood, USA) with a load cell of 30 kN. With the data collected, it is possible to determine the R-curves using the Compliance Based Beam Method (CBBM) [32].

Before testing, a pre-crack was initiated in all specimens to avoid a blunt crack, which could lead to an increase of the energy required for the crack to propagate. After the pre-crack was done, the initial crack length was measured. The specimen was then tested at room temperature and at a constant displacement rate of 0.2 mm/min.

Using the CBBM, the value of G_{Ic} can be determined according to the following expression [32]:

$$G_{Ic} = \frac{6P^2}{b^2h^3}\left(\frac{2a_e^2}{E_f} + \frac{h^2}{5G}\right) \quad (1)$$

Which depends only on the specimen's compliance, corrected flexural modulus (E_f), shear modulus of the adherend (G) and equivalent crack length (a_e) [32,33]. In this equation, P is the load applied and b and h are the width and thickness of the specimen.

2.5.2. ENF test

There are no standards for testing the mode II fracture toughness [32]. The most simple and most common test is the ENF. The equipment and number of specimens used for these tests was the same that was used for the DCB tests.

Using the CBBM, the value of G_{IIc} can be determined according to the follow expression [32]:

$$G_{IIc} = \frac{9P^2 a_{eq}^2}{16 b^2 E_f h^3} \quad (2)$$

2.5.3. Mixed-mode test

To perform the mixed-mode tests, a loading jig, described in the Portuguese patent no 107188 B [34], was used (Fig. 2). This apparatus was designed to perform mixed-mode fracture tests, a combination of mode I and mode II loadings, on adhesively bonded DCB specimens. It can be equipped on a universal testing machine and is possible to apply loadings with a wide array of mode combinations ranging from pure mode I to almost pure mode II, by adjusting the length of the beams supporting the specimen (S_1, S_2, S_3 and S_4) and the fixation points (L_1 and $2L$). A detailed explanation on how the loading jig works is given in the mentioned patent. Furthermore, an article that explains the principles, limitations and all the details regarding the loading jig and its use will be published.

For mixed-mode tests, the fracture ratio can be defined by the angle φ according to the following equation [32]:

$$\varphi = \tan^{-1}\sqrt{\frac{G_{II}}{G_I}} \quad (3)$$

As a result, $\varphi = 0°$ represents pure mode I, $\varphi = 90°$ pure mode II, and as an example, $\varphi = 45°$ would be a mode where $G_I = G_{II}$.

During this test, 3 variables are recorded:

- The load applied to the apparatus, obtained from an Instron® 3367 Universal Testing Machine (Norwood, USA).
- Displacement of the upper and lower adherend, δ_1 and δ_2, obtained from two Linear Variable Differential Transformers (LVDT) attached to each beam.

Using this data and applying the CBBM, it is possible to determine the fracture toughness for mode I and II independently from each other [35]:

$$G_I = \frac{6P^2}{b^2 h^3}\left(\frac{2a_{eI}^2}{E_f} + \frac{h^2}{5G}\right) \quad (4)$$

$$G_{II} = \frac{9P^2 a_{eII}^2}{4 b^2 E_f h^3} \quad (5)$$

Since the fracture toughness for each mode is determined independently, two different equivalent crack lengths are used, for mode I (a_{eI}) and mode II (a_{eII}).

It is also important to note that G_I and G_{II} determined above are two parts of a same toughness, G_C for the respective mixed-mode tested, and should not be confused with G_{IC} or G_{IIC}, which respectively represent the fracture toughness for mode I, obtained through the DCB test, and the fracture toughness for mode II, obtained through the ENF test.

Furthermore, Eqs. (2) and (5), although similar, are deduced for different tests, with slightly different boundary conditions. As a result, only the denominator differs.

3. Experimental results and discussion

3.1. Validation of the ODCB specimens

Changing from DCB to ODCB specimens may have an influence in the fracture toughness measured experimentally. This change is justified by the change of thickness of the adhesive layer, which changes the shape of the fracture process zone and is known to cause differences in the measured toughness [36], and by the inclusion of a secondary adhesive to bond the adhesive plate to the adherend (Fig. 3).

Thus, in order to validate the use of the ODCB specimens, a comparison between the mode I fracture toughness of 3 different specimen configurations was done. The first specimen was a DCB specimen with a 0.2 mm thick adhesive layer. The second, was a DCB specimen with a 0.4 mm thick adhesive layer. The last one, was an ODCB specimen which had an adhesive layer with a total thickness of 0.4 mm (Fig. 4).

With these three configurations it was possible to isolate the influence of the adhesive's thickness and the influence of the secondary bond. In the end, it was possible to understand if the fracture toughness measured was different and what is the cause of this change.

Representative load-displacement curves of the 3 types of specimens used to validate the influence of the adhesive's thickness and of the secondary bond can be seen in Fig. 5. The curve obtained for the DCB with a 0.2 mm thick adhesive layer is the reference. A slight change in the maximum load when the thickness is increased to 0.4 mm can be seen. However, the results obtained for the DCB with 0.4 mm thick adhesive layer and for the ODCB specimen tested in a dry environment are in agreement with each

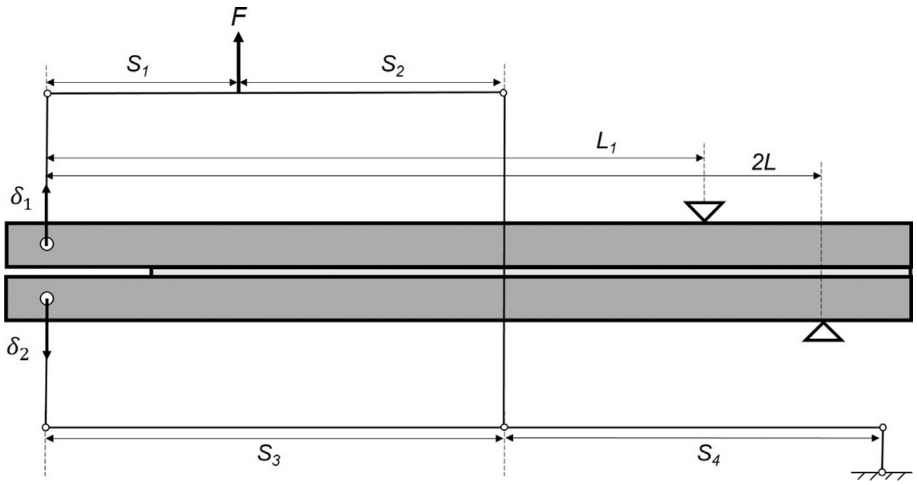

Fig. 2. Mixed-mode apparatus. S_1, S_2, S_3, S_4, $2L$ and L_1 are the six variables that define the configuration of the equipment and, as a result, the loading mode. δ_1 and δ_2 are the displacements of the upper and lower adherend of the specimen and F is the force applied to the apparatus by the universal testing machine.

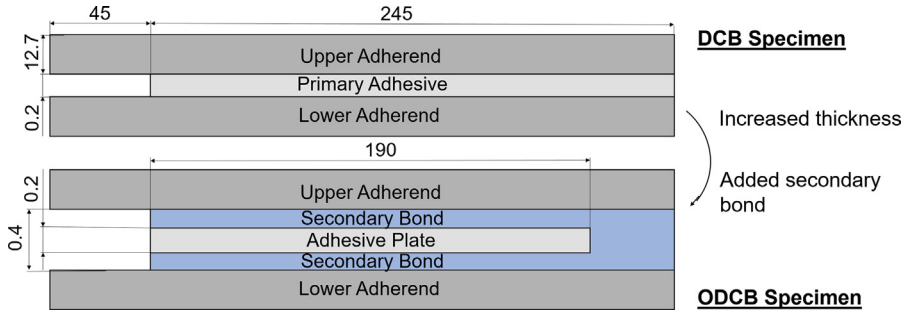

Fig. 3. Differences between the DCB and ODCB specimens (dimensions in mm).

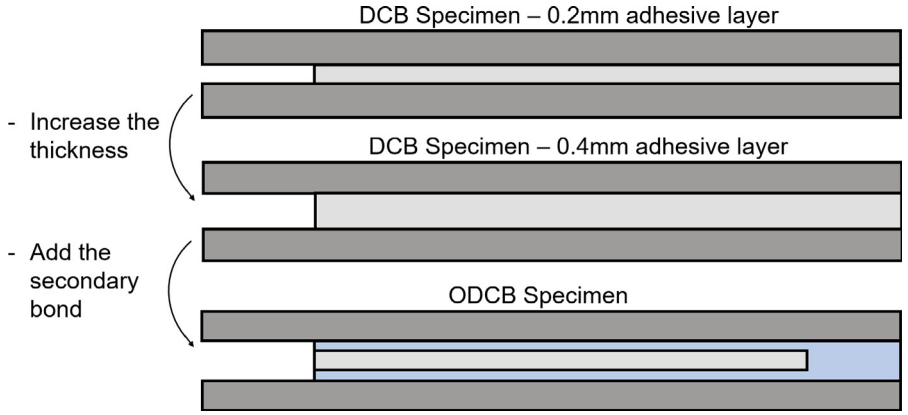

Fig. 4. Three specimen configurations (DCB with 0.2 and 0.4 mm thick adhesive layer and ODCB specimen) and their differences.

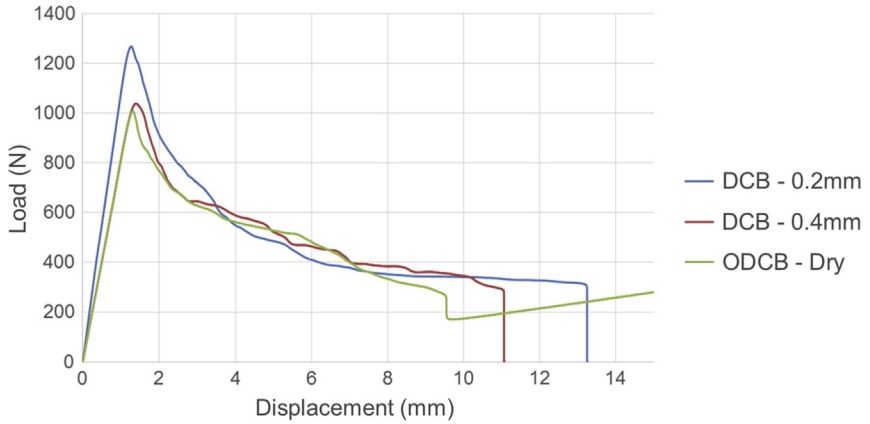

Fig. 5. Representative load-displacement curves of the 3 types of specimens used to validate the influence of the adhesive's thickness and of the secondary bond.

other, suggesting that the introduction of a secondary bond does not affect significantly the obtained properties (Fig. 5).

Analysing the R-curves, a slight increase of G_{IC} is observed when the thickness of the adhesive increases, but no difference is seen with the inclusion of the secondary bond (Fig. 6). As a result, the increase of the adhesive layer's thickness lead to an overestimation of the fracture toughness by 0.2 N/mm. However, the inclusion of the secondary bond did not have an influence on G_{IC}.

In other modified specimens found in the literature, that include the use of a secondary bonding, the influence of the secondary adhesive has also been reported to be close to null. Therefore, this data is in agreement with the results obtained by other authors [16].

This comparison was done using at least 3 valid test results for each different condition.

3.2. Fracture envelopes

With a minimum of three valid results for each experimental tests (Table 5) it was possible to define the fracture envelopes for the three environments studied (Fig. 7). However, it is important to remark that the experimental validation of the use of ODCB specimens, used in the salt water and distilled water environments, has not been done for mixed-mode loadings. This method was validated for mode I and assumed constant for the other cases.

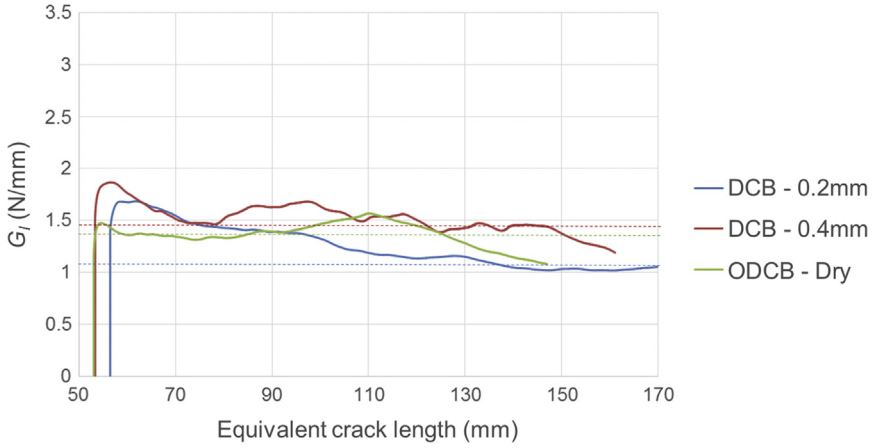

Fig. 6. Representative R-curves of the 3 types of specimens used to validate the influence of the adhesive's thickness and of the secondary bond.

Table 5
Summary of the fracture toughness for the different loading modes as a function of the relative humidity.

		Mode I	Mixed-mode 55°		Mixed-mode 87°		Mode II
Specimen	Environment	G_{IC} (N/mm)	G_I (N/mm)	G_{II} (N/mm)	G_I (N/mm)	G_{II} (N/mm)	G_{IIC} (N/mm)
DCB	Dry	1.15	0.92	1.57	0.04	6.60	4.83
ODCB	Salt water	1.60	1.35	1.08	0.01	7.26	–
	Distilled water	0.61	0.55	0.73	0.02	2.84	–

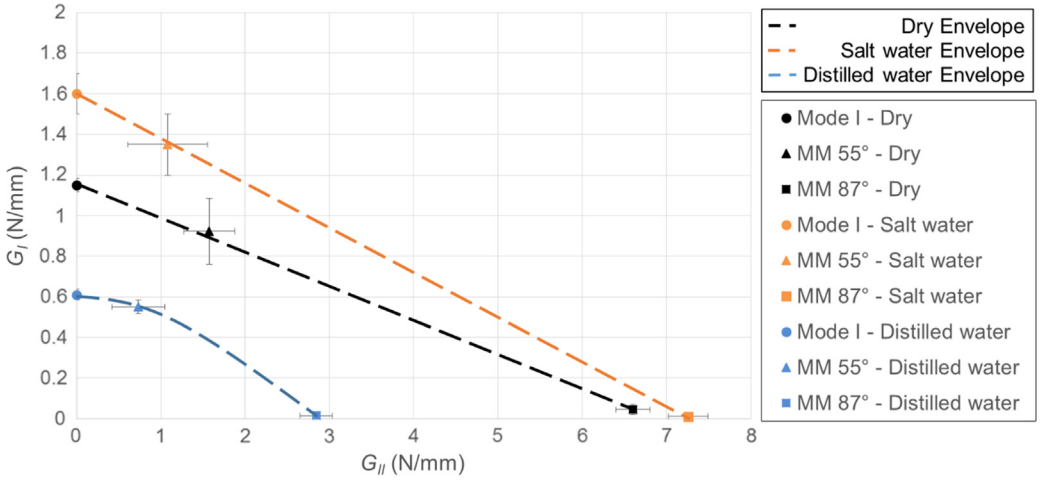

Fig. 7. Fracture envelopes of the specimens tested in a dry, salt water and distilled water environments.

3.2.1. Dry environment

In this envelope, the difference between the values of G_{II} obtained for the ENF and mixed-mode 87° tests stands out (Table 5). It was expected that the mode II component of the fracture toughness measured in the mixed-mode 87° test would be lower than the one measured in the ENF test, as the mixed-mode test introduces an opening load. However, the experimental results show otherwise. Three possible situations may justify this difference. First, it is relevant to point out that these two tests were done using different equipment, with distinct rigidities, which may help explain the difference in the values obtained. To further investigate this possibility, it would be interesting to apply the arcan test, as it can reproduce the loadings in question. In second place, this behaviour is known for composite materials and can be described through the Benzeggagh-Kenane failure criterion [37]. More recently, the same behaviour was reported for adhesives, although the causes of such behaviour are not fully understood [38]. Finally, the third factor to take into account is that the ENF and mixed-mode tests are not standardized and that it is difficult to reproduce pure mode II loadings. All these aspects require further investigation to fully understand the difference between the results obtained for the mixed-mode 87° and for the ENF test.

Ignoring the data obtained with the ENF test, the fracture envelope for the dry environment can be described with a linear function (Eq. (6)).

$$G_I = -0.1658 G_{II} + 1.1576 \quad (6)$$

3.2.2. Salt water environment

Similarly to the results of the dry environment, it seems possible to describe this envelope with a linear function (Eq. (7)). Also,

an increase in the fracture toughness can be observed in comparison with the envelope determined in a dry environment.

$$G_I = -0.2188G_{II} + 1.5946 \quad (7)$$

3.2.3. Distilled water environment

Unlike previous results, the shape of the fracture envelope determined in the distilled water environment can be approximated with a quadratic function (Eq. (8)). It can also be seen that the fracture toughness was reduced when compared to the dry environment.

$$G_I = -0.0658G_{II}^2 - 0.0125G_{II} + 0.5989 \quad (8)$$

In all three environments, the fracture envelope is defined by either a linear or quadratic function. These two types are the most common found in the literature [35]. Less common cases report an initial increase in fracture toughness for mixed-modes close to pure mode I [38]. This situation is known for composite materials and is described by the Benzeggagh–Kenane failure criterion [37].

3.3. Influence of water on the fracture envelope

Analysing the three fracture envelopes and considering the dry environment as a reference, two changes can be identified (Fig. 8). The first one is the change to the distilled water environment, where the fracture toughness of the adhesive is reduced in all loading modes. This behaviour can be explained with the degradation of the adhesive. The second one is the increase of the fracture toughness in the salt water environment. Such change is explained by the plasticization of the adhesive, a phenomenon that allows the polymeric molecules in the adhesive to rearrange themselves more easily, reducing its rigidity and, as a result, increasing its ductility.

In both scenarios, the changes observed can be explained with the adhesive's water mass uptake in each environment, as well as the influence of the ageing environment on the T_g (Fig. 9), which has been reported in the literature [39].

Starting with the distilled water environment, the degradation that occurs can easily be explained with the reduction of the T_g to a point below room temperature. It is known that the toughness of structural adhesives above T_g is very low [40]. As a consequence, any test done above 10 °C will prove a reduction in properties. Furthermore, the adhesive's mass uptake is equal to 35%, which leads to a huge concentration of water within the adhesive and explains why the properties were reduced so significantly within 4 days. Similar results have been obtained by other authors in the past [16,18,19].

In the salt water environment, the increase of fracture toughness can be explained as the result of the interaction between

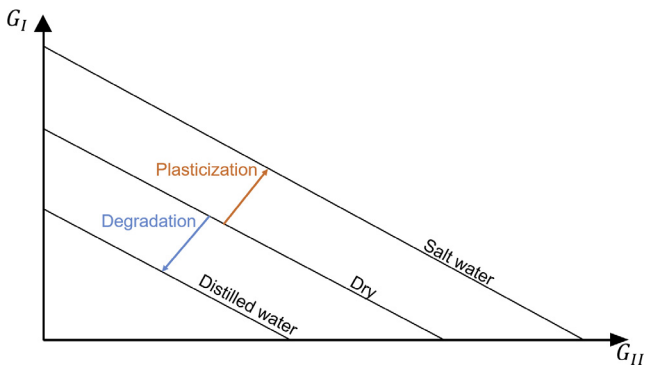

Fig. 8. Schematic representation of the three envelopes and their interactions.

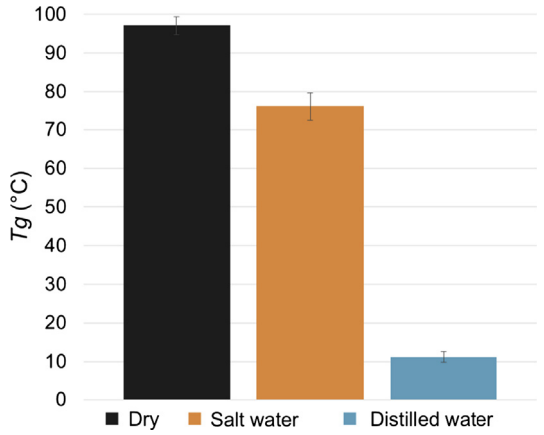

Fig. 9. Glass transition temperature of SikaPower®-4720 as a function of the ageing environment [39].

two opposite factors. On one side, the water absorbed causes a slight degradation, which can be seen in the form of a reduction of T_g. However, the degradation that occurs is not enough to overcome the increase of ductility caused by the plasticization of the adhesive. This explanation becomes more acceptable once it is taken into account that in this environment the mass uptake is approximately 6 times lower (6.5%) than in the distilled water environment. Although not as common, this initial increase has also been reported by other authors in the past [16,19].

4. Numerical modelling

A numerical analysis was carried out to study the time required for the ODCB specimens to saturate and to study the differences between DCB and ODCB specimens in terms of fracture energy obtained. In this section, both fracture and diffusion models are described, followed by the results obtained in each case.

4.1. Diffusion models

Two 1D finite element models were built in ABAQUS® to simulate the diffusion process in the standard DCB joint and in the adhesive plate, used for the ODCB specimens. The objective of these models is to determine the concentration of water in the adhesive. In order to do so, an analogy between heat transfer and moisture diffusion was used [2,41].

In both cases, a 2-node heat transfer link was used (DC1D2). The water sorption parameters of the adhesive SikaPower®-4720, coefficient of moisture diffusion (D) and mass attained at equilibrium (m_∞), were obtained in a previous study (Table 6) [39]. A Fickian behaviour is observed in the distilled water environment, while a sequential dual-fickian behaviour is more suitable for the salt water environment. For this reason, two coefficients of moisture diffusion and two values of mass attained at equilibrium are required for the salt water environment, as opposed to the distilled water environment which only requires one of each.

4.1.1. Diffusion in the DCB specimen

To simulate the diffusion in the DCB specimen, a 1D finite element model representing half the width of the adhesive layer was used (Fig. 10a). The decision of using a 1D model was based on two assumptions:

Table 6
Diffusion parameters of the adhesive SikaPower®-4720 [39].

		D_1 (m^2/s)	m^1_∞ (%)	D_2 (m^2/s)	m^2_∞ (%)
SikaPower®-4720	Distilled water	1.2×10^{-13}	32.5	–	–
	Salt water	2.6×10^{-13}	2.0	2.5×10^{-14}	1.8

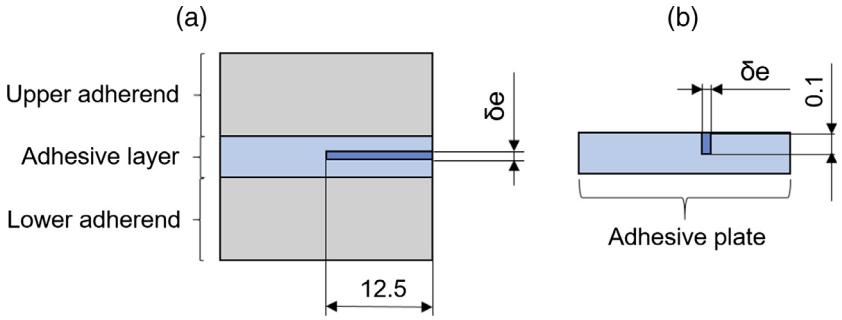

Fig. 10. (a) Scheme of a front view of the DCB specimen. The dark blue area represents the 1D element modelled for the diffusion in the DCB specimen; (b) Scheme of a front view of the adhesive plate. The dark blue area represents the 1D element modelled for the diffusion in the adhesive plate (dimensions in mm). In both cases, the infinitesimal thickness of the element is represented with δe. (For interpretation of the references to colour in this figure legend, the reader is referred to the web version of this article.)

- The water uptake will only occur through the adhesive exposed to the ageing environment. This assumes the inexistence of empty paths between the adhesive layer and the adherend that could accelerate the diffusion process.
- The water uptake perpendicular to the length of the adhesive layer is much larger than the uptake perpendicular to the width. This assumption is based on the geometry of the DCB specimen, where the length is much longer than the width.

Considering these assumption, a unidirectional diffusion process through the adhesive's thickness can be assumed.

4.1.2. Diffusion in the adhesive plate

To simulate the diffusion in the adhesive plate, a 1D finite element model representing half the thickness of the adhesive plate was used (Fig. 10b). In this case, the use of a 1D model was based on the geometry of the adhesive plate. Since the water uptake can occur through all direction, and given the fact that the length and width of the plate are much larger than its thickness, a unidirectional diffusion process through the adhesive's thickness can be assumed.

In total, both models have 500 elements and 501 nodes.

4.1.3. Diffusion model's results

Considering the diffusion parameters mentioned in Table 6 and the experimental measurements of the adhesive's plate mass, the results shown in Fig. 11 were obtained.

The numerical simulations suggested that the adhesive plates would be saturated after 2 days, in both environments. However, the experimental results show that the diffusion process is slower. The reason behind this difference is that the data used for the numerical models was determined with a 1 mm thick specimen, 5 times larger than the adhesive plates. It was shown in the literature that the diffusion coefficient and the saturation levels change as a function of the specimen's thickness [8].

Using the experimental results, the diffusion coefficient and saturation level were updated (Table 7) and reintroduced in the numerical model. The results are shown in Fig. 12.

For the distilled water environment, both experimental and numerical results show a good agreement. In other words, the simulation done to estimate the saturation time was validated. The same can be said for the salt water environment, although the value of D_1 seems to have been overestimated. To accurately determine this value, a thorough diffusion analysis would be required during the first day of ageing.

In the end, it was proven that the adhesive plates are saturated at the end of 4 days, for both salt water and distilled water environments.

4.2. Fracture models

Numerical models were developed in ABAQUS® to simulate the 4 fracture tests (DCB, MM 55°, MM 87° and ENF) for both DCB and ODCB specimens. The models used for the DCB specimens consider elastic elements for the adherends and cohesive elements for the adhesive.

Cohesive zone models (CZM) model three different stages of the failure process: an elastic loading, damage initiation and the propagation that occurs due to local failure within the material. This type of model establishes a relationship between stresses and relative displacements between nodes, allowing the simulation of an elastic behaviour followed by a softening and gradual degradation of the material properties [42].

For the ODCB specimens, two possible scenarios were modelled (Fig. 13):

(1) The primary adhesive is modelled with a cohesive element and the secondary adhesive with an elastic element, making a total of only 1 cohesive layer. This enables the possibility of analysing the stress through the thickness of the secondary bond. However, it assumes that the crack will always propagate in the primary adhesive.
(2) Both primary and secondary adhesives are modelled using a 50% ratio of cohesive elements and elastic elements, making a total of 3 cohesive layers. This gives the possibility of analysing the degradation of both primary and secondary adhesive, as it assumes that the crack can propagate in all three adhesive bonds.

In all three cases, the elastic elements were modelled using 4-node bilinear plane strain quadrilateral elements (CPE4R in ABAQUS®), while the cohesive elements used 4-node two-dimensional cohesive elements (COH2D4 in ABAQUS®). The mechanical and cohesive properties used in the simulations are

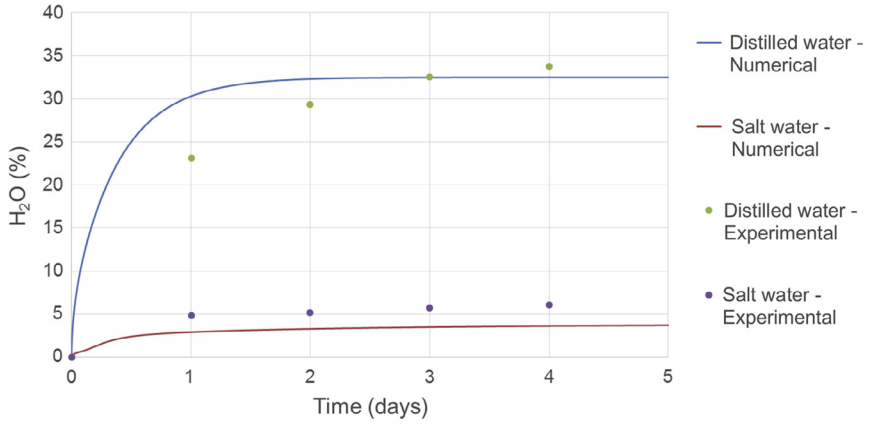

Fig. 11. Experimental and numerical results for the mass uptake of the adhesive plate submerged in distilled water and salt water.

Table 7
Corrected diffusion parameters for the adhesive SikaPower®-4720.

		D_1 (m²/s)	m^1_∞ (%)	D_2 (m²/s)	m^2_∞ (%)
SikaPower®-4720	Distilled water	0.4×10^{-13}	35.0	–	–
	Salt water	3.0×10^{-13}	4.7	1.5×10^{-14}	1.5

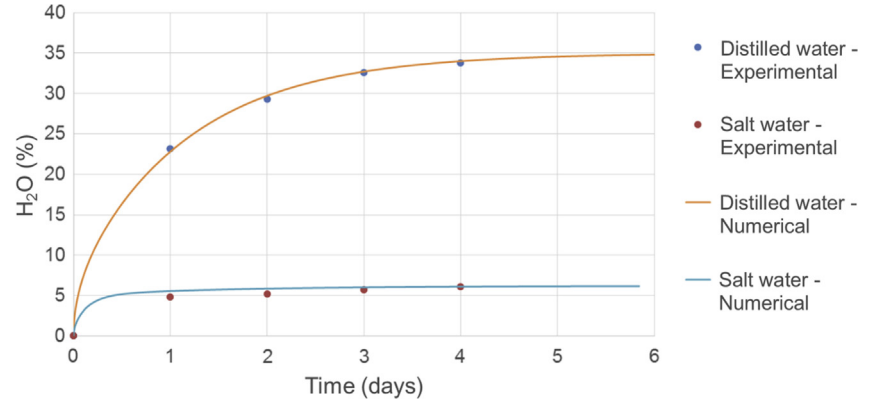

Fig. 12. Updated numerical and experimental results for the mass uptake of the adhesive plate submerged in distilled water and salt water.

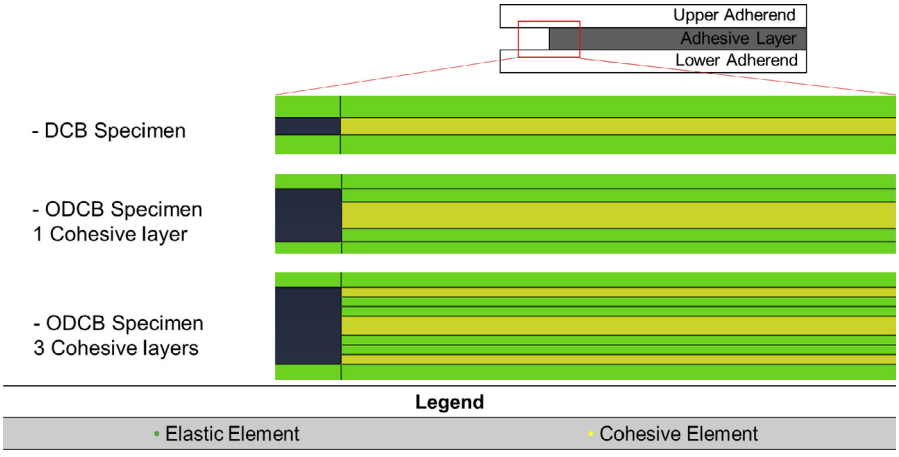

Fig. 13. Pictures of the 3 specimen configurations modelled (not to scale).

shown in Table 8. A triangular traction-separation law available in ABAQUS® was used [43]. This law assumes an elastic behaviour up to σ_f or τ_f. This law approximates the behaviour of the adhesive to a graphic with a shape of a triangle, where the slope of the first

Table 8
Elastic and cohesive properties [23,24,29–31].

	Elastic properties		Cohesive properties				
	E [GPa]	ν	G [MPa]	σ_f [MPa]	τ_f [MPa]	G_{Ic} [N/mm]	G_{IIc} [N/mm]
Aluminium	70	0.33	–	–	–	–	–
SikaPower®-4720	2.171	0.35	750	25.8	15.5	1.15	4.5
Araldite 2021	1.130	0.35	404	26.5	18.4	1.6	3.17

edge is the rigidity, the upper vertex represents σ_f or τ_f, and its area corresponds to the toughness of the material (G_{Ic} and G_{IIc}). The shear maximum relative displacements, correspond to the length of the lower edge, and is calculated based on the parameters mentioned.

Due to the different thickness of the adhesive layers, the mesh applied to each one of these three model types was different. However, all the different mesh refinements used were based on the same principle: maximizing the quality of the mesh in the adhesive layer, where the crack propagates, and applying a less refined mesh in less critical zones, such as the top and bottom of the specimen (Fig. 14). For the DCB and mixed-mode tests, the mesh's element size changes from 1 mm, in the extremes of the specimen, to 0.2 mm or 0.4 mm in the adhesive, depending on the thickness of the adhesive layer. For the ODCB specimens, the mesh's element size decreases to 0.05 mm in the adhesive. The reason behind this refinement is that the secondary bond was divided in two partitions: a 0.05 mm thick layer modelled with elastic elements and another equal layer modelled with cohesive elements, making a total of a 0.1 mm thick secondary bond. Any other component used in these tests, was modelled with a uniform mesh with a 0.2 mm element size.

4.2.1. Model for mode I

To model this test, a pinned support was applied to the lower adherend, representing the pin that connects the specimen to the testing machine, and a vertical displacement was applied to the upper adherend. The boundary conditions used can be seen in Fig. 15(a).

In order to validate the influence of the secondary bonding, another Mode I model was developed. The only difference is the thickness of the adhesive layer, which is 0.4 mm in this case.

4.2.2. Models for mixed-mode 55° and mixed-mode 87°

In the mixed-mode simulations, part of the apparatus used for the experimental tests was modelled. It was necessary to include 4 beams, with a rectangular cross section equal to the real equipment and modelled with beam elements, which were connected to each other and to the specimen with pin multi-point constraints. Similarly to the experimental test, the load is applied to the upper bar, causing the other beams to move and create a combination of both opening and shear modes (Fig. 15b). For the mixed-mode 87°, the same principle was applied. The only difference being the dimensions of the 4 beams and the points where the boundary conditions are applied.

4.2.3. Fracture model's results

Mode I – DCB specimen with 0.2 mm thick adhesive layer

The numerical and experimental R-curves (Fig. 16) show a good agreement with one another, as both of them tend to the same value. Some irregularities can be seen in the experimental curve, which do not appear in the numerical result. This difference is acceptable as the numerical model considers the existence of a perfect adhesive layer and, therefore, no irregularities are shown in the R-curve.

Mode I – DCB specimen with 0.4 mm thick adhesive layer

The comparison between the numerical curve and a representative curve of the experimental tests is shown in Fig. 17. The value obtained for the G_{IC} is approximately the same in both cases.

Mode I – ODCB specimen

In both numerical models, with either 1 or 3 layers of cohesive elements, it can be seen that there is an agreement between the experimental and numerical results regarding the critical energy release rate (Fig. 18). In the model it was considered that the adhesive plate would cover the whole specimen, which is not true. However, since there is an agreement between the experimental and numerical results, it can be concluded that the adhesive plate is long enough to reach a constant crack propagation.

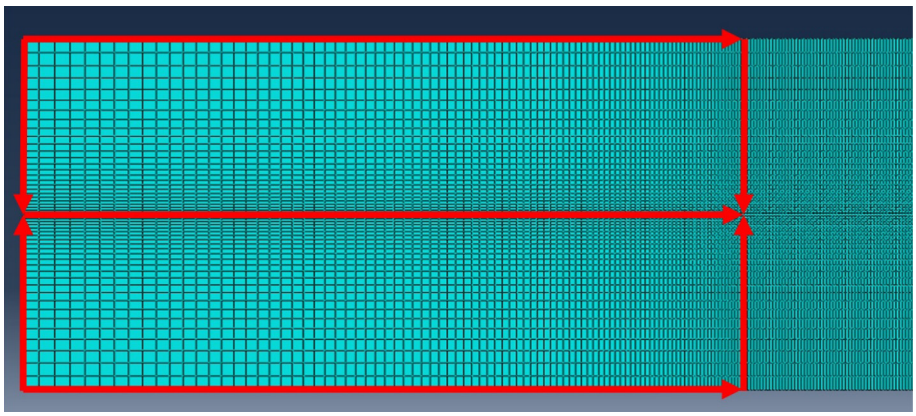

Fig. 14. Example of the mesh refinement applied to the specimen. The mesh is refined towards the adhesive layer and then kept constant throughout the length of the specimen.

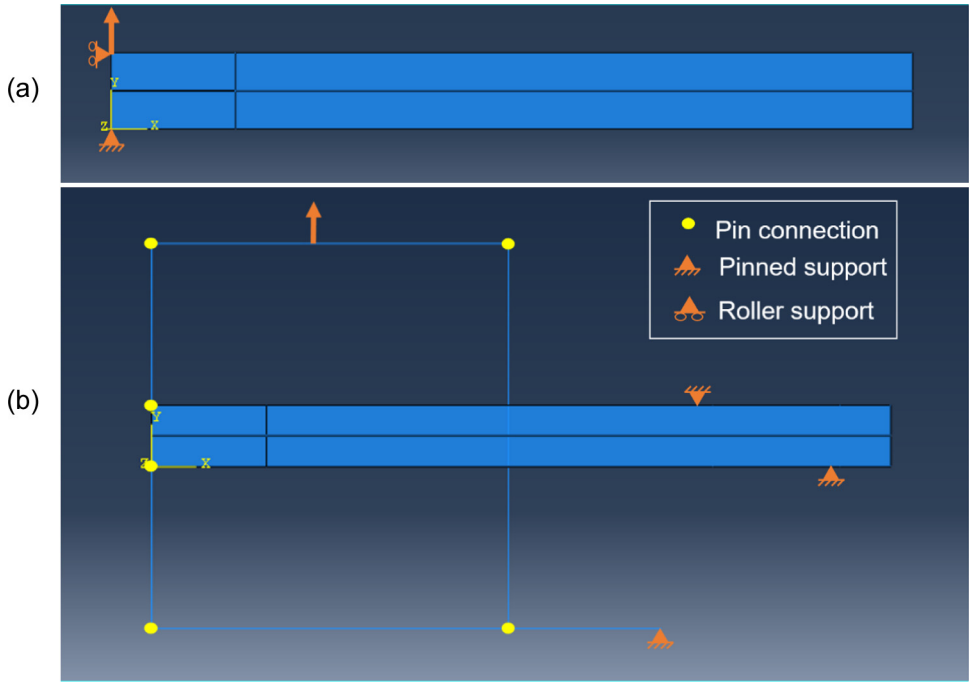

Fig. 15. Assembly and boundary conditions used for the mixed-mode 55° test.

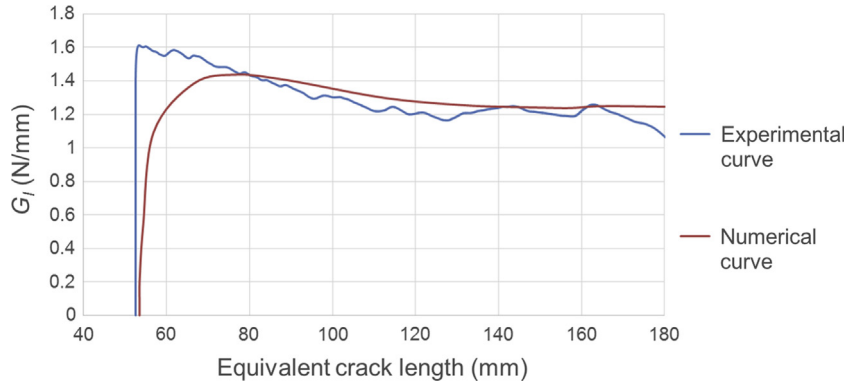

Fig. 16. Numerical and experimental R-curves of the DCB specimens with an adhesive layer of 0.2 mm thickness tested under mode I loading in a dry environment.

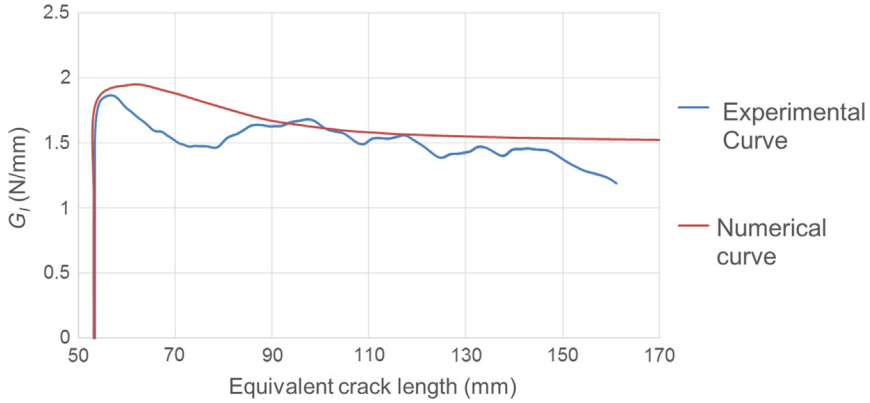

Fig. 17. Numerical and experimental R-curves of the DCB specimens with an adhesive layer of 0.4 mm thickness tested under mode I loading in a dry environment.

According to the same numerical simulation, there is no damage of the CZM elements in the secondary bond (Fig. 19). The damage represented is determined by a reduction of rigidity on each element. This result suggests that the inclusion of the secondary adhesive does not influence the fracture toughness determined experimentally.

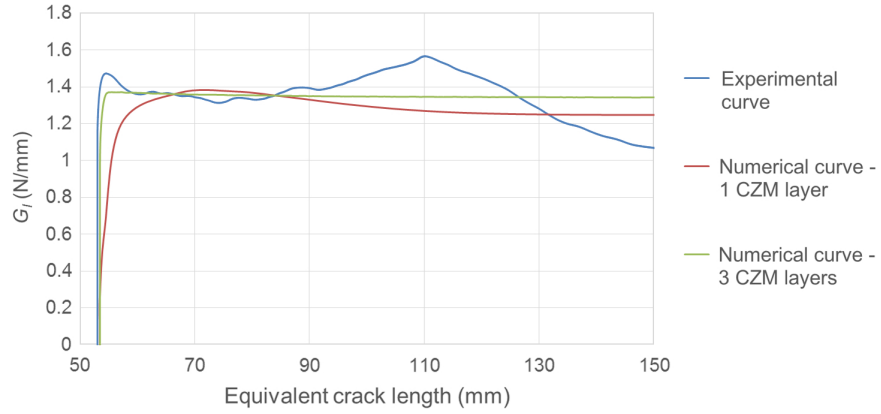

Fig. 18. Numerical and experimental R-curves of the ODCB specimens tested under mode I with a dry adhesive plate.

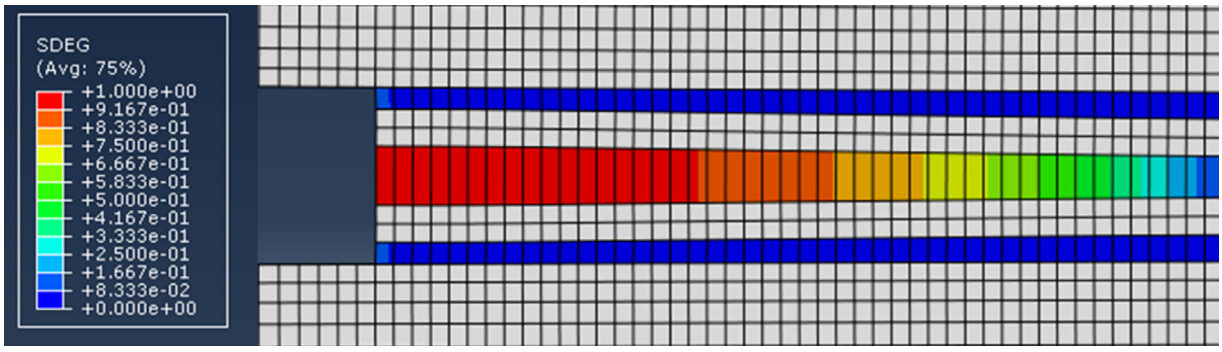

Fig. 19. Damage of CZM elements of the primary and secondary bonds for the ODCB specimens tested under mode I with a dry adhesive plate.

Mixed-mode 55°

The critical energy release rates were determined by the value the plateau reached in the R-curve. Since the simulation considers a stable crack propagation, a good agreement was found between experimental and numerical results (Fig. 20).

Mixed-mode 87°

The value of G_{IIC} obtained from this experimental tests is higher than the value obtained from the ENF test (Fig. 21). This situation should never happen as the mode II critical energy release rate of a mixed-mode loading must be lower than the critical energy release rate of a pure mode II loading. However, the numerical analysis confirms this increase, which must be caused by the influence of the apparatus used to create the mixed-mode loading.

Validation of the ODCB specimens for other loading modes

The influence of this method was studied numerically and the results have shown that the secondary bonds should not influence the fracture toughness measured under mixed-mode 55° and mixed-mode 87°. This conclusion is based on 2 results: the inexistence of degradation in the secondary bonds (Fig. 22) and the equal fracture toughness obtained in the R-curves (Figs. 23 and 24). Regarding the damage of the secondary bonds, only two partially damaged points can be seen at the crack tip, corresponding to a much reduced length of adhesive that does not compromise the results obtained.

On the other hand, the R-curves obtained show equivalent results to what was obtained experimentally for mode I. It can be seen that the increase of the adhesive layer's thickness changes the fracture toughness, while the inclusion of the secondary bond

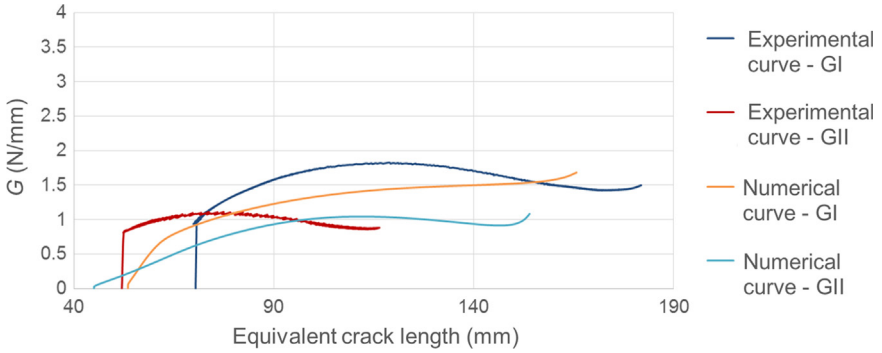

Fig. 20. Numerical and experimental R-curves for the DCB specimens tested under mixed-mode 55° in a dry environment.

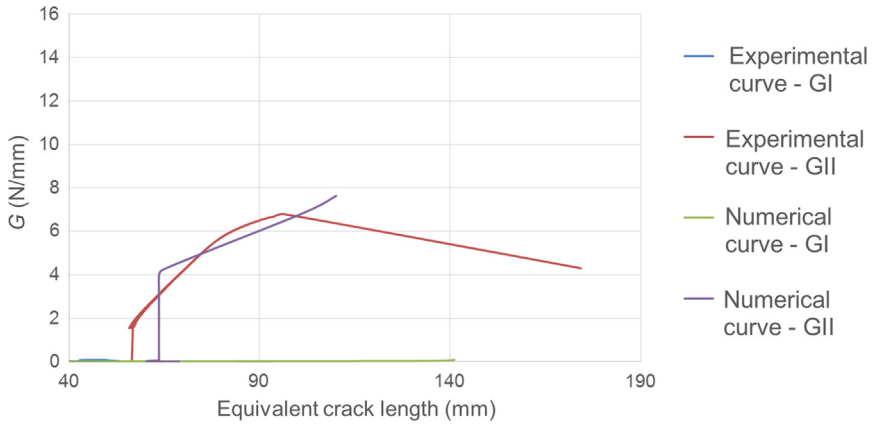

Fig. 21. Numerical and experimental R-curves for the DCB specimens tested under mixed-mode 87° in a dry environment.

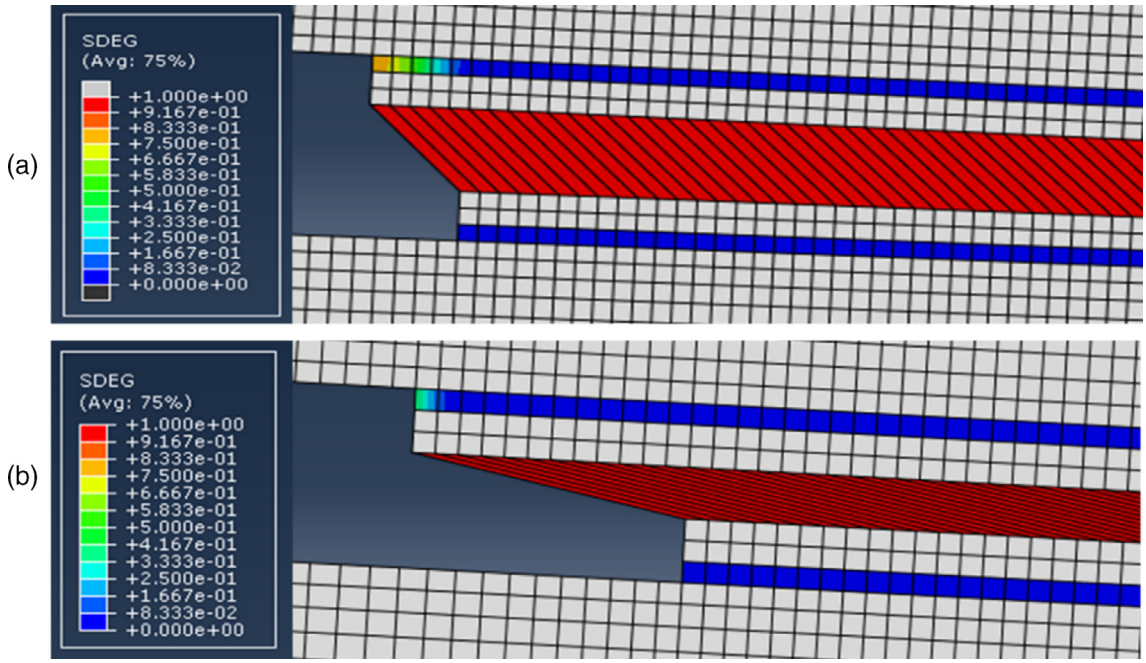

Fig. 22. Damage of the CZM elements of the primary and secondary bonds for the ODCB specimens tested under mixed-mode 55° (a) and mixed-mode 87° (b) with a dry adhesive plate.

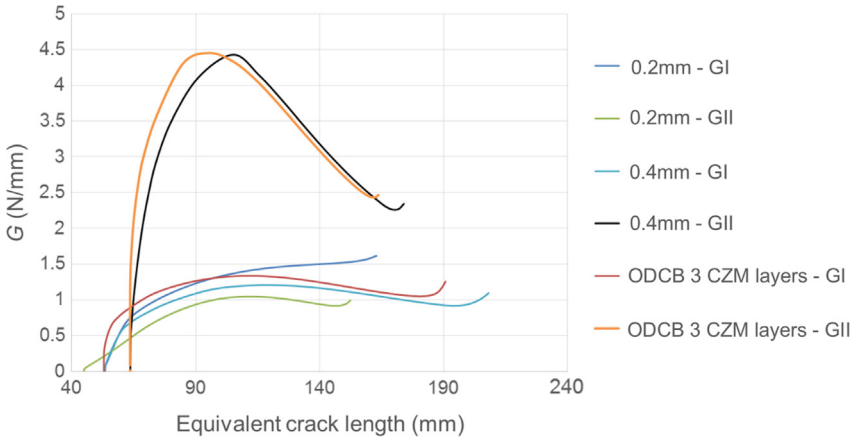

Fig. 23. Numerical R-curves for the DCB and ODCB specimens tested under mixed-mode 55°.

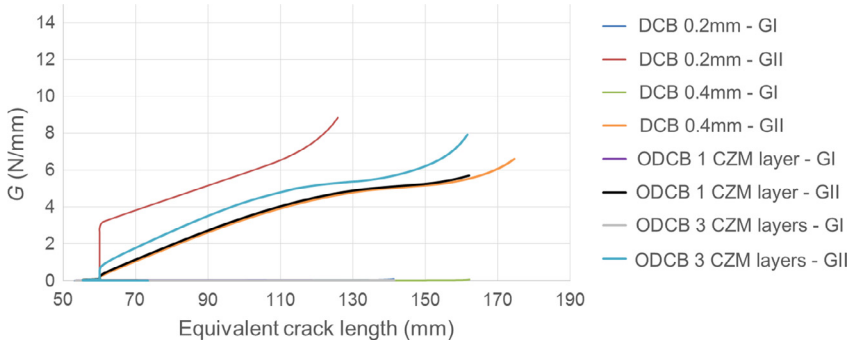

Fig. 24. Numerical R-curves for the specimens tested under mixed-mode 87°.

does not influence the result. The numerical simulations using only 1 or 3 CZM layers reported the same fracture toughness in both mixed-modes. For this reason, and in order to make the graphics more readable, only the latter is shown.

5. Conclusions

The main objectives of this work were the characterization of the three fracture envelopes in a dry, salt saturated solution and distilled water environments as well as determining the relation between them. The fracture envelope in a dry environment has been fully characterized. However, more tests need to be done to define the fracture toughness of the adhesive in the other two environments, in order to allow a better characterization of the changes caused by the ODCB specimen under the mixed-mode loading modes.

Nonetheless, it was possible to identify a trend between the three envelopes, where the distilled water environment causes degradation of the mechanical properties and the salt water environment leads to a higher fracture toughness due to plasticization of the adhesive.

To determine the fracture toughness in the salt water and distilled water environments, a modified specimen was used, allowing the adhesive to saturate in just 4 days. The analysis done in mode I shows that due to an increase of the adhesive layer's thickness, the fracture toughness is overestimated in approximately 0.2 N/mm. This increase is justified with the change of the shape of the FPZ (Fracture Process Zone) as well as the modification of the stress distribution in the adhesive. The inclusion of the secondary bond has proven to have no significant effect on the fracture toughness measured.

The numerical simulations developed in this research suggest that the validation of the ODCB specimens done for mode I can be extrapolated to other loading modes.

Acknowledgements

The authors would like to thank Sika for supplying the SikaPower 4720 adhesive. This study was financed by the Fundação para a Ciência e Tecnologia through grant EXCL/EMS-PRO/0084/2012.

References

[1] L.F.M. da Silva, A. Öchsner, R.D. Adams, Handbook of Adhesion Technology, Springer-Verlag, 2011.
[2] G. Viana, M. Costa, M.D. Banea, L.F.M. da Silva, A review on the temperature and moisture degradation of adhesive joints, Proc. IMechE Part L: J. Mater.: Des. Appl. (2016).
[3] L.F.M. da Silva, C. Sato, Design of Adhesive Joints Under Humid Conditions, Springer, 2013.
[4] J. Comyn, Kinetics and mechanism of environmental attack, in: Durability of Structural Adhesives, Applied Science Publishers, 1983, pp. 85–131.
[5] Y. Zhang, R.D. Adams, L.F.M. da Silva, Absorption and glass transition temperature of adhesives exposed to water and toluene, Int. J. Adhes. Adhes. 50 (2014) 85–92.
[6] J. Crank, The Mathematics of Diffusion, Oxford University Press, 1975.
[7] A. Fick, On liquid diffusion, J. Membr. Sci. 100 (1995) 33–38.
[8] W.K. Loh, A.D. Crocombe, M.M.A. Wahab, I.A. Ashcroft, Modelling anomalous moisture uptake, swelling and thermal characteristics of a rubber toughened epoxy adhesive, Int. J. Adhes. Adhes. 25 (2005) 1–12.
[9] R.A. Pethrick, Design and ageing of adhesives for structural adhesive bonding–a review, Proc. IMechE Part L: J. Mater.: Des. Appl. 229 (2015) 349–379.
[10] A. Mubashar, I.A. Ashcroft, G.W. Critchlow, A.D. Crocombe, Moisture absorption–desorption effects in adhesive joints, Int. J. Adhes. Adhes. 29 (2009) 751–760.
[11] A. Ameli, N.V. Datla, M. Papini, J.K. Spelt, Hygrothermal properties of highly toughened epoxy adhesives, J. Adhes. 86 (2010) 698–725.
[12] X. Han, A.D. Crocombe, S.N.R. Anwar, P. Hu, W.D. Li, The effect of a hot-wet environment on adhesively bonded joints under a sustained load, J. Adhes. 90 (2014) 420–436.
[13] W. Li, M. Ma, X. Han, L. Tang, J. Zhao, E. Gao, Strength prediction of adhesively bonded single lap joints under salt spray environment using a cohesive zone model, J. Adhes. 92 (2016) 916–937.
[14] E.H. Immergut, H.F. Mark, Principles of plasticization, Adv. Chem. Ser. 48 (1965) 1–26.
[15] A.Q. Barbosa, L.F.M. da Silva, A. Öchsner, Hygrothermal aging of an adhesive reinforced with microparticles of cork, J. Adhes. Sci. Technol. 29 (2015) 1714–1732.
[16] J.W. Wylde, J.K. Spelt, Measurement of adhesive joint fracture properties as a function of environmental degradation, Int. J. Adhes. Adhes. 18 (1997) 237–246.
[17] A. Ameli, M. Papini, J. Spelt, Fracture R-curve of a toughened epoxy adhesive as a function of irreversible degradation, Mater. Sci. Eng., B 527 (2010) 5105–5114.
[18] W.K. Loh, A.D. Crocombe, M.M.A. Wahab, I.A. Ashcroft, Environmental degradation of the interfacial fracture energy in an adhesively bonded joint, Eng. Fract. Mech. 69 (2002) 2113–2128.
[19] M. Costa, G. Viana, L.F.M. da Silva, R.D.S.G. Campilho, Effect of humidity on the mechanical properties of adhesively bonded aluminium joints, Proc. IMechE Part L: J. Mater.: Des. Appl. (2016), http://dx.doi.org/10.1177/1464420716645263.
[20] L. Goglio, M. Rezaei, Degradation of epoxy-steel single lap joints immersed in water, J. Adhes. 91 (2015) 621–636.
[21] D. ASTM, 3433–99, Standard Test Method for Fracture Strength in Cleavage of Adhesives in Bonded Metal Joints, 2005.
[22] S.A.P. Limited, SikaPower®-4720, in: Sika® (Ed.), 2014.
[23] M. Costa, G. Viana, C. Canto, L. da Silva, M. Banea, F. Chaves, R. Campilho, A. Fernandes, Effect of the size reduction on the bulk tensile and double cantilever beam specimens used in cohesive zone models, Proc. IMechE Part L: J. Mater.: Des. Appl. (2015), http://dx.doi.org/10.1177/1464420715610248.
[24] J.P.R. Monteiro, R.D.S.G. Campilho, E.A.S. Marques, L.F.M.d. Silva, Experimental estimation of the mechanical and fracture properties of a new epoxy adhesive, Appl. Adhes. Sci. 3 (2015) 1–17.
[25] L. Greenspan, Humidity fixed-points of binary saturated aqueous-solutions, J. Res. Natl. Bur. Stand. A Phys. Chem. 81 (1977) 89–96.
[26] A. Wexler, S. Hasegawa, Relative humidity-temperature relationships of some saturated salt solutions in the temperature range 0-degree to 50-degrees-C, J. Res. Natl. Bur. Stand. 53 (1954) 19–26.
[27] D.F.O. Braga, L.M.C. de Sousa, V. Infante, L.F.M. da Silva, P.M.G.P. Moreira, Aluminium friction-stir weld-bonded joints, J. Adhes. 92 (2016) 665–678.
[28] D.F.O. Braga, L.F.M. da Silva, P.M.G.P. Moreira, Single lap joints numerical modelling and comparison with experimental testing, J. Eng. 2 (2016) 11–20.
[29] L.F.M. da Silva, M.J.C.Q. Lopes, Joint strength optimization by the mixed-adhesive technique, Int. J. Adhes. Adhes. 29 (2009) 509–514.
[30] R. Kottner, R. Hynek, T. Kroupa, Identification of parameters of cohesive elements for modeling of adhesively bonded joints of epoxy composites, Appl. Comput. Mech. 7 (2013) 137–144.

[31] L.F.M. da Silva, G.W. Critchlow, M.A.V. Figueiredo, Parametric study of adhesively bonded single lap joints by the Taguchi method, Int. J. Adhes. Adhes. 22 (2012) 1477–1494.
[32] F.J.P. Chaves, L.F.M. da Silva, M.F.S.F. de Moura, D.A. Dillard, Fracture mechanics tests in adhesively bonded joints: a literature review, J. Adhes. 90 (2014) 955–992.
[33] M.F.S.F. de Moura, R.D.S.G. Campilho, J.P.M. Gonçalves, Crack equivalent concept applied to the fracture characterization of bonded joints under pure mode I loading, Compos. Sci. Technol. 68 (2008) 2224–2230.
[34] F.J.P. Chaves, L.F.M. da Silva, M.F.S.F. de Moura, D.A. Dillard, J.O. Fonseca, Apparatus and method for characterization of bonded joints mixed-mode I+II fracture, in: Provisional Patent Application Portuguese, No. 107188 B, 2013.
[35] F.J.P. Chaves, M.F.S.F. de Moura, L.F.M. da Silva, D.A. Dillard, Numerical validation of a crack equivalent method for mixed-mode I plus II fracture characterization of bonded joints, Eng. Fract. Mech. 107 (2013) 38–47.
[36] M.D. Banea, L. Da Silva, R. Campilho, The effect of adhesive thickness on the mechanical behavior of a structural polyurethane adhesive, J. Adhes. 91 (2015) 331–346.
[37] M.L. Benzeggagh, M. Kenane, Measurement of mixed-mode delamination fracture toughness of unidirectional glass/epoxy composites with mixed-mode bending apparatus, Compos. Sci. Technol. 56 (1996) 439–449.
[38] G. Stamoulis, N. Carrere, J.Y. Cognard, P. Davies, C. Badulescu, On the experimental mixed-mode failure of adhesively bonded metallic joints, Int. J. Adhes. Adhes. 51 (2014) 148–158.
[39] G. Viana, M. Costa, M.D. Banea, L.F.M. da Silva, Behavior of environmentally degraded epoxy adhesives as a function of temperature, J. Adhes. (2016).
[40] M. Banea, L. Da Silva, R. Campilho, Mode I fracture toughness of adhesively bonded joints as a function of temperature: experimental and numerical study, Int. J. Adhes. Adhes. 31 (2011) 273–279.
[41] S. Sugiman, A. Crocombe, I. Aschroft, Modelling the static response of unaged adhesively bonded structures, Eng. Fract. Mech. 98 (2013) 296–314.
[42] J.A.B.P. Neto, R.D.S.G. Campilho, L.F.M. da Silva, Parametric study of adhesive joints with composites, Int. J. Adhes. Adhes. 37 (2012) 96–101.
[43] V. ABAQUS, 6.14 Documentation, Dassault Systemes Simulia Corporation, 2014.

PAPER 7

A new cohesive element to model environmental degradation of adhesive joints in the rail industry

G. Viana[1], R.J.C. Carbas[1,2], M. Costa[2], M.D. Banea[3], L.F.M. da Silva[1,2,*]

[1]Departamento de Engenharia Mecânica, Faculdade de Engenharia da Universidade do Porto (FEUP), 4200-465 Oporto, Portugal, Phone -22 508 14 91, Fax-22 508 22 01

[2]Instituto de Ciência e Inovação em Engenharia Mecânica e Engenharia Industrial (INEGI), 4200-465 Oporto, Portugal

[3]Federal Centre of Technological Education in Rio de Janeiro (CEFET), Av. Maracanã, 229, Rio de Janeiro, Brazil

Abstract

This work addresses the strength of adhesive joints used in the rail industry. The capability of structural adhesives to bond an aluminium rail used to assemble the seats inside the train is investigated. Scaled specimens of these joints were mechanically tested under a wide range of temperatures (from -40ºC to 80ºC) before and after ageing in distilled water in order to simulate real life conditions.

A three dimension numerical simulation was carried out to understand the magnitude of stresses present in the adherends and in the adhesive layer. A new developed cohesive element was used along with the finite element method to predict the behaviour of an adhesive joint after environmental degradation.

Results show that even though a phosphoric acid anodization was applied to the adherends, some specimens suffered interfacial rupture. A new cohesive zone element was developed and was used to predict cohesive failure of the adhesive. The model gave accurate results and was able to successfully predict cohesive failure of every joint that failed cohesively in the adhesive layer.

Keywords: moisture degradation; temperature degradation; numerical simulation, cohesive zone models

1. Introduction

Structural adhesives are increasingly being used in the transport industry. They allow for light weight vehicles, energy savings and reduced emissions. The main advantages include more uniform load distribution, higher fatigue resistance than other traditional joining methods and the ability to join dissimilar materials [1]. Also, due to their high vulnerability to stress concentration, the only viable way to join composite materials, such as fiber reinforced plastic, is with a structural adhesive [2]. However, moisture and temperature degradation are major setbacks in their wide implementation [3], as these materials are very moisture and temperature sensitive.

* Corresponding author. Tel.: +351 22 508 17 06; fax: +351 22 508 14 45.
E-mail address: lucas@fe.up.pt (L. F. M. da Silva).

Moisture degradation of adhesives includes reduction of modulus and strength and increase in ductility [4, 5, 6, 7, 8]. The deleterious effects are greater in adhesive joints as the degradation of the adhesive-adherend interface may cause interfacial failure [9]. The fracture toughness of the adhesive may also increase or decrease, depending on the environmental conditions the adhesive is subjected to [10, 11].

The water diffusion in adhesives is frequently controlled by the Fick's laws. Fickian sorption happens when the diffusion is much slower than relaxation. Although fickian diffusion is the most common uptake behavior in adhesives, non-fickian diffusion is not uncommon. Other models have been developed, such as the dual fickian diffusion [12], delayed dual fickian [13] and the Langmuir model [14]. In many cases the water uptake may be fickian under certain environmental situations and non-fickian under others. Generally non fickian behaviour is more prone to happen at higher temperatures, higher relative humidity and smaller thicknesses of bulk adhesive specimens. There is also evidence that while a bulk adhesive may have a fickian diffusion behaviour, the same adhesive in a joint may have a different water uptake behaviour [15].

The rate at which the water is absorbed and the maximum water uptake depend on environmental factors, such as the relative humidity [14, 16], temperature [14, 17, 18, 19], the adhesive thickness [12, 20] and the stress state of the adhesive [21, 22].

As water diffuses into the adhesive, some of this moisture becomes bound water. Bound water generally increases with exposure time and temperature [23, 24]. Unlike the free water that occupies the free space of the adhesive, this bound water is responsible for the volumetric changes that are observed in adhesives under high humidity environments, which may cause residual stresses in adhesive joints [12, 25, 26, 27]. Type I bound water acts as a plasticizer, increasing the chains segment mobility. It is responsible for decreasing the glass transition temperature (Tg) [23]. If the temperature is high and the exposure time is long, type II bound water may also occur. This type of bound water is responsible for creating secondary cross-linking [24], which lessens the extent of Tg depression [23]. While type I bound water can be removed at low temperature, in order to remove type II bound water, the adhesive must be subjected to relatively high temperatures [23]. Although moisture degradation of adhesive joints is in most cases largely reversible, in some cases, where chemical degradation occurs, the adhesive may recover its original strength after drying [7, 8].

Some studies report that water diffusion in an adhesive joint is much faster than water diffusion through the bulk adhesive alone either due to stress enhanced diffusion [15] or due to water penetrating through the interface between the adhesive and the adherend [28]. Often it is very difficult to predict when an adhesive joint is fully saturated because thin bondlines do not absorb enough water to be measured by common precision scales. Alternative methods to measure the water diffusing through the adhesive in an adhesive joint have been proposed [15, 28, 29].

The main factor affecting the strength of adhesive joints under high and low temperatures is the creation of residual thermal stresses, due to mismatch between the coefficients of thermal expansion (CTE) of adherends and adhesive. This is even more important if the adherends have very dissimilar CTEs. At lower temperatures adhesives are normally stronger. However this does not necessarily mean that the

adhesive joint should be stronger [30] as the adhesive is normally also less ductile. With less ductility two problems arise: there are higher thermal stresses, especially if the substrates are made of different materials and if there is a great mismatch between the CTE of the adhesive and the CTE of the adherends.

At high temperatures the opposite occurs: mismatch between the CTEs of the adhesive and adherends is not very important as the adhesive is usually very ductile. The adhesive is, however, not very strong, which results in low strength of the joint.

Tough the strength and ductility of adhesives may vary considerably with temperature, the toughness does not. Actually, below Tg the toughness of structural adhesives is roughly constant because at low temperature the lack of ductility is compensated by the increased strength and at high temperature the opposite occurs. However, above Tg there is a sharp decrease in toughness [31]. Therefore, structural adhesive joints should not be used when there is the possibility of the service temperature to rise above Tg.

Although the separate effect of moisture and temperature on the mechanical properties of epoxy adhesives is now-a-days relatively well understood, very few studies focus on the mechanical properties of aged adhesives at high and low temperatures [32, 33]. This work aims at shedding light on this subject. This will allow for a more accurate long term prediction of the mechanical behaviour of adhesive joints.

In this study, the ability of a rail used in the rail industry to withstand peel loads was assessed. This joint was tested after and before environmental exposure at 40ºC, 23ºC and 80ºC, which covers the range of temperatures required for the rail industry. A cohesive element that considers moisture and temperature degradation of the adhesive layer was developed and used to predict the mechanical behaviour of the studied adhesive joint.

2. Materials

2.1 Adhesives

Two adhesives which were recommended by Sika® and Nagase® for this durability study were selected:

- The epoxy adhesive XNR 6852-1, supplied by NAGASE CHEMTEX® (Osaka, Japan). This adhesive is a one-part system that cures at 150ºC for 3 h;
- The epoxy adhesive SikaPower 4720 was, supplied by SIKA® (Portugal, Vila Nova de Gaia). This adhesive is a two-part system that cures at room temperature for 24 hours.

A very important parameter to take into account when testing adhesive joints, especially when the joint is subjected to high temperatures, is the adhesive's Tg. This temperature is usually high when the adhesive is dry but normally decreases when the adhesive is exposed to moist environments [23]. The Tg of both adhesives before and after ageing was determined in a previous study [4]. Results showed the Tg of XNR 6852-1 not to be very moisture sensitive. SikaPower 4720, on the other hand, is very moisture dependent, and its Tg when aged in distilled water is actually lower than room temperature (see Figure 1), which

brings severe consequences on its strength and modulus as well as in its water uptake (32.5% at 32.5ºC when aged in distilled water versus only 3.8% when aged in salt water).

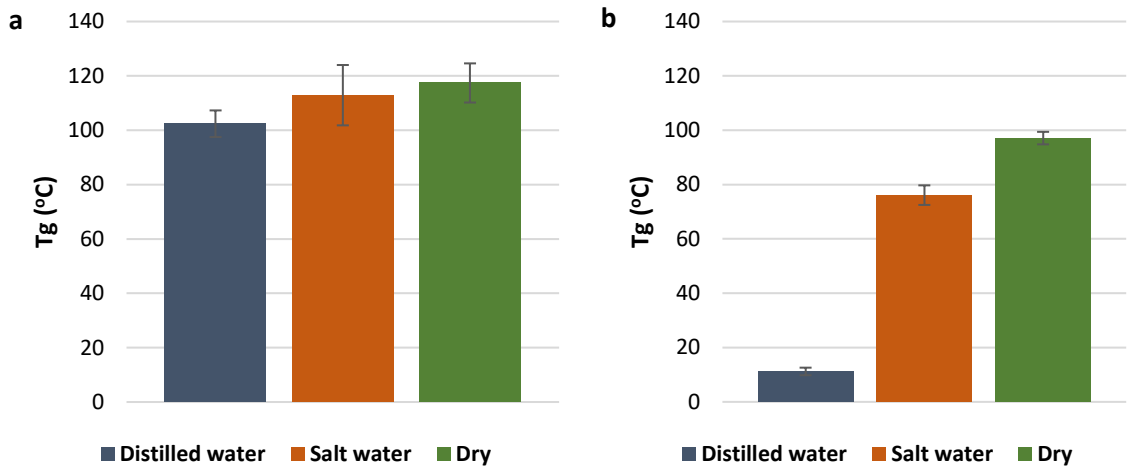

Figure 1: Tg of both adhesives studied [4]:
a- XNR 6852-1
b- SikaPower 4720

2.2 Substrates

The rail that is represented in ***Figure 2***-a is used to assemble the seats of a train to the floor. In order to attach this rail, bolts or rivets are used. This method, however, introduces stress concentration at the holes where the fasteners are attached and reduces its fatigue resistance. The ability of using adhesive bonding instead of mechanical fastening is studied in this paper. This method can reduce the cost of structures, as it can be more easily automatized.

As this substrate is too large to be tested in common universal test machines, a reduced specimen was produced (represented in Figure 3) . Because this kind of profile, which is produced by extrusion, is not available in small dimensions, an alternative profile was made. This was achieved by machining a rectangular shaped profile. The original profile and the test specimen dimensions and geometry can be seen in Figure 2-b. A thread was drilled at one end of the reduced specimen to allow assembly with the test machine. This profile was bonded to a rigid 8 mm thick aluminium plate, which simulates the train floor.

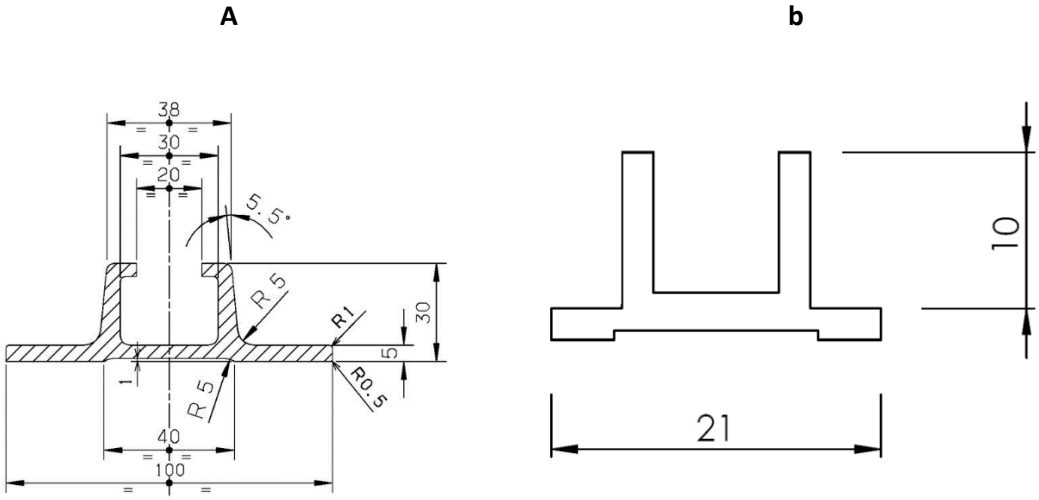

Figure 2: Geometry of a rail used to assemble seats to the train floor (dimensions in millimetres):
a-original geometry (length=2000mm)
b-reduced geometry (length=40mm)

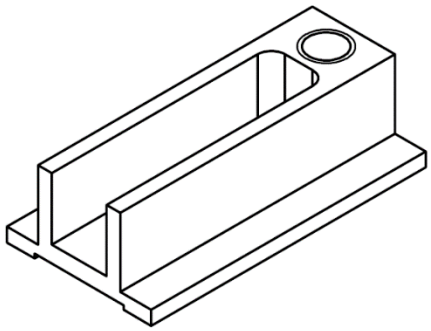

Figure 3: Isometric view of the reduced specimen used in this study.

3. Developed cohesive element

The cohesive element that was developed in this study is based on the element developed by Camanho et al [34]. This is a three dimensional, eight node, zero thickness element that is capable of simulating pure and mixed mode decohesion. This element utilises a triangular cohesive zone law (see Figure 4) to model decohesion between two substrates.

A high initial stiffness (K) is used to hold the top and bottom faces of decohesion element together in the linear elastic range until the yield stress is reached. After this, softening starts and the load decreases linearly until zero. The toughness of the adhesive is given by the area of the triangle.

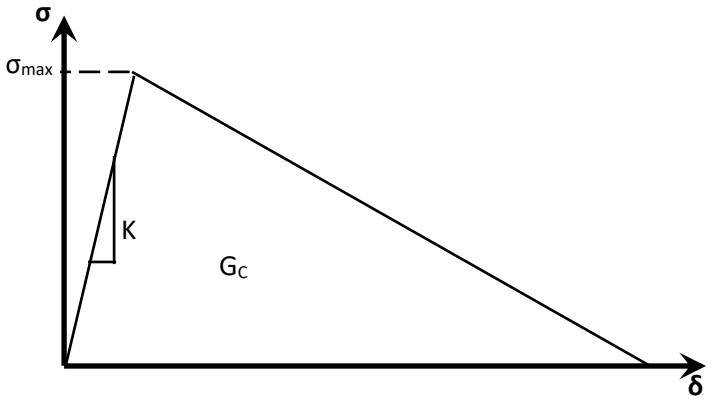

Figure 4: Pure mode cohesive law used in the element proposed in this study.

Modifications were made to this element to make it take into consideration the environmental temperature and absorbed moisture by the adhesive. The element reads the moisture field of the adhesive layer and attributes the yield stress and toughness of the adhesive according to the read moisture and environmental temperature.

The moisture and temperature dependent cohesive properties of the adhesives studied were determined in previous studies [35, 36]. Empirical formulas were used to fit the toughness and yield stress of the adhesive as a function of temperature and moisture. Properties of adhesive XNR6852 was approximated using the following formulas:

$$T_g = 117.4 - 8.23(M)^4 \quad \text{Eq. 1}$$

$$\sigma_y = -15.4 - 0.75\left(T - T_g\right) \quad \text{Eq. 2}$$

$$G_c = 8.46 - 2.27 \times 10^{-4}\left(T - T_g\right)^2 \quad \text{Eq. 3}$$

The following formulas were used with SikaPower 4720:

$$T_g = 91.7 - 2.50\left(T - T_g\right) \quad \text{Eq. 4}$$

$$\sigma_y = 18 - 0.26\left(T - T_g\right) \quad \text{Eq. 5}$$

$$G_c = 0.22 - 9.7 \times 10^{-3}\left(T - T_g\right) \quad \text{Eq. 6}$$

In which σ_y is the yield stress of the adhesive, T is the environmental temperature, T_g is the glass transition temperature, G_c is the fracture toughness and M is the moisture percentage absorbed by the adhesive. Figure 5 shows the variation of the properties with T_g and the comparison with experimental values. The variation of the adhesives' Tg and mechanical properties are graphically represented in Figure 5 and Figure 6 respectively.

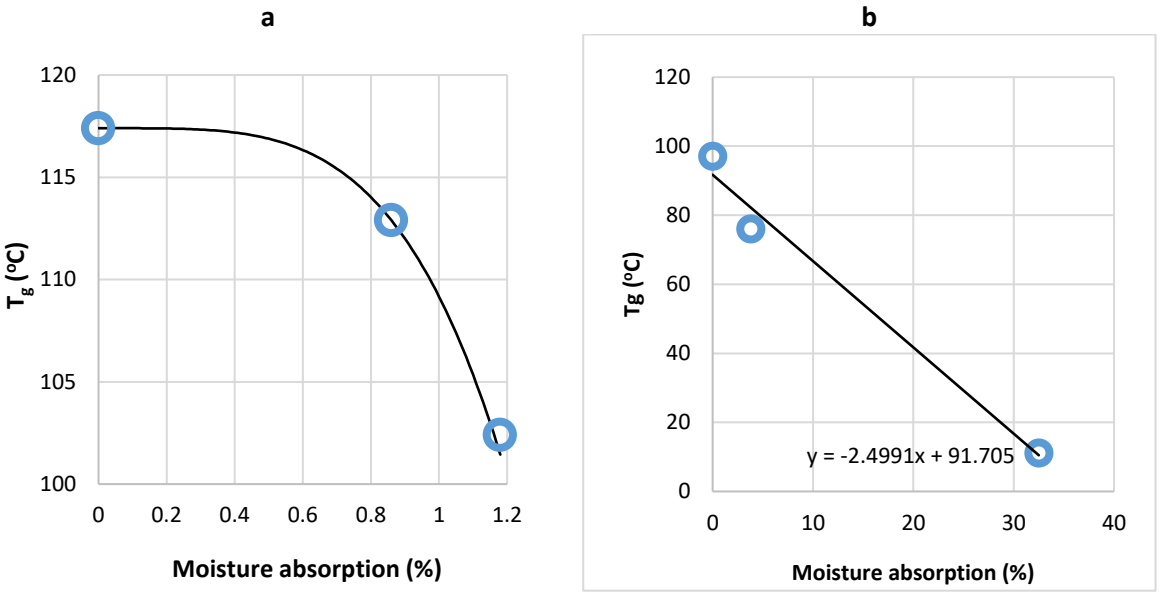

Figure 5: Variation of Tg with moisture absorbed by the adhesive.

As Figure 5 shows, the evolution of the Tg of NXR6852 with moisture concentration is not linear. In this study, a polynomial function was used to approximate the Tg of this adhesive as a function of its moisture absorption. This function matches the experimental values almost perfectly.

However, the evolution of the Tg of SikaPower 4720 with temperature is closer to a straight line. The Tg of this adhesive after exposure in distilled water is lower than the exposure temperature, which in turn affects the amount of water that is absorbed by the adhesive. Nevertheless, a straight line was used to predict the Tg of SikaPower 4720.

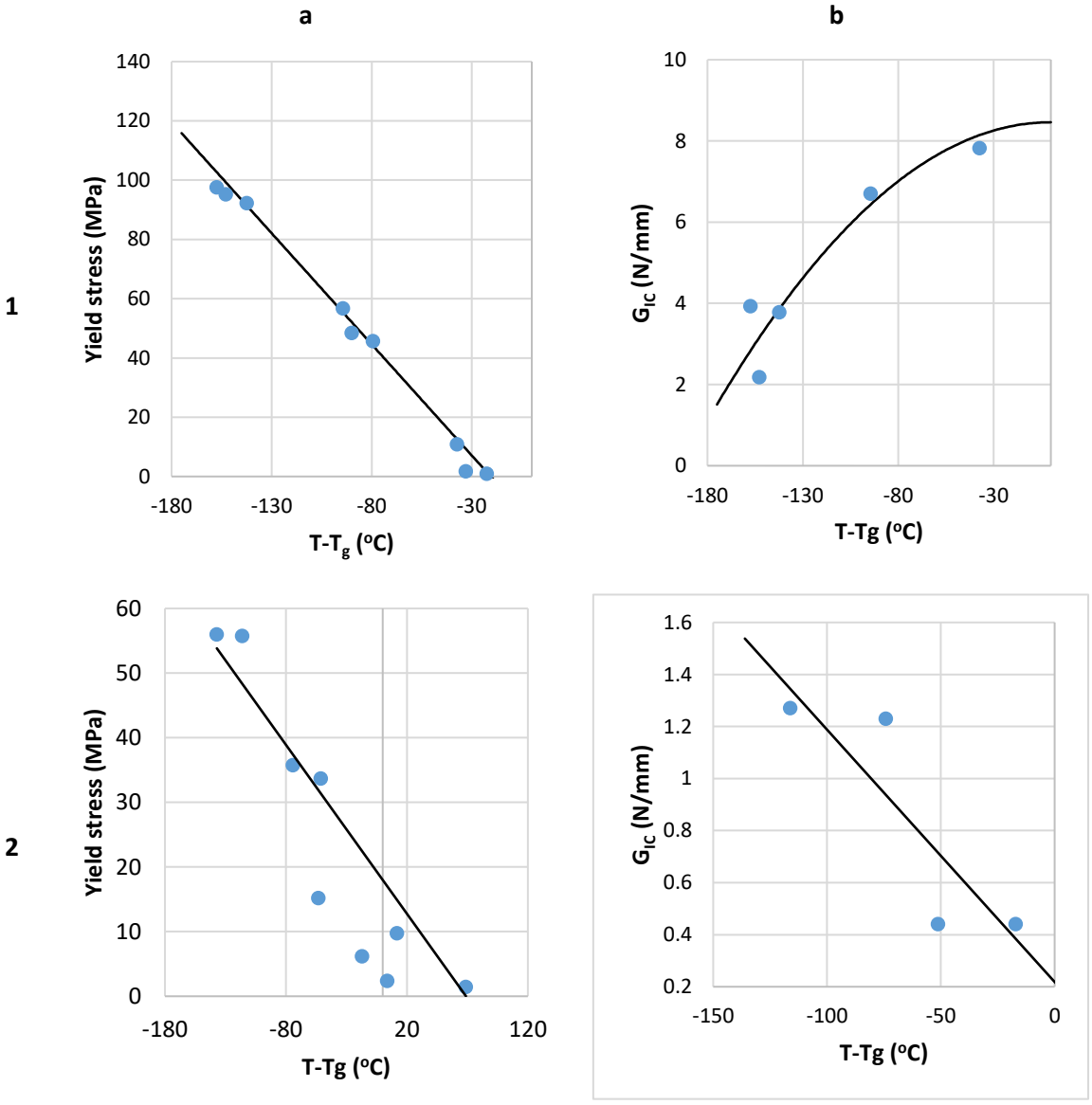

Figure 6: Variation of the yield stress and mode I fracture toughness of both adhesives with T-Tg:
Column a: Variation of yield stress
Column b: Variation of mode I fracture toughness
Row 1: Joints with adhesive XNR6852
Row 2: Joints with adhesive SikaPower 4720

The properties of the adhesives were assumed to be dependent on the difference between the test temperature and Tg. Moisture absorbed by the adhesive will have the effect of decreasing the adhesive's Tg and indirectly affecting the adhesive's properties. This is in line with other studies [37]. In this study, the evolution of the yield stress of both adhesives was considered to be linear, while the evolution of the fracture toughness was modelled with a fourth degree polynomial equation and with a straight line for XNR6852 and SikaPower4720 respectively.

SikaPower 4720 was, under certain environmental conditions, tested above its Tg, which makes the prediction of its cohesive properties a harder task, as there probably is a discontinuity in the mechanical properties around Tg.

It is important to notice that the values obtained for the fracture toughness correspond only to cohesive fracture of the adhesive.

4. Experimental procedure

4.1 Specimen fabrication

Prior to bonding, the surfaces of the substrates were abraded with 80 grit SiC sandpaper, cleaned in an ultrasonic acetone bath and phosphoric acid anodized. Less than a day after being anodised, the specimens were bonded and left to cure for 3h at 150ºC or for 24h at room temperature, according to the indication of the manufacturer of each adhesive used. After the cure cycle, the excess adhesive was removed and the specimens were left to dry for at least 3 weeks in a dry desiccator. After this time, the specimens of each adhesive were divided into two groups:

- Dry specimens, which were ready to be tested;
- Specimens aged in a saturated aqueous solution of NaCl at 32.5ºC;
- Specimens aged in distilled water at 32.5ºC.

As explained above, specimens with reduced dimensions were used. This allowed time efficient production and ageing.

4.2 Test procedure

After all specimens had been produced and dried in a dry desiccator, they were separated into the three different groups mentioned in the previous section. Each specimen was left to cure for at least two weeks. After this time, the dry specimens were ready to be tested. Specimens to be aged were placed in their respective ageing environment for 14 days. This ensured that the bondline was not completely saturated and a gradient in adhesive moisture was present, as demonstrated in section 6.2.

Some studies report that water diffusion in an adhesive joint is much faster than water diffusion through the bulk adhesive alone either due to stress enhanced diffusion [15] or due to water penetrating through the interface between adhesive and adherend [28] or due to stress-enhanced diffusion [15]. Often it is very difficult to predict when an adhesive joint is fully saturated because the thin bondlines do not absorb enough water to be measured by common precision scales.

In order to determine when the specimens reached saturation, some DCB specimens of each adhesive were tested periodically until their toughness stabilized. It was concluded that the specimens needed 13 weeks to be fully saturated. The results of this study were published elsewhere [29].

A special tool was developed to test this joint. This tool, which is represented in Figure 7, allows the adhesive layer to be tested under mode I, which is the most critical situation that the joint must be able to withstand during its work life.

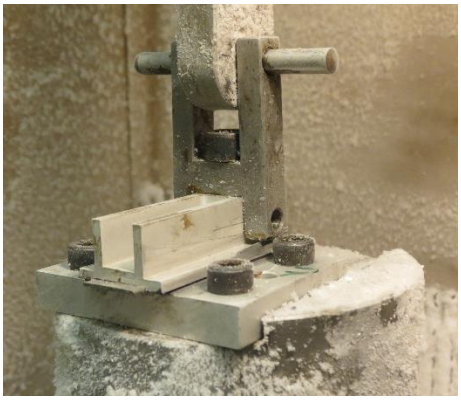

Figure 7: Tool used to test the proposed adhesive joint.

A climatic chamber coupled with a universal test machine (INSTRON® model 3367) allowed to test aged and unaged specimens at -40ºC, 23ºC and 80ºC. Right before testing at -40ºC or 80ºC, the specimens were left inside the climatic chamber at the test temperature for 10 minutes to make sure that the temperature was uniform in the entire specimen. The tests were performed at the constant displacement rate of 0.5mm/min. At least three valid tests were considered for each condition.

5. Numerical simulation

The geometry of the specimen was discretised using the commercial FE software Abaqus®. The substrates wee modelled using C3D8 full integration elements, available in Abaqus® library, to avoid hourglass effects. The bondline has two layers of elastic elements, also discretised using C3D8 elements. Between these two layers of elastic adhesive, the developed cohesive element was placed. The 4 mm wide bondline was modelled with a refined mesh of 20 elements. The rest of the specimen received a courser mesh. Figure 8 shows the mesh used in this study.

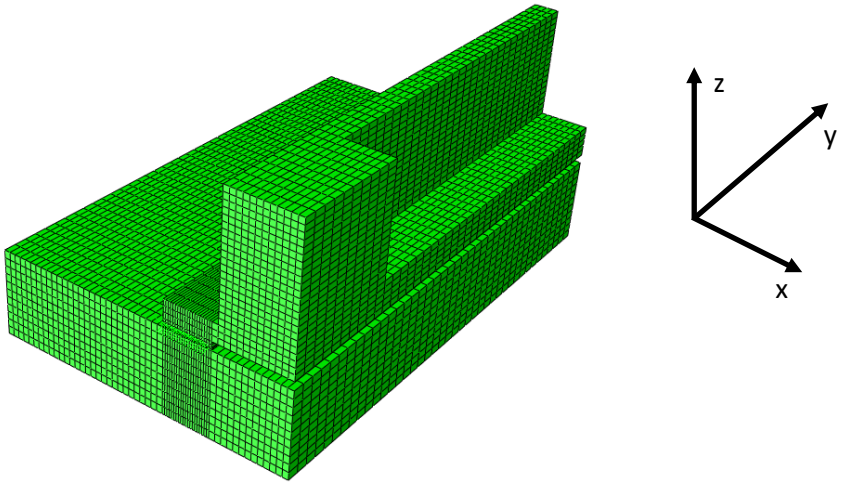

Figure 8: Mesh used in the model.

Due to the symmetry of the specimen, in order to decrease the computational effort, only half of the specimen was modelled. The corresponding boundary conditions were:

1. Every displacement in the down substrate was set to zero;
2. A displacement of 0.5 mm was applied to the loading area of the upper substrate;
3. Displacements in the y and x directions of the middle plane were set to zero.

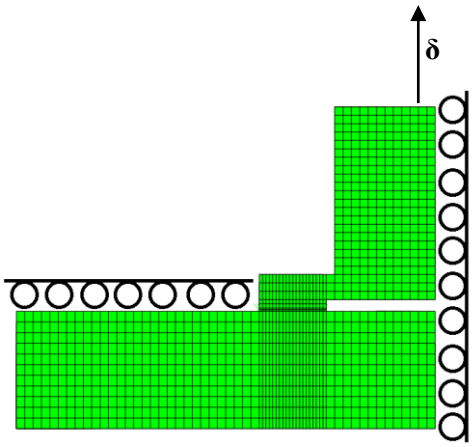

Figure 9: Border condition applied in the FE model.

The numerical prediction of the mechanical behaviour of the tested adhesive joints was made in two stages:

1. Prediction of the moisture gradient across the width of the adhesive taking into account the properties of each adhesive, determined in previous studies [29, 35]. The moisture of each individual element was calculated.
2. Taking into account the moisture of each element calculated in the previous step, the moisture and temperature dependent properties were attributed to each element. This resulted into each

element being assigned a distinct set of properties corresponding to a bondline with graded properties.

6. Results and discussion

6.1 Experimental results

Two types of failure mode were observed: cohesive failure and adhesive failure. Adhesive failure occurred in every environmentally exposed specimen, independently of the test temperature. Examples of failure surfaces of each type of mode of failure can be seen in Figure 10 bellow.

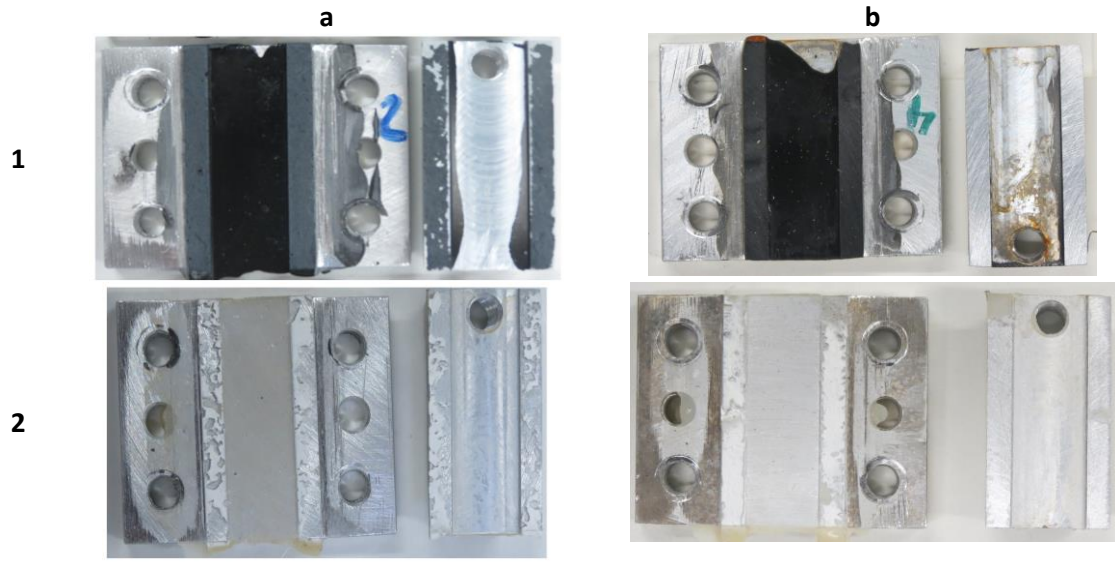

Figure 10: Mode of failure obtained in this study:
Column a: Cohesive failure
Column b: Adhesive failure
Row 1: Joints with adhesive SikaPower 4720
Row 2: Joints with adhesive XNR6852

The average failure load of each kind of specimen is shown in Figure 11 bellow.

a

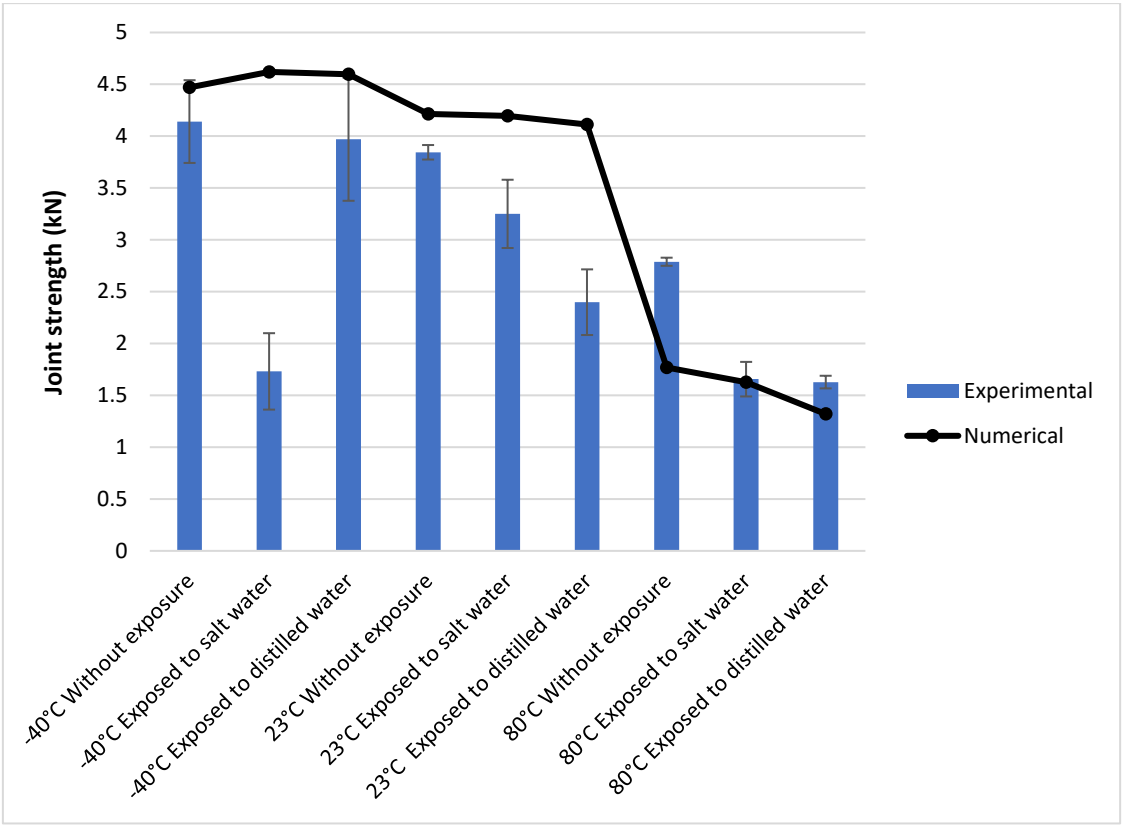

b

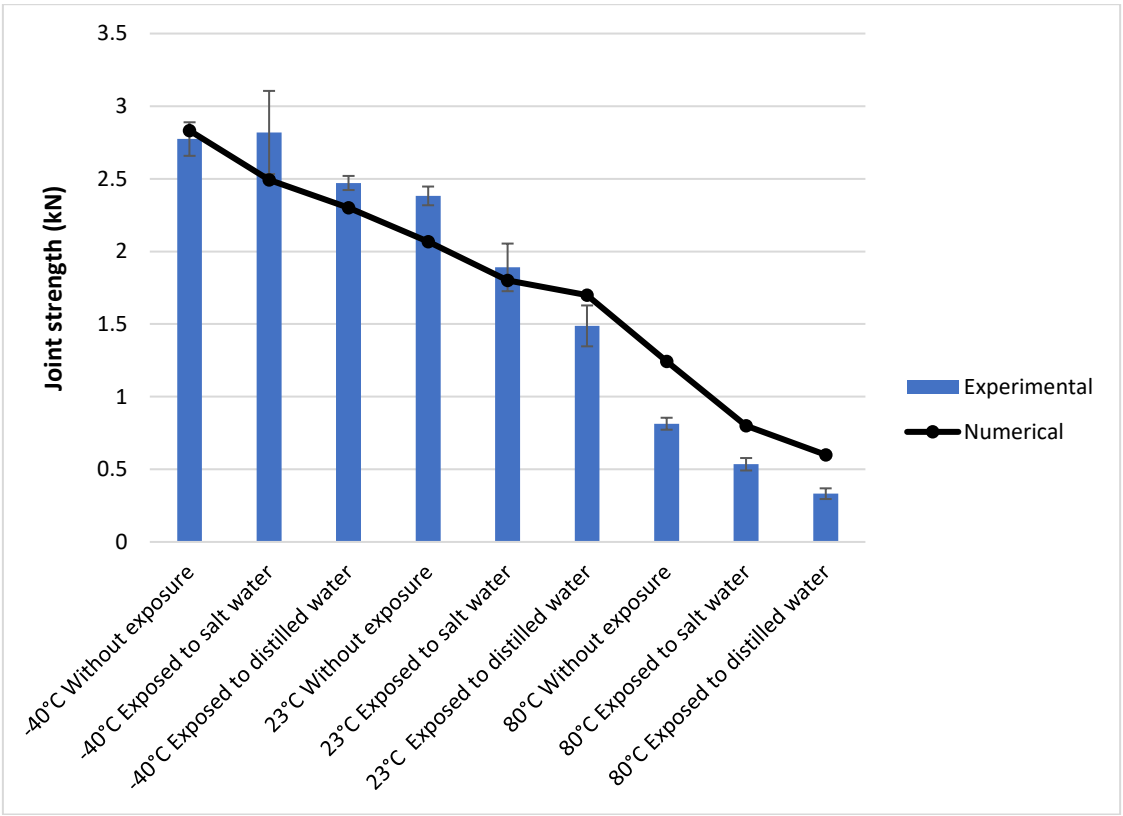

Figure 11: Failure load of joints bonded with:

a- XNR6852

b- SikaPower 4720

Bars in lighter shade correspond to adhesive failure of the specimen, while bars with darker shade correspond to cohesive failure of the adhesive.

Generally, unexposed specimens had higher failure loads than exposed specimens. This is because:

1. Exposed specimens suffered adhesive failure, which typically results into lower failure loads;
2. Due to the plasticizing effect of water, the adhesive becomes weaker, but more ductile, after exposure.

Higher temperatures were also responsible for decreasing the joint strength due to the lower strength of adhesives at these temperatures. This was more apparent in SikaPower joints than in XNR6852 joints probably because SikaPower at 80°C is above or very close to its Tg.

6.2 Prediction of water uptake

The water uptake of each adhesive was computed using the finite element method. Details of the simulation can be found in a previous study [29]. Because the length of the adhesive layer is much longer than the width, moisture uptake in the longitudinal direction can be neglected [38, 39]. This results into a symmetric moisture distribution along the middle of the adhesive layer.

According to the moisture profile that was computed, a different value of absorbed moisture was attributed to each cohesive element. The moisture absorption was discretised into one value for each element across the width of the adhesive layer. Due to the symmetry, only half of the adhesive layer was considered. Results are shown in Figure 12 and Figure 13.

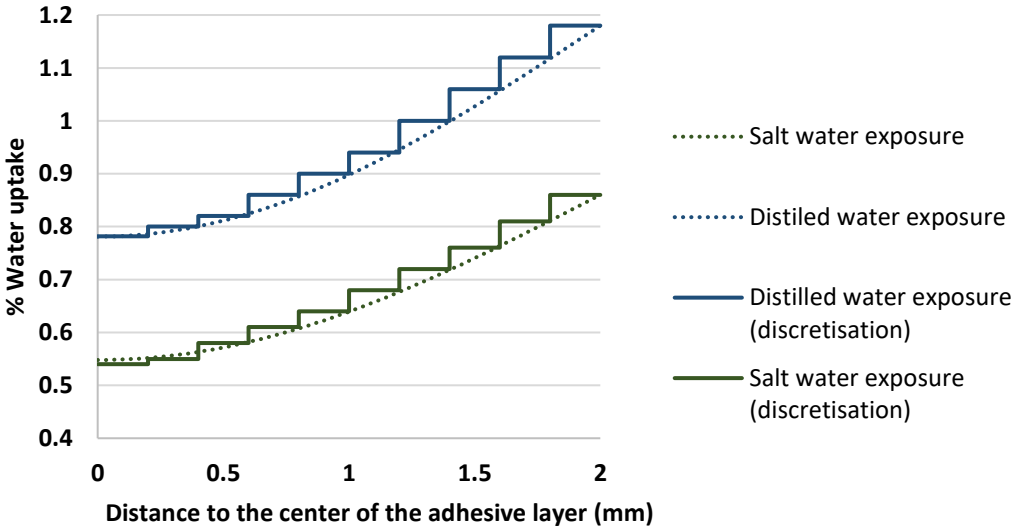

Figure 12: Moisture distribution in the XNR specimens after exposure.

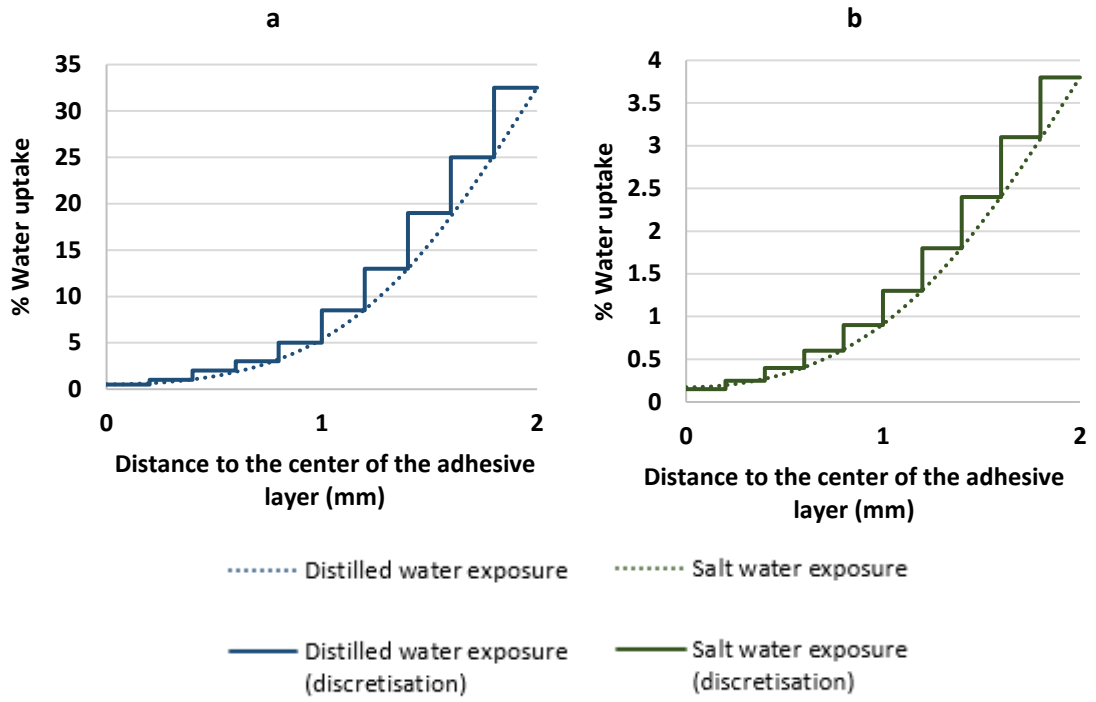

Figure 13: Moisture distribution in SikaPower specimens after exposure.

From Figure 12 and Figure 13 above, it can be noted that water uptake across the width of the adhesive layer is not constant. This is because the specimens were not exposed long enough to allow full saturation of the adhesive. Water uptake of distilled water exposed SikaPower 4720 specimens is higher than the remaining specimens'. This is due to the high moisture dependent Tg of this adhesive. Under high moisture conditions, the Tg of this adhesive is lower than the exposure temperature, which has a great effect on this adhesive's moisture uptake [35].

6.3 Prediction of the mechanical strength of dry and exposed specimens

Generally, results of the numerical model using the developed cohesive element matched the experimental results accurately. Figure 14 shows an example of such prediction.

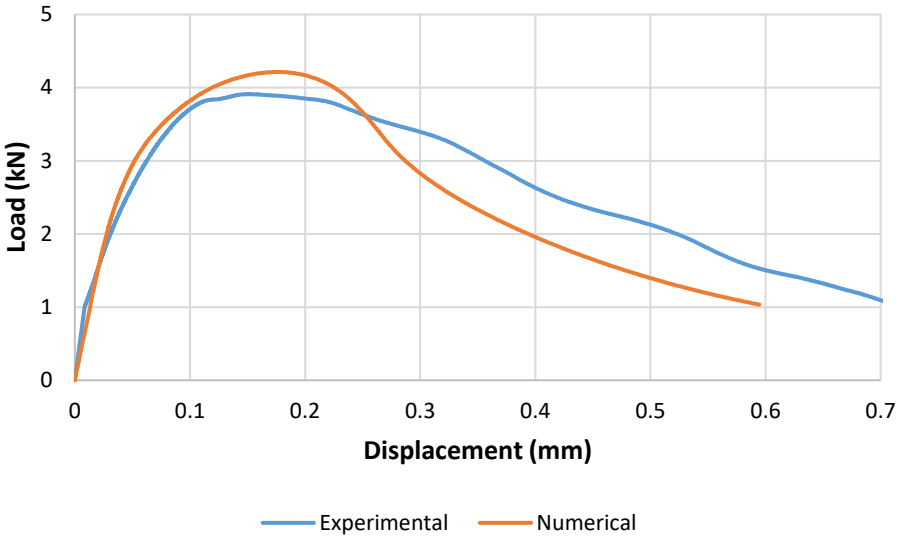

Figure 14: Comparison between experimental and numerical results of unexposed XNR6852specimen tested at 23ºC.

However, because environmentally exposed specimens suffered adhesive failure, the numerical model could not make a good prediction of these specimens, as it only accounts for cohesive failure. Figure 14 shows the comparison between numerical and experimental results.

From Figure 11, it is possible to understand that the numerical predictions of unexposed specimens matched well with the experimental results except when the XNR6852 joints were tested at 80ºC. This is due to the mechanical properties attributed to the adhesive at 80ºC. Obviously the adhesive in an adhesive joint is subjected to higher strain rate than a bulk adhesive if similar cross head speeds are applied. This means that the yield stress of an adhesive determined with a dogbone bulk specimen must be lower than the actual yield stress of an adhesive in an adhesive joint, especially if the adhesive is very ductile and strain rate dependent, such as XNR6852 at high temperature [40]. As the yield strength of the adhesives was determined using bulk dogbone tensile specimens, the strength of the adhesive as calculated by the model is in average lower than the actual strength of the adhesive in a joint, consequently making very conservative predictions if the adhesive is highly strain rate dependent. This could be corrected by simply determining the strength of the adhesive in a joint and adapting the parameters of the equations presented in section 3.

Numerical predictions for -40ºC give roughly the same value for exposed and unexposed conditions. This is because the adhesive is not as affected by environmental humidity at lower temperatures, as it was found in a previous study [35].

It is interesting how salt water exposed XNR6852 specimens had a failure load that was lower than distilled water exposed specimens. Similar behaviour has been witnessed in a previous study [36]. It is thought that, although distilled water is the most aggressive environment for the adhesive, salt water was probably responsible for corrosion of the substrate, resulting in lower interfacial strength.

It was found in a previous study that at lower temperatures, exposed adhesive bonded joints were less likely to suffer adhesive failures than at higher temperatures [36].

7. Conclusion

In this study, adhesive joints used in the railway industry were subjected to different temperature and moisture environments. Results show that generally lower temperatures result into higher strength of the joint. Moisture is responsible for shifting the locus of failure from the adhesive to the interface between adhesive and adherend.

A cohesive element that takes into account moisture and temperature degradation of adhesive joints was developed and used in this study. In the numerical model, the moisture absorption of each cohesive element is considered to make a prediction of the failure load of the joint. Good correlation between the failure load of specimens that suffered cohesive failure in the bondline and results provided by the numerical model was found.

Aknowledgements

The authors would like to thank Sika for supplying the SikaPower 4720 adhesive and Nagase Chemtex for supplying the XNR 6852-1 adhesive. This study was financed by the Fundação para a Ciência e Tecnologia through grant EXCL/EMS-PRO/0084/2012.

References

1. Banea MD, da Silva LFM, Campilho RDSG, Sato C. Smart Adhesive Joints: An Overview of Recent Developments. J Adhesion. 2014;90:16-40.
2. Banea MD, da Silva LFM. Adhesively bonded joints in composite materials: an overview. Proceedings of the Institution of Mechanical Engineers, Part L: Journal of Materials: Design and Applications. 2009;223:1-18.
3. Marques EAS, da Silva LFM, Banea MD, Carbas RJC. Adhesive Joints for Low- and High-Temperature Use: An Overview. J Adhesion. 2015;91:556-85.
4. Costa M, Viana G, da Silva LFM, Campilho RDSG. Environmental effect on the fatigue degradation of adhesive joints: A review. The Journal of Adhesion. 2016;93:127-46.
5. Sugiman S, Crocombe AD, Aschroft IA. Experimental and numerical investigation of the static response of environmentally aged adhesively bonded joints. Int J Adhes Adhes. 2013;40:224-37.
6. Hua Y, Crocombe AD, Wahab MA, Ashcroft IA. Modelling environmental degradation in EA9321-bonded joints using a progressive damage failure model. J Adhesion. 2006;82:135-60.
7. Barbosa AQ, da Silva LFM, Ochsner A. Hygrothermal aging of an adhesive reinforced with microparticles of cork. J Adhes Sci Technol. 2015;29:1714-32.
8. Lin YC, Chen X. Moisture sorption-desorption-resorption characteristics and its effect on the mechanical behavior of the epoxy system. Polymer. 2005;46:11994-2003.
9. Kinloch AJ, Little MSG, Watts JF. The role of the interphase in the environmental failure of adhesive joints. Acta Mater. 2000;48:4543-53.
10. Fernandes P, Viana G, Carbas R, Costa M, da Silva L, Banea M. The Influence of Water on the Fracture Envelope of an Adhesive Joint. Theoretical and Applied Fracture Mechanics. 2017;89.
11. Rodrigues T, Chaves F, Silva LFMd, Costa M, Barbosa A. Determination of the fracture envelope of an adhesive joint as a function moisture. Materialwissenschaft und Werkstofftechnik. 2017;48:1181-90.
12. Loh WK, Crocombe AD, Wahab MMA, Ashcroft IA. Modelling anomalous moisture uptake, swelling and thermal characteristics of a rubber toughened epoxy adhesive. Int J Adhes Adhes. 2005;25:1-12.
13. Mubashar A, Ashcroft IA, Critchlow GW, Crocombe AD. Moisture absorption-desorption effects in adhesive joints. Int J Adhes Adhes. 2009;29:751-60.
14. Ameli A, Datla NV, Papini M, Spelt JK. Hygrothermal Properties of Highly Toughened Epoxy Adhesives. J Adhesion. 2010;86:698-725.
15. Liljedahl CDM, Crocombe AD, Gauntlett FE, Rihawy MS, Clough AS. Characterising moisture ingress in adhesively bonded joints using nuclear reaction analysis. Int J Adhes Adhes. 2009;29:356-60.
16. Vanlandingham MR, Eduljee RF, Gillespie JW. Moisture diffusion in epoxy systems. J Appl Polym Sci. 1999;71:787-98.
17. Suh DW, Ku MK, Nam JD, Kim BS, Yoon SC. Equilibrium water uptake of epoxy/carbon fiber composites in hygrothermal environmental conditions. J Compos Mater. 2001;35:264-78.
18. Shanahan MER, Auriac Y. Water absorption and leaching effects in cellulose diacetate. Polymer. 1998;39:1155-64.
19. Xiao GZ, Shanahan MER. Water absorption and desorption in an epoxy resin with degradation. J Polym Sci Pol Phys. 1997;35:2659-70.
20. Y.C. Lin XC. Moisture sorption–desorption–resorption characteristics and its effect on the mechanical behavior of the epoxy system. Polymer. 2005:11994–2003.
21. X. Han ADC, S. N. R. Anwar, P. Hu and W. D. Li. The Effect of a Hot–Wet Environment on Adhesively Bonded Joints Under a Sustained Load. The Journal of Adhesion. 2014;90:420-36.
22. Liljedahl CDM, Crocombe AD, Wahab MA, Ashcroft IA. The effect of residual strains on the progressive damage modelling of environmentally degraded adhesive joints. J Adhes Sci Technol. 2005;19:525-47.
23. Zhou JM, Lucas JP. Hygrothermal effects of epoxy resin. Part II: variations of glass transition temperature. Polymer. 1999;40:5513-22.
24. Zhou JM, Lucas JP. Hygrothermal effects of epoxy resin. Part I: the nature of water in epoxy. Polymer. 1999;40:5505-12.
25. Adamson MJ. Thermal-Expansion and Swelling of Cured Epoxy-Resin Used in Graphite-Epoxy Composite-Materials. J Mater Sci. 1980;15:1736-45.
26. Xiao GZ, Shanahan MER. Swelling of DGEBA/DDA epoxy resin during hygrothermal ageing. Polymer. 1998;39:3253-60.
27. Chiang MYM, Fernandez-Garcia M. Relation of swelling and Tg Depression to the apparent free volume of a particle-filled, epoxy-based adhesive. J Appl Polym Sci. 2003;87:1436-44.
28. Zannideffarges MP, Shanahan MER. Diffusion of Water into an Epoxy Adhesive - Comparison between Bulk Behavior and Adhesive Joints. Int J Adhes Adhes. 1995;15:137-42.
29. Viana G, Costa M, Banea MD, da Silva LFM. Water diffusion in double cantilever beam adhesive joints. Latin American Journal of Solids and Structures. 2017;14:188-201.
30. Banea MD, Silva LFM. Mechanical Characterization of Flexible Adhesives. J Adhesion. 2009;85:261-85.
31. Banea MD, da Silva LFM, Campilho RDSG. Mode I fracture toughness of adhesively bonded joints as a function of temperature: Experimental and numerical study. Int J Adhes Adhes. 2011;31:273-9.

32. Viana G, Costa M, Banea MD, da Silva LFM. A review on the temperature and moisture degradation of adhesive joints. Proceedings of the Institution of Mechanical Engineers, Part L: Journal of Materials: Design and Applications. 2016;231:488-501.
33. Costa M, Viana G, da Silva LFM, Campilho RDSG. Environmental effect on the fatigue degradation of adhesive joints: a review. The Journal of Adhesion. 2016;DOI: 10.1080/00218464.2016.1179117.
34. Camanho PP, Dávila CG, Moura MFd. Numerical Simulation of Mixed-mode Progressive Delamination in Composite Materials. J Compos Mater. 2003;37:1415 - 38.
35. Viana G, Costa M, Banea MD, da Silva LFM. Behaviour of environmentally degraded epoxy adhesives as a function of temperature. The Journal of Adhesion. 2016;93:95-112.
36. Viana G, Costa M, Banea MD, Silva LFMd. Moisture and temperature degradation of double cantilever beam adhesive joints. J Adhes Sci Technol. 2017;31:1824-38.
37. Jurf RA, Vinson JR. Effect of Moisture on the Static and Viscoelastic Shear Properties of Epoxy Adhesives. J Mater Sci. 1985;20:2979-89.
38. Crocombe AD. Durability modelling concepts and tools for the cohesive environmental degradation of bonded structures. Int J Adhes Adhes. 1997;17:229-38.
39. Crocombe AD, Hua YX, Loh WK, Wahab MA, Ashcroft IA. Predicting the residual strength for environmentally degraded adhesive lap joints. Int J Adhes Adhes. 2006;26:325-36.
40. Viana G, Machado J, Carbas R, Costa M, Silva LFMd, Vaz M, Banea MD. Strain rate dependence of adhesive joints for the automotive industry at low and high temperatures. Int J Adhes Adhes. 2018;Submitted.